MECHANISTIC REGULATION OF HMGB1 FUNCTION IN DRUG-INDUCED LIVER INJURY

Thesis submitted in accordance with the requirements of the University of Liverpool for the degree of Doctor in Philosophy

By

Jonathan David Lea

September 2014

DECLARATION

This thesis is the result of my own work. The material contained within this thesis has not been presented, nor is currently being presented, either wholly or in part for any other degree or qualification.

Jonathan David Lea

This research was carried out in the Department of Molecular and Clinical Pharmacology, University of Liverpool, UK.

CONTENTS

ACKNOWLEDGMENTS

I would like to thank my supervisors Prof Kevin Park and Dr Daniel Antoine for their guidance and scientific discussion over the course of my PhD, and to Dr Dominic Williams for his guidance and support over the first 12months of my PhD. I would also like to acknowledge the financial support I have received from the MRC.

I am also very grateful to Peter Lundbäck and the other members of Prof Helena Harris' group at the Karolinska Institutet who helped with the h2G7 project, Prof Anja Kipar for her assistance with histological analysis, Dr Roz Jenkins for mass spectrometry assistance, Dr Maxine Seaton for microscopy assistance. Thank you also to Phill Roberts, Pete Metcalfe and Luke Palmer for technical assistance.

I would like to say thank you to the PhD students and Post-docs with whom I've spent a lot of time over my PhD for their friendship, help and advice; in particular Phil, Hannah, Jack, George, James F, James H, Luke S, Ali, Holly, Áine, Agnés and Nicola and all the other members of G27a.

I would also like to thank all my friends outside of the University who have supported me during my PhD, and taken the time to ask and care about how my studies have been going – usually over a pint!

Finally, I would like to thank my family and especially Sophie for their love, support, advice and unbelievable patience and understanding throughout! Sophie has been amazing at being there for me, keeping me motivated and giving me invaluable help, including the unenviable proofreading! I would also like to reserve a special thank you for my Grandad Jeff, who sadly passed away during my studies. He always encouraged me to do my best, and achieve the most I could. Thank you.

PUBLICATIONS

Papers

JD Lea, JI Clarke, DJ Antoine. HMGB1 as a mechanistic biomarker and pivotal co-ordinator of drug-induced liver injury (DILI). *Manuscript in preparation.*

P Lundbäck, **JD Lea,** L Ottosson, JW Sharkey, A Sowinska, JI Clarke, BK Park, U Andersson, H Harris, DJ Antoine. A chimeric anti-HMGB1 antibody protects against acetaminophen-induced liver injury in mice. *Manuscript in preparation.*

Abstracts

JD Lea, P Lundbäck, L Ottosson, JW Sharkey, A Sowinska, K Palmblad, JI Clarke, BK Park, U Andersson, H Harris, DJ Antoine. Humanized anti-HMGB1 antibody therapy attenuates *in vivo* acetaminophen-induced liver injury. *Toxicol Lett 229S (2014) S69-70*

ABBREVIATIONS

ADCC	antibody-dependent cell cytotoxicity
ADR	adverse drug reaction
AIF	apoptosis-inducing factor
AILI	acetaminophen-induced liver injury
ALF	acute liver failure
ALT	alanine aminotransferase
AMAP	acetyl-m-aminophenol
amu	atomic mass units
AP	alkaline phosphatase
APAP	acetaminophen (paracetamol)
ATP	adenosine triphosphate
BCRP	breast cancer resistance protein
BSA	bovine serum albumin
°C	degrees centigrade
CDC	complement-mediated cytotoxicity
CDR	complementarity determining region
CXCL1	chemokine (C-X-C motif) ligand 1
CYP	cytochrome P450
DAMP	damage-associated molecular pattern
DILI	drug-induced liver injury
DISC	death-induced signaling complex
DMSO	dimethyl sulphoxide
d_5NEM	deuterated NEM
DMEM	Dulbecco's modified eagle media
DNA	deoxyribonucleic acid
DTT	dithiothreitol
ECL	electrochemiluminescence reagent
EDTA	ethylenediaminetetraacetic acid
Fab	fragment (antigen binding)
FBS	fetal bovine serum
Fc	fragment (crystallisable)
FcγR	Fc gamma receptor
FasL	Fas ligand
GGT	γ-glutamyltransferase
GSH	glutathione
H&E	hematoxylin and eosin
HDAC	histone deacetylase
HMGB1	high mobility group box 1 protein
HMGB1-Ub	ubiquitinated hmgb1

HSA	human serum albumin
HSP	heat shock protein
IAP	inhibitor of apoptosis proteins
ICAD	
IFNγ	interferon-gamma
IL-1β	interleukin 1 beta
IL-6	interleukin 6
i.p.	intraperitoneal
kDa	kilodalton
KC	Kupffer cells
LC-MS/MS	liquid chromatography tandem mass spectrometry
LCA	*Lens culinaris* Agglutinin
LPS	lipopolysaccharide
miR	microRNA
MCP-1	macrophage chemoattractant protein 1
MEFs	mouse embryonic fibroblasts
MP	microparticles
MPO	myeloperoxidase
MPT	mitochondrial permeability transition pore
MRP	multidrug resistance-associated protein
MS/MS	tandem mass spectrometry
MTS	3-(4,5-dimethylthiazol-2-yl)-5-(3-carboxymethoxyphenyl)-2-(4-sulphophenyl)-2H-tetrazolium)
m/z	mass-to-charge ratio
NAC	N-acetylcysteine
NEM	N-ethylmaleimide
NAPQI	N-acetyl-*p*-benzoquinonimine
NF-κB	nuclear factor kappa-light-chain-enhancer of activated B cells
NK/NKT	natural killer cells
NL	neutrophilic leukocytes
NLS	nuclear localisation sequence
p	probability
PAMP	pathogen-associated molecular pattern
PAS	periodic acid-Schiff
PBS	phosphate buffered saline
PFA	paraformaldehyde
PI	propidium iodide
PIC	protease inhibitor cocktail
PKC	protein kinase C
PS	phosphatidyl serine
PTM	post-translational modification

qPCR	quantitative PCR
RAGE	receptor for advanced glycation end products
ROS	reactive oxygen species
RT	room temperature
SEM	standard error of the mean
SSA	sulphosalicylic acid
STS	staurosporine
TBL	total bilirubin
TBS-T	tris-buffered saline-Tween
TLR	Toll-like receptor
TMB	3,3',5,5'-tetramethyl-benzidine
TNFα	tumour necrosis factor alpha
TNFR1	tumour necrosis factor receptor 1
TNFR2	tumour necrosis factor receptor 2
U	units
ULN	upper limit of normal
v/v	volume/volume
w/v	weight/volume
Z-VAD-FMK	N-Benzyloxycarbonyl-Val-Ala-Asp(O-Me) fluoromethyl ketone

ABSTRACT

Drug-induced liver injury (DILI) is a major cause of attrition during drug development, and also a leading cause of hospital admissions. In order to identify novel biomarkers that may improve the diagnosis and treatment of DILI, well characterised hepatotoxins such as acetaminophen (APAP) are used. High mobility group box 1 (HMGB1) protein is a ubiquitously expressed protein involved in the facilitation of gene transcription. However, extracellular HMGB1 acts as a key mediator of inflammation. During APAP-induced liver injury (AILI), HMGB1 is passively released from necrotic hepatocytes in a fully reduced, hypoacetylated isoform, or actively released from immune cells following acetylation of HMGB1 at key lysine residues within nuclear localisation sequences. Extracellular HMGB1 can bind to a range of receptors including TLR2, TLR4, TLR9, CXCR4 and RAGE to mediate cytokine-inducing or chemotactic effects and has been shown to be a more sensitive and predictive serum biomarker of AILI outcome than ALT. Additionally, anti-HMGB1 antibodies have been used to successfully attenuate injury in animal models of inflammatory conditions, including DILI. Mechanistic understanding of HMGB1 regulation and function is essential for this emerging biomarker of AILI.

A murine monoclonal anti-HMGB1 antibody (2G7) has previously been used to attenuate AILI. A chimeric anti-HMGB1 monoclonal antibody (h2G7) was investigated, alongside 2G7 and a human isotype control antibody (E2) in an experimental model of AILI. C57BL/6 mice dosed with 530mg/kg APAP by intraperitoneal (*i.p.*) injection, followed by antibody or PBS treatment *i.p.* at 2hr post-APAP and euthanisation at 10hr post-APAP showed that 300µg h2G7 treatment afforded protection from AILI by significantly attenuating serum ALT, miR-122 and chemo/cytokine increases seen in the isotype control group. Liver histology and MPO revealed reduced neutrophil infiltration and activity in anti-HMGB1 treated animals. No significant differences were seen between 2G7 and h2G7 animals, and there was no effect on hepatic GSH in antibody-treated animals. Mechanism of action studies using Fc region modified forms of h2G7 ruled out complement-mediated and FcγR-mediated effects of h2G7 in the AILI model, as these did not significantly affect the h2G7 effect on AILI.

Redox modulation of HMGB1 function had been proposed as a mechanism of regulation of proinflammatory activity of HMGB1. Investigations into the cytokine-inducing capability of different redox isoforms of HMGB1 in THP-1 and RAW264.7 cells demonstrated that HMGB1 needs to be in a Cys23-Cys45 disulphide conformation with a reduced thiol at Cys106 in order to induce cytokine release via NF-κB activation. During apoptosis, HMGB1 can be oxidised by activated caspases. Oxidation has previously been shown to regulate the structure of proteins and facilitate other post-translational modifications (PTM). LC-MS/MS characterisation of HMGB1 from APAP overdose patients with high levels of apoptosis revealed ubiquitination at Lys30 (HMGB1-Ub). Ubiquitination was shown *in vitro* not to direct HMGB1 for proteasomal degradation, but HMGB1-Ub was detectable in apoptotic microparticles (MP), membrane vesicles that are shed from a cell during late apoptosis.

In summary, HMGB1 was shown to be critical for the coordination of AILI, as antibody-mediated inhibition lead to a reduction in hepatic injury. Chimeric anti-HMGB1 antibody was effective at attenuating liver injury and advances anti-HMGB1 antibody treatment towards clinical utility. HMGB1 redox regulation of inflammatory signalling and the identification of HMGB1-Ub demonstrate the importance of PTM in governing HMGB1 function. HMGB1 shows promise as an acute, sensitive and predictive biomarker of AILI in man. Through the use of *in vitro* and *in vivo* systems, the work presented in this thesis expands our current understanding of the mechanistic and functional roles of HMGB1 in DILI and has further defined mechanisms that can be used to inform the clinical situation.

Chapter One

General Introduction

CONTENTS

1.1 Adverse drug reactions (ADRs)

An adverse drug reaction (ADR) can be defined as "an appreciably harmful or unpleasant reaction, resulting from an intervention related to the use of a medicinal product, which predicts hazard from future administration and warrants prevention or specific treatment, or alteration of the dosage regimen, or withdrawal of the product" (Edwards and Aronson, 2000).

ADRs can be classified into either “on-target” or “off-target” reactions. “On-target” reactions are directly related to the primary or secondary pharmacology of the drug and are usually an exaggeration of the pharmacological effect of the drug. For instance, on-target reactions include commonly seen ADRs such as bleeding caused by warfarin. On-target reactions can generally be avoided by reduction of the dose given to the patient. By contrast, “off-target” (or idiosyncratic) reactions are often dose-independent, often patient-specific and can be related to metabolic or immune-related variations of the individual, leading to increased sensitivity of the individual to the parent drug or one or more of its metabolite(s). Additionally, as off-target reactions affect only a very small proportion of a population, they are much harder to determine in pre-clinical testing and suitable animal models for their detection may be unavailable. Hypersensitivity reactions to β-lactam antibiotics such as amoxicillin, the anticonvulsant carbamazepine or hepatotoxicity with the NSAID diclofenac are examples of idiosyncratic ADRs (Park et al., 2011, Pirmohamed and Park, 2003).

ADRs are a leading cause of hospital admissions in the developed world and a major cause of drug attrition in the pharmaceutical industry. The financial burden of ADRs to both these sectors is great, and as the incidence of ADRs has increased in the last 10 years this is an area of healthcare that requires effective strategies to counter this growth (Wu et al., 2010, U.S. Food and Drug Administration (FDA)).

Within the pharmaceutical industry ADRs are a major concern, with 30% of compound attrition in drug development due to ADRs (Kola and Landis, 2004). The estimated cost of a new chemical entity from discovery to market is projected at around $1billion (DiMasi et al., 2003) and a large part of this expenditure is due to attrition of other prospective compounds.

Recent clinical studies of ADRs have defined the proportions of ADRs caused by different classifications of drugs and additionally, which organs are most prevalently targeted by ADRs (Pirmohamed et al., 2004, Wu et al., 2010). The consensus amongst these studies is that the reporting of ADRs may be underestimating the true incidence of ADRs, and hence the impact on hospitals may be greater than estimated.

In 2004, Pirmohamed *et al* undertook a study of hospital admissions to two NHS hospitals in the Northwest of England over a 6-month period. This study showed that 6.5% of admissions were classified as ADRs, and the projected national cost to the NHS of ADRs was £466million (Pirmohamed et al., 2004). A more recent study by Wu *et al* looked at hospital admissions over a 10-year study of all NHS hospitals. This study showed ADRs to be responsible for 0.9% of admissions, that within the study time there was a 76.8% increase in admissions, and an in-hospital mortality rate increase of 10% (from 4.3 to 4.7%) (Wu et al., 2010). Furthermore, another study has shown that approximately one-in-seven in-patients may experience an ADR whilst in hospital, which increases the length of stay by 0.25day/patient admission episode and is both a significant cause of morbidity and increased burden on hospitals. Worryingly, about half of the ADRs recorded could potentially have been avoided (Davies et al., 2009). A major contributor to the costs associated with ADRs is the shortcomings of current clinically used biomarkers and this establishes the need for novel biomarkers of ADRs that can be used to improve clinical assessment and direct treatment.

1.2 Drug Induced Liver Injury (DILI)

Drug-induced liver injury (DILI) is a leading cause of acute liver failure (ALF) in the developed world, with 52% of cases of ALF being attributable to DILI (Ostapowicz et al., 2002). Hepatotoxicity is a leading cause of drug withdrawal from the market and issuing of black box warnings. Of the 548 new drugs brought to market between 1975 and 1999, 4 withdrawals and 10 black box warnings were issued due to hepatotoxicity (Lasser et al., 2002). Current models of hepatotoxicity are only able to detect about half of hepatotoxic compounds (approximately half of known hepatotoxins being detectable in animal models (Olson et al., 2000) and 60-70% in *in vitro* human hepatocyte testing (Xu et al., 2008)), so in order to detect compounds that could lead to idiosyncratic reactions, better models and biomarkers are required.

Clinically, DILI can present with a wide range of symptoms, and can appear like other forms of liver injury (Navarro and Senior, 2006). Hence the clinician needs to be able to associate drug dose, disease onset and be able to exclude other hepatic conditions in order to diagnose DILI. Patients may also present with non-specific symptoms such as upper right quadrant pain or fatigue. Additionally, existing medical conditions such as alcoholism or cirrhosis may complicate disease onset and diagnosis. Moreover, clinical manifestations of DILI can range from mild asymptomatic changes through to fulminant liver failure. A liver biopsy is the only definitive form of diagnosis of DILI, but this is an invasive procedure, so non-invasive serum biomarkers of DILI are utilised as a diagnostic tool.

Current serum biomarkers of hepatotoxicity can be split into markers of hepatocellular and cholestatic damage, with alanine aminotransferase (ALT) and aspartate aminotransferase (AST) being classified as hepatocellular markers and alkaline phosphatase (AP), and γ-glutamyltransferase (GGT) being classified as cholestatic markers (Laverty et al., 2010). Reference ranges from healthy individuals are key to identifying abnormal elevations in

these enzymes and the upper limit of normal (ULN) for ALT is 40 IU/L, AST is also 40 IU/L, AP has a ULN of 120 IU/L, and GGT of 51 IU/L (Antoine et al., 2009a). Raised serum ALT and AST often precede elevations in bilirubin levels (TBL), a liver function biomarker, and together are indicative of serious liver injury. In clinical scenarios, these serum biomarkers are also assessed alongside albumin and prothrombin time, which are additional markers of liver function, providing a fuller picture of the status of the liver - as liver injury may not necessarily affect liver function. The internationally defined criteria for liver toxicity classification are according to serum ALT and AP levels (Benichou, 1990):

- Cholestatic injury is a defined as AP > 2×ULN or ALT/AP ≤ 2
- Mixed Hepatocellular/cholestatic injury is defined as an ALT/AP ≤ 2-5.
- Hepatocellular injury is determined by the ALT > 2×ULN or ALT/AP ≥ 5

However, the current gold standard biomarkers of DILI have significant shortfalls that limit their effectiveness. Firstly, elevations ALT and AST do not definitively confirm DILI as the cause, as other disease processes such as fatty liver disease and viral hepatitis also lead to elevations in these enzymes (Ozer et al., 2008). Secondly, thresholds for the definition of a significant elevation of ALT and AST vary between different DILI studies. Thirdly, the absolute height of elevation of ALT does not correlate with the severity of injury (Ozer et al., 2008). Furthermore, elevations in serum ALT and AST can be detected following muscle or cardiac injury, thus diminishing the liver-injury specificity of ALT (Ozer et al., 2008). Total bilirubin may be increased due to non-hepatic reasons such as haemolysis. Finally, elevations in ALT, AST and bilirubin are not as rapid as other potential biomarkers, and so more acute biomarkers may be useful for improving speed of diagnosis and subsequently earlier appropriate treatment. Together these shortfalls with current gold standard biomarkers leave areas of potential improvement that could be addressed through the discovery and validation of novel DILI biomarkers. Utilisation of a panel of novel biomarkers

alongside the existing biomarkers (ALT, AST, bilirubin, prothrombin time) will result in greater knowledge of a patient's liver health and improve prognosis.

1.3 Drug metabolism

Drug metabolism consists of three phases: Phase I, Phase II and Phase III, corresponding to drug bioactivation/toxification, conjugation and drug transportation respectively. The products of drug metabolism may be more or less reactive than the parent compound. Those metabolites that have increased reactivity than the parent compound can be referred to as having undergone bioactivation. Reactive metabolites are able to act as electrophiles, which can be categorised into hard or soft electrophiles, which also determines the molecular target bound by the metabolite. Hard electrophiles tend to bind to hard nucleophiles, whereas soft electrophiles bind to soft nucleophiles (Ma and Subramanian, 2006). Hard nucleophiles include DNA bases and lysine residues and usually contain nitrogen, which can act as the electron donor, whereas soft nucleotides include sulphur-containing species, as the lone electron pair are further from the nucleus. Imbalance between the phases of drug metabolism that result in a build-up of reactive metabolites can lead to cellular stress, cell death and DILI (Pachkoria et al., 2007).

Phase I metabolism results in the addition or formation of a chemically reactive group, such as -OH, -COOH, -SH or $-NH_2$, primarily through oxidation, reduction or hydrolysis reactions (Gibson, 2001).

Phase I reactions are often catalysed by the mixed-function oxidase system, which is found in the smooth endoplasmic reticulum. This system comprises cytochrome P450 (CYP) enzymes and NADPH cytochrome P450 reductase. CYP enzymes are heme-containing monooxygenase enzymes that catalyse the addition of oxygen to drugs, and reduction of the iron within the CYP. NADPH cytochrome P450 reductase acts as an electron carrier to

facilitate the transfer of electrons from NADPH to the CYP substrate (Meyer, 1996). Ultimately reactions catalysed by this system rely upon the presence of molecular oxygen and NADPH, and result in the insertion of a single oxygen atom into the substrate/drug molecule (Gibson, 2001).

Phase II metabolism consists of conjugation reactions that usually produce inactive compounds that can be excreted. These reactions often involve a high-energy co-factor or substrate derivative, which leads to the formation of a water-soluble metabolite that can be excreted in bile or urine (Gibson, 2001). Conjugation reactions include sulphation, glucuronidation and glutathione (GSH) conjugation.

GSH conjugation is a common form of bioinactivation when sulphation and glucuronidation pathways are saturated. GSH is a tripeptide (Glu-Cys-Gly) which can become conjugated to an electrophile via the formation of a thioester bond with the cysteine residue of GSH (Meister, 1983, Coles et al., 1988). This process can happen spontaneously, or enzymatically, under the control of GSH S-transferases. Phase II metabolism of neutrophilic metabolites are controlled by UDP-glucuronosyl transferases and sulphotransferases (Bock et al., 1987).

However, there are examples of Phase II metabolism leading to the formation of toxic metabolites. Diclofenac is a non-steroidal anti-inflammatory drug that is associated with idiosyncratic toxicity. The mechanism of toxicity has been attributed to the formation of an acyl glucuronide that can then bind to cellular and plasma proteins (Boelsterli, 2003, Zhou et al., 2005, Kretz-Rommel and Boelsterli, 1993).

Phase III metabolism refers to the use of drug transporters to eliminate a metabolite or drug from the liver. These transporters are responsible for the transport of a drug from the sinusoid to the hepatocyte surface, transport into the hepatocyte cytosol via the

basolateral membrane, intracellular trafficking and subsequent movement across the canalicular membrane into the bile (Evans, 1996).

As Phase I metabolism usually does not alter the lipophilicity of the compound, the metabolites produced can passively diffuse out of hepatocytes. However due to the conjugation reactions, Phase II metabolites are of greater molecular weight and hydrophilicity. Hence drug transporters are critical for the removal of these metabolites. The main transporters involved in the removal of metabolites from hepatocytes are multidrug resistance-associated proteins 3 and 4 (MRP3 and MRP4) on the basolateral membrane and MRP2 and breast cancer resistance protein (BCRP) on the apical membrane (Zamek-Gliszczynski et al., 2006).

1.4 Acetaminophen-induced liver injury (AILI)

Acetaminophen (APAP) is the one of the most commonly administered analgesic drugs in the western world. However, APAP overdose is the most common cause of DILI, causing 39% of acute liver failure (ALF) cases in the US, with the majority being defined as suicide attempts or accidental overdose (Ostapowicz et al., 2002). In the UK alone, APAP is responsible for 200-500 deaths per year and 20-40 liver transplants (Hawton et al., 1995). APAP is metabolised in the liver by three pathways (Fig.1.1): The majority of the dose is metabolised by Phase II sulphation and glucuronidation reactions to form stable metabolites that are readily excreted in urine. However, CYPs, primarily CYP2E1, CYP1A2 and CYP3A4 can metabolise up to 15% of APAP dose to form N-acetyl-*p*-benzoquinone imine (NAPQI) (Raucy et al., 1989). There is also a reported role for CYP2D6, a highly polymorphic CYP that may be associated with inter-individual differences in APAP metabolism and toxicological effects. NAPQI is a reactive metabolite, but at therapeutic doses of APAP, the NAPQI formed is detoxified by conjugation with intracellular glutathione

(GSH). However, in cases of APAP overdose excessive NAPQI production leads to depletion of GSH stores and excess NAPQI can bind irreversibly to cellular macromolecules such as proteins. NAPQI binds to mitochondrial proteins at a much higher level than the quinone-derivatives produced from the regioisomer of APAP, acetyl-m-aminophenol (AMAP) (Matthews et al., 1997, Myers et al., 1995). Irreversible binding of NAPQI to a wide range of proteins is associated with mitochondrial dysfunction and other cellular stresses. Ultimately these lead to massive hepatocyte cell death (James et al., 2003, David Josephy, 2005, Jollow et al., 1973).

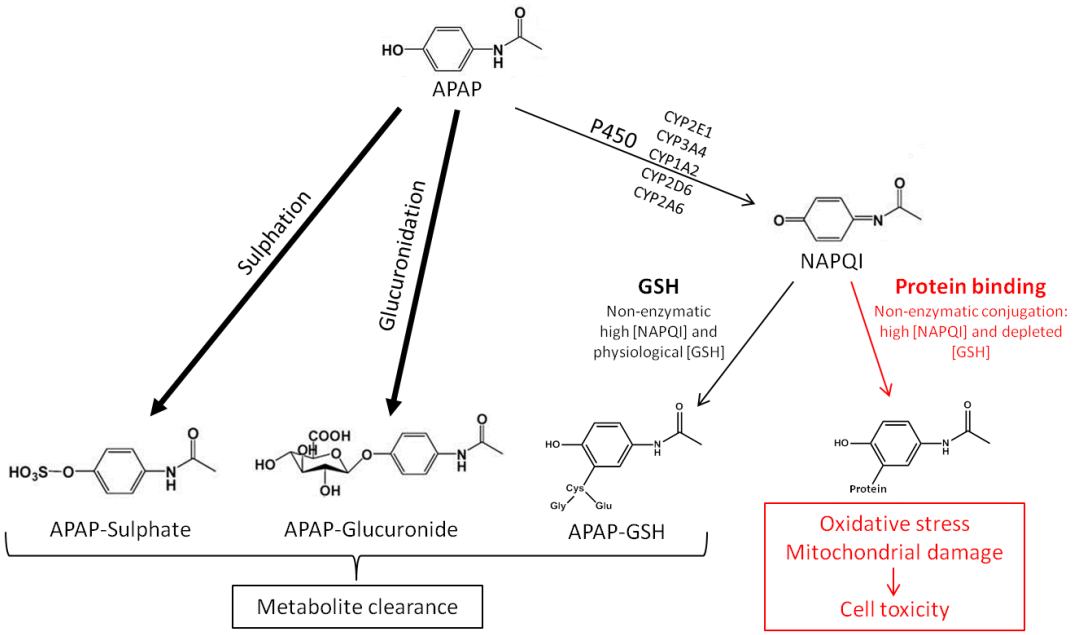

Fig.1.1 – APAP metabolism. APAP is primarily metabolised by Phase II reactions to form sulphate and glucuronide conjugates which can then be easily cleared. However, up to 15% of APAP is metabolised by CYP enzymes to form a reactive metabolite, NAPQI. NAPQI is detoxified by intracellular GSH. However, if GSH stores are depleted, NAPQI can bind to intracellular macromolecules such as proteins, leading to mitochondrial damage and oxidative stress, ultimately resulting in cell death and the development of liver injury.

Clinical intervention in cases of APAP overdose is treatment with N-acetylcysteine (NAC), a precursor in the synthesis of GSH. This enables the regeneration of hepatic glutathione, and detoxification of NAPQI. Treatment is usually via the intravenous route, although oral NAC

is sometimes used in the US. NAC treatment is most effective within 8hr of overdose (Prescott et al., 1979). Untreated APAP overdose can lead to fulminant liver failure. In these cases the only way to avoid death is liver transplantation.

The role of the immune system in AILI is a controversial subject, with conflicting reports as to the level of importance of the innate immune response to hepatocyte cell death. However, it is agreed that the innate immune system plays a role in the progression and resolution of AILI, with resident liver immune cells such as Kupffer cells (KC), natural killer (NK/NKT) cells and neutrophils appearing to be key modulators. These cells all produce chemokines and cytokines that are vital coordinators of inflammation. AILI is characterised by centrilobular hepatic necrosis and leukocyte infiltration, particularly neutrophils. However, the role of neutrophils in AILI is controversial. Antibody-induced neutrophil depletion and inhibition of neutrophils infiltration through CXCR2 knockout greatly reduces the severity of liver injury (Ishida et al., 2006, Liu et al., 2006). Neutrophils are responsible for production, through inducible nitric oxide synthase (iNOS), and release of nitric oxide, which leads to further oxidative damage. However, others argue that the protective role is actually due to induction of protective genes in response to the anti-neutrophil antibody (Jaeschke and Liu, 2007) and neutrophils do not contribute to the initiation or propagation of AILI (Lawson et al., 2000).

The role of KC is also controversial, as depletion of KC has been shown to result in both a decrease and increase in susceptibility to AILI (Goldin et al., 1996, Ju et al., 2002), although this may be dependent on the timepoint of injury, with KC depletion being protective at early timepoints but detrimental at later timepoints. However, recent characterisation of macrophages in AILI suggests that KC are proinflammatory, and infiltrating macrophages are resolution-associated (Holt et al., 2008).

NK and NKT cells, as the primary source of IFNγ, have been shown to be important in the propagation of inflammation during AILI. Initially, depletion of NK and NKT cells appeared

to be protective against AILI in mice (Liu et al., 2004). However, this study was shown to be compromised as the effects seen were shown to be attributable to the use of DMSO, the vehicle for APAP, which can itself induce leukocyte infiltration (Masson et al., 2008). Despite debate surrounding the importance of particular innate immune cell types in the pathogenesis of AILI, it is known that these immune cells, particularly macrophages, are key sources of inflammatory chemo- and cytokines.

1.4.2 Idiosyncratic DILI

Although APAP is the xenobiotic responsible for the majority of DILI-associated hospital admissions, other drugs and herbal remedies are also responsible for a large number of hospital admissions. Idiosyncratic DILI is the second greatest cause of ALF in the US - accountable for 13% of cases. Idiosyncratic DILI is most commonly caused by antibiotics, with amoxicillin-clavulanate being the most frequent cause. Drugs often associated with idiosyncratic DILI are shown in Table 1.1, produced by combining two recent studies taken from different Western European populations.

Table 1.1: Common idiosyncratic hepatotoxins arranged by drug class

Drug class	Drug name	References
Antibiotic	Amoxicillin-clavulanate	[a][b]
	Isoniazid	[b]
	Erythromycin	[b]
	Trovafloxacin	[b]
Psychotropic	Carbamazepine	[a][b]
	Paroxetine	[a][b]
	Valproic acid	[b]
	Tetrabamate	[b]
	Bentazepam	[b]
NSAID	Diclofenac	[a][b]
	Ibuprofen	[a][b]
	Nimesulide	[b]
Immunosuppressive	Azathioprine	[b]
	Methotrexate	[a]
Hypolipidemic	Atorvastatin	[a]
	Fenofibrate	[a]
Antiretroviral	Nevirapine	[a]
Chemotherapeutic	Flutamide	[a][b]
Anti-platelet	Ticlopidine	[a][b]
H2-receptor antagonist	Ebrotidine	[b]
Anti-thyroid	Thiamazole	[b]

[a] (Sgro et al., 2002), [b] (Andrade et al., 2005)

1.5 Drug-induced cell death mechanisms

Drug toxicity can result in cell stress mediated through many mechanisms, such as oxidative stress and irreversible binding of cellular macromolecules. Cell stress can be alleviated through cellular defence mechanisms, however if these pathways are overwhelmed or exhausted, cells can proceed to cell death. The mechanism of cell death plays a major role in the magnitude and coordination of the inflammatory response. ADRs can result in an inflammatory response through toxicity of either the parent compound or a metabolite or metabolites. This inflammatory response can be a source of prospective biomarkers that could be used to aid clinical diagnosis and direct patient treatment.

1.5.1 Apoptosis

Apoptosis is a tightly regulated, ATP-dependent form of cell death (Kerr et al., 1972), which comprises compartmentalisation of cellular macromolecules and leads to a general suppression of proinflammatory signalling. Morphologically, apoptosis presents as the rounding of cells, including withdrawal of podocytes, a reduction in cellular volume, nuclear condensation and fragmentation and membrane blebbing (Kroemer et al., 2009). These blebs are also known as apoptotic bodies, and are phagocytosed *in vivo*. Apoptosis can be coordinated by caspase proteins. Caspase proteins are a family of proteases that possess a cysteine-containing active site and cleave target molecules after aspartate residues (Hengartner, 2000, Thornberry et al., 1997). Caspases can be categorised into initiator or effector caspases, according to their role in apoptosis. Apoptosis in mammalian cells can be initiated through two major mechanisms: through a death-receptor (extrinsic) pathway or via a mitochondrial (intrinsic) pathway (Fig.1.2).

The death receptor pathway can be initiated by tumour necrosis factor alpha (TNFα) binding to TNFα receptor 1 (TNFR1) or FasL (CD95 ligand) binding to Fas (CD95).The ligand-receptor binding mediates formation of a signalling complex with adaptor molecules.

TNFR1 activation leads to recruitment of TRADD, and subsequent recruitment of FADD and RIP which can then recruit multiple procaspase-8 proteins. Fas activation leads to direct recruitment of FADD. FADD and procaspase-8 form a complex known as the death-induced signalling complex (DISC). The low intrinsic caspase activity of procaspase-8 coupled with its high localised concentration at the signalling complex leads to activation (by cleavage) of caspase-8 (Muzio et al., 1998), which can subsequently cleave substrate proteins including effector caspases such as caspase-3. Caspase-3 can then target other proteins for cleavage such as the inhibitor of caspase-activated DNase (ICAD), to induce further pro-apoptotic pathways.

The intrinsic apoptotic pathway is mitochondria-mediated and can be activated through diverse stimuli, such as DNA damage and chemical or oxidative stress. Common to these stimuli is the formation of the mitochondrial permeability transition pore (MPT) due to changes in the inner mitochondrial membrane. The MPT pore formation leads to loss of mitochondrial potential and release of two groups of proteins. The first group consists of cytochrome *c*, Smac/DIABLO and HtrA2/Omi. Cytochrome *c* can (with Apaf-1 and procaspase-9) then form a protein complex known as the apoptosome, which activates caspase-9 and subsequently activate effector caspases (Rodriguez and Lazebnik, 1999). Smac/DIABLO and HtrA2/Omi are responsible for the binding and inhibition of a group of proteins known as inhibitor of apoptosis proteins (IAP), leading to further pro-apoptotic signalling. A second group of mitochondrial proteins are released later, including apoptosis inducing factor (AIF), endonuclease G and ICAD/CAD. These proteins translocate to the nucleus to cause DNA fragmentation. Mitochondrial permeability is regulated by members of the Bcl-2 family, and hence the intrinsic pathway is dependent on a shift in the balance of these proteins from an anti-apoptotic to a pro-apoptotic signal. Bcl-2 and Bcl-x_L are anti-apoptotic members of the family and Bax, Bad and Bid are pro-apoptotic (Robertson and Orrenius, 2000). Bad acts by binding to Bcl-2 and Bcl-x_L , thus inhibiting them from

preventing cytochrome *c* release. There are at least another 20 members of the Bcl-2 family that include Puma and Noxa, which are pro-apoptotic members associated with p53-mediated apoptosis.

There is also significant evidence of cross-talk between the two pathways. Firstly, the executioner phase of apoptosis is common to both pathways, with caspase-3 playing a key role in both pathways. Caspase-3 substrates when cleaved act to cause cytoskeletal remodelling and DNA fragmentation. Additionally, Fas-mediated apoptosis leads to the cleavage of Bid by caspase-8 and hence mitochondrial damage (Li et al., 1998). Fig.1.2 shows an overview of the two major apoptotic pathways.

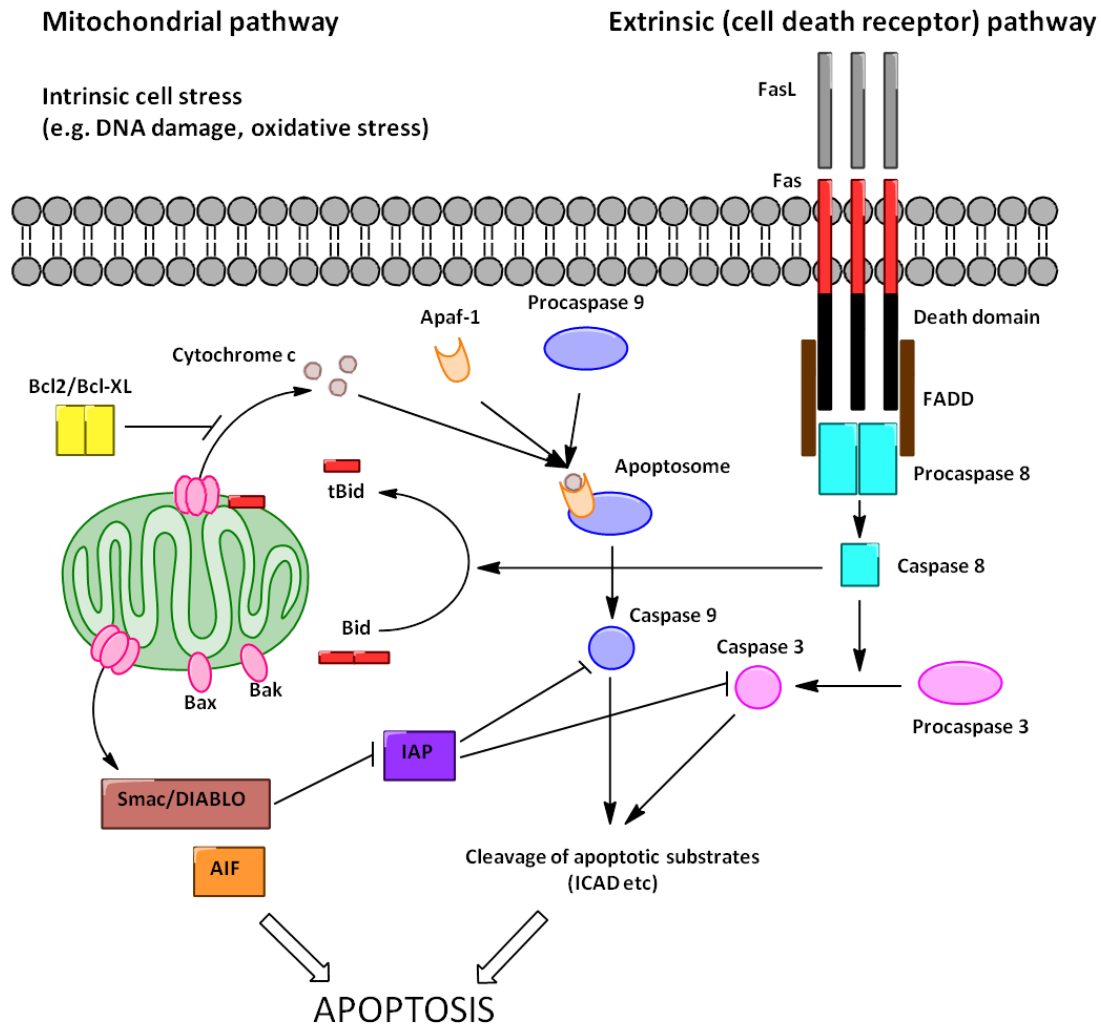

Fig.1.2 - An overview of the intrinsic and extrinsic pathways of apoptosis and how cross-talk is possible between the two. Adapted from (Bellance et al., 2009)

1.5.2 Necrosis

In contrast to apoptosis, necrosis is a largely unregulated mode of cell death characterised by cytoplasmic organelle swelling and loss of cell membrane integrity resulting in the release of intracellular molecules, such as lysosomal proteins and DNA. As there are no generally accepted mechanisms of unregulated necrosis, necrosis is classified according to the absence of apoptotic or autophagic markers (Kroemer et al., 2009). The passive release of intracellular molecules during necrosis leads to a proinflammatory response. Despite necrosis classically being recognised as an unregulated form of cell death, increasing evidence points to a regulated form of necrosis termed "necroptosis" that proceeds via RIP1 and RIP3 activation (Declercq et al., 2009). In addition, there is cross-talk between cell death mechanisms, hinting at a partial regulation of necrosis. For instance, high levels of TNFα can induce hepatocyte necrosis (Malhi et al., 2006), suggesting an overwhelming of the extrinsic pathway of apoptosis. Additionally, caspase inhibition has been shown to redirect cells from apoptosis to necrosis instead. Intracellular ATP levels are also pivotal to whether a cell undergoes apoptosis or necrosis, with apoptosis being an ATP-dependent process, whereas necrosis predominates in conditions of ATP depletion (Leist et al., 1997, Hotchkiss et al., 2009, Nicotera et al., 1998).

1.5.3 Autophagy

Autophagy, literally meaning "self-eating", is an ATP-dependent cellular process that presents morphologically through vacuolisation of the cytosol, a lack of chromatin condensation and accumulation of double membrane autophagic vacuoles, known as autophagosomes. There is little phagocytosis of autophagic cells *in vivo*. The double-membraned autophagosomes that are characteristic of autophagy fuse with lysosomes to enable enzymatic degradation of the contents. For this reason autophagy is a pathway used to degrade and recycle cellular contents, including organelles and damaged or redundant

proteins and is characteristic of a pro-survival mechanism during cell stress. However, in some cases autophagy is also implicated in cell death. Autophagy can be an alternative mechanism of cell death in cells where apoptosis is unable to occur (either through caspase inhibition or perturbation of the function of Bcl-2 family members) (Tsujimoto and Shimizu, 2005).

1.5.4 Pyroptosis

Pyroptosis is a recently identified form of cell death that is seen in bacterially infected or LPS-treated macrophages, and is dependent on the presence of caspase-1. Caspase-1 can form a complex with an adapter protein, ASC, to form the "pyroptosome" which activates caspase-1 and leads to cell death with the release of the cytokines IL-1β and IL-18. For this reason pyroptosis is classified as a programmed proinflammatory mechanism of cell death (Bergsbaken et al., 2009).

1.6 Innate immune response

The innate immune system is the frontline response to acute injury, and is characterised by a generalised response to injury regardless of the stimulus. The cells involved in the innate immune response have the capability to detect, combat and resolve injury, whilst also activating the adaptive immune response through antigen presentation. The key cell types involved in the innate immune response are macrophages, dendritic cells, mast cells, NK cells, neutrophils, basophils and eosinophils. Macrophages, dendritic cells and NK cells can act as antigen presenting cells to cells of the adaptive immune system through phagocytosis of non-self macromolecules and processing to antigens. Neutrophils, basophils and eosinophils are members of the granulocyte family, named due to the presence of a high concentration of cytoplasmic granules containing oxidising enzymes, which can be used against invading pathogens during infection. The innate immune response is coordinated

through highly conserved and specialised intra- and intercellular signalling mechanisms. Together these pathways enable the activation of inflammation, removal of insult and resolution of injury. The innate immune response mediates inflammation in response to injury, regardless of the source of injury, for this reason, it is helpful to classify the resulting inflammatory response according to the presence or absence of a pathogen. This has lead to the definition of sterile and non-sterile inflammation. An innate immune response to an invading pathogen (such as a bacterial infection) is defined as non-sterile, whereas an innate immune response to non-pathogen mediated injury (such as an ADR) is defined as sterile inflammation.

1.6.1 Pathogen-associated molecular patterns (PAMPs)

Pathogen-associated molecular patterns (PAMPs) are exogenously-derived patterns including lipoproteins, lipopolysaccharide (LPS), lipoteichoic acid, flagellin, unmethylated DNA and single or double stranded RNA. PAMPs can be recognised by Toll-like receptors (TLRs) and other pattern recognition receptors (PRRs), which then initiate an innate immune response (Table 1.2) (Kumar et al., 2011). LPS is considered the prototypical PAMP and is a ligand for TLR4 (Park et al., 2009).

1.6.2 Damage-associated molecular patterns (DAMPs)

Damage-associated molecular patterns (DAMPs) are endogenous molecules released extracellularly upon cell activation, cell injury or cell death. DAMPs including high mobility group box 1 protein (HMGB1), heat shock proteins (HSPs), some S100 proteins (S100A8, S100A9, S100A12 and S100B), DNA, ATP and uric acid (which exists extracellularly as monosodium urate crystals) (Bianchi, 2007) (Table 1.2). There are no receptors exclusively for each DAMP, instead DAMPs signal through receptors with other known ligands. For instance, S100A12, S100B and HMGB1 have all been shown to act as ligands for the receptor for advanced glycation end products (RAGE), and HMGB1, HSP70, S100A8 and

S100A9 can all interact with TLRs (Bianchi, 2007). DAMP release has been shown to be associated with the progression of inflammation in APAP-induced DILI (Antoine et al., 2009b, Martin-Murphy et al., 2010).

Table.1.2. – A summary of DAMPs, PAMPs and their receptors.

DAMP	DAMP Receptors	PAMP	PAMP Receptor
HMGB1	TLR2, TLR4, TLR9, RAGE	LPS	TLR4
S100 proteins	RAGE, TLR2, TLR4	Lipoproteins	TLR2
Heat shock proteins	TLR2, TLR4	Flagellin	TLR5
Extracellular DNA	TLR9	CpG-ODN DNA	TLR9
Extracellular ATP	$P2X_7$	dsRNA	TLR3
Uric acid	NLRP3 Inflammasome, TLR2		

(Park et al., 2004, Hori et al., 1995, Ivanov et al., 2007, Maher, 2009, Foell et al., 2007, Bianchi, 2007, Chen et al., 2006, Liu-Bryan et al., 2005, Kumar et al., 2011).

1.6.3 Toll-like receptors (TLRs)

Toll-like receptors (TLRs) are a family of single membrane bound receptors that are responsible for the detection of conserved molecular sequences, either derived from exogenous (invading pathogens) or endogenous sources (from activated, injured or dead cells). There are ten human TLRs, each with the ability to recognise unique molecule patterns. During non-sterile inflammation by gram negative bacteria, TLR2 is responsible for the detection of bacterial lipoproteins and TLR4 is responsible for the detection of LPS. TLR9 is responsible for the detection of unmethylated CpG-OpN DNA and TLR5 is responsible for the detection of flagellin. Together these TLRs define the innate immune response to bacterial infection (Kumar et al., 2011). DAMPs can also signal through TLRs although the mechanistic understanding of the recognition of different DAMPs is still a major area of investigation. For example, HMGB1 can signal through TLR2, TLR4 and TLR9, through interaction with a partner molecule, which itself is a ligand for the specific TLR (e.g. HMGB1 interacts with LPS and signals through TLR4) (Hreggvidsdottir et al., 2009).

1.6.4 Nuclear Factor Kappa-light-chain-enhancer of activated B cells (NF-κB) signalling

Multiple different intracellular signalling pathways can be activated depending upon the array of membrane and intracellular receptors activated. Collectively, these pathways determine the inflammatory response to proinflammatory signals.

Inflammation-associated intracellular signalling is mediated through the transcription factor nuclear factor kappa-light-chain-enhancer of activated B cells (NF-κB). NF-κB signalling is highly regulated through post-translational modifications of the proteins that make up the signalling complexes. NF-κB itself is a heterodimer, comprising a p65 and a p50 subunit (also known as RelA and RelB respectively). In unstimulated cells, the heterodimer is sequestered in the cytoplasm by IκB, which retains NF-κB in an inactivated form. Upon cell activation (for example through TLR4 activation by LPS), an NF-κB activating complex (IKK complex) comprising IKKα, IKKβ and IKKγ (also known as NEMO) is formed which phosphorylates IκB causing a conformational change, targeting IκB for degradation and nuclear translocation of the p50/p65 heterodimer (Hayden and Ghosh, 2004, Bonizzi and Karin, 2004). Upon nuclear translocation, NF-κB can bind to promoter regions of inflammation-associated genes and cause their transcription. NF-κB signalling is pivotal in the progression of the inflammatory response, as target genes of NF-κB include TNFα and interleukins. However, NF-κB also plays an important role in apoptosis inhibition as it induces expression of Inhibitor of apoptosis protein (IAP). A schematic summary of NF-κB signalling is shown in Fig.1.3.

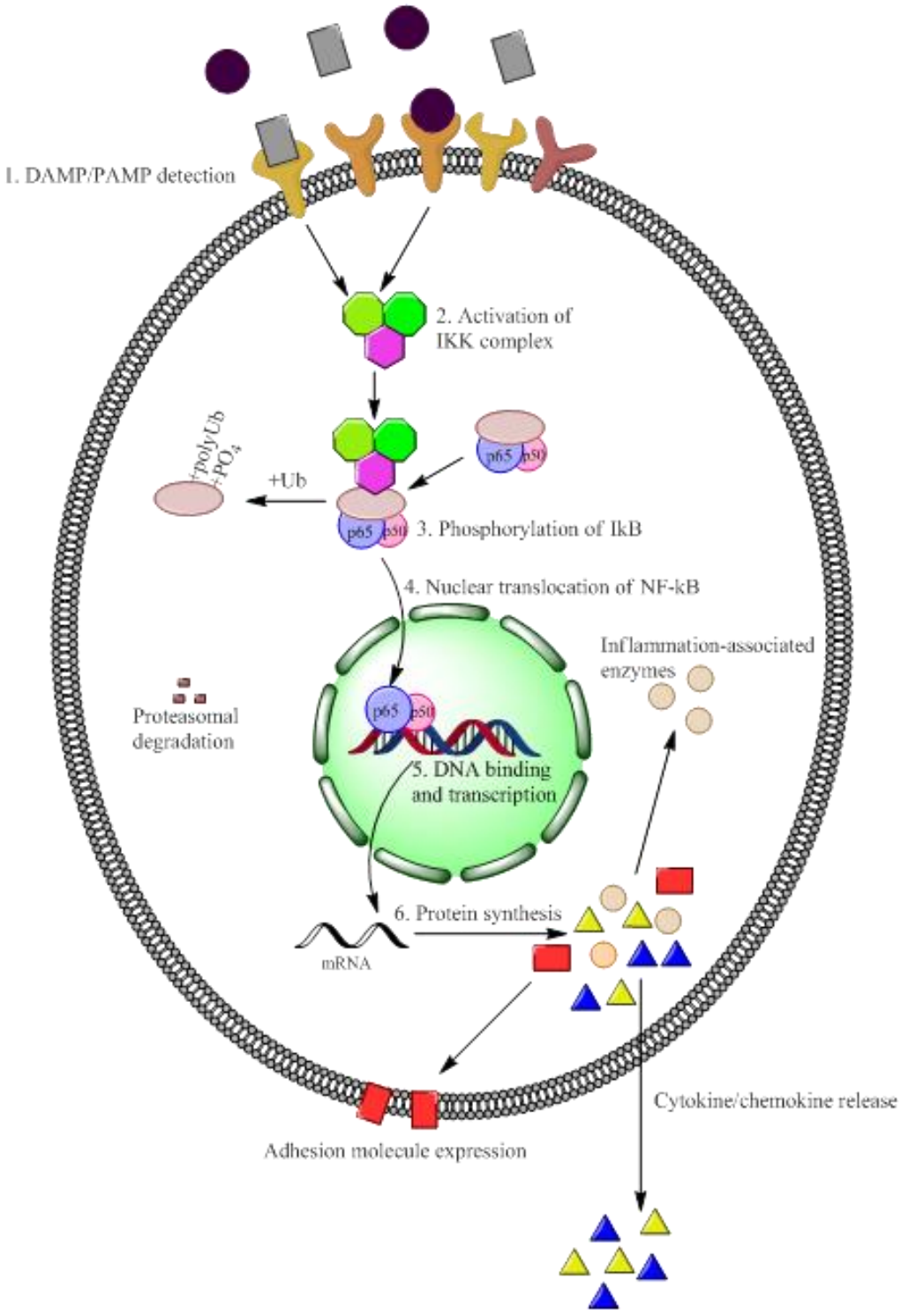

Fig.1.3 – Overview of the inflammatory pathway of classical NF-κB signalling. Adapted from (Bonizzi and Karin, 2004). Cell stimulation by endogenous or exogenous stimuli leads to the activation of NF-κB signalling. NF-κB is a multifunctional transcription factor that upregulates expression of proinflammatory proteins as well as inhibiting pro-apoptotic signals.

1.6.5 Cytokines

Amongst the inflammation-associated genes are genes encoding cytokines. Cytokines can exhibit pro- or anti-inflammatory activity, depending upon the cytokine, receptor expression on the target cells and the extracellular environment into which they are released. During inflammation, the extracellular environment dictates the role of cytokines through modulation of the redox environment. The collective interactions of multiple cytokines and chemokines can coordinate and define the inflammatory response.

Tumour necrosis factor alpha (TNFα) is generally considered to be a proinflammatory cytokine, which can be released by activated immune cells. TNFα is released rapidly upon immune cell activation and is the endogenous ligand for TNF receptor 1 and TNF receptor 2 (TNFR1 and TNFR2). TNFα signalling can stimulate proinflammatory signalling through NF-κB, however it can also result in cell apoptosis and regeneration through signalling via TNFR1. In models of DILI, TNFα has been shown to be a key coordinator of proinflammatory activity (Blazka et al., 1996).

Interleukin 6 (IL-6) is a cytokine associated with both pro- and anti-inflammatory activity. IL-6 signalling is mediated through the IL-6 receptor, which is a heterodimer complex comprised of the IL-6Rα chain (CD126) and gp130 (CD130). IL-6 binding to IL-6Rα recruits gp130 and promotes complex formation. This complex activation then initiates signal transduction. In the context of hepatotoxicity, IL-6 null mice have shown increased liver injury following toxic or drug insult (Kovalovich et al., 2000, Masubuchi et al., 2003), demonstrating the important role IL-6 plays in the resolution of liver injury.

Interleukin 1β (IL-1β) is a proinflammatory cytokine which is the ligand for the IL-1R family. There are two IL-1 receptors, designated type I and type II. The type I receptor is located to the plasma membrane and is a shared receptor which is also utilised by IL-1α. The type II

receptor is a decoy receptor as it lacks the cytoplasmic domain and functions to reduce the effects of IL-1, effectively acting as a competitive inhibitor of IL-1 signalling.

Both members of the IL-1 family exist as precursor molecules that require processing before release. IL-1β undergoes both processing and active secretion in response to inflammatory signals. IL-1β secretion is via a non-classical pathway. PAMPs can induce pro-IL-1β production and DAMPs can cause inflammasome formation, which in turn leads to activation of caspase-1 that is responsible for cleavage of pro-IL-1β into the mature cytokine. The initial PAMP signal alone is sufficient to induce IL-1β release, due to autocrine action of DAMPs released in response to the initial PAMP stimulus.

The role of IL-1β in DILI is a topic of contention, as in many scenarios IL-1β is a key propagator of the inflammatory response. However, recently a study of the role of IL-1β in AILI showed that IL-1R null mice do not show less toxicity than wildtype counterparts (Williams et al., 2010) which contradicts earlier reports (Blazka et al., 1996).

1.7 High mobility group box 1 (HMGB1)

HMGB1 is a 215 amino acid, ubiquitous, highly conserved, non-histone DNA-binding protein. It is comprised of three major regions, designated the A box, the B box and the C-terminal acidic tail (Fig.1.4). There is a 99% sequence homology between rodents and humans, demonstrating that HMGB1 is highly conserved between mammalian species and will likely lend itself to translational investigations. *Hmgb1* knockout mice die shortly after birth, demonstrating a critical role of HMGB1 in cell survival (Calogero et al., 1999). Under physiological conditions, HMGB1 shuttles between nuclear and cytosolic compartments, governed by the acetylation and methylation status of two lysine-rich nuclear localisation sequences (NLSs) in HMGB1 (Bonaldi et al., 2003, Ito et al., 2007). NLS1 is located in the A box, and NLS2 is located in the linker region between the B box and the C-terminal acidic

tail. Acetylation or methylation of the lysine residues leads to cytosolic localisation, whereas deacetylation or demethylation leads to nuclear localisation of HMGB1. A detailed review of HMGB1 post-translational modifications is given in section 1.9.7. Within the nucleus, the role of HMGB1 is to facilitate transcription through manipulation of nucleosome complexes (Sutrias-Grau et al., 1999) and loosening DNA-wrapped histone complexes (Travers, 2003). The HMG box comprises three α helices in an "L" shape configuration, which fit into the minor groove of duplex DNA (Thomas and Travers, 2001). HMGB1 can also induce bending of linear DNA through action of the B box, and the A box shows a high preference for distorted DNA, such as that distorted by UV- (Pasheva et al., 1998) or cisplatin damage (Hughes et al., 1992, Pil and Lippard, 1992). The function of cytosolic HMGB1 under non-pathological situations is unknown, however it could simply be that excess HMGB1 resides in the cytosol when the necessity for gene transcription is lower. However, during pathological scenarios, HMGB1 can be released into the extracellular environment whereby it can act as a proinflammatory cytokine. The extracellular activity of HMGB1 is governed by the mechanism of release. During necrotic cell death, HMGB1 is passively released in a hypoacetylated form into the extracellular environment where it conveys proinflammatory cytokine activity. Conversely, during early apoptosis HMGB1 is sequestered in the nucleus (Scaffidi et al., 2002). HMGB1 release has been seen during late apoptosis/secondary necrosis (Bell et al., 2006), but this HMGB1 lacks proinflammatory activity.

Fig.1.4 – Schematic structure of HMGB1. HMGB1 comprises two HMG boxes, designated A box and B box (which convey the DNA binding activity of the protein) and a C-terminal acidic tail (comprised solely of glutamate and aspartate residues) joined together by linker regions. HMGB1 contains two lysine-rich NLSs: NLS1 is located in the A box and NLS2 is located in the linker region between the B box and the acidic tail.

In addition to being released upon cell death in a hypoacetylated form, HMGB1 can be actively secreted from activated immune cells in a hyperacetylated form. Acetylation of key lysine residues within the lysine-rich NLSs of HMGB1 results in cytoplasmic translocation of HMGB1 and directs HMGB1 for secretion via a non-classical vesicle mediated pathway. Hyperacetylated HMGB1 released from activated immune cells has cytokine stimulating activity. Extracellular HMGB1 has been shown to bind to a multitude of receptors, either directly or through formation of proinflammatory complexes with PAMPs. HMGB1 receptors include multiple TLRs: TLR2, TLR4, TLR9 and RAGE. These HMGB1 receptors all have other ligands: TLR2 is the receptor for many bacterial, viral and fungal proteins, including bacterial lipoproteins. TLR4 binds to lipopolysaccharide (LPS), TLR9 binds to extracellular DNA. Proinflammatory HMGB1-partner molecule complexes signal through the partner molecule receptor. For instance, HMGB1-LPS complexes bind to TLR4. The binding of HMGB1-containing proinflammatory complexes to receptors leads to synergistic proinflammatory activity compared to HMGB1 or the partner molecule alone (Hreggvidsdottir et al., 2009). The intracellular mechanisms behind the production of a synergistic inflammatory response to these HMGB1-partner molecule complexes are currently unknown and are an area of ongoing research.

1.8 HMGB1-targeting therapeutic interventions

Following the identification of a role for HMGB1 as a mediator of inflammation, recent focus has been on investigating a range of different strategies to inhibit HMGB1 release and function. These include both exogenous agents comprising anti-HMGB1 antibodies, small molecule inhibitors of HMGB1 (both naturally occurring and chemically synthesised) and endogenous peptides.

1.8.1 Anti-HMGB1 antibodies

Anti-HMGB1 antibodies have been developed for a range of species, and with epitopes in a range of regions within HMGB1. These antibodies have been tested in a range of *in vitro* systems and rodent models of inflammation (Table.1.3). These models show that anti-HMGB1 antibody treatment can prevent extracellular HMGB1 function and the development of inflammatory disease situations through the inhibition of normal extracellular HMGB1 signalling. Anti-HMGB1 antibodies have been shown to be effective in both acute and chronic conditions.

Table.1.3. – Applications of anti-HMGB1 antibodies

Anti-HMGB1 antibody	Inflammatory model	References
Rabbit polyclonal IgG	Sepsis (LPS)	(Wang et al., 1999)
Rabbit polyclonal IgG (B box binding)	Arthritis	(Kokkola et al., 2003)
	Sepsis (CLP)	(Yang et al., 2004b)
	Hemorrhagic shock	(Yang et al., 2006)
Chicken polyclonal IgY	Sepsis (CLP)	(Suda et al., 2006)
	Acute pancreatitis	(Sawa et al., 2006)
	AILI	(Antoine et al., 2010)
	Acute liver failure (d-galactosamine)	(Takano et al., 2010)
Rat monoclonal IgG2a (C-terminal binding)	Brain ischemia	(Liu et al., 2007)

LPS = lipopolysaccharide, CLP = cecal ligation and puncture, AILI = acetaminophen-induced liver injury

Recombinant A box protein has also be shown to be effective at preventing extracellular HMGB1 function in a rodent model of arthritis (Kokkola et al., 2003) and can bind to RAGE, competing with full-length HMGB1 for target cell signalling. Additionally, it is known that A box can bind to HMGB1 itself, and suppress HMGB1 signalling through disablement of HMGB1-receptor binding (Li et al., 2003).

1.8.2 Other HMGB1-targeting therapeutics

Other HMGB1-targeting therapeutics include chemically synthesised compounds, plant/herbal extracts and endogenous peptides (Table.1.4)

Chemical inhibitors

Ethyl pyruvate was one the first compounds identified that was able to prevent release of HMGB1, and protect from lethality in a sepsis model (Ulloa et al., 2002). Ethyl pyruvate prevents nuclear-cytosolic translocation of HMGB1, a pivotal step in HMGB1 release (Dave et al., 2009). Recently, other compounds such as gold sodium thiomalate, dexamethasone, acteoside, forsythoside B, Tanshinone IIA and atorvastatin have all proved effective in attenuating HMGB1-mediated injury in a range of models. (Wang et al., 2010b, Schierbeck et al., 2010, Lee et al., 2004, Wang et al., 2010a, Jiang et al., 2010)

Naturally occurring small molecule inhibitors

Natural inhibitors of HMGB1 include glycyrrhizin (which occurs in liquorice), quercetin (a plant flavonoid) and a range of Chinese herbal medicines. Glycyrrhizin acts by binding directly to both HMG boxes of HMGB1, preventing signalling of extracellular HMGB1 (Mollica et al., 2007). Quercetin prevents macrophage-derived HMGB1 release *in vitro* and resulted in a reduction in circulating levels of HMGB1 in an *in vivo* model of endotoxemia (Tang et al., 2009). Chinese medicinal compounds have been shown to successfully prevent lethality in sepsis models (Wang et al., 2006, Li et al., 2007a, Li et al., 2007b).

Endogenous inhibitors

In addition to exogenous inhibitors of HMGB1, there are endogenous peptides or mechanisms that attenuate HMGB1-mediated inflammatory signalling. These include the hormones ghrelin and vasoactive intestinal peptide (VIP) and the anti-coagulation protein thrombomodulin. Ghrelin prevents HMGB1 release and protects against sepsis (Chorny et al., 2008) and radiation damage (Jacob et al., 2010). Cholinergic agents such as nicotine can

inhibit HMGB1 release through vagus nerve stimulation, leading to improved survival in a model of sepsis (Wang et al., 2004).

Table.1.4 - Non-antibody anti-HMGB1 targeting therapeutics

Exogenous HMGB1 Inhibiting Agents	
Agent	**References**
HMGB1 A box protein	(Yang et al., 2004a, Li et al., 2003, Kokkola et al., 2003)
Ethyl pyruvate	(Ulloa et al., 2002, Dave et al., 2009)
Glycyrrhizin (derived from liquorice)	(Mollica et al., 2007)
Atorvastatin	(Wang et al., 2010b)
Tanshinone IIA	(Wang et al., 2010a)
Quercetin (plant flavonoid)	(Tang et al., 2009)
Gold sodium thiomalate	(Schierbeck et al., 2010)
Dexamethasone	(Schierbeck et al., 2010)
Forsythoside B	(Jiang et al., 2010)
Acteoside	(Lee et al., 2004)
Chinese medicinal herbs	
Angelica sinenis (Danggui)	(Wang et al., 2006)
Camellia sinesis (Green tea)	(Li et al., 2007a)
Salvia militorrhiza (Danshen)	(Li et al., 2007b)
Endogenous HMGB1 Inhibiting Agents	
Ghrelin	(Chorny et al., 2008, Jacob et al., 2010)
Vasoactive intestinal peptide (VIP)	(Chorny and Delgado, 2008, Luo et al., 2009)
Thrombomodulin	(Abeyama et al., 2005)
Pituitary adenylate cyclise activating protein (PACAP)	(Tang et al., 2008)
Cholinergic agents	(Wang et al., 2004)

1.9 Post-translational modifications of proteins

Post-translational modifications (PTMs) are enzyme-mediated chemical alterations to a protein that occur following translation of the mRNA to protein at ribosomes. These chemical alterations can vastly alter the chemical and structural properties of the protein, and hence can alter the functional properties, localisation and fate of the protein. There is a wide range of PTMs that can be applied to a protein, depending upon the amino acids present within said protein. Collectively PTMs have a diverse effect on the proteins expressed within a cell. The balance between these different PTMs is vital for the maintenance of signalling pathways pivotal to cell function and survival.

1.9.1 Phosphorylation

The most-heavily studied PTM is phosphorylation, with around 200,000 peer reviewed publications available. Phosphorylation involves the addition of a phosphate group (PO_4^{3-}) to a protein, usually substitution for a hydrogen atom, which is then eliminated as a water molecule. Phosphorylation is mediated by enzymes with kinase activity and conversely dephosphorylation is mediated by phosphatase enzymes. Serine, threonine and tyrosine are the most commonly phosphorylated amino acids, but there are rare occurrences of histidine and aspartate residues. Commonly, phosphorylation is associated with a change in function of the target protein from an off-to-on or conversely on-to-off configuration. HMGB1 is subject to phosphorylation, that causes nucleocytoplasmic translocation, but the specific residues have not yet been defined (Youn and Shin, 2006).

1.9.2 Acetylation

Acetylation is the addition of an acetyl ($-CH_2CH_3$) group to an amino acid residue. Acetylation reactions are substitutions of an acetyl group for an active hydrogen, resulting in the formation of an acetoxy group. The most commonly acetylated amino acid is lysine, which is acetylated by acetyltransferase enzymes in presence of acetyl-coenzyme A, which

acts as the acetyl group donor. Conversely, deacetylation, mediated by deacetylases can reverse the effects of acetylation. Histone acetylation has been widely studied in the context of the regulation of gene regulation. Histone acetyltransferases (HATs) are opposed by histone deacetylases (HDACs) although these enzymes do not exclusively acetylate or deacetylate histones. Acetylation of lysine residues within the NLSs of HMGB1 are important for the nucleocytosolic shuttling of HMGB1 in immune cells (Bonaldi et al., 2003).

1.9.3 Methylation

Methylation is the addition of a methyl ($-CH_3$) group to an amino acid residue. Methylation can occur on arginine or lysine residues, and is catalysed by methyltransferase enzymes. Histone methylation is a fundamental aspect of gene regulation and expression. Methylation of HMGB1 has been observed, specifically in neutrophils (Ito et al., 2007), suggesting cell type-specific post-translational modification of proteins.

1.9.4 Oxidation

The balance between oxidation and reduction (redox) of cysteine residues can greatly determine the function and expression of a protein. Oxidative PTMs can be reversible or irreversible, with reversible modifications generally associated with physiological situations, whereas irreversible oxidative PTMs are generally associated with pathological scenario (Spickett and Pitt, 2012). Oxidases and reductases are enzymes with opposing functions that can, amongst a range of functions, catalyse the oxidation and reduction of proteins respectively. Cysteine and methionine residues have sulphur-containing side chains, and as such are the most readily oxidised residues. Oxidation of these sulphur-containing residues can cause conformational changes in the structure of the protein, and result in modulation of protein expression, function or localisation. The oxidising agent can also determine the type of oxidative PTM, with reactive oxygen species such as hydroxyl radicals ($OH\cdot$), hydrogen peroxide (H_2O_2) and superoxide (O_2^-), reactive nitrogen species such as nitric

oxide (NO), nitrogen dioxide (NO_2) and peroxynitrite ($ONOO^-$) and reactive chlorine species such as hypochlorous acid (HOCl) being produced by activated phagocytes and reacting with proteins in oxidation, nitrogenation or chlorination reactions. The oxidisation of a cysteine residue is determined by the pKa of the residue, which is influenced by the local amino acid environment and the structural accessibility of the cysteine. Cysteines in HMGB1 are subject to redox regulation, which appear to affect extracellular function (Kazama et al., 2008).

1.9.5 Ubiquitination

Ubiquitination is the conjugation of the 8.5kDa protein ubiquitin to a target protein, in an ATP-dependent process. The target protein may be directed for ubiquitination by other PTMs or due to misfolding. Ubiquitin is a 76 amino acid protein, and it is the C-terminal glycine residue that becomes conjugated to (primarily) lysine residues in the target protein. Ubiquitin itself can also be ubiquitinated, leading to polyubiquitin chain formation on the target protein. Ubiquitination is mediated by a highly target-specific multi-step enzymatic cascade; usually comprising three enzymes from families designated E1, E2 and E3 (Ciechanover, 1998) (Fig.1.5). E1 enzymes are ubiquitin-activating enzymes which form a high energy thioester intermediate with ubiquitin in an ATP-dependent reaction. In humans, there are known to be two E1 enzymes (UBE1, UBE1L2) which catalyse the activation of ubiquitin. Following ubiquitin activation, the E1-ubiquitin complex reacts with a specific ubiquitin conjugating enzyme (E2) (of which in humans there are at least 38 E2 enzymes (Ciechanover, 1998)) that catalyse the transfer of the ubiquitin to the E2 enzyme, forming another thioester intermediate. E3 enzymes are responsible for the binding of the target protein and facilitating the transfer of ubiquitin from the E2 enzyme onto the target protein. E3 enzymes are classified into one of three groups, HECT-domain, U-box or RING finger, depending upon the homology and mechanism of action (Komander, 2009,

Hatakeyama and Nakayama, 2003). HECT-domain E3s contain a catalytic cysteine residue and interact directly with the substrate protein to conjugate ubiquitin. RING finger E3s instead bring together the E2 enzyme and the substrate protein and acts as a scaffold protein in the conjugation. In some cases proteins have been identified that catalyse the activity of E3 to form polyubiquitin chains, these have been designated as having E4 activity (Koegl et al., 1999, Shi et al., 2009). The diverse number of combinations of E1, E2 and E3 enzymes leads to a highly specific mechanism of regulation of protein expression through ubiquitination (Ciechanover, 1998, Komander, 2009).

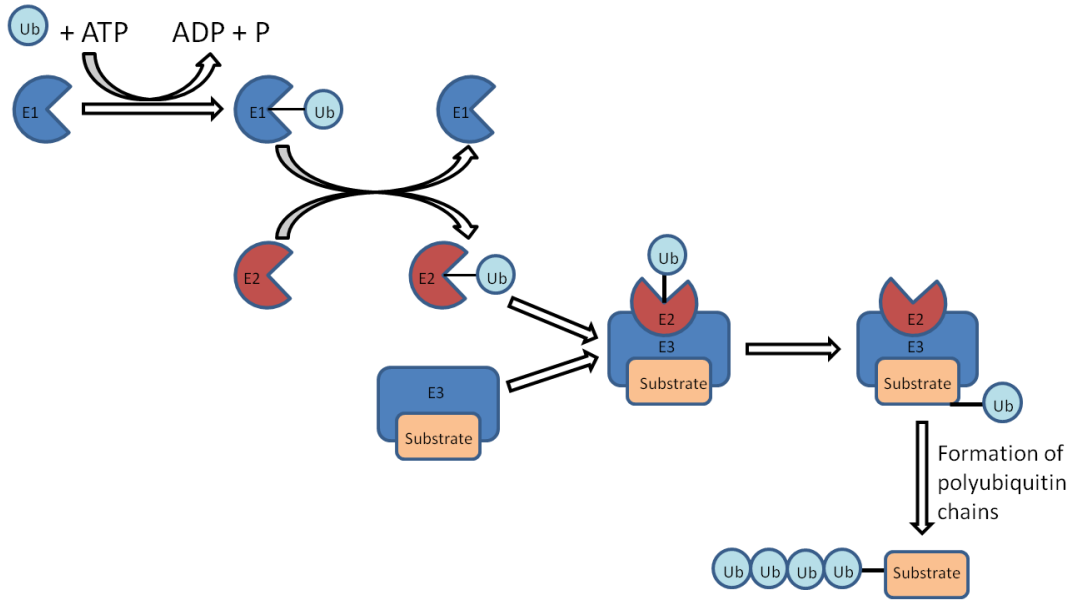

Fig.1.5 – The ubiquitination cascade. Ubiquitination is an ATP-dependent process. Ubiquitin is activated by E1 enzymes, which then transfer the activated ubiquitin molecule to E2 enzymes, E3 enzymes then facilitate the transfer of ubiquitin to the target protein. Polyubiquitination can occur sequentially, through conjugation of ubiquitin to further ubiquitin molecules. The linkages between the ubiquitin molecules determine the fate of the polyubiquitinated protein.

The fates of ubiquitinated proteins are varied, and polyubiquitin chains formed between each lysine residue in ubiquitin have been observed. The conjugated lysines in a polyubiquitin chain define the subsequent targeting of the polyubiquitinated protein

(Komander, 2009). Classically, polyubiquitination via lysine 48 leads to targeting of the target protein to the 26S proteasome for proteolytic degradation (Ciechanover, 1998).

1.9.6 Cross-talk between PTMs

PTMs can often direct the target protein for further PTMs. For example, oxidation can target proteins for ubiquitination, such as in the case of IRP2 (Yamanaka et al., 2003), and phosphorylation can also target for ubiquitination as is seen with IκB (Chen et al., 1995, Alkalay et al., 1995). Additionally, PTMs can crosstalk with each other to direct protein responses. Lysine residues are the target of many PTMs, however these PTMs are mutually exclusive and so acetylation precludes ubiquitination or methylation and vice-versa (Kim et al., 2006). This mutual exclusivity of enzyme-linked lysine modifications can tightly regulate the function and localisation of the protein, and play an integral role in signalling pathways and the maintenance of homeostasis within a cell.

1.9.7 Roles of PTMs on HMGB1 structure and function

HMGB1 is subject to many PTMs that collectively can govern HMGB1 expression and function (Zhang and Wang, 2008) (Fig.1.6). Oxidation of cysteine 106 in HMGB1 results in loss of the immunostimulatory activity of HMGB1 (Kazama et al., 2008) and may be due to a conformational change in the structure of HMGB1. Oxidation of the thiol groups of cysteine 23 and cysteine 45 can lead to the formation of a disulphide bond between the two residues, leading to a conformational change in the structure of HMGB1 (Sahu et al., 2008). Acetylation of lysine residues within NLS1 and NLS2 of HMGB1 can direct HMGB1 for nuclear→cytosolic translocation and active release (Bonaldi et al., 2003). Similarly, phosphorylation of key serine residues in the NLSs can also direct HMGB1 for nuclear→cytosolic translocation and subsequent release (Youn and Shin, 2006). Additionally, a single methylation of lysine 42 was able to induce nuclear→cytosolic translocation of HMGB1 in neutrophils (Ito et al., 2007). Acetylation, phosphorylation and

methylation of HMGB1 are all reversible processes, whereas caspase-dependent oxidation of cysteine residues within HMGB1 during apoptosis has been show to be an irreversible modification, potentially due to formation of sulphonate ($-SO_3^-$) group on the cysteine residue 106.

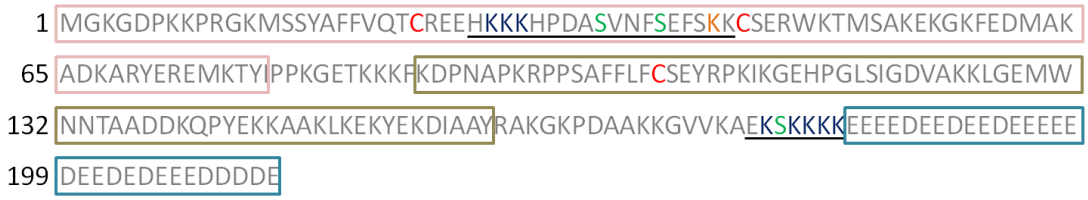

Fig.1.6 – Post-translational modifications of HMGB1. HMGB1 is subject to many post-translational modifications, notably oxidation of conserved cysteine residues 23, 45 and 106 (red), methylation of lysine 42 (orange), phosphorylation of serine residues (green) and acetylation of lysine residues (dark blue). A box, B box and C-terminal tail are defined by coloured boxes (pink, bronze and light blue respectively). NLSs are indicated by the underlined regions. Adapted from (Harris et al., 2012, Zhang and Wang, 2008).

1.10 Current understanding of HMGB1 in liver injury

HMGB1 is released from necrotic hepatocytes (Antoine et al., 2009b, Martin-Murphy et al., 2010) and in a model of AILI both hypo- and hyperacetylated HMGB1 being detectable at 10hr post-APAP (530mg/kg), indicating both necrosis and the activation of immune cells (Antoine et al., 2009b). Serum HMGB1 shows promise as a circulating biomarker of AILI, with levels of hypoacetylated HMGB1 strongly correlating with the histological evidence of AILI in mice, and also proving to be more sensitive than ALT (Antoine et al., 2009b).

Recent studies have also shown that the extracellular activity of HMGB1 is dependent on the oxidation state of the three cysteine residues within HMGB1, although the precise regulation of function by redox is unknown. These residues (C23, C45 and C106) are highly conserved and oxidisable and have been shown to be essential for determining the inflammatory activity of HMGB1. A very recent study has shown the critical role of intracellular ATP in the caspase-dependent oxidation of HMGB1 during apoptosis. In

starved mice compared with fed mice, basal ATP levels are depleted, thus inhibiting the ATP-dependent process of caspase-activation, and hence apoptosis and caspase-dependent oxidation of HMGB1. In the absence of apoptosis, only necrotic cell death is observed, and a much greater increase in inflammatory cell infiltration and increased inflammatory response is seen. To support the key role of HMGB1 in coordinating the inflammatory response, an anti-HMGB1 antibody reduced the inflammatory response (Antoine et al., 2010).

In addition to AILI, HMGB1 may have potential as a biomarker of all forms of liver injury, such as ischemia/reperfusion injury (Tsung et al., 2005, Watanabe et al., 2005) and chronic injury conditions such as alcoholic liver disease (Ge et al., 2014).

The immune cell exclusivity of acetylated HMGB1 provides insight into the mechanism of release of serum HMGB1, and together with redox status is indicative of the mechanisms involved in the inflammatory response. PTMs regulate the function and intracellular expression profile of HMGB1. However, the precise functional definitions of the effects of HMGB1 oxidation are unknown at the start of this thesis. Additionally, other, currently undiscovered PTMs of HMGB1 may exist that may play a crucial role in the regulation, function and dynamics of the protein.

1.11 Aims of thesis

HMGB1 has been widely investigated in a range of *in vitro* and *in* vivo models of inflammatory conditions as a potential biomarker of cellular injury and innate immune activation. However mechanistic understanding of how HMGB1 contributes to inflammatory processes is an incomplete and exciting field of study. The aims of this thesis are to investigate different aspects of HMGB1 regulation in the context of DILI, through anti-HMGB1 antibody treatment and HMGB1 PTMs.

Anti-HMGB1 antibody treatments have been utilised in a range of inflammatory models, including DILI, ischaemia-reperfusion injury and arthritis. Further examination of the translational potential and the mechanism of action of anti-HMGB1 antibodies will enhance our knowledge and potentially lead to clinical trials of anti-HMGB1 antibodies.

HMGB1 is subject to many PTMs that could govern its expression, localisation and functions. Subsequently, HMGB1 PTMs could play a significant role in the coordination and propagation of innate immune responses during different forms of cell death and cell activation. Greater knowledge of the function of HMGB1 PTMs is required and could be used to investigate ADRs, with particular potential to improve the diagnosis and treatment of DILI.

The aims of this thesis are to address the following hypotheses:

1. Aim: To determine the effects of a chimeric anti-HMGB1 antibody (h2G7) in an *in vivo* model of APAP-induced liver injury (AILI). Hypothesis: h2G7 can attenuate proinflammatory signalling and limit HMGB1-mediated injury in a preclinical animal model of AILI.

2. Aim: To determine the mechanism of action of the anti-HMGB1 antibody, h2G7, in an *in vivo* model of AILI. Hypothesis: h2G7 attenuation of proinflammatory signalling and HMGB1-mediated injury in a preclinical animal model of AILI is through neutralisation of HMGB1 signalling by HMGB1 binding and elimination, but may have complement or Fcγ receptor-mediated mechanisms.

3. Aim: To define the role of redox of cysteine residues in the proinflammatory capability of extracellular HMGB1. Hypothesis: The proinflammatory activity of HMGB1 is dependent upon the redox status of the three conserved cysteine

residues of HMGB1. HMGB1 will undergo redox-dependent modulation of function in order to regulate the innate immune response to cellular injury.

4. Aim: To define HMGB1 PTMs and the regulation of HMGB1 localisation and expression during apoptotic cell death. Hypothesis: Apoptosis-dependent oxidation leads to the modulation of HMGB1 localisation and function, and also subsequent PTMs of HMGB1 that may have a role in signalling.

The above aims intend to provide greater insight into the regulation of HMGB1 expression and function, with the view to gaining a greater understanding of the mechanistic controls behind this emerging novel biomarker of cellular injury and immune activation. This knowledge could then provide greater understanding of the role of HMGB1 in the coordination of DILI and potentially direct therapeutic explorations to tackle a prevalent clinical issue.

Chapter Two

Investigating the effects of a chimeric anti-HMGB1 antibody on acetaminophen-induced liver injury

CONTENTS

2.1 Introduction

Antibodies (or immunoglobulins) are glycoproteins of approximately 150kDa responsible for the highly specific binding of molecular structures called antigens. Within an antigen, a specific molecular sequence known as the epitope is the precise recognition target for the antibody. Antibodies are comprised of two heavy and two light chains, arranged in a Y-shaped configuration, held together by disulphide bonds (Fig.2.1) (Woof and Burton, 2004). Mammalian antibodies are classified into fives isotypes (IgA, IgD, IgE, IgG and IgM) according to their heavy chain type (α, δ, ε, γ or μ). Isotypes vary in functional localisation, biological properties and types of antigen recognised. Heavy chains contain two regions, the constant region and the variable region. α, δ and γ heavy chains have constant regions comprised of three Ig domains, whereas ε and μ constant regions consist of four Ig chains (Woof and Burton, 2004). Variable regions are comprised of one Ig domain, that is identical between all antibodies produced by one individual B cell, but vary between different B cells. Light chains contain one variable and one constant domain, and are either of κ or λ chain type. Both light chains on the same antibody molecule are always of the same type (κ or λ) (Woof and Burton, 2004). The arms of the "Y" are known as the Fab (fragment, antigen-binding) regions, and contain the variable region and one Ig domain of the constant region of the heavy chain, and the entire light chain. The epitope-recognising region of the Fab is called the complementarity determining region (CDR) and it is made up of the six variable loops of the β-strands (three each from the heavy and light chains) from within the variable regions. The base of the antibody is known as the Fc (fragment, crystallisable) region and is comprised of the two or three Ig domains of the heavy chains that are not bound to the light chains (Woof and Burton, 2004). The Fc region can bind to Fc receptors (FcγR) or other immune molecules such as complement proteins, and mediate immune responses in the presence of antigen. Antibody isotypes can be further divided into subclasses, based upon differences in the structure of the hinge region between the Fab and Fc regions. Human IgG

has four subclasses, designated IgG1-4, whereas mouse IgG has four subclasses designated IgG1, IgG2a, IgG2b and IgG3 (Woof and Burton, 2004). Subclasses also differ in their abundance in plasma and their differing complement activating and FcγR binding properties.

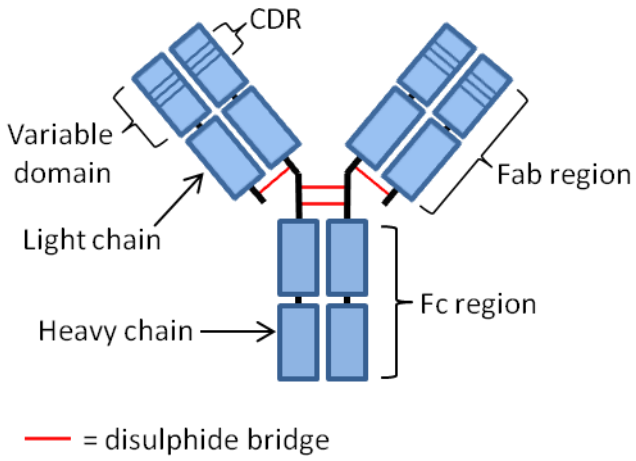

Fig.2.1 – A schematic representation of an antibody. Antibodies are glycoproteins comprised of four peptide chains (two heavy and two light) linked by disulphide bridges. The hinge regions allow some flexibility in the antibody to facilitate antigen binding. Two antigen binding sites (defined by the CDRs) are present within each antibody molecule, although this does not necessarily mean that two separate antigen molecules will be bound by one antibody molecule as two binding sites may be present on one antigen molecule. Figure modified from (Carter, 2001)

Non-human antibodies are effective tools for exploring the role of target proteins in preclinical models, however due to species differences they are generally unsuitable for clinical application. In order for an antibody to be tolerated by a patient, modification of the antibody with human subunits is required. Subsequently, chimeric or humanized antibodies targeting other cytokines have been developed. At least 25 antibody therapies have been approved for use in human disease, with many more under clinical development (Chan and Carter, 2010).

The simplest form of adaption of an antibody for clinical use is chimerisation. Chimeric antibodies possess the variable domains of the non-human antibody (usually mouse), including the CDRs, conjugated to the constant domains from a human antibody. Chimeric antibodies have been used successfully in clinical inflammatory diseases, for example anti-TNFα monoclonal antibodies (such as infliximab) are approved for use for the treatment of Crohn's disease and rheumatoid arthritis (Elliott et al., 1994). However, despite the effectiveness of chimeric antibodies, there is still non-human protein within the antibody. This can, in cases, be recognised by the patient immune system, leading to an anti-chimeric immune response, and toxicity. Humanized antibodies are more human than chimeric antibodies as they only utilise the CDRs from the non-human antibody, cloned into the human antibody backbone, thus removing almost all potentially immunogenic regions. However the development of humanized antibodies requires X-ray crystallography in order to accurately define the CDR-encoding residues. A summary of clinically useful antibodies is shown in Fig.2.2.

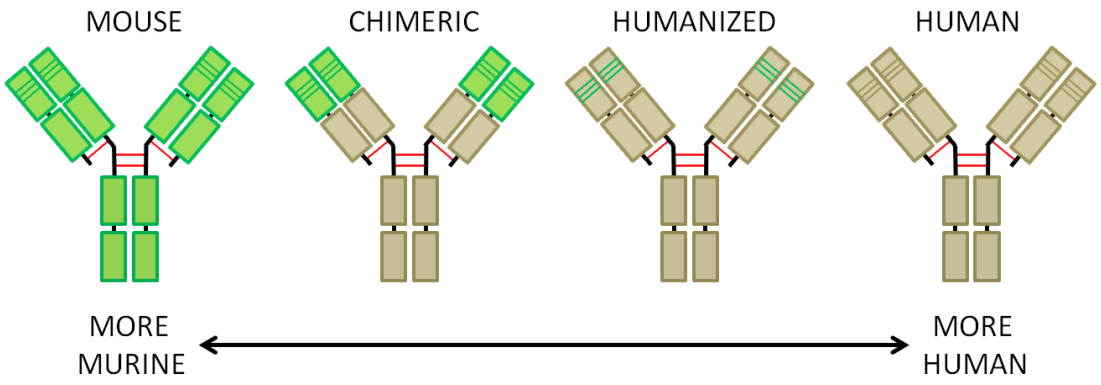

Fig.2.2 – The differences in protein domains between murine, chimeric, humanized and human antibodies. Chimeric and humanized antibodies both have their constant domains from the human antibody. Humanized antibodies are more closely related to human antibodies than chimeric antibodies, as only the CDRs are taken from the non-human (in this case mouse) antibody. However, chimeric antibodies do have clinical utility. Figure modified from (Carter, 2001).

Acetaminophen (APAP) overdose is the most common cause of drug-induced liver injury (DILI), causing around a third of acute liver failure cases in the US (Ostapowicz et al., 2002). In the UK, APAP-induced liver injury (AILI) is responsible 20-40 liver transplants and more than 200 deaths each year (Antoine et al., 2012, Hawton et al., 1995) and in England alone was responsible for 38,000 emergency hospital admissions in the financial year of 2010-11 (Antoine et al., 2014).

AILI is well characterised in animal studies and replicates the human pathogenesis (Antoine et al., 2014). In AILI, hepatocyte necrosis is the predominant form of cell death, with little, but some, apoptosis seen, depending upon the ATP-status of the hepatocytes (Antoine et al., 2010).

HMGB1 is a key coordinator and modulator of the inflammatory response in AILI (Antoine et al., 2010), as it is responsible for the recruitment and activation of innate immune cells. HMGB1 acts as an important driver of the proinflammatory response through the induction of cytokine release, and serum HMGB1 has been shown to correlate with the development and prognosis of AILI in man (Antoine et al., 2012). Hence therapeutics that target HMGB1 may have the potential to be extremely useful in the control of inflammation, both during AILI and other inflammatory conditions.

A range of HMGB1-targeting therapeutics have been explored in preclinical models of inflammatory conditions (Lu et al., 2014, Chen et al., 2013, Musumeci et al., 2014). These therapeutics act via inhibition of HMGB1 release, function or both. Anti-HMGB1 antibodies are a widely researched class of therapeutics (Table.2.1). One such anti-HMGB1 antibody therapy is the monoclonal antibody 2G7

The 2G7 antibody (Merck Serono) is a mouse monoclonal IgG2b antibody which binds to the A box of HMGB1 with an epitope between residues 53-63 (SAKEKGKFEDM) (Wahamaa et al., 2007) and recognises human, bovine and murine HMGB1, but not HMGB2. 2G7 has been used to successfully attenuate AILI in a CD-1 murine model (Antoine DJ, unpublished

data) and two experimental models of arthritis (Schierbeck et al., 2011). 2G7 has also been used *in vitro* to inhibit TNFα release from activated immune cells (Yang et al., 2010).

Table.2.1 – Anti-HMGB1 therapeutic strategies in preclinical models

Anti-HMGB1 antibody	Inflammatory model	References
Rabbit polyclonal IgG	Sepsis (LPS)	(Wang et al., 1999)
Rabbit polyclonal IgG (B box binding)	Arthritis	(Kokkola et al., 2003)
	Sepsis (CLP)	(Yang et al., 2004)
	Hemorrhagic shock	(Yang et al., 2006)
Chicken polyclonal IgY	Sepsis (CLP)	(Suda et al., 2006)
	Acute pancreatitis	(Sawa et al., 2006)
	AILI	(Antoine et al., 2010)
	Acute liver failure (d-galactosamine)	(Takano et al., 2010)
Rat monoclonal IgG2a (C-terminal binding)	Brain ischemia	(Liu et al., 2007)
	Blood-brain-barrier dysfunction	(Zhang et al., 2011)
	Atherosclerosis	(Kanellakis et al., 2011)
Mouse monoclonal IgG2b (2G7, A box binding)	AILI	(Antoine, unpublished data)
	Arthritis	(Schierbeck et al., 2011)
Polyclonal, species not disclosed (Shino-test)	Crush injury	(Shimazaki et al., 2012)
Rabbit monoclonal (Abcam)	Acute-on-chronic liver failure	(Li et al., 2013)
Mouse monoclonal (Abnova)	Autoimmune encephalomyelitis	(Uzawa et al., 2013)
Rabbit polyclonal IgG	Acute lung injury	(Entezari et al., 2014)

LPS= lipopolysaccharide, CLP = cecal ligation and puncture

As a result of the successful inhibition of HMGB1 in both *in vitro* and *in vivo* models, Merck Serono and the Karolinska Institutet have agreed to investigate the production and testing of a chimeric form of 2G7, designated h2G7. This is the next step towards the development of an anti-HMGB1 antibody with clinical therapeutic potential.

2.1.1 Aims

The aims of the work in this chapter were to:

- Assess the protective effect of h2G7, a chimeric IgG1 version of the 2G7 antibody, in a murine model of AILI. This work will be carried out in parallel, and in comparison, with the murine 2G7 counterpart.
- Identify the lowest effective dose of h2G7 in the murine AILI model.

2.2 Materials and Methods

2.2.1 Materials

Bio-Rad Protein Assay Dye Reagent, Precision Plus Kaleidoscope Standards (molecular weight markers) and non-fat milk was purchased from Bio-Rad Laboratories Ltd (Hemel Hempstead, UK). HRP-coupled Goat anti-human IgG Fc region was purchased from Bethyl Laboratories (Montgomery, Texas, USA). Amersham Hybond ECL membrane and Amersham Hyperfilm ECL were purchased from GE Healthcare (Little Chalfont, UK). Western Lightning Plus-ECL was purchased from Perkin Elmer (Beaconsfield, UK). All other materials were purchased from Sigma-Aldrich (Poole, UK) or Fisher Scientific (Loughborough, UK) unless otherwise indicated.

2.2.2 Experimental animals

The protocols described were undertaken in accordance with criteria outlines in a licence granted under the Animals (Scientific Procedures) Act 1986 and approved by the University of Liverpool Animal Ethics Committee. 8 week old male C57BL/6J mice (20-25g) were purchased from Charles River laboratories and had a 5-day acclimatisation period prior to experimentation. Animals were also maintained in a 12hr light/dark cycle with free access to food and water.

2.2.3 Antibody Expression and Purification

Mouse IgG2b monoclonal anti-HMGB1 antibody (2G7), chimeric human IgG1 monoclonal anti-HMGB1 antibody (h2G7) and monoclonal isotype-matched (IgG1) human anti-tetanus toxin antibody (E2) were expressed and purified by Peter Lundbäck (Karolinska Institutet) as previously described (Wahamaa et al., 2007). 2G7 antibody was produced by mouse B-cell hybridoma. h2G7 was produced by inserting the Fab-encoding segments of 2G7-encoding DNA into human IgG1 antibody-encoding DNA and transfected into “Freestyle” HEK293

cells. The same approach was taken for E2. Following successful transfection, cell culture supernatants were collected for 14 days. Antibodies were purified from the supernatants using Protein G.

2.2.4 Animal dosing regime

Male C57BL/6J mice (20-25g, *n=6* per group) were fasted overnight for 16hr, to reduce basal ATP levels. The following morning animals were administered a single intraperitoneal (*i.p.*) injection of APAP (530mg/kg) in 0.9% saline, or vehicle (0.9% saline) control. 2hr post-APAP, animals were then administered a single *i.p.* injection (on the opposite side) of antibody (E2, 2G7, h2G7) at the doses indicated or PBS. At 10hr post-APAP, mice were sacrificed using a rising concentration of CO_2 and blood was taken by cardiac puncture. Serum was isolated from blood by allowing the blood to clot at room temperature for 30min and centrifugation (1500*g*, 10min, 4°C) before aliquoting and storage at -80°C. Liver and spleen samples were snap frozen in liquid nitrogen and stored at -80°C, or fixed in 4% PFA. Samples fixed in 4% PFA overnight were then washed with PBS and transferred into 70% EtOH, prior to paraffin embedding.

2.2.5 Determination of total hepatic glutathione (GSH)

Total hepatic GSH was determined as described previously (Williams et al., 2007). 30-50mg of liver was weighed and homogenised in 800µL of GSH stock buffer (143mM NaH_2PO_4, 6.3mM EDTA, pH 7.4) supplemented with 200µL of 6.5% (w/v) SSA. Liver homogenates were incubated on ice for 10min to precipitate out proteins. Homogenates were centrifuged (18400*g*, 5min, 4°C) and the supernatants were transferred to a new eppendorf tube and stored at -80°C until analysis. Protein pellets were dissolved in 1M NaOH at 60°C for 1hr and also stored at -80°C. The protein content of protein samples was determined using Bio-Rad protein assay at 570nm (Bradford, 1976). GSH content was measured spectromically (at 412nm) by kinetic reaction between total GSH and glutathione reductase

(Vandeputte et al., 1994) on a MRX microtiter-plate reader with Max Revelation software (Dynatech Laboratories, Billinghirst UK). GSH in samples was compared to a 0-40nmoles/mL standard curve.

2.2.6 Determination of alanine aminotransferase (ALT) activity in serum

Serum ALT activity was determined by kinetic assay according to the manufacturer's instructions (Thermo Scientific) and as previously published (Goldring et al., 2004). 30µL of sample was loaded in duplicate into 96-well plates. ALT reagent was warmed to 37°C and 300µL per well was added to samples and assayed on a Varioskan Flash machine (Thermo Scientific). Pyruvate (and L-glutamate) is produced by the transfer of the amino group from L-alanine to 2-oxoglutarate, in a reaction catalysed by ALT. The reduction of pyruvate to L-lactate by LDH results in the oxidisation of NADH to NAD. This oxidation leads to a decrease in absorbance at 340nm when assayed spectromically.

2.2.7 MicroRNA 122 (miR-122) quantification in serum

miR-122 was quantified in serum using the previously published method (Antoine et al., 2013). miRNA was extracted and purified using a miRNeasy kit followed by an RNeasy MinElute Cleanup Kit (Qiagen, Venlo, Netherlands), in accordance with the manufacturer's instructions. 200µL of serum, diluted in nuclease-free H_2O, was incubated at RT with 700µL Qiazol for 5min in order to disrupt nucleo-protein interactions. 140µL of chloroform was then added and the samples centrifuged (12000*g*, 15min, 4°C). 350µL of the aqueous supernatant was mixed with 350µL 70% EtOH and applied to miRNeasy mini spin columns and centrifuged (>8,000*g*, 15sec, RT). The flow-through was added to 450µL of 100% EtOH, samples applied to RNeasy Min Elute columns and centrifuged (>8,000*g*, 15sec, RT). The elute was then purified by washing with RWT and RPE buffers and 80 % EtOH. The columns were then dried by centrifugation (>8,000*g*, 5min, RT) and the small RNA fraction eluted in 14µL of nuclease-free water before storing at -80°C.

Reverse transcription was performed using TaqMan miRNA reverse transcription kit (Applied Biosystems) and miR-122 and Let-7d (endogenous miRNA control) primers using a GeneAmp PCR9700 machine. Briefly, 2µL purified miRNA was used to synthesise cDNA with a total reaction volume of 15µL via thermal cycling (30min at 16°C, 30min at 42°C, 5min at 85°C and then held at 4°C).

qPCR reactions were run in duplicate in 384-well plates using TaqMan PCR Primers and Master Mix (Applied Biosystems) according to manufacturer's instructions. 1.33µL of cDNA was used and the total reaction volume was made up to 20µL with primer/master mix, and subject to thermal cycling (2min at 50^{o}C, 10min at 95^{o}C and 50 cycles of 15sec at 95^{o}C and 60sec at 60^{o}C) on a ViiA7 machine (Life Technologies). Levels of miRNA were measured by the fluorescent signal produced from the TaqMan assay probes. miR-122 levels were subsequently normalised to the level of the endogenous miRNA, let-7d.

2.2.8 Serum HMGB1 quantification

This assay was performed by a collaborator at the Karolinska Institutet. Serum HMGB1 measurement was determined by sandwich ELISA according to the manufacturer's instructions (Shino-Test/IBL International) using a chicken anti-HMGB1 polyclonal antibody as the capture antibody. Samples were compared against a pig HMGB1 standard curve. HMGB1 content was detected by turnover of 3,3',5,5'-tetramethyl-benzidine (TMB) by a peroxidise-linked anti-HMGB1 antibody. The lower limit of detection was 0.1ng/mL.

2.2.9 Chemo- and cytokine quantification in serum

This assay was performed by Peter Lundbäck at the Karolinska Institutet as part of our collaboration. Serum MCP-1, CXCL1, TNFα and IL-6 concentration was determined by cytokine bead array (CBA) according to the manufacturer's instructions (BD Biosciences).

2.2.10 Liver myeloperoxidase (MPO) activity assay

Myeloperoxidase (MPO) activity was assayed in liver homogenates. 30-50mg of liver was homogenised in 1mL Buffer A (3.4mM KH_2PO_4, 16mM Na_2HPO_4 pH7.4) and centrifuged (10000*g*, 20min, 4°C). The pellet was resuspended in 500µL Buffer B (43.2mM KH_2PO_4, 6.5mM Na_2HPO_4, 10mM EDTA, 0.5% hexadecyltrimethylammonium, pH6.0). The resuspended pellet was heated at 60°C for 2hr. The sample was centrifuged again (10000*g*, 20min, 4°C) and the supernatant removed. Protein content in the supernatants was determined by Bradford assay, and samples were diluted to equal protein concentrations. 20µg of total protein was loaded in duplicate into 96-well plates and 100µL of TMB was added per well. Plates were incubated in the dark at RT, and the reaction was stopped after 30min using 50µL of 2N H_2SO_4. Plates were run at 450nm on a MRX microtiter-plate reader with Max Revelation software (Dynatech Laboratories, Billinghirst UK).

2.2.11 Anti-human IgG Western blot on mouse liver lysates

Liver pieces (30-50mg) were homogenised in 500µL RIPA buffer and kept on ice for 15min. Samples were then centrifuged (18400*g*, 5min, 4°C). Supernatants were assayed for protein content by Bio-Rad protein assay and 20µg of total protein was loaded onto 10% acrylamide gels. Gels were run and proteins transferred onto nitrocellulose membranes. Membranes were blocked with 10% (w/v) non-fat milk for 1hr and then probed with goat polyclonal anti-human IgG Fc region (1:5000, 1hr, RT). Membranes were washed with 0.1% TBS-T and probed using electrochemiluminescence reagent (ECL Plus – Perkin Elmer). Membranes were imaged onto X-ray film, developed and fixed.

2.2.12 Histology

Hepatotoxicity was assessed through histological examination of liver and spleen tissues in collaboration with Prof A Kipar from the Department of Veterinary Pathology, University of Liverpool. All examination and scoring of sections was performed by Prof Kipar in a blinded

manner. Fixed liver sections were embedded in paraffin wax and 3µm sections were prepared and stained with hematoxylin and eosin (H&E) or Periodic Acid Schiff (PAS) stain. All sections were examined and the degree of hepatotoxicity was scored according to the criteria in Table.2.2 (Taken from (Antoine et al., 2009)).

Table.2.2 – Criteria for histological scoring of hepatotoxicity by APAP in C57BL/6 mice

Score	Definition
0	Normal histology – no evidence of hepatocyte necrosis
1	Hepatocellular necrosis is minimal to mild, Focal Limited to centrilobular region Less than 1/4 of affected lobules are necrotic Associated with vacuolar degeneration or haemorrhages
2	Hepatocellular necrosis is mild to moderate, Focal or multifocal Extends from central to midzonal lobular region 1/2 of affected lobules necrotic Associated with vacuolar degeneration or haemorrhages
3	Hepatocellular necrosis is moderate to severe, Multifocal May extend from centrilobular region to portal area More than 1/2 – 3/4 affected lobules necrotic Associated with vacuolar degeneration or haemorrhages
4	Hepatocellular necrosis is severe, Multifocal May extend from centrilobular region to portal area More than 3/4 affected lobules necrotic Associated with vacuolar degeneration or haemorrhages
5	Massive hepatocellular necrosis (severe) involving entire lobules Necrosis extends from central vein to portal area (bridging necrosis) Necrosis extends to adjacent lobules (multilobular necrosis) Associated with vacuolar degeneration or haemorrhages

2.2.13 Statistical analysis

Statistical analysis of data was undertaken using GraphPad Prism 5 software. All results are presented as mean±standard error of the mean (SEM). Data were assayed for normality by Shapiro-Wilk test. Normal data were compared by One-Way ANOVA or unpaired t-test as indicated. Non-parametric data were compared by Kruskal-Wallis or Mann-Whitney tests as indicated. Results were considered significant when $p<0.05$.

2.3 Results

2.3.1 The impact of APAP and anti-HMGB1 treatment on total hepatic glutathione (GSH)

GSH content was not significantly different between groups of mice given any of the saline+antibody treatments when compared to saline+PBS animals (Fig.2.3A). However in all groups of animals receiving APAP there was significant depletion of liver GSH in comparison with saline animals (Fig.2.3B). The reduction in total hepatic GSH was not significantly different between APAP-treated mice given PBS or any of the antibodies (Fig.2.3C).

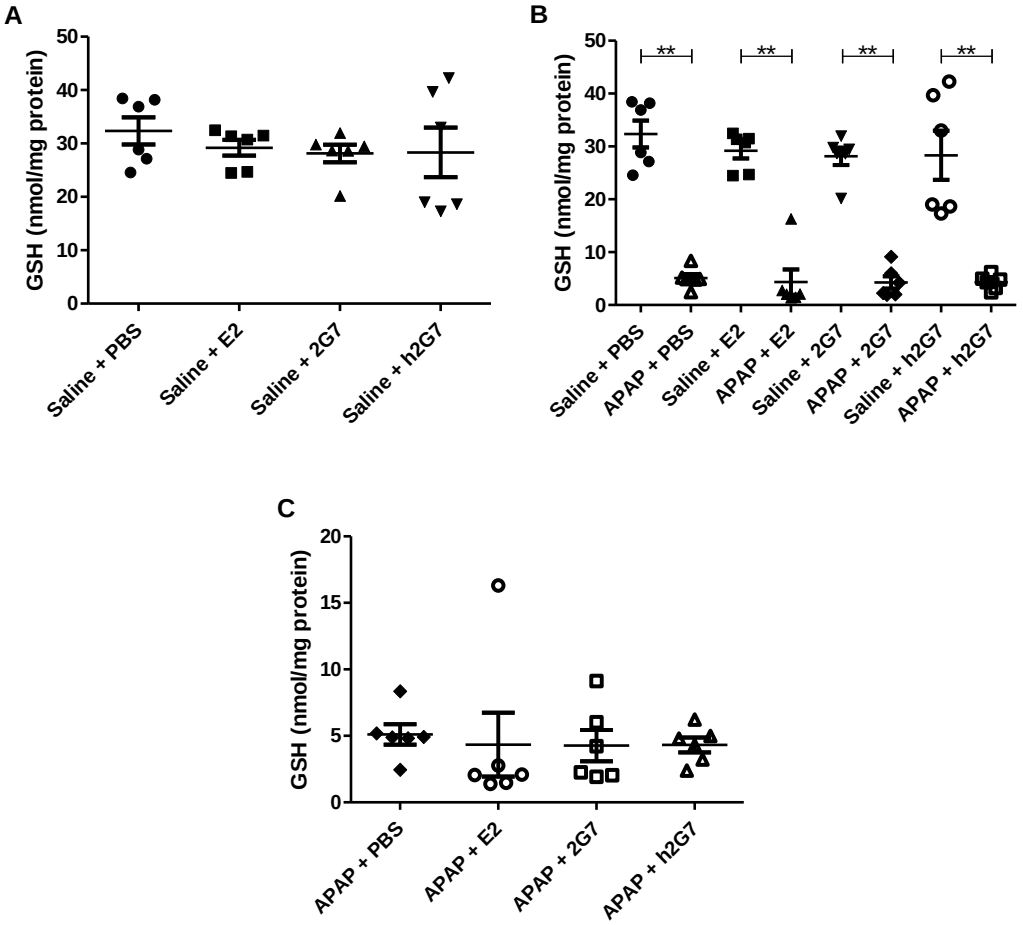

Fig.2.3 – Liver GSH in APAP-treated mice. A) Liver GSH saline+antibody treated animals in comparison with saline+PBS. B) APAP-induced depletion of liver GSH compared with saline treated animals. C) Antibody treatment does not affect APAP-induced GSH depletion. All antibodies were administered at 300µg/mouse. Data is represented as mean±SEM, *n=6* per group. ** = $p<0.01$ as determined by One-Way ANOVA.

2.3.2 The impact of APAP and anti-HMGB1 treatment on serum ALT activity

Serum ALT activity was not elevated in saline+antibody treated animals in comparison with saline+PBS treated animals (Fig.2.4A). However, following APAP treatment in PBS or E2 treated animals a significant elevation in ALT activity was seen compared with saline control groups (APAP+PBS 5050±445 U/L vs saline+PBS 34.30±4.63 U/L, $p<0.001$) or (APAP+E2 4915±590 U/L vs saline+E2 51.14±17.0 U/L) (Fig.2.4B). No effect on the elevation in ALT activity caused by APAP was observed by E2 antibody post treatment. However 2G7 (1987±486 U/L) caused a significant attenuation of the ALT rise seen in APAP+PBS animals.

Similarly, h2G7 (2168±419 U/L) caused dose dependent attenuation of the ALT elevation in response to APAP compared to the isotype control group (E2) (Fig.2.4B-C) that was first evident in the 300µg antibody treatment group (Fig.2.4C).

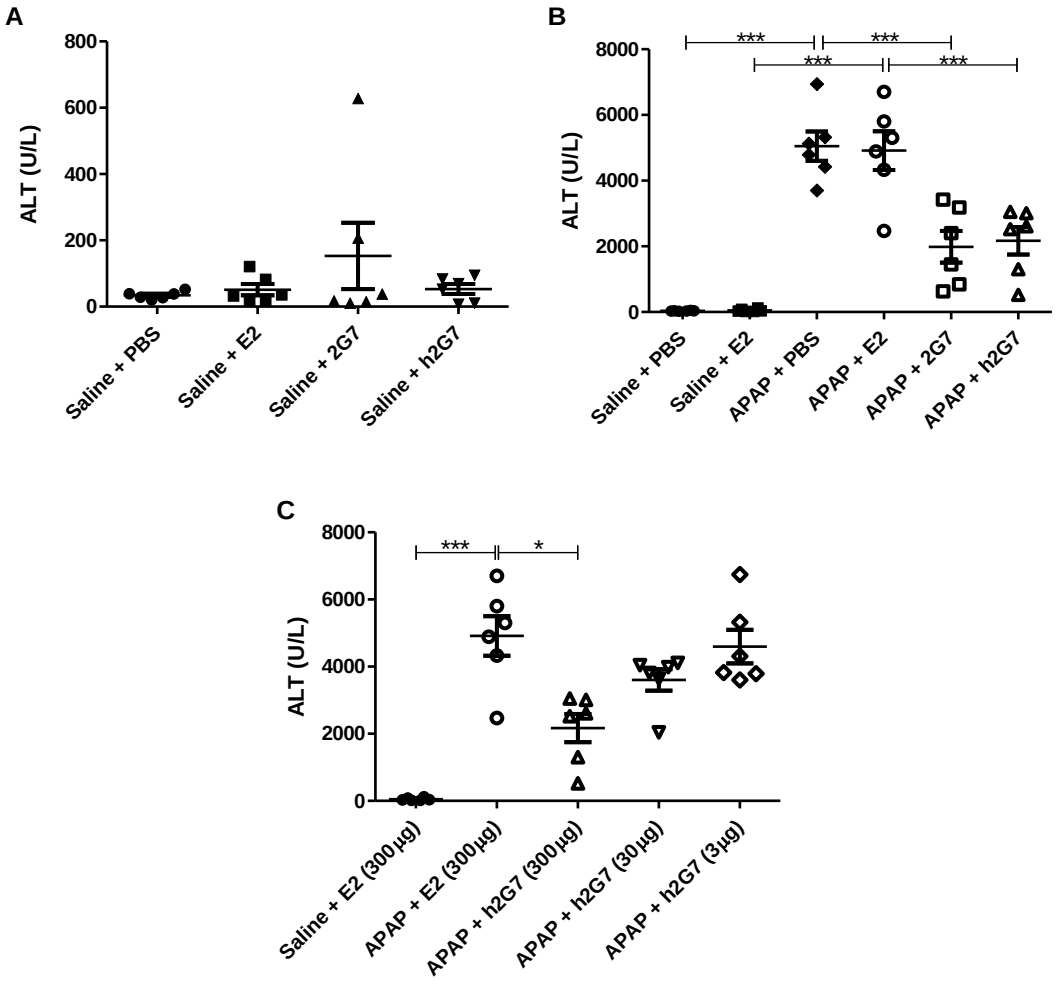

Fig.2.4 – Serum ALT activity in APAP-treated mice. A) Serum ALT activity in saline+antibody treated animals compared with saline+PBS. ALT values are within the expected range (<200 U/L) for healthy mice. B) Serum ALT activity is significantly elevated following APAP treatment, in comparison with saline animals, and attenuated by anti-HMGB1 treatment. All antibody treatments are at 300µg/mouse C) Serum ALT activity over a h2G7 dose response in comparison with APAP and saline control groups. Data is represented as mean±SEM, *n=6* per group. * = p<0.05, *** = p<0.001 as determined by One-Way ANOVA.

2.3.3 The impact of APAP and anti-HMGB1 treatment on serum miR-122

Baseline serum miR-122 was not elevated above that seen with saline+PBS treated animals following antibody treatment (Fig.2.5A). However, following APAP+PBS treatment, a significant increase in serum miR-122 was seen (8671±6466 ΔΔCt miR-122/Let-7d) when compared with saline+PBS animals (53.56±17.13 ΔΔCt miR-122/Let-7d). A similar significant effect was seen with APAP+E2 treatment (6988±2105 ΔΔCt miR-122/Let-7d) in comparison with saline+E2 treatment (594.5±505.3 ΔΔCt miR-122/Let-7d). No effect on the elevation in miR-122 caused by APAP was observed with E2 antibody treatment. Decreases in circulating miR-122 in comparison to APAP+PBS or APAP+E2 were seen with 2G7 (530.1±139.0 ΔΔCt miR-122/Let-7d) and h2G7 (663.7±102.5 ΔΔCt miR-122/Let-7d) treatment, respectively, although these were not significant (Fig.2.5B). There was a dose dependent attenuation of the rise in serum miR-122 by h2G7 that was significant in the 300μg antibody treatment group, but not lower doses (Fig.2.5C).

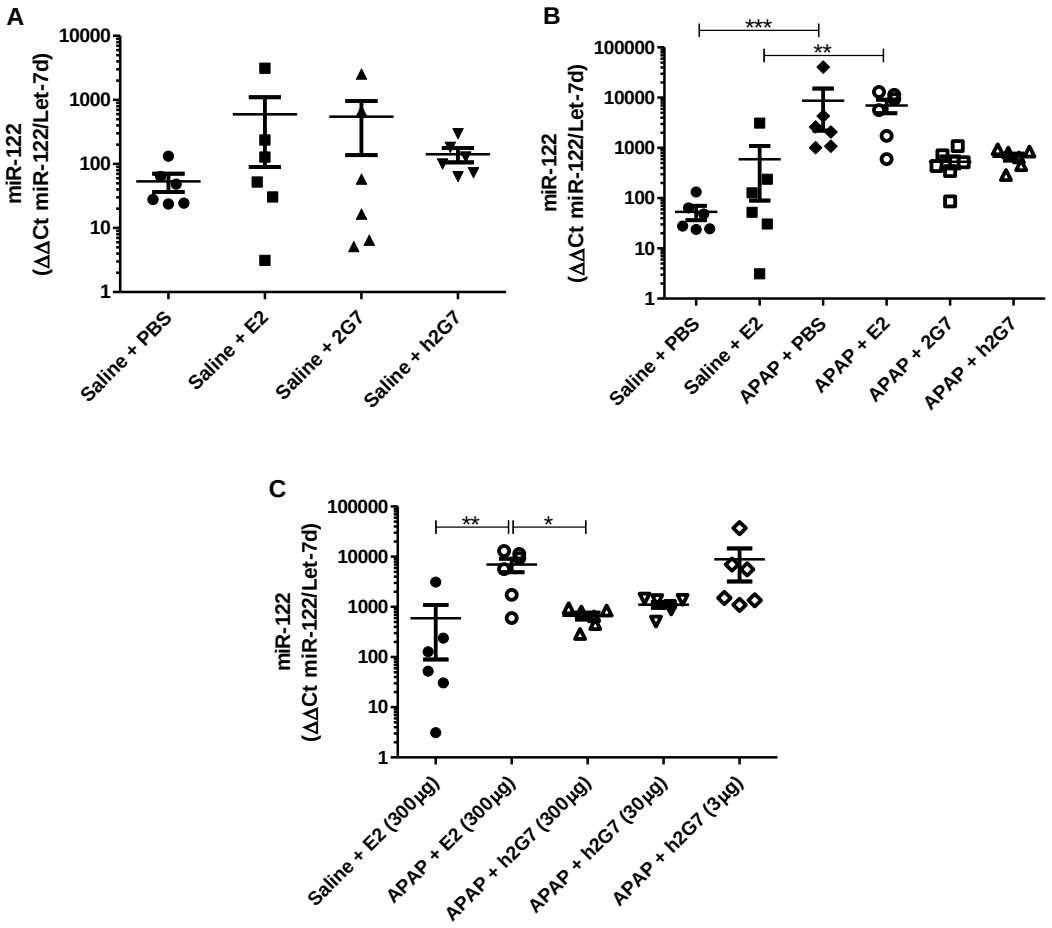

Fig.2.5 – Serum miR-122 in APAP-treated mice. A) Serum miR-122 in saline+antibody treated animals. B) Serum miR-122 in APAP treated animals, in comparison with saline treated and APAP+antibody treated animals. C) Serum miR-122 over a h2G7 dose response in comparison with APAP and saline control groups. Data is represented as mean±SEM, *n=6* per group. * = p<0.05, ** = p<0.01, *** = p<0.001 as determined by Kruskal-Wallis test.

2.3.4 Correlation between serum biomarkers of liver injury

A positive correlation of miR-122 and ALT has been determined previously in AILI in man (Starkey Lewis et al., 2011). In our C57BL/6 model there is also positive correlation between serum biomarkers of liver injury (miR-122 and ALT), with a Pearson R value of 0.5904 ($p<0.0001$) and shows that at the 10hr timepoint miR-122 is still elevated and correlates with the later marker of liver injury (ALT). (Fig.2.6)

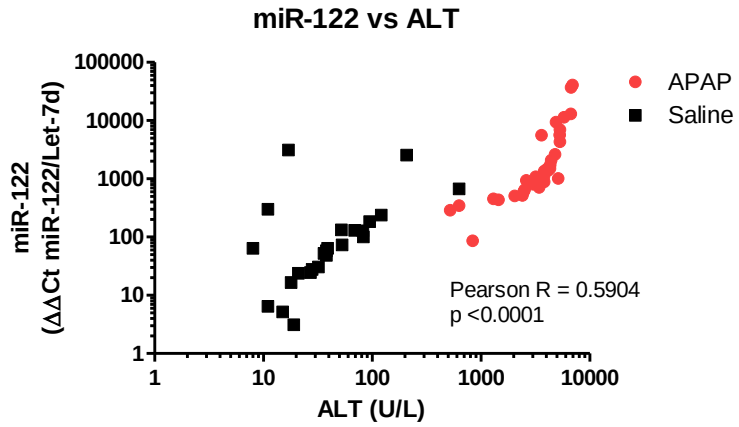

Fig.2.6 – Correlation between miR-122 and ALT in APAP-treated mice. miR-122 and ALT correlation in male C57BL/6 mice at 10hr APAP (530mg/kg) (*n*=36) or saline (*n*=24). All antibody interventions or PBS were grouped together according to APAP or saline treatment.

2.3.5 The impact of APAP and anti-HMGB1 treatment on serum HMGB1

Serum HMGB1 levels were determined by collaborators at the Karolinska Institutet. The effect of anti-HMGB1 treatment on serum HMGB1 levels in APAP-treated animals was investigated by ELISA. Somewhat surprisingly, there was no significant difference in serum HMGB1 level observed between any of the APAP-treated groups (Fig.2.7). This may be a result of interaction between the anti-HMGB1 antibodies tested (2G7/h2G7) and the anti-HMGB1 antibodies used in the ELISA.

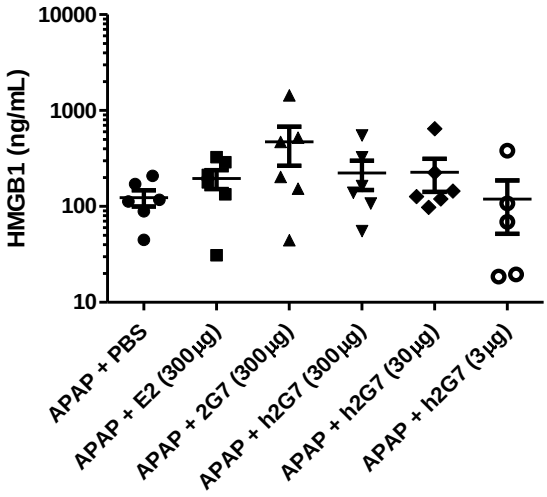

Fig.2.7 – Serum HMGB1 in APAP-treated mice. HMGB1 ELISA shows no significant difference in serum HMGB1 content between any of the APAP-treated groups (PBS, E2, 2G7, h2G7). Data is represented as mean±SEM, *n=6* per group.

2.3.6 The impact of APAP and anti-HMGB1 treatment on serum chemo- and cytokines

Serum HMGB1 levels were determined by collaborators at the Karolinska Institutet. In APAP-treated mice, serum MCP-1 (A), CXCL1 (B) and TNFα (C) release were significantly attenuated in comparison with APAP+PBS or APAP+E2 animals, by 2G7 and h2G7 treatment respectively, at all antibody doses, except for MCP-1 in response to h2G7 at 300µg

(p=0.113) (Fig.2.8). E2 antibody had no effect on the serum levels of MCP-1 or CXCL1, but did cause a small, but significant decrease in TNFα release.

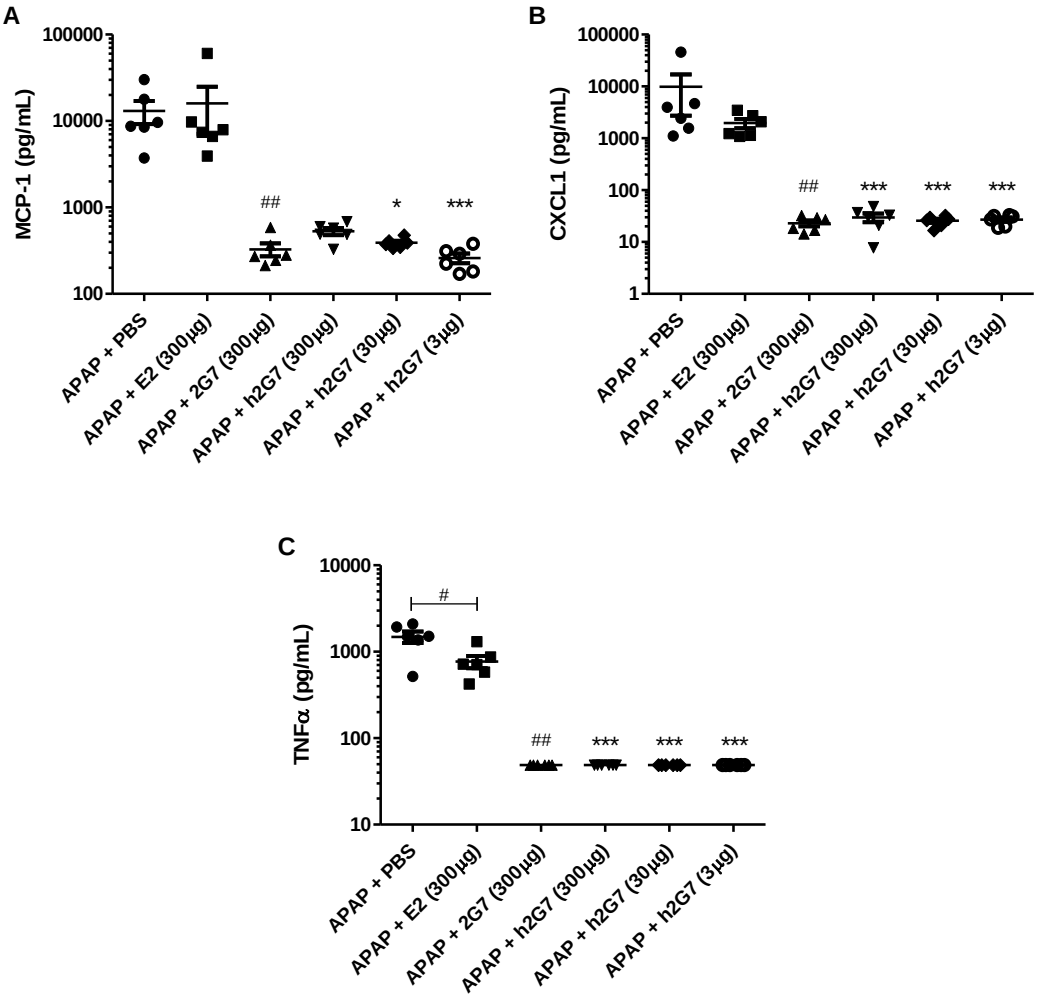

Fig.2.8 – Serum chemo- and cytokines in APAP-treated mice. A) MCP-1, B) CXCL1 and C) TNFα release following APAP treatment and APAP+antibody treatment. Data is represented as mean±SEM, *n=6* per group. # = p<0.05, ## = p<0.01 compared with APAP+PBS as determined by t-test. * = p<0.05, *** = p<0.001 compared with APAP+E2 as determined by Kruskal-Wallis test.

2.3.7 The impact of APAP and anti-HMGB1 treatment on liver myeloperoxidase (MPO) activity

No significant increase in liver MPO activity was observed in saline animals given any of the antibodies, when compared with saline+PBS animals (Fig.2.9A). However, a significant elevation in MPO activity was seen in APAP+PBS or APAP+E2 treated animals compared with corresponding saline control groups (Fig.2.9B). h2G7 (300µg) significantly attenuated the APAP-induced rise in MPO activity in comparison with the isotype control antibody (E2) treatment (Fig.2.9C).

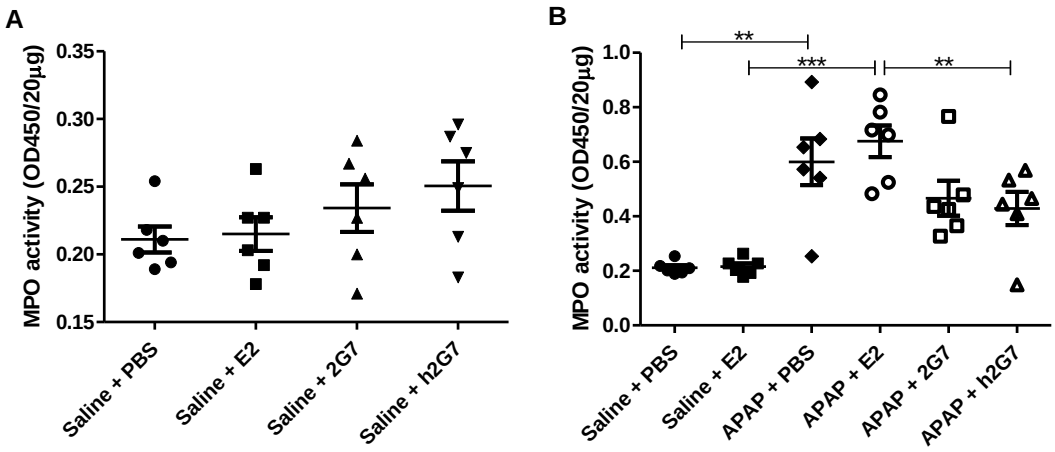

Fig.2.9 – Liver MPO activity in APAP-treated mice. A) MPO activity in saline+antibody treated animals. B) MPO activity seen with APAP treatment in comparison with saline treatment and APAP+antibody treatments. C) Data is represented as mean±SEM, *n=6* per group. ** = $p<0.01$, *** = $p<0.001$ as determined by One-Way ANOVA.

2.3.8 Liver localisation of antibodies

Western blotting for human IgG Fc region showed liver localisation of E2 and h2G7 antibodies in mice in these treatment groups, but not the PBS group (Fig.2.10). 2G7 was not detected by the anti-human antibody. More antibody was detectable in APAP-treated mice than the corresponding saline-treated antibody group for both E2 and h2G7. (Fig.2.10).

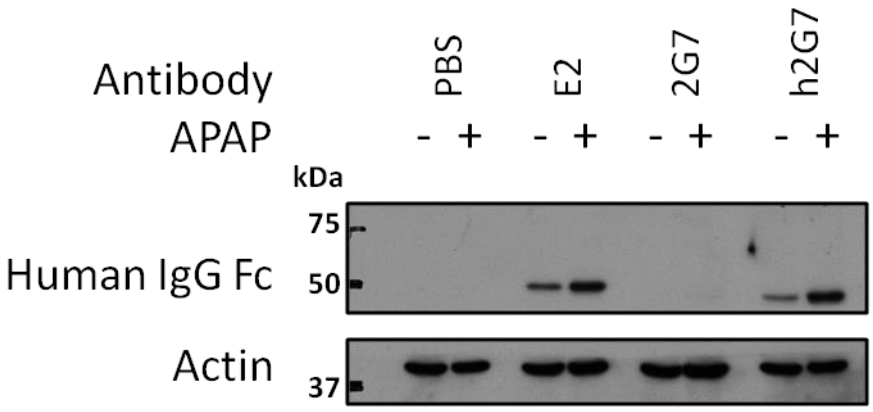

Fig2.10 – Anti-human Fc Western blotting of mouse liver lysates. Representative blot of livers from each treatment group (*n=6* animals/group). All antibodies are at 300µg/mouse. E2 and h2G7 localise to the liver, with more liver expression in APAP-treated mice.

2.3.9 The impact of APAP and anti-HMGB1 treatment on liver histology

Histological examination of livers from APAP-treated mice was undertaken as per the method in (Antoine et al., 2010), using the scoring system detailed in the methods section (Table.2.2). Histological scoring and notes are shown in Table.2.3. This revealed that APAP+PBS and APAP+E2 treated mice underwent moderate-to-severe AILI, characterised by a reduced number of centrilobular hepatocytes due to necrosis and neutrophil infiltration into the central veins and central zone. This demonstrates the hepatotoxic and immune components of AILI. However, following anti-HMGB1 treatment (both 2G7 and h2G7 at 300µg/mouse) there was a clear reduction in liver injury, characterised by a less hepatocellular necrosis, and no infiltration of neutrophils. Tissue glycogen levels were normal in these animals. h2G7 also showed dose-dependent attenuation of liver injury with 30µg treatment resulting in mild attenuation of liver injury, whereas 3µg h2G7 treatment resulted in no attenuation of histological liver injury compared with control animals.

Table.2.3 – Histological scoring of liver injury. Scoring of livers was on a 0-5 scale (according to Table.2.2 in Section 2.2.12) with 0 representing normal histology, and 5 representing massive hepatocellular damage. NL = neutrophilic leukocytes.

GROUP	HISTOLOGY SCORE	HISTOLOGY NOTES
APAP+PBS	2.67±0.21	Reduced number of centrilobular cells, with swelling (or coagulative necrosis) of remaining hepatocytes; often a few NL within central veins and central zone
APAP+E2 (300µg/mouse)	2.33±0.33	Reduced number of centrilobular cells, with swelling (or coagulative necrosis) of remaining hepatocytes; often a few NL within central veins and central zone
APAP+2G7 (300µg/mouse)	1.50±0.22	Centrilobular several remaining cells (with hydropic swelling) (mainly in zone 3); unaffected tissue diffuse glycogen
APAP+h2G7 (300µg/mouse)	1.17±0.31	Centrilobular several remaining cells (with hydropic swelling) (mainly in zone 3); unaffected tissue diffuse glycogen
APAP+h2G7 (30µg/mouse)	2.42±0.15	Centrilobular several remaining cells (with hydropic swelling); occ. a few NL in central vein; unaffected tissue diffuse glycogen
APAP+h2G7 (3µg/mouse)	2.83±0.48	Reduced number of centrilobular cells, with swelling (or coagulative necrosis) of remaining hepatocytes; often a few NL within central veins and central zone

2.4 Discussion

HMGB1 is an emerging target of therapeutics in inflammatory conditions including DILI. Recent publications have demonstrated the key role that HMGB1 plays in the coordination and execution of the inflammatory response to injury or infection (Yang et al., 2004, Antoine et al., 2010, Tsung et al., 2005, Harris et al., 2012, Schierbeck et al., 2011, Yang et al., 2013). Amongst HMGB1 targeting therapeutics, anti-HMGB1 antibodies have shown an ability to suppress inflammatory responses through the inhibition of HMGB1 proinflammatory signalling. The experiments in this chapter are the first known study of a chimeric anti-HMGB1 antibody (h2G7) in an *in vivo* model.

Liver GSH is responsible for the adduction and removal of reactive species formed as a result of oxidative cell stress. Depletion of GSH can occur in conditions of excessive cell stress when the high levels of reactive metabolites exhaust the GSH pool (Mitchell et al., 1973). Liver GSH was significantly depleted in all APAP-treated animals in comparison with saline-treated animals, showing APAP-dependent depletion of GSH. In saline-treated animals, administration of the antibodies did not affect basal GSH levels (Fig.2A). Additionally, antibodies had no effect on the GSH depletion seen following APAP treatment (Fig.2B). Antibodies were administered at 2hr post-APAP to allow bioactivation of APAP. No effect on hepatic GSH was observed in antibody control groups, indicating that the antibodies are unlikely to affect APAP bioactivation to NAPQI and subsequent GSH depletion. However, this would need confirmation through covalent binding assays, HPLC or mass spectrometry, which could be an area of future investigation.

APAP (530mg/kg, 10hr) has been shown previously to induce elevated serum ALT activity in CD-1 mice (Antoine et al., 2009). Additionally, elevated serum ALT activity has been observed in C57BL/6 mice at 300mg/kg APAP by 6hr (Salhanick et al., 2006) and 12hr (Vaquero et al., 2007), although there are no studies at 10hr, 530mg/kg APAP in C57BL/6

mice for direct comparison with the data in this thesis. In our C57BL/6 AILI model, serum ALT activity was significantly elevated in APAP+PBS treated mice in comparison with the saline+PBS group.

Administration of E2 antibody at 2hr post-APAP had no effect on serum ALT activity level, demonstrating the inert nature of the E2 antibody in this inflammatory model. However, significant reduction of the serum ALT level was seen when 2G7 or h2G7 were administered at 300μg at 2hr post-APAP. This was similar to another mouse study of anti-HMGB1 antibody intervention in AILI that showed a significant reduction in ALT elevation with anti-HMGB1 antibody treatment (Antoine et al., 2010). This shows that anti-HMGB1 antibody treatment significantly attenuates hepatocellular injury, as has been shown with 2G7 in previous studies (Antoine, unpublished). There was no significant difference in serum ALT activity between 2G7 and h2G7 at 300μg antibody in APAP-treated mice, suggesting no difference in protective effect at this dose. Additionally, there was dose dependent action of h2G7 seen, as there was a greater reduction in ALT activity seen with 300μg than 30μg, and in turn 30μg more than 3μg, with only 300μg causing a significant decrease in ALT activity compared with the APAP+E2 group.

A significant elevation in miR-122 has been shown to be a highly specific marker of AILI in man (Starkey Lewis et al., 2011) and miR-122 is elevated in a BALB/c model of AILI (Wang et al., 2009). Additionally, a recent study has shown elevation of miR-122 in a C57BL/6 model of obstructive cholestasis (Woolbright et al., 2013). Unfortunately, due to no consensus on the normalising miRNA this precludes the direct quantitative comparison of miR-122 elevations between these studies and the data in this thesis. Serum miR-122 was unaffected by the presence of any of the antibodies tested in saline-treated animals. Following APAP treatment, there was a significant elevation in serum miR-122. The data also showed a significant decrease in miR-122 in APAP-treated mice following h2G7

treatment in comparison with the isotype control group, and with 2G7 treatment in comparison with the APAP+PBS group. As seen with ALT, there is a dose-dependent trend in the reduction in serum miR-122 by h2G7, with mean miR-122 values lower in 300μg than 30μg and 30μg than 3μg, and only 300μg showing significant depletion. Serum miR-122 is strongly correlated with serum ALT, as shown by a Pearson R value of 0.5904. This data is similar to the value previously published Pearson R of 0.46 in AILI patients (Starkey Lewis et al., 2011).

Serum HMGB1 level was not affected by antibody treatment in APAP-treated animals. However, this may be because of an interaction between 2G7/h2G7 and the anti-HMGB1 antibody used in the ELISA. The epitope for 2G7 and h2G7 is amino acids 53-63, but the specific antibody and epitope used in the ELISA is not disclosed by the manufacturer (Shino-Test IBL). 2G7 binding could lead to a conformational change in HMGB1, or steric hindrance of the ELISA anti-HMGB1 antibody binding to HMGB1.

Immune activation following APAP-treatment was characterised by chemo- (MCP-1 and CXCL1) and cytokine (TNFα) release and myeloperoxidase (MPO) activity. MCP-1 and CXCL1 are important mediators of immune cell recruitment, especially macrophages and neutrophils (Antoniades et al., 2012, Takada et al., 1995, Dambach et al., 2002). Serum MCP-1 has been shown to correlate with toxicity in APAP overdose (James et al., 2005). CXCL1 has been shown to be released in an *in vivo* model of AILI (Pires et al., 2014). Hence the reduction in the amount of MCP-1 and CXCL1 release following anti-HMGB1 treatment (both 2G7 and h2G7) is indicative of a reduction in AILI severity. Anti-HMGB1 treatment has also been shown to attenuate the immune component of AILI in CD-1 mice through suppression of TNFα release (Antoine et al., 2010). MPO is an important source of reactive oxygen species during inflammation, and is indicative of the accumulation of polymorphonuclear leukocytes (PMN) at the site of injury (Schierwagen et al., 1990). The

reduction in MPO activity seen with h2G7 treatment in comparison with the E2 treatment in APAP treated mice indicates that h2G7 successfully inhibits the neutrophil activation in the liver, and hints at reduced neutrophil infiltration.

Western blotting for human IgG Fc region showed that the E2 and h2G7 antibodies were present in the liver, showing that the antibodies are located at the site of injury. It also appears that there is an enrichment of antibody in APAP-treated mice, in comparison with the antibody-matched saline-treated animals. Enrichment of h2G7 antibody in the APAP-treated animals may be due to localisation of the anti-HMGB1 antibody to the site of injury to sequester its antigen (HMGB1). Interestingly, there is also a small decrease in the observed MW of h2G7 in comparison with E2, which could be due to differences in the total amino acid mass of the Fab regions.

H&E staining demonstrated that there was significantly less centrilobular hepatocyte necrosis and neutrophil infiltration in anti-HMGB1 animals in comparison with APAP+PBS treated animals. This demonstrates a hepatoprotective effect of anti-HMGB1 treatment, and the data complements the serum and liver AILI marker findings. Necrosis was the predominant form of cell death in APAP-treated animals, and apoptosis was absent. This is presumably due to the depletion of hepatic ATP as shown previously (Antoine et al., 2010). The neutrophil infiltration, as also seen previously in CD-1 mice (Antoine et al., 2010), is indicative of the release of chemokines and DAMPs from necrotic hepatocytes and resident immune cells (Brenner et al., 2013). In APAP-treated animals there was significant attenuation of AILI (centrilobular hepatocyte necrosis and neutrophil infiltration) with 2G7 and h2G7 treatment, compared with APAP+PBS animals. The histological evidence also show no difference in the level of attenuation of liver injury between 2G7 and h2G7, suggesting that there is no difference in efficacy between 2G7 and h2G7 (at 300µg antibody). PAS staining showed no glycogen depletion in the anti-HMGB1 treated animals,

which suggests that the reduction in liver injury had an positive effect on appetite and GSH synthesis. Faster resynthesis of GSH has previously been shown in fed vs fasted mice (Antoine et al., 2010).

The data in this chapter indicates that h2G7 has equivalent anti-HMGB1 activity to 2G7. This suggests that the CDRs that are conserved between 2G7 and h2G7 are the only regions that are essential for anti-HMGB1 function. This is expected as the CDRs are the region responsible for HMGB1 recognition. The serum biomarkers and liver markers of inflammation and injury all show no difference in response between 2G7 and h2G7, suggesting that the antibodies have identical anti-inflammatory profiles in AILI, resulting from similar, if not identical, efficacies for HMGB1. Whilst this is certainly the case at 300µg, a caveat in this conclusion is that the 2G7 and h2G7 antibodies were only compared at 300µg, and as such this may be the dose point at which the antibody dose response curves intersect. Further work to compare the responses to 2G7 and h2G7 over a range of doses will be required to definitively confirm this conclusion.

Given that h2G7 is a chimeric antibody and therefore should be tolerated in patients, the data in this chapter indicates that h2G7 may have clinical usefulness for the treatment and attenuation of AILI, and possibly other forms of DILI and inflammatory diseases. Future experiments should investigate the temporal effectiveness of h2G7 in AILI, as h2G7 may be effective at timepoints beyond the 8-10hr post-ingestion recommendation for N-acetylcysteine therapy (Prescott et al., 1979). N-acetylcysteine is a precursor for GSH production, and hence can protect against NAPQI-induced cell stress. HMGB1 is elevated at first presentation to hospital, and precedes rises in ALT (Antoine et al., 2013), so h2G7 could also be applied prior to ALT rises. Future clinical trials of h2G7 in APAP-overdose patients will be able to determine the clinical utility of h2G7, but the preclinical data in this chapter indicate that h2G7 has therapeutic promise.

Future work with h2G7 should also focus on determining the mechanism of action of h2G7 when attenuating preclinical AILI. The data in this chapter would indicate that HMGB1 sequestration and elimination would be the likely mechanism, as no differences in response to 2G7 and h2G7 were observed. If other mechanisms such as complement-mediated or Fcγ receptor (FcγR) mediated-effects were involved with helping to suppress AILI (for example through phagocytosis of HMGB1/injured hepatocytes and prevention of further DAMP release), a difference in response between 2G7 and h2G7 would have been expected. This is because of species differences in the Fc region, which is responsible for mediating these functions.

Other investigations that should be pursued include assessment of the formation of h2G7-HMGB1 immune complexes and their clearance, and the determination of binding affinities of h2G7 and 2G7 to different redox and acetyl isoforms of HMGB1. Recent investigations have demonstrated distinct mechanistic and functional roles of different HMGB1 redox isoforms (Chapter 4, (Venereau et al., 2012)) and clinical data shows the predictive capability of acetylated HMGB1 on AILI outcome (Antoine et al., 2012). Yet no isoform-specific antibodies for HMGB1 exist, and this is a key challenge for future HMGB1 research.

Chapter Three

Investigating the mechanism of action of a chimeric anti-HMGB1 antibody in acetaminophen-induced liver injury

CONTENTS

3.1 Introduction

Previously in Chapter 2, we have shown that the chimeric antibody, h2G7, targeted towards HMGB1 can modulate DILI in murine models by a hypothesis linked to the neutralisation of circulating HMGB1 released from necrotic or inflammatory cells. However, as well as antigen neutralisation, IgG antibodies can mediate and modulate inflammation through two other main mechanisms: complement-mediated effects such as complement-dependent cytotoxicity (CDC) and FcγR-mediated effects such as antibody-dependent cell cytotoxicity (ADCC). These are Fc region-dependent mechanisms of action and are dependent on residues located in the hinge and CH2 regions of the antibody (Idusogie et al., 2000, Jefferis and Lund, 2002).

The complement system is a collection of proteins that facilitate the immune response by enabling phagocytosis, chemotaxis and cell lysis. There are three pathways of activation of the complement system, with only the classical pathway being activated by antibody-antigen complexes (Hughes-Jones and Gardner, 1979) (Fig.3.1).

Residue K322 has been shown to be critical for C1q activation by human IgG antibodies (Idusogie et al., 2000). There are species differences observed between mice and human IgG isotypes, resulting in differences in the C1q binding regions, however, K322 has been shown to be important in both species (Idusogie et al., 2000, Duncan and Winter, 1988). The K322A mutant may have mild effects on ADCC, which are mediated through C5a, but these are minor compared with the massive decrease in C1q binding or CDC activation (Hezareh et al., 2001, Sorkin et al., 2010).

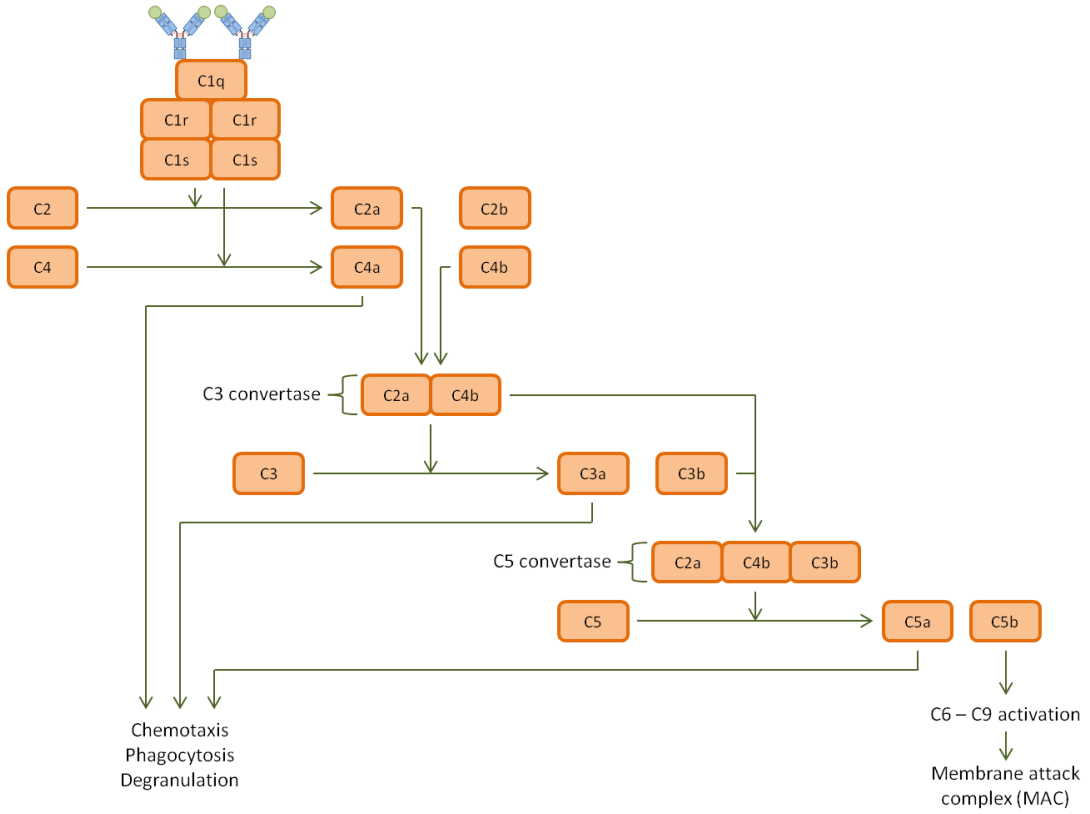

Fig.3.1 – The "classical" antibody-mediated complement signalling cascade. The classical pathway is initiated by binding of IgG or IgM to the protein C1q, a component of the C1 complex that is comprised of one C1q, two C1r and two C1s subunits. Multiple IgG molecules are needed to bind to C1q to activate the C1 complex. IgG binding leads to a conformational change in C1q that then activates the two C1r subunits. C1r subunits then cleave the C1s subunits. This $C1r^2 1s^2$ complex then cleaves C2 and C4 proteins, into C2a and C2b, and C4a and C4b. C4b and C2a then bind together to form the C3 convertase that then cleaves C3 into C3a and C3b. C3b binds to the C3 convertase to form the C5 convertase, which then cleaves C5 into C5a and C5b. C3a, C4a and C5a are involved in the recruitment of inflammatory cells to the site of injury, increase in phagocytosis, and degranulation. C5b subsequently activates a cascade of activation of C6, C7, C8 and C9 to form the membrane attack complex (MAC) that facilitates target cell lysis.

Binding of IgG antibodies to Fcγ receptors (FcγR) on the surface of immune cells, particularly NK cells but also macrophages, neutrophils, and eosinophils leads to activation of the immune cells, with a wide range of responses (such as phagocytosis, ADCC, cytokine release and respiratory burst). Humans express FcγRI, FcγRIIa, FcγRIIb, FcγRIIIa and FcγRIIIb receptors, with differential expression profiles on different cell types (Guilliams et al., 2014). Additionally, different immunoglobulin isotypes have different affinities for the

different FcγR isotypes, with FcγRI being the highest affinity and FcγRIIb being the lowest affinity for IgG (Bruhns et al., 2009). Of the aforementioned receptors, FcγRIIb is the only inhibitory isotype. FcγRI and FcγRIIa receptor activation signals for phagocytosis, a process aided by FcRn (Vidarsson et al., 2006). FcRn is a specialised FcR that is unable to bind to IgG at pH7.4, but can bind at pH6.0-6.5, protecting IgG from lysosomal degradation following phagocytosis (Junghans and Anderson, 1996). FcγRIIIa receptors are responsible for ADCC initiation by NK cells (Sun, 2003). ADCC is a process of elimination of target cells mediated through the activation of immune cells by antibody-bound cell surface antigen.

A pivotal aspect of the recognition of antibodies by FcγR is the presence of glycosylated residue N297 (Arnold et al., 2007). These N-linked glycosyl chains coordinate the interaction between FcγR and antibody. Deglycosylation of N297, either by mutation of the arginine to an alanine (N297A) or through enzymatic deglycosylation of the chains by EndoS, a *Streptococcus pyogenes* endoglycosidase, leads to loss of function of ADCC initiation by antigen-bound IgG (Collin and Olsen, 2001, Allhorn et al., 2008). N297A mutation eliminates the ability for glycosyl chains from forming at position 297, however there is evidence showing an effect of N297A mutation on C1q binding (10-fold decrease in C1q binding (Lund et al., 1996)) which may limit its utility in this mechanism of action study.

By contrast, EndoS deglycosylation can suppress inflammation without affecting complement (Nandakumar et al., 2013). EndoS treatment has also been used to suppress inflammation in a range of inflammatory models such as systemic lupus erythematosus (SLE) (Lood et al., 2012), glomerulonephritis (Yang et al., 2010), encephalomyelitis (Benkhoucha et al., 2012) and arthritis (Nandakumar et al., 2007).

Mutation of residues within the CH2 and hinge region can modulate CDC and FcγR-mediated effects, with both increased and decreased activities being possible (Armour et al., 1999, Shields et al., 2001, Lazar et al., 2006). The majority of research into the effects of residue mutation has been focussed on increasing ADCC activity in antibody-based

therapeutics, such as in cancer immunotherapy (Lazar et al., 2006, Kubota et al., 2009). CDC and ADCC mechanisms are often linked, with mutations that affect CDC also affecting ADCC. For example substitution of residues 233-236 of human IgG2 or residues 327, 330 and 331 of human IgG4 into human IgG1 greatly reduce C1q and ADCC activation (Armour et al., 1999, Shields et al., 2001).

Consequently mutation or modification of K322 and N297 can be utilised to investigate the effects of knocking down CDC and FcγR-mediated responses in inflammatory models (human IgG1 is recognised by mouse FcγRs) (Lux and Nimmerjahn, 2013, Overdijk et al., 2012).

As has been shown in the previous chapter, the chimeric anti-HMGB1 antibody, h2G7 can successfully attenuate HMGB1-mediated liver injury in a murine model of acetaminophen overdose. In animals given an intraperitoneal dose of APAP (530mg/kg), h2G7 treatment caused a significant reduction in serum ALT activity and cytokine release compared with PBS or control antibody, and was comparable with the murine 2G7 antibody. Additionally, other injury markers such as miR-122 and myeloperoxidase were reduced with h2G7 treatment. However, the mechanism of action of h2G7 is unknown. In order to investigate the mechanism of action, a K322A mutated form of h2G7 and an EndoS-treated h2G7 will be utilised to identify if complement-mediated and FcγR-mediated responses play a role in the mechanism of h2G7-mediated attenuation of AILI.

3.1.1 Aims

The aim of the work in this chapter was to identify the potential mechanism of action of h2G7 in an *in vivo* model of AILI. This was achieved through investigation of the effectiveness of modified forms of h2G7 to reduce AILI, in comparison with unmodified h2G7. The modified forms of h2G7 used were a K322A mutant, which had no C1q binding ability, and hence was not able to activate complement, and an EndoS-treated form of

h2G7, which was deglycosylated, and therefore was unable to initiate FcγR-mediated responses. Through excluding the role of complement-mediated and FcγR-mediated effects, it can be suggested that any responses seen are due to neutralisation of HMGB1 by h2G7.

3.2 Materials and Methods

3.2.1 Materials

Bio-Rad Protein Assay Dye Reagent, Precision Plus Kaleidoscope Standards (molecular weight markers) and non-fat milk were purchased from Bio-Rad Laboratories Ltd (Hemel Hempstead, UK). HRP-coupled Goat anti-human IgG Fc region was purchased from Bethyl Laboratories (TX, USA). Amersham Hybond ECL membrane and Amersham Hyperfilm ECL were purchased from GE Healthcare (Little Chalfont, UK). Western Lightning Plus-ECL was purchased from Perkin Elmer (Beaconsfield, UK). All other materials were purchased from Sigma-Aldrich (Poole, UK) or Fisher Scientific (Loughborough, UK) unless otherwise indicated.

3.2.2 Experimental animals

The protocols described were undertaken in accordance with criteria outlines in a licence granted under the Animals (Scientific Procedures) Act 1986 and approved by the University of Liverpool Animal Ethics Committee. 8 week old male C57BL/6J mice (20-25g) were purchased from Charles River laboratories and had a 5-day acclimatisation period prior to experimentation. Animals were also maintained in a 12hr light/dark cycle with free access to food and water.

3.2.3 Antibody Expression and Purification

Mouse IgG2b monoclonal anti-HMGB1 antibody (2G7), chimeric human IgG1 monoclonal anti-HMGB1 antibody (h2G7) and monoclonal isotype-matched (IgG1) human anti-tetanus toxin antibody (E2) were expressed and purified by Peter Lundbäck (Karolinska Institutet) as described in Chapter 2.

3.2.4 K322A mutation and validation

This work was carried out by and in collaboration with investigators at the Karolinska Institutet.

An 18 cycle PCR reaction was performed with the h2G7 IgGγ plasmid as a template, K322A forward primer: CAAGGAGTACAAGTGCGCGGTCTCCAACAAAGC and K322A reverse primer: GCTTTGTTGGAGACCGCGCACTTGTACTCCTTG. Template DNA was degraded by DpnI digestion for 1hr at 37°C. The PCR produced plasmid was purified by gel extraction and propagated plasmid was sequenced (Eurofins DNA) in order to verify the codon change (AAG/GCG) and that no additional undesired mutations were introduced.

Complement C1q binding of h2G7 and the K322A mutant were assayed by immobilising the antibody onto a plate and exposing to C1q in normal human serum (NHS) diluted in PBS. Human serum albumin (HSA) was used as a negative control protein, as this does not bind to C1q. Human IgG complexes were used as a positive control for C1q binding.

3.2.5 EndoS deglycosylation and validation

This work was carried out by and in collaboration with investigators at the Karolinska Institutet.

Deglycosylation of h2G7 at N297 was performed using deGlycIT columns according to manufacturer's instructions (Genovis, Lund, Sweden). Briefly, h2G7 was applied to deGlycIT

columns, incubated for 15min at RT before centrifugation (1000*g*, 1min) and storage at -80°C.

Gel shift assay: 3.75µg of EndoS-treated antibody was subjected to SDS-PAGE on Tris-glycine 4-20% gradient gels (Bio-Rad). Gel was stained with Coomassie blue and destained in 10% acetic acid/40% MeOH. The deglycosylation effect was verified by a small mass-shift decrease for IgGγ.

***Lens Culinaris* Agglutinin (LCA) binding assay:** A microtiter ELISA plate (Corning) was coated with h2G7 or EndoS-treated h2G7 at 37°C for 2hr. The plate was washed 5x with 0.1% TBS-T. The plate was then blocked in 0.1% TBS-T for 1hr at RT. Equilibration of plate was performed by 5x washes with TC buffer (1mM Tris pH 7.5, 1mM $CaCl_2$, 1mM $MgCl_2$, 1mM $MnCl_2$ and 0.1% Tween). The plate was washed 5x with 0.1% TBS-T. Biotinylated LCA (Vector Labs) was diluted to 1µg/mL in TC buffer and added to the plate for 1h at 37°C. The plate was washed 5x with 0.1% TBS-T. Streptavidin-HRP was diluted according to manufacturer's instructions in 0.1% TBS-T and incubated for 20min at RT. The plate was washed 5x with 0.1% TBS-T. TMB liquid substrate solution was added and plates were incubated in the dark and the reaction stopped with 2N sulphuric acid.

FcγR binding assay: Human recombinant FcγRI (Life Technologies) was diluted to 1µg/mL in PBS and coated on a microtiter ELISA plate (Corning) at 37°C for 2hr. Plates were washed 3x with PBS-T (0.05%). Plate was blocked in 1% BSA in PBS for 1hr at RT. Plates were washed 3x with PBS-T (0.05%). Various concentrations of h2G7 and EndoS-treated h2G7 was diluted in antibody diluent (0.1% BSA, 0.05% Tween 20 in Tris-buffered saline) and added to the plate for 90min at RT. Plates were washed 3x with PBS-T (0.05%). Rabbit F(ab')2 anti-human (whole IgG, Dako P0406) was diluted 1:800 in antibody diluent and incubated for 45min at RT. Plates were washed 3x with PBS-T (0.05%). TMB liquid substrate solution was added and plates were incubated in the dark and the reaction stopped with 2N sulphuric acid.

3.2.6 Animal dosing regime

Male C57BL/6J mice (20-25g, *n=6* per group) were fasted overnight for 16hr. The following morning animals were administered a single intraperitoneal (*i.p.*) injection of APAP (530mg/kg) in 0.9% saline, or vehicle (0.9% saline) control. 2hr post-APAP, animals were then administered a single *i.p.* injection (on the opposite side) of antibody (E2, h2G7, K322A h2G7 or EndoS-treated h2G7) at 300µg/mouse, or PBS. At 10hr post-APAP, serum, liver and spleen samples were collected as described in Chapter 2, Section 2.2.4.

3.2.7 Determination of total hepatic glutathione (GSH)

Total hepatic GSH was determined as described in Chapter 2, Section 2.2.5 and as previously (Vandeputte et al., 1994).

3.2.8 Determination of alanine aminotransferase (ALT) activity in serum

Serum ALT activity was determined by assay according to the manufacturer's instructions (Thermo Scientific) and as previously described in Chapter 2, Section 2.2.6 and published (Goldring et al., 2004).

3.2.9 MicroRNA 122 (miR-122) quantification in serum

miR-122 was quantified in serum using the previously described method in Chapter 2, Section 2.2.7 and as published (Antoine et al., 2013).

3.2.10 Chemokines and cytokine quantification in serum

Serum MCP-1, CXCL1, TNFα and IL-6 concentration was determined by cytokine bead array (CBA) as described in Chapter 2, Section 2.2.9, according to the manufacturer's instructions (BD Biosciences). This assay was done in collaboration with colleagues at the Karolinska Institutet.

3.2.11 Liver myeloperoxidase (MPO) activity assay

Myeloperoxidase (MPO) activity was assayed in liver homogenates as described in Chapter 2, Section 2.2.10 according to a method derived from (Scaffidi et al., 2002).

3.2.12 Anti-human IgG Western blot on mouse liver lysates

Anti-human Western blots were run on liver RIPA lysates as described in Chapter 2, Section 2.2.11.

3.2.13 Statistical analysis

Statistical analysis of data was undertaken using GraphPad Prism 5 software. All results are presented as mean±standard error of the mean (SEM). Data were assayed for normality by Shapiro-Wilk test. Normal data were compared by One-Way ANOVA or unpaired t-test as indicated. Non-parametric data were compared by Kruskal Wallis or Mann-Whitney tests as indicated. Results were considered significant when $p<0.05$.

3.3 Results

3.3.1 Validation of K322A mutant: Determination of C1q binding

Validation of the K322A mutation of h2G7 was determined by collaborators at the Karolinska Institutet through investigating the binding of human C1q to immobilised antibody. The antibody was either coated directly onto the plate (Fig.3.2A), or was coated via binding to immobilised HMGB1 (Fig.3.2B) and tested for C1q binding using normal human serum (NHS). The K322A mutation of h2G7 completely eliminated C1q binding to a level comparable to the negative control protein human serum albumin (HSA). When the antibodies were coated directly, unmodified h2G7 bound to C1q with a similar affinity as positive control aggregated IgG immune complexes (Fig.3.2A). When the antibodies were coated through binding to pre-coated HMGB1, the aggregated IgG complexes did not bind to the plate, and hence did not subsequently bind C1q (Fig.3.2B).

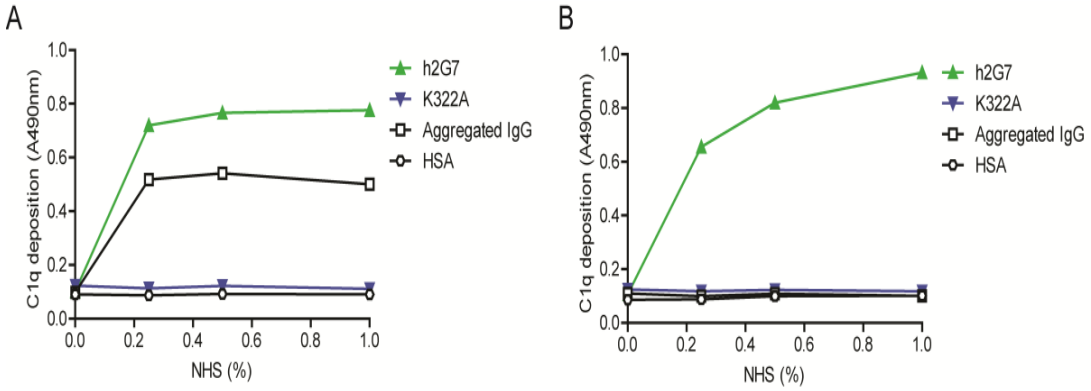

Fig.3.2 – C1q binding capability of h2G7 and K322A h2G7. (A) Antibodies or control protein (human serum albumin (HSA)) were directly coated onto the detection plate. (B) The antibodies were coated through conjugation to pre-coated HMGB1 on the detection plate. Normal human serum (NHS) was applied to the plate at 0, 0.25, 0.5 and 1% concentrations diluted in PBS. Bound C1q was detected using an anti-C1q antibody.

3.3.2 Validation of deglycosylation of h2G7 by EndoS treatment by Gel shift, LCA and FcγR binding assays

Validation of the deglycosylation of h2G7 was undertaken by collaborators at the Karolinska Institutet. A small decrease in the molecular weight of the IgG heavy chain, from approximately 55kDa to 53kDa was observed following EndoS treatment, indicating deglycosylation of h2G7 (Fig.3.3A). No effect was seen on the light chain (25kDa). The LCA assay detects the glycosylated asparagine residue at N297 (Nandakumar et al., 2007). Deglycosylation by EndoS treatment resulted in a loss of signal in the LCA assay in comparison with the untreated h2G7 antibody (Fig.3.3B-C). EndoS-mediated deglycosylation reduced the luminescence reading to background levels up to 100ng/mL antibody. h2G7 binds to immobilised FcγRI, however following EndoS treatment this binding was inhibited, up to a concentration of 3ng/mL (Fig.3.3D-E).

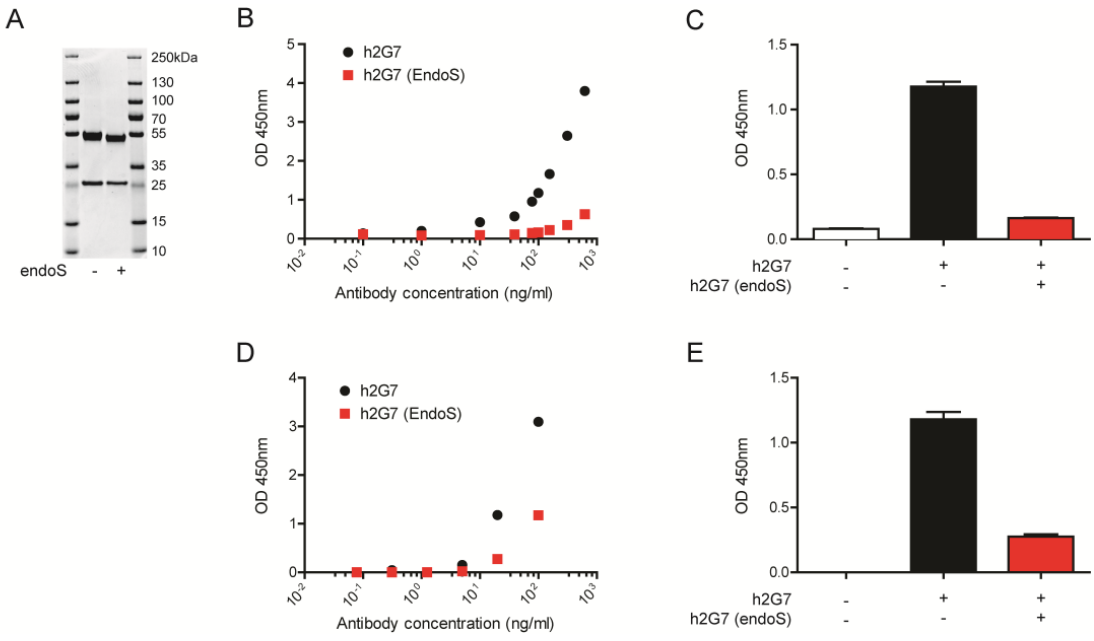

Fig.3.3 – Validation of the EndoS-mediated deglycosylation of h2G7. (A) Gel shift assay, (B and C) *Lens Culinaris* agglutinin (LCA) assay, (D and E) FcγRI binding assay. Data is representative of the batch of EndoS-treated antibody that was used in the later *in vivo* experiments.

3.3.3 The impact of APAP and different chimeric anti-HMGB1 antibodies on total hepatic glutathione (GSH)

There was no effect on hepatic GSH seen in response to any of the antibodies in saline control animals. However hepatic GSH was significantly depleted in all APAP treated animals in comparison with the corresponding saline group. There was a significant difference seen between APAP+E2 (6.34±0.93 nmol/mg protein) and APAP+h2G7 (21.54±2.28 nmol/mg protein) (Fig.3.4). More importantly, there was no difference observed between any of the h2G7 variants.

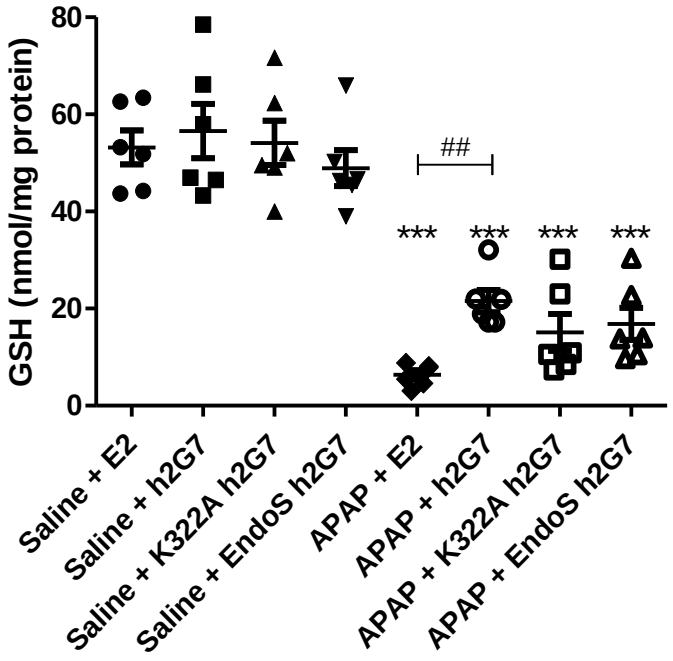

Fig.3.4 – Liver GSH levels in male C57BL/6 mice administered saline or APAP (530mg/kg, *i.p.*) for 10hr, with h2G7 variants or E2 at 2hr post-APAP/saline (*i.p.*). Data is represented as mean±SEM of *n=6* mice per group. *** = p<0.001, as compared with antibody-matched saline group. ## = p<0.01 between the indicated groups as determined by One-Way ANOVA.

3.3.4 The impact of APAP and different chimeric anti-HMGB1 antibodies on serum ALT activity

Serum ALT activity was significantly elevated in APAP+E2 treated animals in comparison with saline+E2 treated animals (5628±157.3 vs 43.38±7.03 U/L). Treatment with h2G7 (3177±669.7 U/L) and K322A h2G7 (3096±754.8 U/L) showed significant attenuation of the APAP-dependent rise in ALT activity seen with APAP+E2. There was a decrease in ALT activity observed in the EndoS h2G7 treated animals, however this was not significant (3495±703.2 U/L). Additionally, there was no difference in ALT activity seen between the h2G7 variants (Fig.3.5).

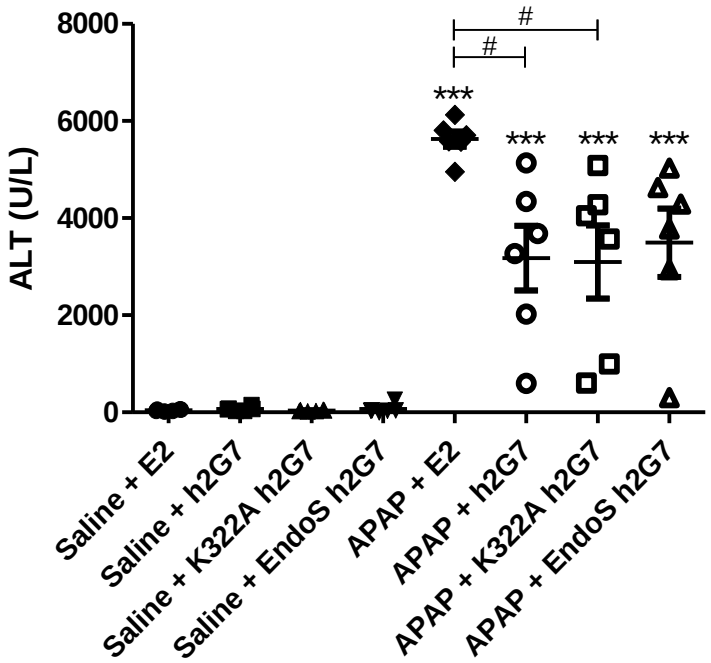

Fig.3.5 – Serum ALT levels in male C57BL/6 mice. Mice were administered saline or APAP (530mg/kg, *i.p.*) for 10hr, with h2G7 variants or E2 at 2hr post-APAP/saline (*i.p.*). Data is represented as mean±SEM of *n=6* mice per group. *** = p<0.001, as compared with antibody-matched saline group. # = p<0.05 between the indicated groups as determined by Kruskal-Wallis test.

3.3.5 The impact of APAP and different chimeric anti-HMGB1 antibodies on serum miR-122

Serum miR-122 was significantly elevated in APAP+E2 treated animals (14866±4746 ΔΔCt miR-122/Let-7d) in comparison with saline+E2 treated animals (94.99±29.92 ΔΔCt miR-122/Let-7d). This elevation was significantly attenuated with h2G7 (3366±729.8 ΔΔCt miR-122/Let-7d), but not significantly with K322A h2G7 (4564±2218 ΔΔCt miR-122/Let-7d) and EndoS-treated h2G7 (3958±1960 ΔΔCt miR-122/Let-7d), although a decrease was seen (Fig.3.6). There were no significant differences between h2G7 variants.

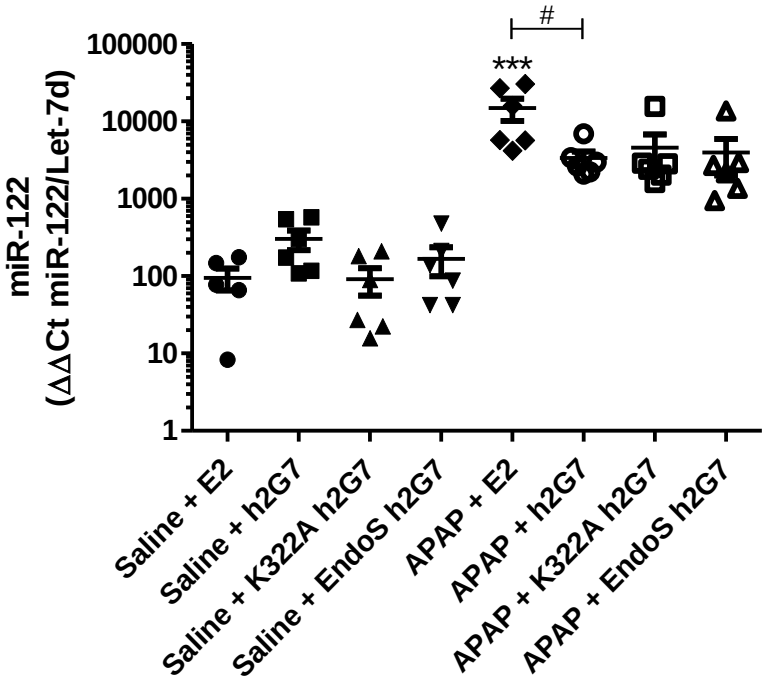

Fig.3.6 – Serum miR-122 levels in male C57BL/6 mice. Mice were administered saline or APAP (530mg/kg, *i.p.*) for 10hr, with h2G7 variants or E2 at 2hr post-APAP/saline (*i.p.*). Data is represented as mean±SEM of *n=6* mice per group. *** = p<0.001, as compared with antibody-matched saline group. # = p<0.05 between the indicated groups as determined by Kruskal-Wallis test.

3.3.6 The impact of APAP and different chimeric anti-HMGB1 antibodies on serum chemo- and cytokines

Serum MCP-1, CXCL1 and TNFα were all elevated in response to APAP. Significant attenuation of serum MCP-1 was seen for h2G7 and K322A h2G7, but not EndoS-treated h2G7. Significant reduction in CXCL1 and TNFα were seen with all h2G7 variants, to the lower limit of detection of the assay. No differences were observed between the variants for all chemokines/cytokines (Fig.3.7A-C).

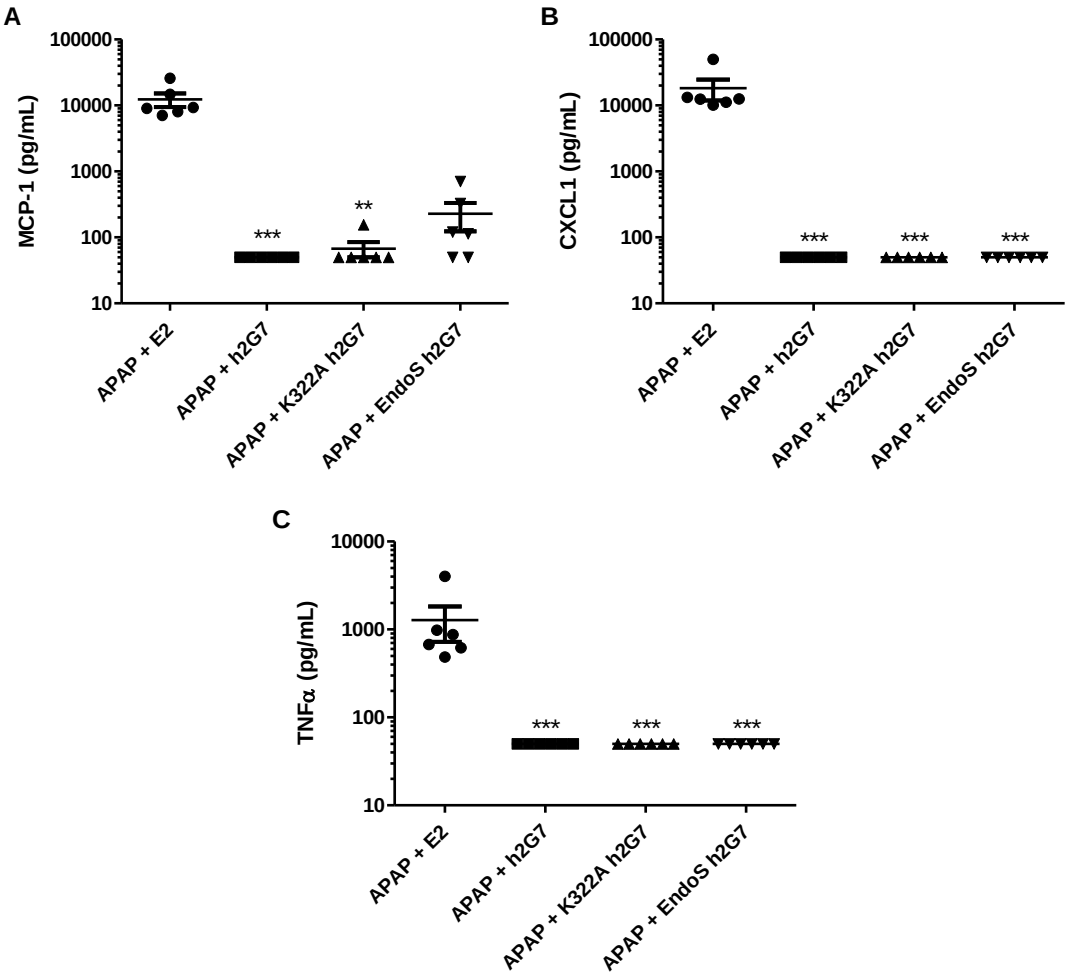

Fig.3.7 – Serum cytokine and chemokine levels in APAP-treated male C57BL/6 mice. A) MCP-1, B) CXCL1 and C) TNFα release in male C57BL/6 mice administered APAP (530mg/kg *i.p)* for 10hr, with h2G7 variants or E2 at 2hr post-APAP/saline (*i.p.*). Data is represented as mean±SEM of *n=6* mice per group. ** = p<0.01, *** = p<0.001 compared with APAP+E2 as determined by Kruskal-Wallis test. The lower limit of detection was 49pg/mL.

3.3.7 The impact of APAP and different chimeric anti-HMGB1 antibodies on liver myeloperoxidase (MPO) activity

An increase in hepatic MPO activity was evident in the APAP-treated animals (0.466±0.129 OD_{450}/20µg protein) in comparison with the saline+E2 (0.326±0.019 OD_{450}/20µg protein) control group, although this was not significant. Non-significant decreases in MPO activity, in comparison to APAP+E2, were seen in animals given the anti-HMGB1 therapy, regardless of the h2G7 variant (Fig.3.8).

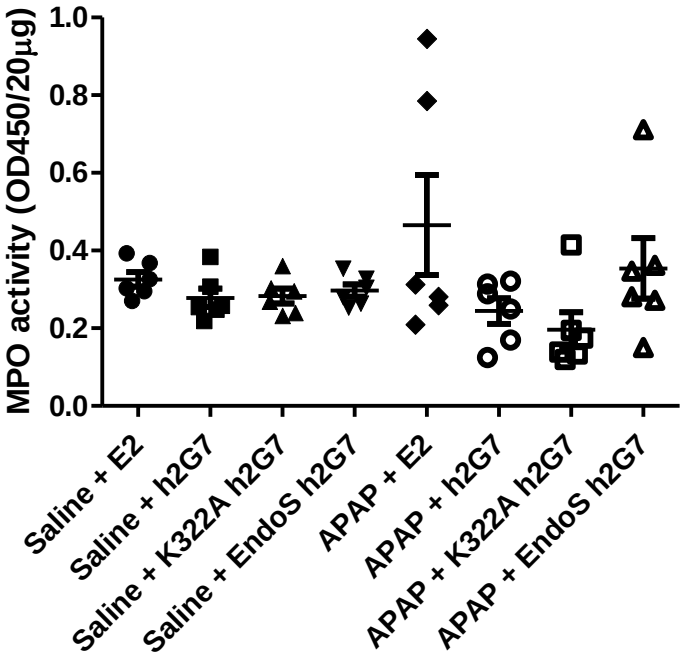

Fig.3.8 – Liver MPO activity in male C57BL/6 mice. Mice were administered saline or APAP (530mg/kg, *i.p.*) for 10hr, with h2G7 variants or E2 at 2hr post-APAP/saline (*i.p.*). Data is represented as mean±SEM of *n=6* mice per group.

3.3.8 Liver localisation of antibodies

Western blots for human IgG contained in RIPA lysates of liver tissue showed enrichment of antibody in APAP-treated animals in comparison with the saline-treated animals given the same dose of antibody. This was the case for E2 as well as the three h2G7 variants. In APAP-treated animals there were no differences in human IgG liver expression between the different antibody groups. In saline-treated animals there was greater liver expression of E2 than there was for any of the h2G7 variants. There is a slight shift in MW between E2 and h2G7 and K322A, and also a small decrease from the MW of h2G7 to that of EndoS-treated h2G7 (Fig.3.9).

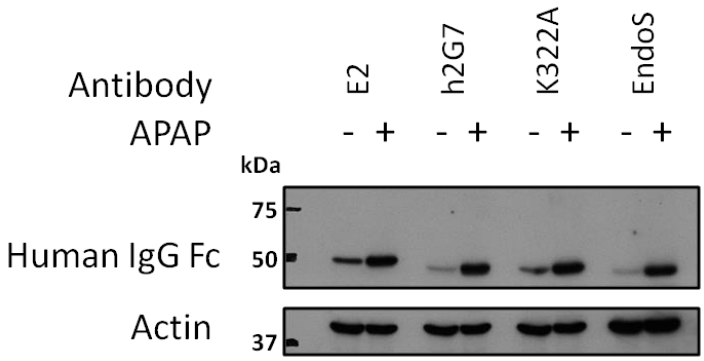

Fig.3.9 – Liver expression of human IgG-containing antibodies. Representative Western blot for human IgG heavy chain in the liver of C57BL/6 mice administered saline or APAP (530mg/kg, *i.p.*) for 10hr, with h2G7 variants or E2 at 2hr post-APAP/saline (*i.p.*). Actin was used as a loading control.

3.4 Discussion

Complement activation is an important aspect of the immune response to infection and injury, aiding the innate immune system in resolving the insult appropriately. Complement activation though antibody-C1q binding can lead to the removal of antigen from the site of injury through phagocytosis by activated immune cells. The C1q binding assay shows that there is significant human C1q binding to unmodified h2G7, independent of whether the antibody is either directly, or via HMGB1, coated onto the assay plate. However the K322A mutant displays no C1q binding in either test system, indicative of successful mutation of the key residue required for C1q binding. This data fits well with literature that shows the elimination of CDC capability of IgG with the K322A mutation (Idusogie et al., 2000). As a result of the absence of C1q binding, K322A mutated h2G7 would not activate the classical complement signalling cascade *in vivo*, and hence the K322A mutant h2G7 was suitable for investigating the effects of the complement system in the mechanism of action of h2G7.

FcγR-mediated effects are another potential mechanism of action of h2G7. The Fc region of antigen-bound IgG antibodies binds to FcγR and activates immune cells, leading to a range of cytotoxic responses such as phagocytosis and release of lysozyme enzymes (Jefferis and Lund, 2002). Recognition of the Fc region of IgG antibodies is dependent upon the glycosyl chains bound to N297, as they help to mediate the interaction between FcγR and Fc region by maintaining the structure of the Fc region (Krapp et al., 2003). EndoS treatment to remove N297 glycosyl groups, and hence the capability of h2G7 to bind to FcγR, was verified by three different assays (gel shift, LCA and FcγR binding). The gel shift and LCA assays demonstrated a deglycosylation of N297, and the FcγR binding assays showed a loss of FcγR binding function. These assays confirm that EndoS-treated h2G7 was unable to activate FcγR-mediated responses, and fit with previous literature demonstrating a lack of

FcγR function of deglycosylated IgG antibodies (Allhorn et al., 2008, Nandakumar et al., 2013).

The use of GSH levels as a marker of APAP bioactivation has previously been discussed in Chapter 2. The level of GSH depletion was similar to that seen in Chapter 2, and seen in other models of AILI (Antoine et al., 2010, Antoine et al., 2009). There were no significant differences between liver GSH in any of the anti-HMGB1 treated groups, demonstrating no effect of the K322A mutation or EndoS treatment on the bioactivation of APAP in comparison with h2G7. However, there was a significant difference in GSH observed between APAP+E2 and APAP+h2G7 groups. As a result of the anti-HMGB1 treatment, these animals underwent less severe toxicity than the APAP+E2 mice, and therefore may have had an increased appetite, allowing greater GSH resynthesis. Faster resynthesis of GSH has been shown in fed vs fasted mice (Antoine et al., 2010). This hypothesis could be explored by investigating the expression of GSH synthesis enzymes in the livers of the animals, by Western blot, and also quantification of GSH adduct formation by LC-MS/MS to ascertain any differences in bioactivation.

Serum ALT activity was significantly elevated in APAP+E2 treated animals in comparison with saline+E2. This fits with the data in Chapter 2 and other murine models of AILI (Amaral et al., 2013, Antoine et al., 2010, Williams et al., 2014). There was significant attenuation of the rise in ALT in animals given APAP+h2G7 or K322A h2G7, but there was not quite a significant depletion in the APAP+EndoS-treated h2G7 group. However there was no significant difference between the ALT levels of any of the h2G7 variants, demonstrating that modification of h2G7 by either K322A or EndoS does not affect the amount of attenuation of liver injury caused by h2G7. This indicates that neither CDC nor FcγR-mediated responses are implicated in the mechanism of action of h2G7, and suggest that neutralisation of HMGB1 through sequestration is the likely mechanism of action of the

h2G7 antibody. The level of attenuation of ALT activity in h2G7 treated animals is similar to that seen in Chapter 2 and previous experimental studies of anti-HMGB1 antibodies in AILI in mice (Antoine et al., 2010).

Serum miR-122 data further supports the absence of a role of CDC and FcγR-mediated responses in the mechanism of action of h2G7. Serum miR-122 was significantly elevated in APAP+E2 animals compared with saline+E2 controls, indicating miR-122 release in AILI, as has previously been seen in BALB/c mice (Wang et al., 2009). This elevation was significantly reduced by administration of anti-HMGB1 antibody, regardless of residue 322 or the glycosylation status of N297.

MCP-1, CXCL1 and TNFα are important amplifiers of the inflammatory response that recruit (MCP-1, CXCL1) and activate (TNFα) immune cells to the site of injury (Takada et al., 1995, Antoniades et al., 2012, Dambach et al., 2002). Anti-HMGB1 antibody treatment has previously been shown to attenuate TNFα release in mice (Antoine et al., 2010). Serum levels of all three proteins were significantly elevated in APAP+E2 treated animals in comparison with saline+E2 animals. This elevation in serum chemokines and cytokine release was diminished by anti-HMGB1 treatment, with h2G7, K322A h2G7 and EndoS-treated h2G7 all significantly reducing serum levels of all three chemokines/cytokines. As seen with both ALT and miR-122, there was no difference between any of the h2G7 variants, again supporting the hypothesis that neither CDC nor FcγR-mediated responses are implicated in the mechanism of action of h2G7.

Liver MPO is indicative of neutrophil activation, and is elevated in APAP+E2 treated animals compared with saline+E2 animals, although not significantly. This increase in MPO activity is reduced in h2G7 treated animals, as well as in K322A and EndoS-treated h2G7 variants. This data shows that anti-HMGB1 treatment successfully inhibits APAP-induced neutrophil activation, potentially through a reduction in hepatic necrosis (as indicated by the ALT data

and miR-122), leading to less DAMP release and hence less neutrophil recruitment. However, the role of neutrophils in AILI still remains controversial, with conflicting reports of the contribution of neutrophils to injury (Williams et al., 2014, Marques et al., 2012).

Investigation of the localisation of h2G7, K322A h2G7 and EndoS-treated h2G7 to the liver show clear enrichment of the antibody to the liver in the APAP-treated animals in comparison with the saline-treated animals for all antibodies. Additionally, in APAP treated animals there is no difference in the expression of the antibodies between h2G7 variants. This suggests that the modification of h2G7 does not affect the ability of the antibody to locate to the site of injury and HMGB1 release. This would be expected as the high affinity for antigen (HMGB1), large size (approximately 150kDa) and hydrophilic nature of monoclonal antibodies hamper their movement between tissues and mean that they localise at the site antigen (Keizer et al., 2010).

In our model we would not expect much elimination of the antibodies. Due to the size of monoclonal antibodies (mAbs), they are not eliminated in the urine, and are instead subject to metabolism to peptides and amino acids that can then be used for protein synthesis or are excreted by the kidney (Keizer et al., 2010). Elimination mechanisms for mAbs are not well defined, but mechanisms include FcγR-mediated internalisation by monocytes and macrophages and non-specific endocytosis. Both of these mechanisms result in lysosomal degradation of the antibody (Keizer et al., 2010). However, generally the half-lives of monoclonal antibody treatments are long, so little elimination of the antibodies would be expected in the 8hr treatment time of the experiment (Keizer et al., 2010).

There is a small decrease in the observed MW of h2G7 variants in comparison with E2, which, as discussed in Chapter 2, could be due to differences in the total amino acid mass of the Fab regions. Furthermore, there is another decrease in MW of the EndoS-treated

h2G7 relative to h2G7 and K322A h2G7, suggesting further evidence of the successful deglycosylation following EndoS treatment.

Future studies will investigate if any histological differences are seen between the h2G7 variants with regards to hepatocellular damage, neutrophil infiltration and HMGB1 release. Given the data obtained within this chapter and Chapter 2, differences between any of the h2G7 variants would not be anticipated. However, as observed in the previous chapter, there should be a significant decrease in hepatocellular necrosis and neutrophil infiltration in h2G7-treated animals.

Another important consideration with regards to future development of an anti-HMGB1 antibody as a therapeutic for the treatment of APAP overdose is the effect of the antibody on regeneration of the liver. Evidence suggests that HMGB1 impairs hepatocyte regeneration following APAP overdose in C57BL/6 mice (Yang et al., 2012a) but yet compounds with anti-HMGB1 effects such as ethyl pyruvate may also impair regeneration (Yang et al., 2012b).

The work in this chapter demonstrates that the mechanism of action of the anti-HMGB1 antibody, h2G7, in a model of APAP overdose is not dependent on complement-mediated or FcγR-mediated pathways. Instead it appears that the mechanism of action of h2G7 is through neutralisation of the target molecule, HMGB1, and that this results in the phenotypic attenuation of AILI. It is perhaps not unexpected that there is no ADCC-mediated mechanism of action of h2G7 as this relies on antigen (HMGB1) to be bound on the cell surface, and HMGB1 expression has not previously been seen on the surface of hepatocytes. However, the experiments indicate that there are no other FcγR-mediated effects. Additionally, due to species differences, it was unlikely that the human IgG1 backbone of h2G7 would activate the murine complement system. Assessment of the

ability of h2G7 to bind to murine C1q should be investigated, to confirm the findings in this chapter.

As a result of the investigations in this chapter, a better understanding of the mechanism of action of h2G7 was established, and now h2G7 has the potential to be utilised in other *in vivo* models of inflammatory conditions. However, despite this, further work should also be undertaken to develop antibodies that target specific post-translationally modified forms of HMGB1, to allow investigation into the role of specific HMGB1 isoforms at different stages of the inflammatory process and the role of different PTMs on HMGB1 function. PTM-specific antibodies could then also be developed as a therapeutic intervention to lead to decreased initiation and improved resolution of HMGB1-mediated injury.

Chapter Four

Redox regulation of HMGB1 cytokine-inducing function

CONTENTS

4.1 Introduction

Reduction and oxidation (redox) of proteins is a key post-translational modification, which can lead to substantial modifications in protein structure, localisation and function. Oxidative modification of sulphur-containing residues (cysteine or methionine) can also be important in regulating the expression of proteins, as conformational changes associated with oxidation can lead to modulation of protein function and downstream signalling (Spickett and Pitt, 2012).

Cysteine is a sulphur containing amino acid that can be oxidised at its sulphydryl group (Fig.4.1). In the cytosol, the sulphydryl usually exists in the thiol state, due to the reducing environment (Go and Jones, 2008). However, in the presence of an oxidising environment (e.g. endoplasmic reticulum or extracellular), the cysteine sulphydryl group can be oxidised to a sulphenic acid (R-SOH) by reactive oxygen species (ROS). The sulphenic acid is generally unstable and can subsequently be irreversibly oxidised to sulphinic ($R\text{-}SO_2H$) or sulphonyl ($R\text{-}SO_3H$) acid derivatives. The sulphenic acid may also form a disulphide bridge through reacting with the thiol group on another cysteine residue, either within the same protein or with another protein. Disulphide bridges can also occur through thiol-disulphide exchange reactions, for example with oxidised glutathione (GSSG) (Spickett and Pitt, 2012, Paget and Buttner, 2003). Additionally, cysteine can be oxidised by reactive nitrogen species (RNS) such as nitric oxide (NO) to form a S-nitrosothiol (R-SNO) or by peroxynitrite ($ONOO^-$) to an S-nitrothiol (Cooper et al., 2002). Methionine, the other sulphur containing residue cannot form disulphide bridges. Disulphide bridges can link peptide chains as seen classically in the linking of the heavy chains of immunoglobulins. Disulphide bridges can also hold a protein in a new conformation. Cysteine redox has been associated with the modulation of the function of other DAMP molecules (Rubartelli and Lotze, 2007).

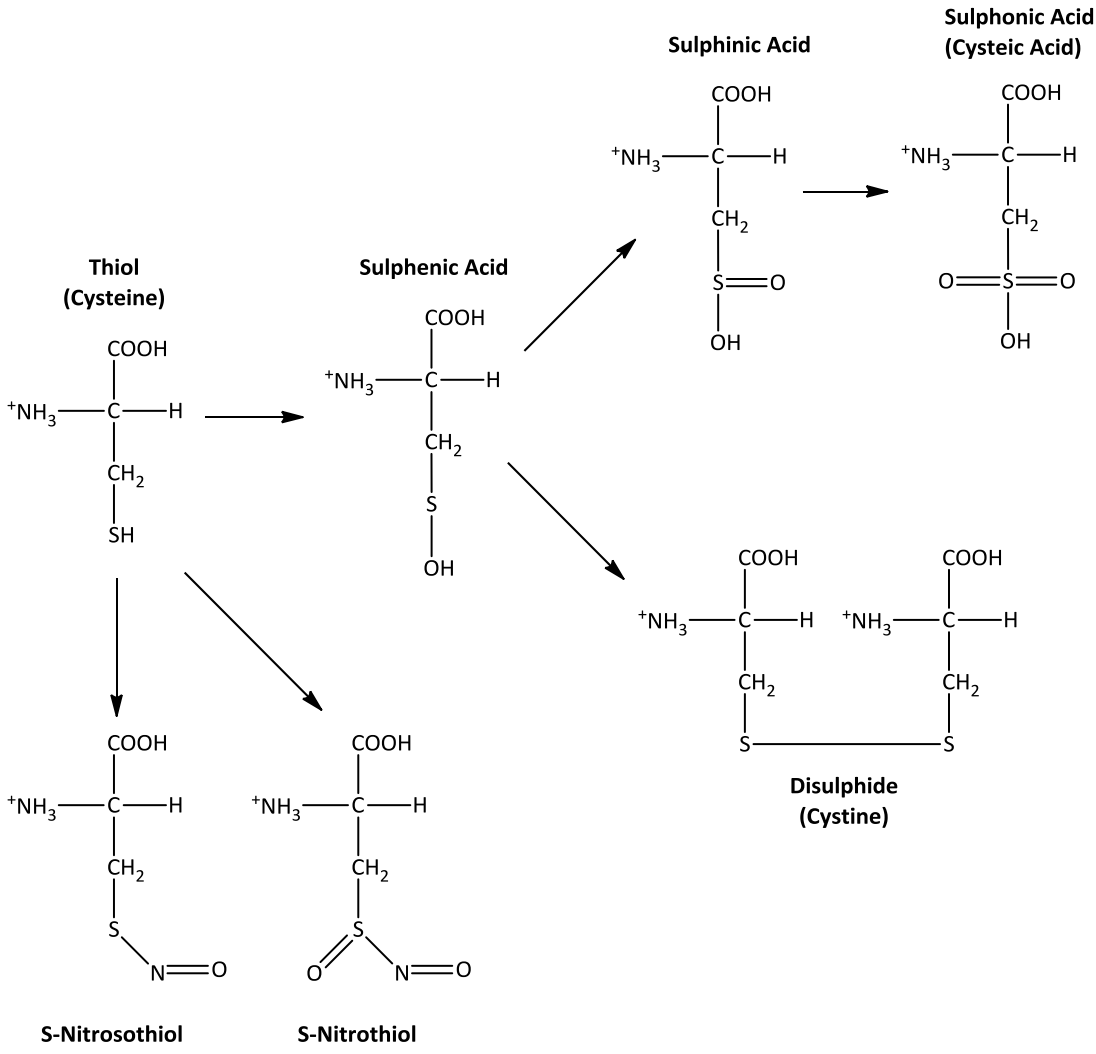

Fig.4.1 – Overview of cysteine redox states. Adapted from (Paget and Buttner, 2003, Griffiths et al., 2002).

HMGB1 contains three conserved cysteine residues (Cys 23, 45 and 106) which are subject to redox modification. Cysteine 23 and 45 are located in the A box region, and can form a disulphide bridge in the presence of mild oxidising conditions. Cysteine 106 is located in the B box, and does not form a disulphide bridge. In strongly oxidising conditions, such as those occurring during caspase-mediated cleavage of mitochondrial complex 1 and subsequent ROS release, HMGB1 can be terminally oxidised at all cysteines leading to a loss of proinflammatory activity (Kazama et al., 2008). Disulphide bridge formation has been shown to cause a conformational change in HMGB1 A box (Sahu et al., 2008).

HMGB1 receptors include TLR2, TLR4, TLR9 and RAGE (Park et al., 2006, Hori et al., 1995, Tian et al., 2007, Ivanov et al., 2007, Yu et al., 2006) . TLR4 has been the focus of much research of HMGB1 function, as this receptor has been shown to be responsible for HMGB1-mediated cytokine release, with both HMGB1 alone (Yang et al., 2010) or in complex with the prototypical TLR4 ligand, LPS, able to induce cytokine release (Hreggvidsdottir et al., 2012). HMGB1 induces cytokine release from macrophages through TLR4 binding in a MD-2 dependent manner. A requirement of HMGB1-induced cytokine release is the presence of a cysteine at residue 106 (Yang et al., 2010). HMGB1 can also induce chemotaxis of immune cells through RAGE and CXCL4 binding (Yang et al., 2007, Venereau et al., 2013, Schiraldi et al., 2012).

TLR4 binding leads to NF-κB signalling activation. Activation of the NF-κB system results in translocation of NF-κB (p65/p50) to the nucleus and transcription of target genes. Some of the most important target genes for the NF-κB signalling pathway are those encoding cytokines. Cytokines are proteins that are released into the extracellular environment whereby they bind to receptors on target cells and facilitate pro- or anti-inflammatory signalling processes. The tight regulation of cytokine production and release allows immune cells to regulate inflammatory signalling. TNFα and IL-6 are two cytokines whose expression and release are regulated by NF-κB signalling.

TNFα is a transmembrane protein that arranges into stable homotrimers. TNFα can be released as a result of proteolytic cleavage by ADAM17, to form soluble TNFα (sTNFα). Both the sTNFα and membrane-bound forms have biological activity. TNFα can be actively released by a range of cell types, although classically TNFα release from macrophages has predominated in the literature. Other TNFα secreting cell types include fibroblasts, NK cells, and CD4+ lymphocytes. TNFα acts through binding to two receptors TNFR1 and TNFR2. TNFR2 is exclusively expressed on immune cells and is responsive to membrane-bound

TNFα. TNFR1 is able to bind both the sTNFα and membrane-bound forms, and then activate three different downstream signalling cascades: NF-κB signalling, MAPK signalling and the cell-death receptor pathway. In models of DILI, TNFα has been shown to be a key coordinator of proinflammatory activity (Blazka et al., 1996).

IL-6 is a cytokine secreted from macrophages which exhibits pro- and anti-inflammatory activities. IL-6 binds to the IL-6 receptor, IL-6Rα (CD126), and upon ligand binding, gp130 (CD130) is recruited to the IL-6Rα chain, forming a complex. Additionally, a soluble form of IL-6Rα is released into the extracellular environment, which can bind to extracellular IL-6 and then insert into the membrane of non-IL-6Rα expressing cells, and form the signalling complex with gp130. This form of IL-6 recognition is responsible for signalling the results in the proinflammatory responses to IL-6. Binding of IL-6 to membrane bound IL-6Rα is responsible for anti-inflammatory effects of IL-6 (Scheller et al., 2011). IL-6 binding to the IL-6 receptor complex leads to activation of JAK/STAT signalling. JAK (Janus kinases) are responsible for phosphorylating STAT proteins that translocate to the nucleus and are responsible for binding to genes with a GAS promoter region. These genes encode proteins involved in cell proliferation and differentiation. In the context of hepatotoxicity, IL-6 null mice have shown increased liver injury following toxic or drug insult (Kovalovich et al., 2000, Masubuchi et al., 2003), demonstrating the important role IL-6 plays in the resolution of liver injury.

A schematic representation of the proinflammatory signalling pathways activated following TLR4 activation is shown in Fig.4.2.

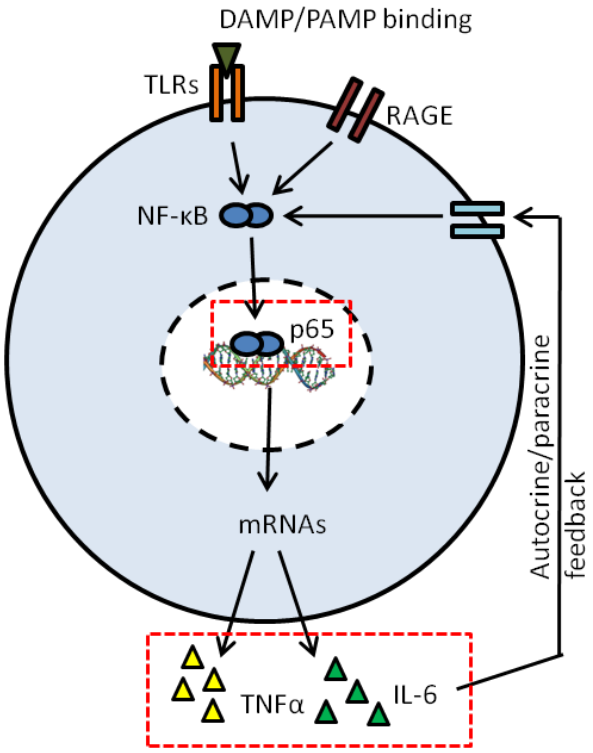

Fig.4.2 – Overview of the proinflammatory signalling pathways following TLR4 activation. Dashed red boxes indicate areas to be used to investigate the proinflammatory capability of different redox isoforms of HMGB1

THP-1 cells are a human monocyte-like cell line and RAW264.7 cells are a mouse macrophage cell line. These cell lines were chosen as model cell lines for investigating the role of different redox forms of HMGB1 as they are sensitive to other proinflammatory stimuli such as LPS, and are capable of proinflammatory cytokine production and release (Lozanski et al., 1992, Jang et al., 2006, Yang et al., 2010).

4.1.1 Aims

The first aim of this chapter was to optimise an *in vitro* system for assessing proinflammatory capability, using LPS as a positive control stimulator of proinflammatory signalling in THP-1 or RAW264.7 cell lines.

Subsequently the aim was to determine the cytokine stimulating activity of different cysteine redox isoforms of HMGB1.

4.2 Materials and Methods

4.2.1 Materials

Fetal bovine serum, fluorescent antibodies for immunofluorescence and Prolong Gold was purchased from Life Technologies (Paisley, UK). Donkey serum was purchased from Jackson Immunoresearch (PA, USA). Anti-p65 antibody was purchased from Santa Cruz Biotech (Heidelberg, Germany). Bio-Rad Protein Assay Dye Reagent, Precision Plus Kaleidoscope Standards (molecular weight markers) and non-fat milk was purchased from Bio-Rad Laboratories Ltd (Hemel Hempstead, UK). Amersham Hybond ECL membrane and Amersham Hyperfilm ECL were purchased from GE Healthcare (Little Chalfont, UK). Western Lightning Plus-ECL was purchased from Perkin Elmer (Beaconsfield, UK). TNFα and IL-6 ELISA kits were purchased from R&D Systems (Abingdon, UK). CellTiter 96® Aqueous One Solution assay kit was purchased from Promega (Southampton, UK). All other materials were purchased from Sigma-Aldrich (Poole, UK) or Fisher Scientific (Loughborough, UK) unless otherwise indicated.

4.2.2 Cell culture

THP-1 cells were purchased from the ATCC and cultured in RPMI-1640 media supplemented with 10% heat-inactivated fetal bovine serum (FBS), 2mM L-glutamine and 100U/mL penicillin and 100µg/mL streptomycin at 37°C in 5% CO_2. Cells were used up to passage 32, after which a noticeable drop in the sensitivity of the cells was observed.

RAW264.7 cells were purchased from the ATCC and cultured in Dulbecco's Modified Eagle Medium (DMEM) supplemented with 10% heat-inactivated FBS, 2mM L-glutamine, 100U/mL penicillin and 100µg/mL streptomycin at 37°C in 5% CO_2.

4.2.3 NF-κB activation in response to LPS

Dose response sample preparation:

THP-1 ($5x10^6$ in 7mL) or RAW264.7 ($3x10^6$ in 5mL) cells were cultured in complete growth media for 24hr at 37°C in 5% CO_2 in T25 flasks. THP-1 cells were then dosed with LPS (from Escherichia coli 0111:B4) by addition of 3mL fresh complete growth media containing the different doses of LPS, to bring the total volume of each flask to 10mL. Alternatively, RAW264.7 ($3x10^6$) cells were dosed by replacement of the media with 5mL of fresh complete growth media containing the different doses of LPS. Cells were then incubated for 1hr at 37°C in 5% CO_2 before whole cell or cytosolic and nuclear lysis. Whole cell lysis was performed by pelleting the cells (300*g*, 5min), removal of the media, washing twice with Hank's balanced salt solution (HBSS) and resuspension of the cell pellet in 200µL of RIPA buffer supplemented with protease inhibitor cocktail (PIC). Samples were incubated on ice for 15min and then centrifuged (18400*g*, 5min, 4°C). Supernatants were stored at -80°C. Cytosolic and nuclear extraction was performed using a modified version of the method of Dignam et al (Dignam et al., 1983). Cells were pelleted (300*g*, 5min) and media removed. Cells were washed twice in HBSS and then subject to cell membrane lysis using Buffer A (50mM NaCl, 0.5M sucrose, 1mM EDTA, 10mM HEPES (at pH8), 0.5mM spermidine, 0.15mM spermine and 0.2% Triton X-100) and centrifuged (1150*g*, 5 min, 4°C). The supernatant was removed (cytosolic lysate), the pellet resuspended in Buffer B (50mM NaCl, 25% glycerol, 1mM EDTA, 10mM HEPES (at pH8), 0.5mM spermidine and 0.15mM spermine) and centrifuged (1150*g*, 5 min, 4°C). The supernatant was discarded and the pellet resuspended in Buffer C (350mM NaCl, 25% glycerol, 1mM EDTA, 10mM HEPES (at pH8), 0.5mM spermidine and 0.15mM spermine). The resuspended pellet was then incubated on ice for 30min and then centrifuged (1150*g*, 5 min, 4°C). The supernatant was removed (nuclear lysate) carefully to avoid taking up DNA. Cytosolic and nuclear lysates

were stored at -80°C. All buffers were supplemented with 0.5µL/mL β-mercaptoethanol and 2µL/mL protease inhibitor cocktail.

Timecourse sample preparation:

The same conditions as for the dose response (above), however, instead of multiple LPS concentrations, a single concentration (THP-1: 3ng/mL, RAW264.7: 100ng/mL) was applied to cells, and cells were lysed at 0, 1, 4, 8, 16 and 24hr.

4.2.4 Western blotting for p65 nuclear translocation

Nuclear and cytosolic samples were assessed for p65 expression in order to determine cytonuclear translocation of NF-κB in response to LPS. 5µg (total protein) of each sample was mixed with reducing agent and sample buffer, then denatured at 85°C for 5min. Samples were then loaded onto 10% acrylamide gels and proteins separated by electrophoresis in a Tris-Glycine running buffer. Proteins were electro-transferred onto a nitrocellulose membrane using 20% MeOH buffer for 1hr at 80V. Successful transfer and even loading was then checked using Ponceau Red. Membranes were washed with 0.1% Tween-TBS and blocked using 10% non-fat milk for 30min at RT with shaking. Membranes were cut membrane at the 50kDa marker using scalpel, to allow simultaneous probing for p65 (65kDa) and actin (42kDa). The appropriate membranes were then incubated with shaking for 1hr at RT with mouse monoclonal anti-p65 (1:1000 in 2% milk) or mouse monoclonal anti-actin (1:160,000 in 2% milk). Membranes were then washed (4x5min) with 0.1% Tween-TBS before addition of secondary anti-mouse IgG (1:5000 in 2% milk for p65 membrane, 1:10,000 for actin membrane) and incubation for 1hr at RT on shaker. Membranes were then washed (4x5min) with 0.1% Tween-TBS, and treated with electrochemiluminescence reagent (ECL Plus, Perkin Elmer) for 1min. Proteins were visualised using exposure to X-ray film. Films were scanned using a Bio-Rad GS800

calibrated densitometer (Bio-Rad, Hemel Hempstead, UK) and analysed using TotalLab TL100 software (TotalLab Ltd, Newcastle, UK).

4.2.5 IL-6 ELISA

Media samples from THP-1 or RAW264.7 cells treated with LPS or different redox molecular forms of HMGB1 were analysed for release of IL-6 by ELISA according to manufacturer's instructions (R&D Systems). Briefly, 96-well ELISA plates were coated at RT overnight with capture antibody (mouse anti-human IL-6 for THP-1, or rat anti-mouse IL-6 for RAW264.7), unbound capture antibody was then removed by washing with 0.05% Tween in PBS and plates were blocked with 1% BSA in PBS. Plates were washed and samples or recombinant human or mouse IL-6 standards (100µL) were added and incubated for 2hr at RT. Plates were rewashed to remove unbound protein, and a detection antibody (biotinylated goat anti-human or anti-mouse IL-6) added for 2hr. Plates were washed, streptavidin-HRP solution was added to the wells and incubated at RT in the dark for 20min. Excess streptavidin-HRP was removed by washing and a 3,3',5,5'-tetramethyl-benzidine (TMB) based substrate solution added for 10min in the dark. 50µL of 2N H_2S0_4 was then added to stop the colour development reaction and plates were read at 450nm on a MRX microtiter-plate reader with Max Revelation software (Dynatech Laboratories, Billinghirst UK).

4.2.6 TNFα ELISA

Media samples from THP-1 or RAW264.7 cells treated with LPS or different redox molecular forms of HMGB1 were analysed for release of TNFα by ELISA according to manufacturer's instructions (R&D Systems). Assay procedure was identical to that used for the IL-6 ELISA above, with the exception that the capture antibody, detection antibody and standards were mouse anti-human TNFα, biotinylated goat anti-human TNFα and recombinant human TNFα respectively for THP-1 samples or goat anti-mouse TNFα, biotinylated goat anti-mouse TNFα and recombinant mouse TNFα respectively for RAW264.7 samples.

4.2.7 Immunofluorescence (IF) of RAW264.7 activation in response to LPS

13mm glass coverslips were coated with 0.1% gelatin and placed into 12-well plates. RAW264.7 cells ($1x10^5$ cells/well) were plated into the wells, and allowed to adhere overnight. After adherence, cells were dosed with LPS for 24hr. Cells were washed with PBS and fixed with 4% PFA for 15min. 50mM NH_4Cl was used to quench the fixation. Cells were washed three times with PBS and permeabilised using 0.2% Triton X-100 for 10min. Cells were washed twice in TBS. Coverslips were blocked using 1% BSA and 5% donkey serum in TBST for 1 hr at RT. Coverslips were washed with TBST and probed with rabbit IgG polyclonal anti-HMGB1 (1:1000, 1hr, RT) in 1% BSA in TBST. Coverslips were washed x 3 in TBST. Secondary antibody (fluorescent-labelled donkey anti-rabbit (1:1000, 1hr, RT) and phalloidin (1:250, 1hr, RT) in 1% BSA in TBST were added to the coverslips and shielded from light. Coverslips were washed, and Hoechst stain (2µg/mL) was added to cells for 10min. Coverslips were washed in TBST and coverslips were mounted onto microscope slides along with 10µl of Prolong Gold. Coverslips were sealed using nail varnish. Slides were imaged using a Zeiss Axio Observer Z.1 microscope at 40x magnification using an Apotome.2 device.

4.2.8 Cytotoxicity assessment

RAW264.7 cells ($4x10^4$ cells/well) were plated into 96-well plates, allowed to adhere for 24hr, and then dosed with LPS (0-1000ng/mL) for 24hr. Cell viability was determined by CellTiter 96® Aqueous One Solution assay kit. Briefly, 20µL of 3-(4,5-dimethylthiazol-2-yl)-5-(3-carboxymethoxyphenyl)-2-(4-sulphophenyl)-2H-tetrazolium) (MTS) solution was added to the 100µL of cells in each well. Plates were incubated in the dark at 37°C for 1hr. The absorbance of 80µL of the contents of each well was measured at 490nm on a MRX microtiter-plate reader with Max Revelation software (Dynatech Laboratories, Billinghirst UK).

4.2.9 Mass spectrometric analysis of different molecular forms of HMGB1

Different molecular redox forms of rat recombinant HMGB1 were a gift from Dr H Yang (Feinstein Institute, NY, USA). HMGB1 redox isoforms were produced through exposure of recombinant HMGB1 to H_2O_2 (50 mM) or dithiothreitol (DTT) (5mM) for up to 120min. The different molecular forms of HMGB1 were defined by LC-MS/MS by and in collaboration with Dr D Antoine, and as discussed in Yang et al (Yang et al., 2012). Reduced cysteine residues within HMGB1 were characterised by thiol-specific alkylation with *N*-ethylmalemide (NEM) (50mM, 5min). Alkylation with NEM yields a mass-shift of 125amu (atomic mass unit). Sulphonyl (SO_3H) oxidative modification was determined by looking for a mass increase of 48amu on each particular cysteine residue. After the first alkylation step, rHMGB1 preparations were precipitated in ice-cold methanol (MeOH). MeOH was recovered by centrifugation (14000g, 10min, 4°C). Remaining cysteine residues engaged in a disulphide bond were reduced with DTT (1mM, 15min, 4°C). Newly reduced cysteines were then alkylated with deuterated NEM (d_5NEM) (50mM, 5min) which yields a mass shift of 130amu compared with unexposed thiols and 5amu compared with NEM-alkylated thiols. Samples were subject to tryptic digest (40ng/µL, 16hr, 37°C).

Samples were run on a hybrid triple quadrupole-linear ion trap mass spectrometer (QTRAP 5500, AB Sciex, Foster City, CA, USA) equipped with a NanoSpray II source by in-line LC using a U3000 HPLC System (Dionex, CA, USA) connected to a 180µm x 20mm nanoAcquity UPLC C_{18} trap column and a 75µm x 15cm nanoAcquity UPLC BEH130 C_{18} column (Waters, MA, USA) via reducing unions. Spectra were acquired automatically in positive ion mode using information-dependent acquisition (Analyst; Applied Biosystems). Database searching was performed using ProteinPilot 2 (Applied Biosystems) with the latest version of the SwissProt database, with the confidence level set at 80%, and with biological modifications

allowed. Individual peptide fragmentation to produce *b* and y ions was used to determine the amino acid sequence and confirm the presence of specific modifications.

4.2.10 NF-κB activation in THP-1 cells in response to different molecular forms of HMGB1

As per the LPS dose response and timecourse experiments described above, THP-1 cells ($5x10^6$) were cultured in 7mL complete growth media for 24hr at 37°C in 5% CO_2 in T25 flasks. After this 24hr period, a 40µL sample of the cells was taken and counted to determine the cell number (approximately $7x10^6$ cells). THP-1 cells were then treated with 1µg/mL of the four different molecular redox forms of HMGB1 for 0-24hr by addition of 3mL of complete growth media containing each molecular form of HMGB1 to give a final volume of 10mL. At 1hr, cells were lysed, nuclear and cytosolic lysates were produced and nuclear p65 expression was determined by Western blotting. At 24hr, the release of TNFα and IL-6 were determined by ELISA. In both cases, 100ng/mL LPS was used as a positive control for proinflammatory signalling induction.

4.2.11 Statistical analysis

Statistical analysis of data was undertaken using GraphPad Prism 5 software. All results are presented as mean±standard error of the mean (SEM). Data were assayed for normality by Shapiro-Wilk test. Normal data were compared by One-Way ANOVA or unpaired t-test as indicated. Non-parametric data were compared by Kruskal Wallis or Mann-Whitney tests as indicated. Results were considered significant when $p<0.05$.

4.3 Results

4.3.1 Whole cell p65 expression in THP-1 cells

In order to confirm p65 expression in THP-1 cells and the effects of LPS treatment on p65 expression, THP-1 cells were treated with 10µg/mL LPS for 0-24hr. Whole cell RIPA lysates were made, protein content assessed and Western blots for p65 expression were run. Densitometric data are shown in Fig.4.3. Western blotting shows that although there is a downward trend in p65 expression, there is no significant perturbation in whole cell p65 content following LPS treatment in THP-1 cells.

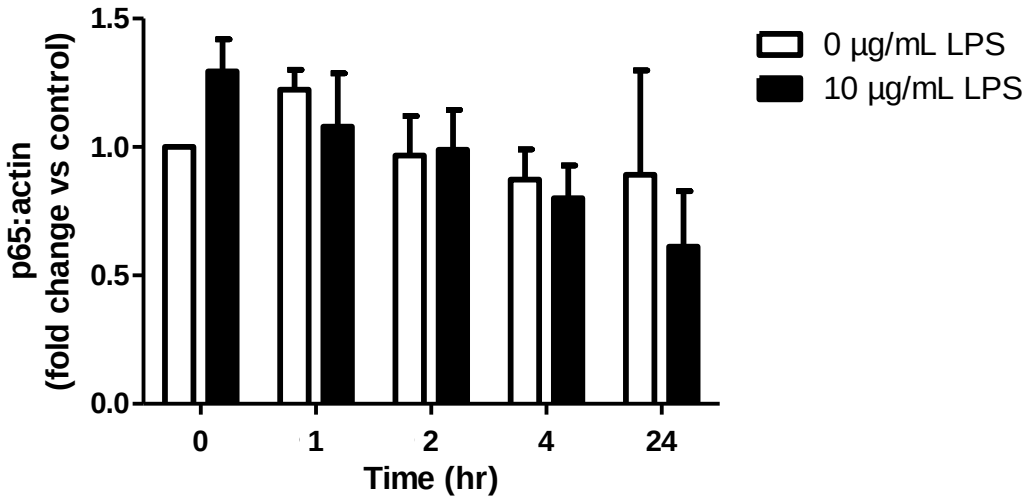

Fig.4.3 – Whole cell p65 expression in THP-1 cells following LPS treatment. THP-1 cells were treated with LPS (10µg/mL) for 0, 1, 2, 4 or 24hr. Numerical representation of Western blots for p65 expression on 5µg of RIPA whole cell lysates. Actin used as a loading control. Data is represented as mean±SEM of *n=3* individual experiments.

4.3.2 Nuclear p65 expression following LPS treatment in THP-1 and RAW264.7 cells

The transcription factor NF-κB is responsible for upregulation of proinflammatory signalling. Following LPS treatment, increased nuclear expression of p65, indicative of NF-κB signalling activation, was detectable in a dose- and time-dependent manner in both THP-1 and RAW264.7 cells (Fig.4.4 and Fig.4.5).

Dose-dependent nuclear p65 expression

In THP-1 cells, in the absence of LPS stimulation basal nuclear p65 expression was minimal. However following LPS stimulation up to a 75-fold increase in nuclear p65 (observed at 100ng/mL) was detectable compared with untreated controls. Statistically significant elevation in nuclear p65 content was observed at concentrations of 3ng/mL LPS and above. Maximal nuclear p65 was observed at 100ng/mL. The EC_{50} for nuclear p65 expression was determined to be 1.2ng/mL (Fig.4.4B).

In RAW264.7 cells, in the absence of LPS stimulation basal nuclear p65 expression was minimal. However following LPS stimulation up to a 6-fold increase in nuclear p65 (observed at 100ng/mL) was detectable compared with untreated controls. Statistically significant elevation in nuclear p65 content was observed at 100ng/mL LPS (Fig.4.4D).

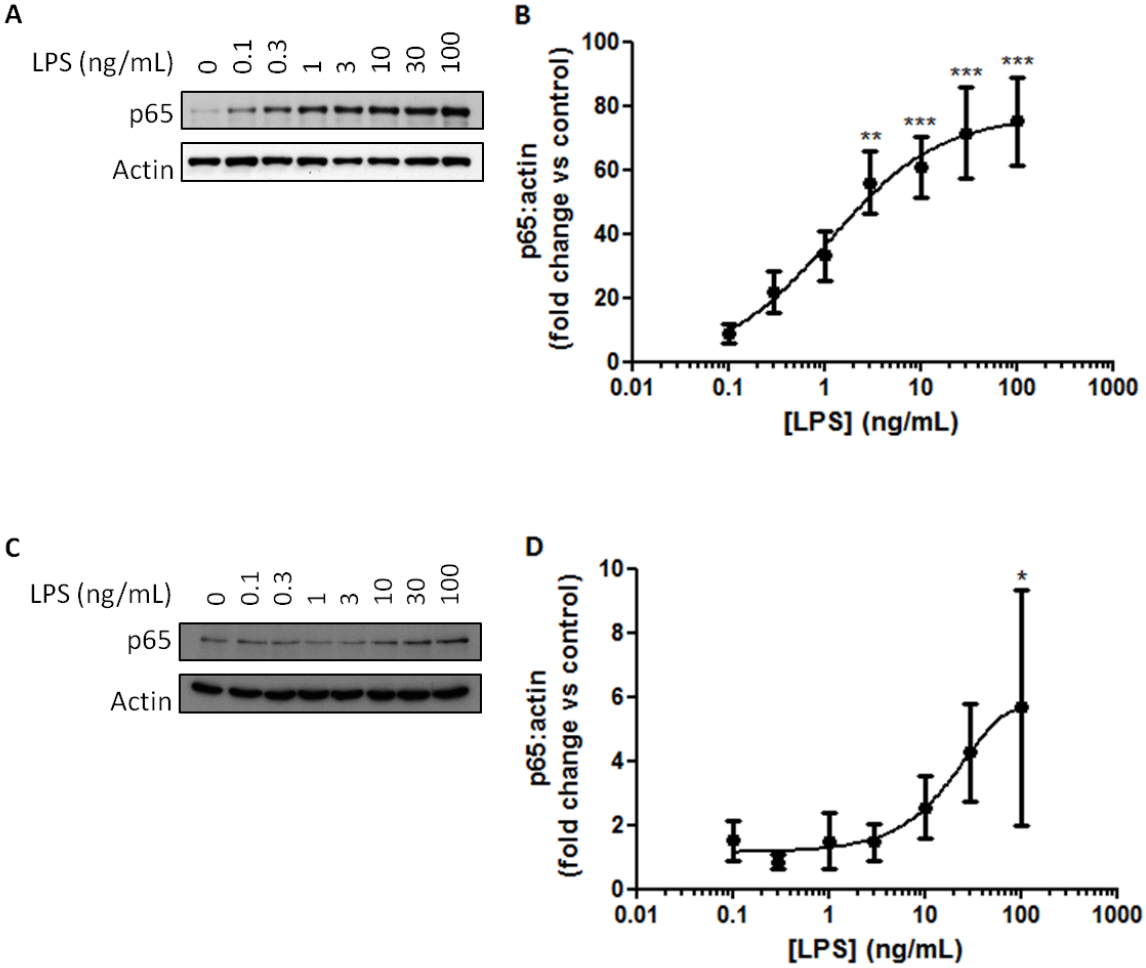

Fig.4.4 – LPS induced nuclear expression of p65 in THP-1 and RAW264.7 cells. LPS treatment induces nuclear translocation of p65 in a dose-dependent manner at 1hr as detected by Western blot. (A) Representative blot of THP-1 nuclear p65. (B) Fold change of THP-1 nuclear p65 following LPS stimulation (C) Representative blot of RAW264.7 nuclear p65. (D) Fold change of RAW264.7 nuclear p65 following LPS stimulation. Data is represented as mean±SEM of *n=5* (THP-1) or *n=3* (RAW264.7) separate experiments. * = p<0.05, ** = p<0.01, *** = p<0.001 compared with 0ng/mL control.

Time-dependent nuclear p65 expression

In THP-1 cells, the time-dependent translocation of p65 in response to LPS was determined over a 24hr timecourse using 3ng/mL LPS, as this was the lowest concentration that resulted in a statistically significant increase in nuclear p65 at 1hr. Peak nuclear p65 expression was seen at 1hr LPS treatment, with a slight, non-significant drop in nuclear p65 content seen up to 24hr treatment. Statistically significant elevations in nuclear p65 were seen with LPS treatment at all timepoints compared with the time-matched control sample (Fig.4.5B).

In RAW264.7 cells, the time-dependent translocation of p65 in response to LPS was determined over a 24hr timecourse using 100ng/mL LPS, as this was the lowest concentration that resulted in a statistically significant increase in nuclear p65 at 1hr. Peak nuclear p65 expression was seen at 1hr LPS treatment, with a significant drop in nuclear p65 content seen up between 1hr and 24hr LPS treatment. Statistically significant elevations in nuclear p65 were seen with LPS treatment at all timepoints compared with the time-matched control sample (Fig.4.5D).

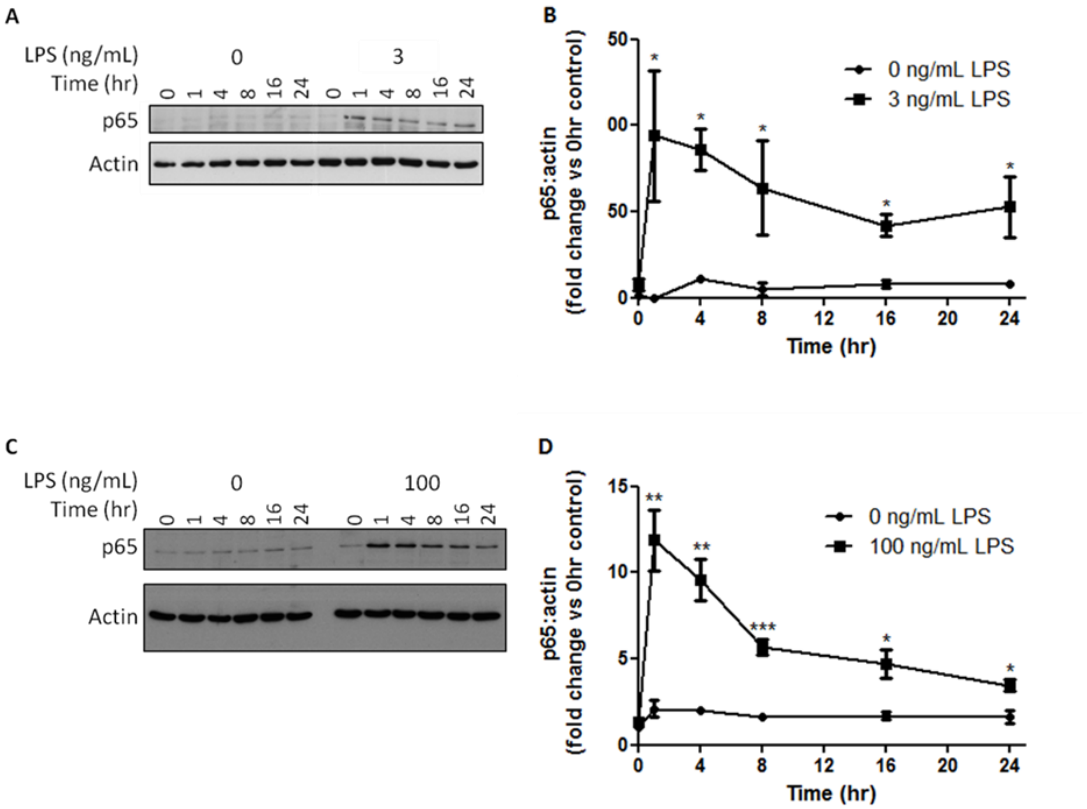

Fig.4.5 – Temporal dynamics of LPS-induced nuclear translocation of p65, as detected by Western blot. (A) Representative blot of THP-1 nuclear p65. (B) Fold change of THP-1 nuclear p65 following LPS stimulation (C) Representative blot of RAW264.7 nuclear p65. (D) Fold change of RAW264.7 nuclear p65 following LPS stimulation. Data is represented as mean±SEM of *n=3* (THP-1) or *n=3* (RAW264.7) separate experiments. * = $p<0.05$, ** = $p<0.01$, *** = $p<0.001$ compared with time-matched control.

4.3.3 Proinflammatory cytokine release from THP-1 cells following LPS treatment

The proinflammatory cytokines TNFα and IL-6 have been shown to be heavily implicated with the progression of inflammation and are also under transcriptional regulation by NF-κB. Therefore, cytokine release provides an endpoint for inflammatory signalling. Release of these cytokines into cell media by LPS-stimulated THP-1 cells was assayed by ELISA.

Dose dependent TNFα and IL-6 release

Dose-dependent TNFα release from THP-1 cells was observed at 24hr in response to LPS (0-2000ng/mL), with maximal TNFα release (625±102pg/mL) observed at 2000ng/mL LPS. (Fig.4.6A) Dose-dependent IL-6 release from THP-1 cells was also observed at 24hr in response to LPS (0-2000ng/mL) with maximal IL-6 release (230.5±46.8pg/mL) seen at 200ng/mL LPS. (Fig.4.6B)

Dose-dependent TNFα release from RAW264.7 cells was observed at 24hr in response to LPS (0-1000ng/mL), with significant release seen at 10ng/mL and greater. Maximal TNFα release (1588±157pg/mL) was observed at 100ng/mL LPS and an EC_{50} of 5.126ng/mL (Fig.4.6C). Dose-dependent IL-6 release from THP-1 cells was also observed at 24hr in response to LPS (0-1000ng/mL) with significant release seen at 30ng/mL and greater and maximal IL-6 release (856.8±16.74pg/mL) seen at 100ng/mL LPS and an EC_{50} of 29.00ng/mL (Fig.4.6D).

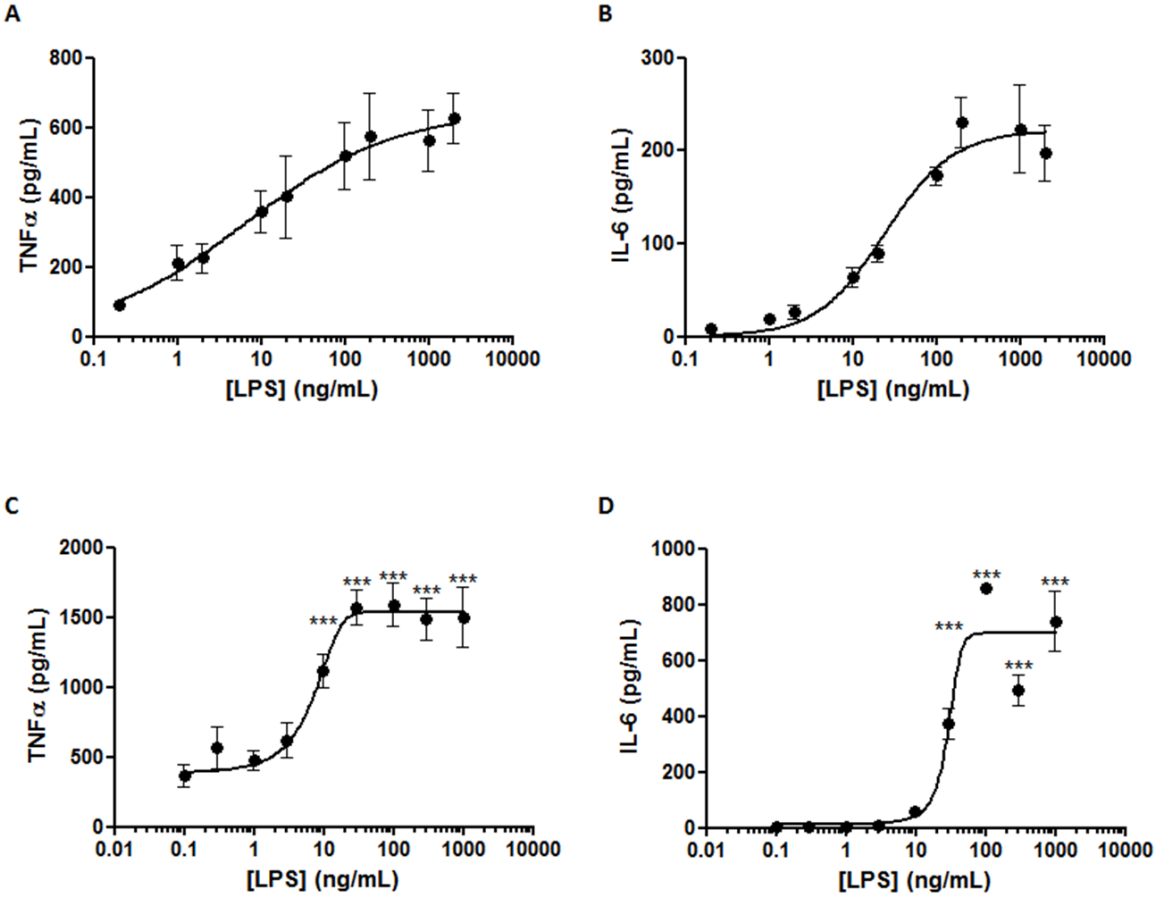

Fig.4.6 – Dose-dependent LPS induced cytokine release from THP-1 and RAW264.7 cells. LPS induced TNFα and IL-6 release from THP-1 cells (A-B) and RAW264.7 (C-D) in a dose-dependent manner, as determined by ELISA. Cells were treated with LPS at the indicated concentrations for 24hr. All data is presented as mean±SEM of *n=3* individual experiments with duplicate wells. *** = $p<0.001$ as compared with the 0ng/mL control.

Time dependent TNFα and IL-6 release

The timecourse of TNFα and IL-6 release from LPS stimulated THP-1 cells was determined over a 24hr period. Significant TNFα release compared to time-matched control was detectable at 4hr LPS treatment and this was also the peak level of TNFα detected (1516±464pg/mL). TNFα remained significantly elevated compared with time-matched controls at all later timepoints up to 24hr. A decrease in media TNFα level from the peak level was seen at 16 and 24hr (Fig.4.7A). IL-6 release from LPS stimulated THP-1 cells was determined over a 24hr period. Significant IL-6 release was detectable at 4hr LPS treatment (23.81±3.12pg/mL) compared with time-matched control (0.22±1.33pg/mL), however the peak IL-6 level was observed at 24hr (127.46±5.55pg/mL) compared with time-matched control (16.55±1.53pg/mL) (Fig.4.7B).

The timecourse of TNFα and IL-6 release from LPS stimulated RAW264.7 cells was determined over a 24hr period. Significant TNFα release was detectable at 1hr LPS treatment (21.5±6.10pg/mL) compared to time-matched control (5.56±2.07pg/mL) and TNFα remained significantly elevated compared with time-matched controls at all later timepoints up to 24hr. Peak level of TNFα (2604±246pg/mL) was reached at 16hr, but was decreasing by 24hr (Fig.4.7C). IL-6 release from LPS stimulated THP-1 cells was determined over a 24hr period. Significant IL-6 release was detectable at 4hr LPS treatment (13.80±4.78pg/mL) compared with time-matched control (2.04±0.55pg/mL), however the peak IL-6 level was observed at 16hr (485.4±260.7pg/mL) compared with time-matched control (2.26±0.24pg/mL) (Fig.4.7D).

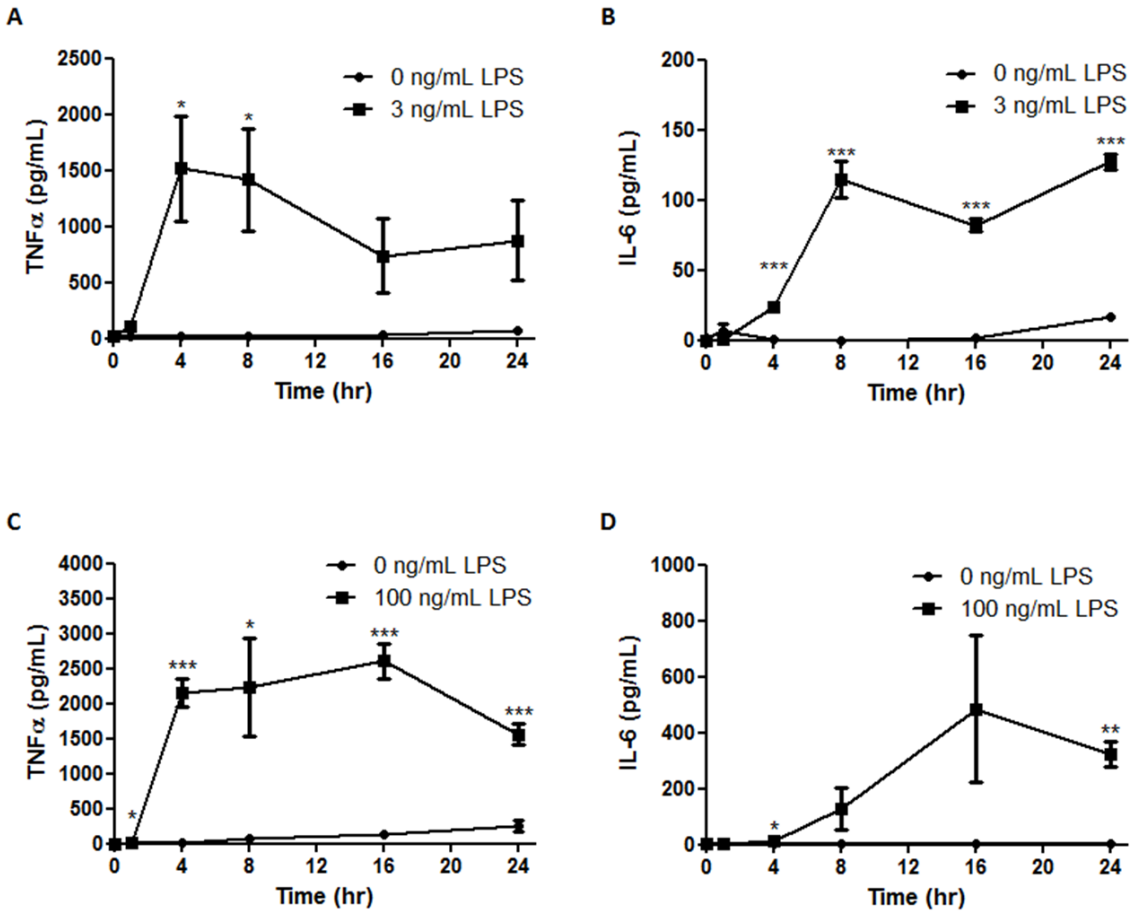

Fig.4.7 – Time-dependent LPS induced cytokine release from THP-1 and RAW264.7 cells. LPS induced TNFα and IL-6 release from THP-1 cells (A-B) and RAW264.7 (C-D) in a time-dependent manner, as determined by ELISA. Cells were treated with LPS at the indicated concentrations for 0-24hr. All data is presented as mean±SEM of *n=3* individual experiments with duplicate wells. * = p<0.05, ** = p<0.01, *** = p<0.001 as compared with the time-matched 0ng/mL control.

4.3.4 LPS stimulation causes HMGB1 translocation and release from RAW264.7 cells

In response to 100ng/mL LPS, HMGB1 is exported out of the nucleus with depletion seen at 16hr and significant depletion seen at 24hr (Fig.4.8). This HMGB1 is translocated into the cytosol as seen by immunofluorescence microscopy (Fig.4.9B).

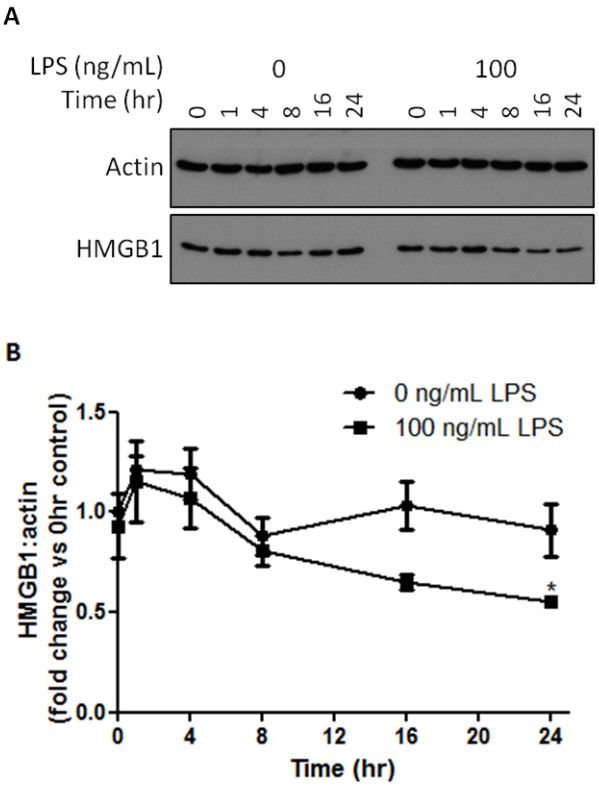

Fig.4.8 – LPS induces nuclear HMGB1 depletion from RAW264.7 cells in a time-dependent manner. Nuclear HMGB1 depletion in RAW264.7 cells in response to LPS, in a time-dependent manner, as determined by Western blot. Cells were treated with 100ng/mL LPS for 0-24hr. (A) Representative Western blot. (B) Fold change in nuclear HMGB1 compared to time-matched control. Data is presented as mean±SEM of *n=3* individual experiments with duplicate wells. * = $p<0.05$ as compared with the time-matched 0ng/mL control.

Following LPS treatment, HMGB1 (green) expression in RAW264.7 cells is altered from solely nuclear (0ng/mL LPS) (round areas of expression that co-localise with DNA staining) to both nuclear and cytosolic expression (10-1000ng/mL LPS) (elongated and hazy expression, no co-localisation with DNA) (Fig.4.9A and Fig.4.9B). The elongated morphology of the cells is also shown by staining for actin (red) which demonstrates that the RAW264.7 cells are being activated by LPS (Fig.4.9A).

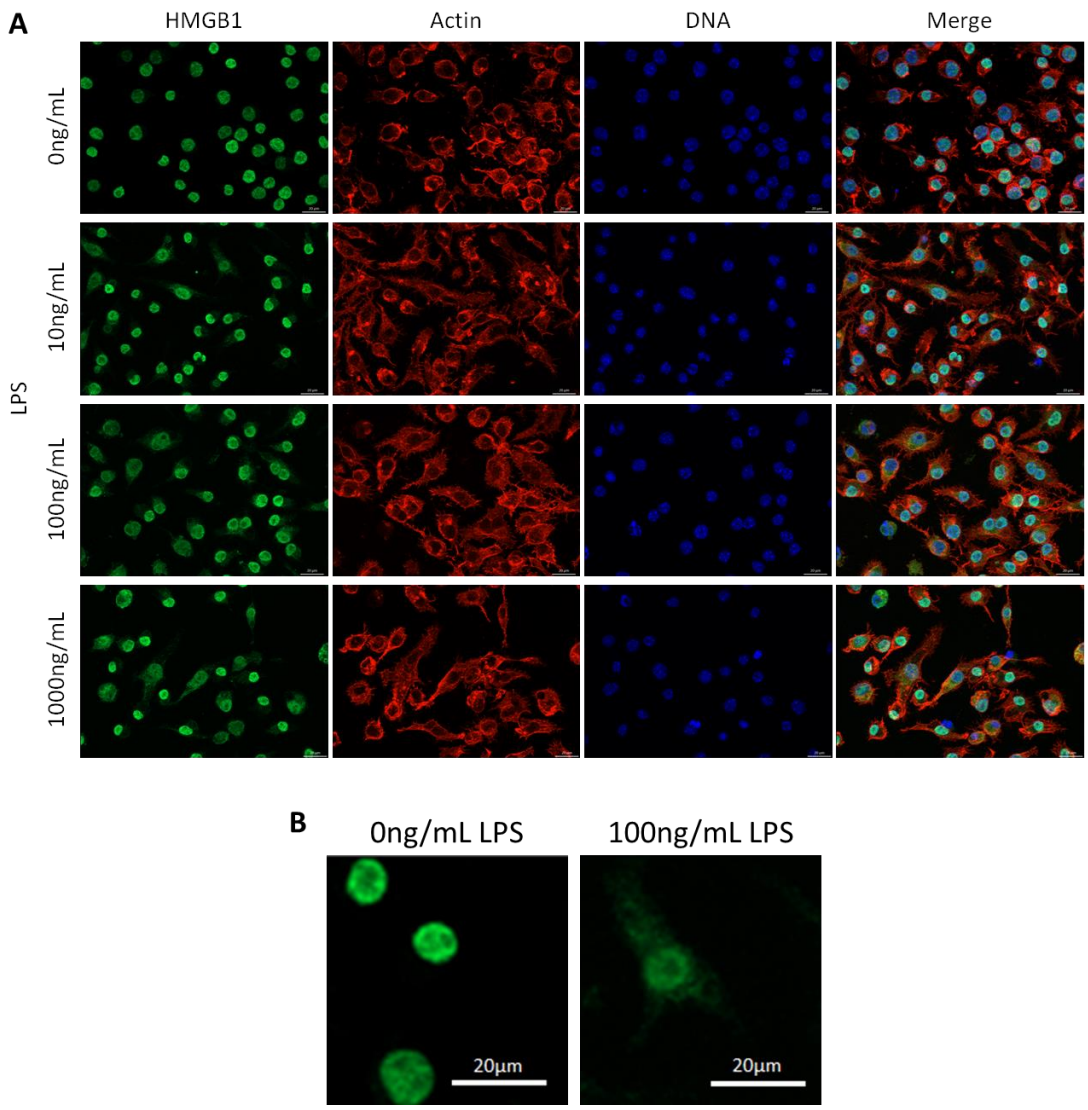

Fig.4.9 – LPS activates RAW264.7 cells and induces cytosolic HMGB1 translocation in a dose-dependent manner at 24hr. (A) Immunofluorescent staining of HMGB1 in LPS–stimulated (0-1000ng/mL) RAW264.7 cells. HMGB1 was stained using Abcam rabbit polyclonal (ab18256) primary followed by Alexa Fluor 488 donkey anti-rabbit secondary, DNA was stained using Hoechst, actin was stained using phalloidin. Scale bar is 20µm. (B) Representative HMGB1 staining from 0ng/mL and 100ng/mL LPS-treated RAW264.7 cells. Data is representative of *n=3* experiments.

4.3.5 LPS does not induce cell death of RAW264.7 cells

No effect on RAW264.7 cell viability was observed in response to LPS (0-1000ng/mL) at 24hr, displaying that the responses displayed in the other experiments are not a consequence of cell death (Fig.4.10).

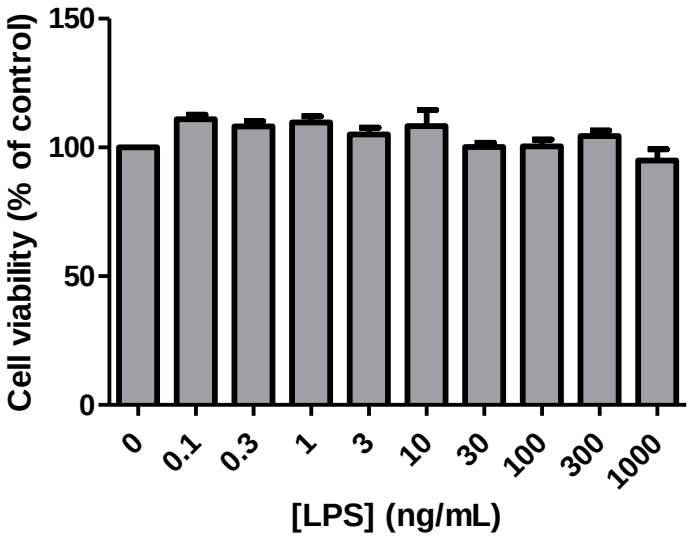

Fig.4.10 – LPS has no effect on RAW264.7 cell viability at 24hr. RAW264.7 cells ($4x10^4$ cells/well) were treated with the indicated doses of LPS for 24hr. Cell viability was tested by CellTiter 96® Aqueous One Solution assay kit. All data is presented as mean±SEM of *n=3* individual experiments with duplicate wells.

4.3.6 LC-MS/MS characterisation of HMGB1 redox isoforms

HMGB1 redox isoforms were characterised by LC-MS/MS (Fig.4.11). Recombinant HMGB1 isoforms underwent tryptic digest into peptides of interest corresponding to amino acid sequences MSSYAFFVQTCS (corresponding to amino acids 13-24), CSER (corresponding to amino acids 45-48) and RPPSAFFLFCSEYRPK (corresponding to amino acids 97-112).

Peptide characterisation of untreated recombinant HMGB1 showed a MSSYAFFVQTCS peptide chain with a mass of 1569.7Da, 130amu greater than the mass of the individual amino acids, demonstrating that this was alkylated with d_5NEM and previously C23 was engaged in a disulphide bridge (Fig.4.11A). Similarly, the CSER peptide had a mass of 623.5Da, 130amu greater than the mass of the individual amino acids, demonstrating that this was alkylated with d_5NEM and previously C45 was engaged in a disulphide bridge (Fig.4.11B). The RPPSAFFLFCSEYRPK peptide (2070.2Da) was modified with an increased mass of 125amu, demonstrating that this was alkylated with NEM, and had previously been a thiol (Fig.4.11C). This redox isoform was subsequently designated HMGB1 A (Fig.4.12).

Peptide characterisation of H_2O_2-treated recombinant HMGB1 showed a MSSYAFFVQTCS peptide chain with a mass of 1487.7Da (Fig.4.11D), a CSER peptide with a mass of 541.5Da (Fig.4.11E), and a RPPSAFFLFCSEYRPK peptide with mass 1993.2Da (Fig.4.11F). All of these peptides had a shift of 48amu, and analysis of b and y ions showed that this was due to all three cysteines being in a sulphonyl state. This redox isoform was designated HMGB1 B (Fig.4.12).

Peptide characterisation of DTT-treated recombinant HMGB1 showed a MSSYAFFVQTCS peptide chain with a mass of 1564.7Da (Fig.4.11G), a CSER peptide with a mass of 618.5Da (Fig.4.11H) and a RPPSAFFLFCSEYRPK peptide with a mass of 2070.2Da (Fig.4.11H), demonstrating that all three peptides had a 125amu shift in mass. Through analysis of b and y ions, this was confirmed to be due to cysteine alkylation with NEM, and hence all

cysteines had been in the fully-reduced thiol state. This redox isoform was subsequently designated HMGB1 C (Fig.4.12).

Mild oxidation with H_2O_2 lead to a MSSYAFFVQTCS peptide chain with a mass of 1569.7Da and a CSER peptide with a mass of 623.5Da. Both of these are 130amu greater than the mass of the individual amino acids, demonstrating alkylation with d_5NEM and engagement in a disulphide bridge (Fig.4.11A,B). The RPPSAFFLFCSEYRPK peptide had a mass of 1993.2Da and corresponded to the sulphonyl form (Fig.4.11E). This redox isoform was subsequently designated HMGB1 D (Fig.4.12).

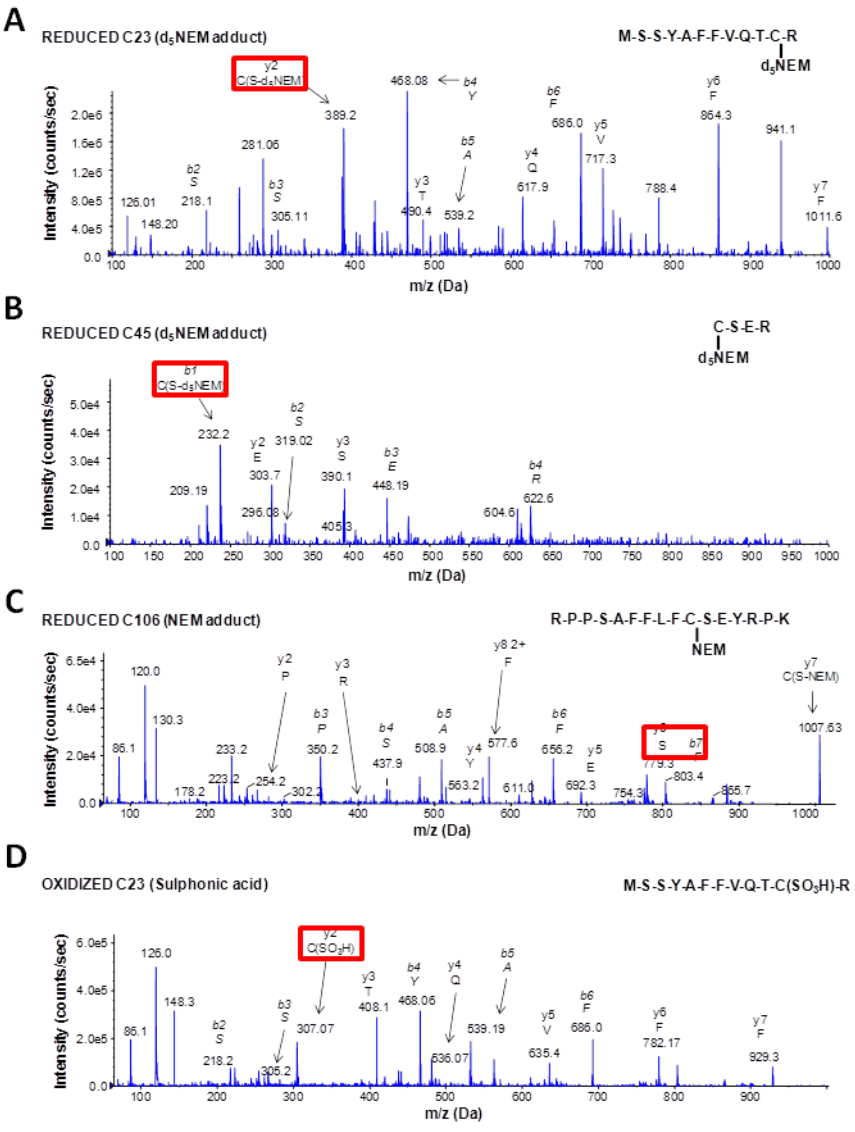

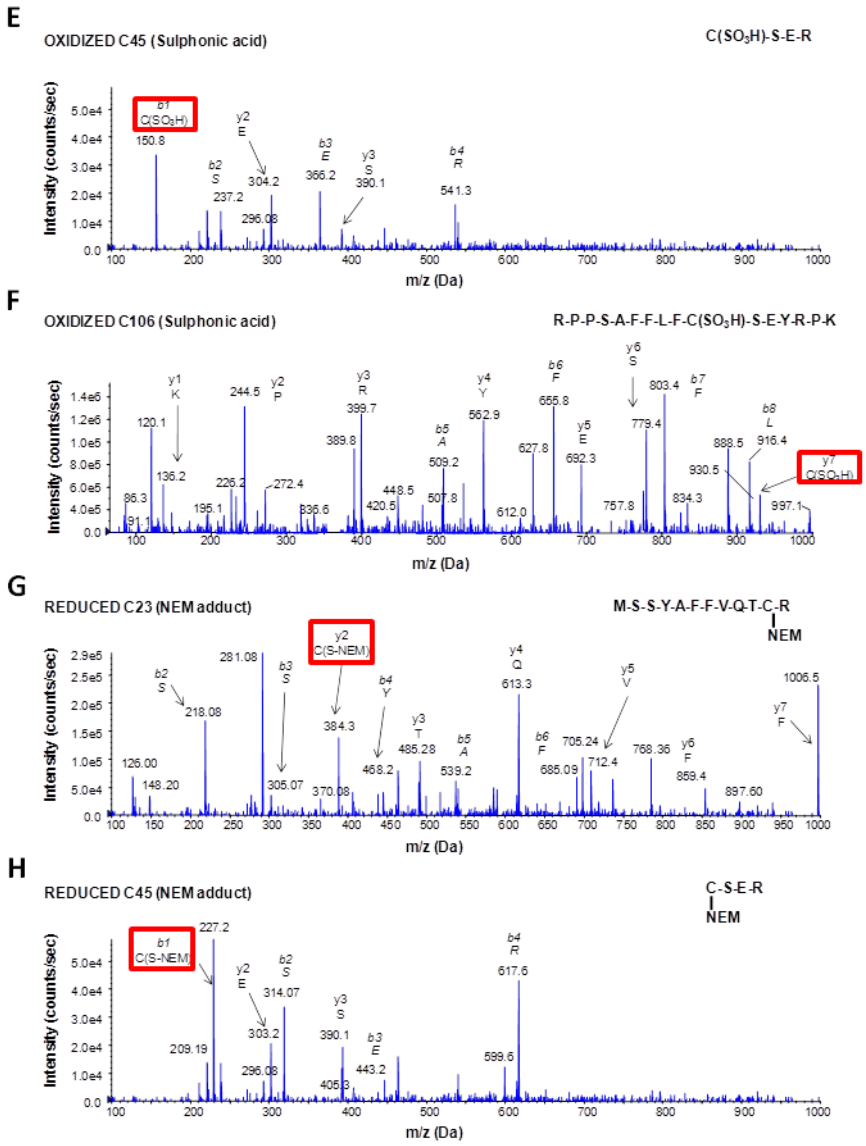

Fig.4.11 – LC-MS/MS characterisation of the redox state of recombinant HMGB1s. (A) Characterisation of C23: MS/MS trace of the peptide containing amino acids 13-24, with a d_5NEM adduct after DTT reduction of a C23-C45 disulphide bond. (B) Characterisation of C45: MS/MS trace of the peptide containing amino acids 45-48, with a d_5NEM adduct after DTT reduction of a C23-C45 disulphide bond. (C) Characterisation of C106: MS/MS trace of the peptide containing amino acids 97-112 with an NEM adduct indicating reduced thiol C106. (D) MS/MS trace of the peptide containing amino acids 13-24, with a sulphonyl group on C23. (E) MS/MS trace of the peptide containing amino acids 45-48, with a sulphonyl group on C45. (F) MS/MS trace of the peptide containing amino acids 97-112, with a sulphonyl group on C106. (G) Characterisation of C23: MS/MS trace of the peptide containing amino acids 13-24 with an NEM adduct indicating reduced thiol. (H) Characterisation of C45: MS/MS trace of the peptide containing amino acids 45-48 with an NEM adduct indicating reduced thiol.

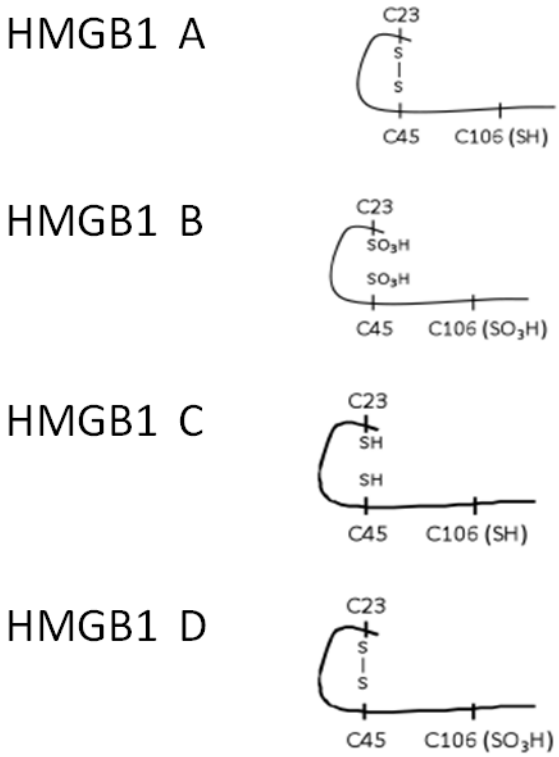

Fig.4.12: Summary of the redox isoforms of HMGB1. Modified from (Yang et al., 2012).

4.3.6 Nuclear p65 expression in THP-1 cells following treatment with different HMGB1 redox isoforms

HMGB1 redox isoforms show different abilities to induce nuclear p65 translocation (Fig.4.13). HMGB1 A (C23-C45 disulphide, C106 –SH) is able to cause significant translocation of p65 to the nucleus of THP-1 cells (0.359±0.044 p65:actin) compared with control (0.039±0.015 p65:actin), whereas all other redox isoforms are unable to cause p65 translocation. This data shows that HMGB1 A is the only isoform able to induce proinflammatory signalling through NF-κB activation.

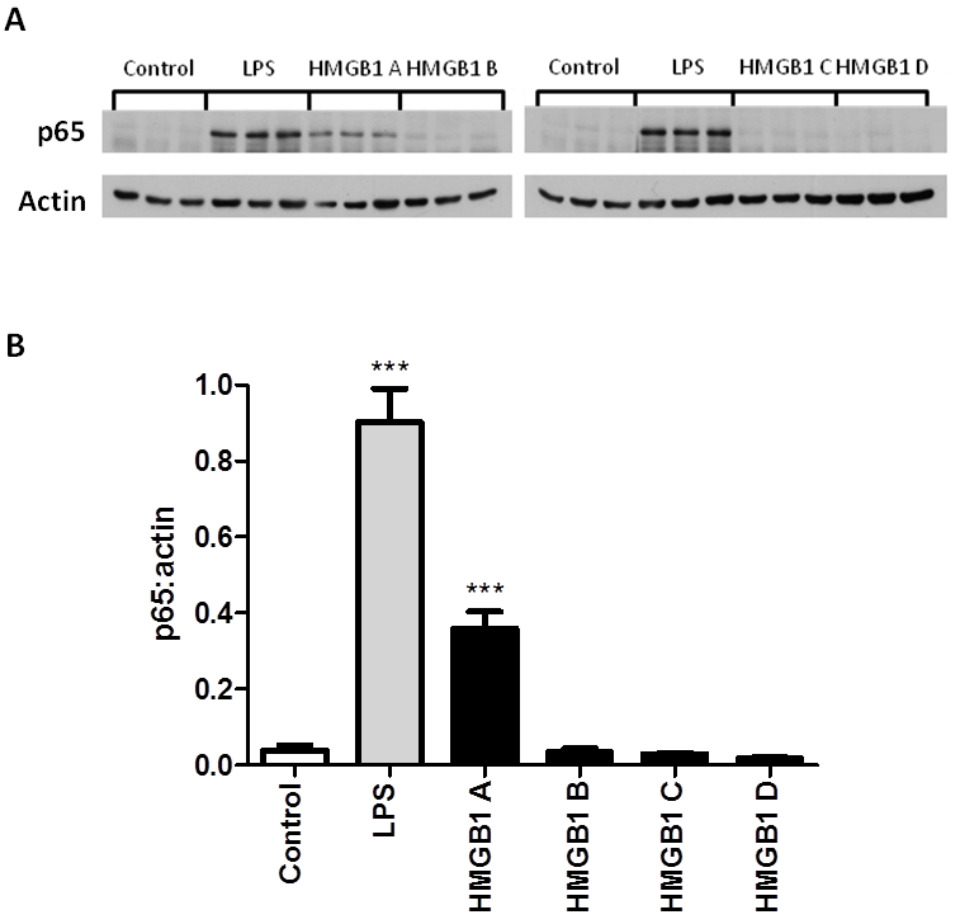

Fig.4.13 – Nuclear p65 expression in THP-1 cells following treatment with HMGB1 redox isoforms. (A) Representative Western blot for nuclear p65 in THP-1 cells treated with either 100 ng/mL LPS or redox isoforms of HMGB1 for 1hr. Each condition was run in triplicate. (B) Actin normalised nuclear p65 expression in THP-1 cells in response to LPS (100ng/mL) or HMGB1 redox isoforms (1µg/mL). Data is presented as mean±SEM of *n=4* experiments with triplicate samples. *** = p<0.001 when compared with control (media only).

4.3.7 Proinflammatory cytokine release from THP-1 cells following treatment with different HMGB1 redox isoforms

HMGB1 redox isoforms show different abilities to induce cytokine release from THP-1 cells (Fig4.14). HMGB1 A (C23-C45 disulphide, C106 –SH) is able to cause both significant TNFα and IL-6 release from THP-1 cells compared with control (media only). All other HMGB1 redox isoforms are unable to cause TNFα or IL-6 release and were significantly different from the HMGB1 A response. This suggests that HMGB1 A is the only isoform able to induce proinflammatory cytokine release.

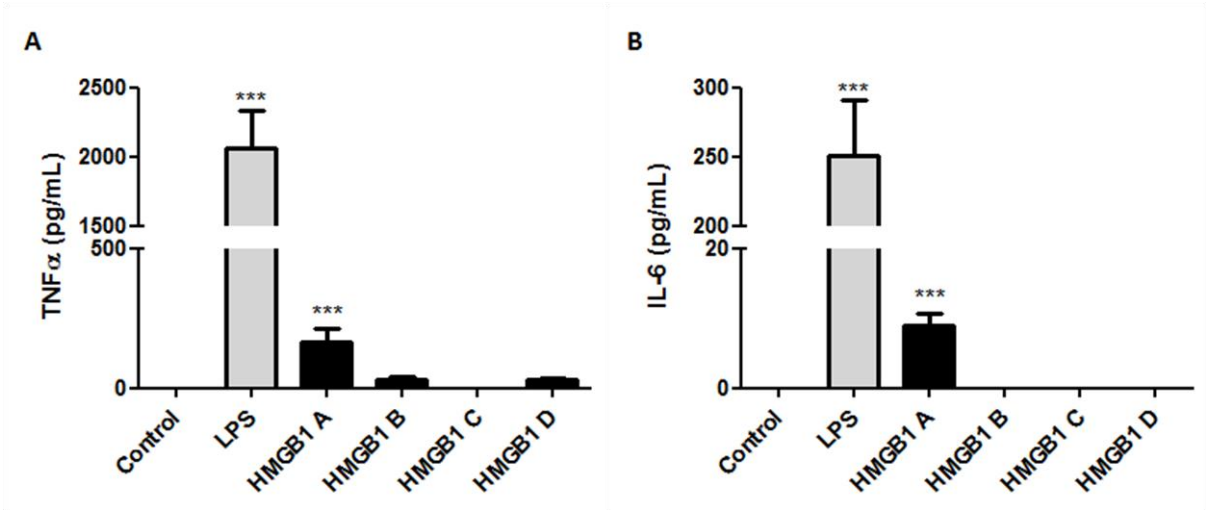

Fig.4.14 – Cytokine release by THP-1 cells following treatment with HMGB1 redox isoforms. A) TNFα or B) IL-6 release from THP-1 cells in response to LPS (100 ng/mL) or HMGB1 redox isoforms (1µg/mL). Data is presented as mean±SEM of *n=3* experiments with duplicate wells. *** = p<0.001 compared with control (media only).

4.4 Discussion

LPS is the chief component of Gram-negative bacteria cell walls, and is the prototypical ligand agonist for TLR4. LPS binds to TLR4 through a specific binding site to activate TLR signalling (Park et al., 2009). Recent work has implicated TLR4 as the important receptor for the release of cytokines in response to HMGB1 (Yang et al., 2010).

In THP-1 whole cell lysates, no perturbation in p65 expression was observed with LPS at 24hr. This was not unexpected as LPS has been shown to have little effect on whole cell p65 expression under these conditions, however subcellular localisation of p65 should change following LPS treatment, with p65 undergoing nuclear translocation following TLR4 stimulation (Cordle et al., 1993).

As a TLR4 agonist, LPS induces proinflammatory responses, mediated through activation of NF-κB signalling and cytokine release from activated immune cells. The effect of LPS on THP-1 and RAW264.7 cell activation was investigated, and as expected, it caused both NF-κB signalling activation and TNFα and IL-6 release in a time- and dose-dependent manner. In THP-1 cells whole cell p65 expression was unaffected over this time period, showing that p65 is translocating to the nucleus rather than simply undergoing greater protein synthesis and increasing total expression, which fits with previous observations (Cordle et al., 1993). Similarly, cytokine production in response to LPS was seen from both THP-1 and RAW264.7 cells, which corresponds with literature (Jeong and Jue, 1997, Jang et al., 2006). Significant release of both TNFα and IL-6 were seen in response to 3ng/mL LPS over a 24hr timecourse in THP-1 cells and in response to 100ng/mL LPS in RAW264.7 cells. In both cell lines, peak TNFα release preceded peak IL-6 release. This observation may be attributable to TNFα mediated IL-6 release, as TNFα is known to be released more rapidly following LPS stimulation (Kemna et al., 2005). In both cell lines a minor decrease in detectable TNFα occurred between peak level and 24hr. This may be due to cytokine binding to receptors on

THP-1 cells (and internalisation) leading to a reduction in the available detectable cytokines in the media.

Additionally, LPS activation of RAW264.7 cells also resulted in HMGB1 translocation from the nucleus (as shown by Western blot) and translocation into the cytosol (IF) suggesting active HMGB1 release. HMGB1 release from immune cells is regulated by acetylation (Bonaldi et al., 2003), and is another important feature of inflammation (Lu et al., 2012).

The data confirmed that LPS was suitable positive control for the proinflammatory activation of THP-1 and RAW264.7 cells with a TLR4 agonist. Hence investigations into the proinflammatory activity of different redox forms of HMGB1 was undertaken in THP-1 cells as they showed more consistent p65 activation.

The data show that the different redox conformations of HMGB1 have differing cytokine release inducing capabilities, with HMGB1 requiring a C23-C45 disulphide bridge and C106 as a thiol (HMGB1 A) in order to induce NF-κB activation and proinflammatory cytokine release. The disulphide bridge between cysteines 23 and 45 is known to alter the conformational shape of HMGB1 (Sahu et al., 2008), and this may reconfigure HMGB1 into a 3D structure that allows interaction with TLR4. Additionally, it is known that cysteine 106 is essential for the propagation of inflammatory signalling through TLR4 as substitution mutation to serine removes this capability (Yang et al., 2010). The data shows that C106 also needs to be in a thiol conformation for successful proinflammatory signalling induction, as HMGB1 D (C23-C45 disulphide, C106 sulphonyl) lacks proinflammatory activity. This suggests that terminal oxidation of C106 can preclude HMGB1-TLR4 binding. The redox isoforms HMGB1 B-D lack cytokine-stimulating activity, probably due to no being in the correct 3D conformation to interact with TLR4 and induce NF-κB signalling.

The results from investigations in this chapter have shown that HMGB1 A is the only isoform to be able to induce cytokine release. Data in THP-1 cells conforms with the observations of Yang et al who showed in RAW264.7 cells and PBMCs that HMGB1 A is the only isoform capable of causing cytokine release (Yang et al., 2012). Recently a standardised nomenclature for different redox isoforms of HMGB1 has been established, with the HMGB1 A isoform known as disulphide HMGB1 (Antoine et al., 2014).

Furthermore, other recent studies have determined that fully reduced HMGB1 (C23, C45 and C106 as thiols) also plays a key role in inflammatory signalling by acting as a chemoattractant for immune cells through interaction with CXCL12 and signalling via CXCR4 (Venereau et al., 2013, Venereau et al., 2012). Venereau et al demonstrate that HMGB1 released from necrotic cells is in the all-thiol conformation and undergoes time-dependent oxidation in the extracellular environment, proceeding to the proinflammatory (C23-C45 -S-S-, C106 -SH) conformation, before further oxidation to a non-inflammatory fully oxidised form. These published data show that HMGB1 is under dynamic redox regulation that strictly regulates extracellular HMGB1 functions. As the cysteine redox isoforms are mutually exclusive, these results demonstrate the pivotal role that redox has in the coordination of the HMGB1-mediated inflammatory response. As a result, the redox potential of the extracellular environment can govern the extent of propagation of inflammatory signalling. As mentioned above, the intracellular environment is largely reducing, and as a result most intracellular HMGB1 exists in the fully reduced conformation. This means that upon necrotic cell death, this isoform of HMGB1 is immediately able to induce chemotaxis of immune cells to the site of injury.

Following immune cell recruitment, HMGB1 can become mildly oxidised to the cytokine stimulating isoform, due to the oxidising extracellular environment. Additionally, activated immune cells can contribute to this oxidising environment through ROS production. At this

stage there will be a positive proinflammatory feedback cycle in place whereby activated immune cells actively secrete HMGB1, in addition to the HMGB1 lost by necrotic parenchymal cells, and together these can cause further HMGB1 (and other proinflammatory mediators) release (Venereau et al., 2013).

Activated immune cells, particularly neutrophils, can release ROS into the extracellular environment, resulting in terminal oxidation of HMGB1 cysteines to sulphonyl residues. The fully sulphonyl form (HMGB1 C) has been shown to be immunologically inert, and is likely to be involved in the resolution of injury. HMGB1 can also undergo caspase-dependent oxidation in apoptotic cells, leading to production of sulphonyl HMGB1. This immunologically inert redox isoform coupled with the lack of release of HMGB1 from early apoptotic cells may act as a safety mechanism to prevent proinflammatory signalling during apoptotic cell death (Kazama et al., 2008).

As apoptosis is associated with HMGB1 caspase-dependent oxidation to an inert form, this demonstrates the critical role of intracellular ATP in injury. In fasted mice, basal ATP levels are depleted, thus preventing the ATP-dependent process of caspase activation. Hence apoptosis and caspase-dependent oxidation of HMGB1 is prevented. Following ATP depletion, necrotic cell death predominates and a distinct lack of apoptosis is observed. Fasted mice also show a much greater increase in inflammatory cell infiltration and increased inflammatory response compared with fed mice (Antoine et al., 2010).

In addition to cases of injury, HMGB1 redox may affect intracellular HMGB1 functions, although this area is currently under-researched. The cysteine residues have been shown to be important for nuclear translocation of HMGB1, with particular dependence on cysteine 106. Mutation of C106 to a serine, or triple cysteine to serine mutations prevents HMGB1 nuclear translocation under non-pathological conditions (Hoppe et al., 2006). Furthermore, HMGB1 redox has been shown to be important at modulating the interaction of HMGB1 A

box with cisplatin-modified DNA. Fully reduced HMGB1 can bind to cisplatin-modified DNA with 10-fold greater affinity than disulphide A box (Park and Lippard, 2011). Very recently, HMGB1 redox has been shown to be important for the association of histone H1 with DNA. HMGB1 redox has been shown to modulate the ability of HMGB1 to bind to and bend DNA. Fully reduced HMGB1 and Histone H1 have similar (if not identical) binding sites on DNA, and as a result HMGB1 can displace Histone H1 from DNA. Fully reduced HMGB1 is able to displace Histone H1 from bent DNA, whereas oxidised HMGB1 has lower ability. As a result, HMGB1 redox could affect DNA transcription (Polanska et al., 2014).

In summary, the results in this chapter show that HMGB1 proinflammatory function is under strict redox regulation that directly affects the ability of HMGB1 to induce NF-κB signalling and cytokine release. Recent publications have also defined the role for fully-reduced HMGB1 in chemotaxis. Whilst HMGB1 redox has been shown to be crucial for the regulation of extracellular function, little is known about potential cross-talk between different post translational modifications on HMGB1. For example, it is not known if redox modification can affect acetylation, it may seem that this is likely given that disulphide bridge formation changes the 3D conformation of HMGB1 A box. However, no acetylated lysine residue is located within 8Å of the cysteine residues, suggesting that acetylation of HMGB1 lysines will not affect the pKa of the cysteine residues (Sahu et al., 2008). This potential cross-talk between acetylation and oxidation of HMGB1 will be an important area of HMGB1 biology to investigate, as acetylated HMGB1 is actively released from activated immune cells, and is a sensitive, mechanistic and acute biomarker of DILI in APAP overdose patients. A higher serum concentration of hyperacetylated HMGB1 is associated with a poorer prognosis and is more predictive of patient outcome (death/requirement for transplant by King's College criteria (KCC)) than ALT (Antoine et al., 2012).

Additionally, protein oxidation can modulate protein function and protein-protein interactions, including aiding the subsequent modification of the protein. It will be important to explore if oxidation can affect the formation of other post-translational modifications on HMGB1.

Chapter Five

HMGB1 ubiquitination – a novel PTM in apoptosis

CONTENTS

5.1 Introduction

HMGB1 is proving to be an important emerging biomarker of inflammation, and as a result a greater understanding of the molecular mechanisms that regulate HMGB1 expression, localisation and function is essential for directing hypotheses and experimental investigations.

Recent work investigating the role of PTMs in the regulation of HMGB1 function and localisation have been focussed on cysteine redox-regulation of extracellular proinflammatory function ((Yang et al., 2010), Chapter 4) and acetylation-directed nucleocytosolic translocation and active release of HMGB1, through acetylation of lysine residues within the NLS regions of HMGB1 (Bonaldi et al., 2003). Additionally, preliminary investigations into the roles of methylation (Ito et al., 2007) and phosphorylation (Youn and Shin, 2006) on the nucleocytosolic translocation of HMGB1 have been explored. However, a comprehensive investigation of the roles of all HMGB1 PTMs, in both healthy and disease conditions is lacking.

Additionally, whilst studies into the functional roles of HMGB1 have expanded our understanding, little is known of the mechanisms of regulation of HMGB1 expression or the fate of HMGB1 during apoptosis.

Apoptosis is a tightly regulated, non-inflammatory mechanism of cell death, characterised by cell shrinkage, blebbing and nuclear condensation (Kerr et al., 1972). The two main pathways of apoptosis induction exhibit significant cross-talk, and both result in the activation of an effector caspase (often caspase-3) that acts as a tipping point for proceeding to apoptotic cell death.

During apoptosis, HMGB1 is oxidised in a caspase-dependent manner and may also be oxidised by reactive oxygen species during inflammation, resulting in a loss of

immunological function (Kazama et al., 2008, Yang et al., 2012). Reports have shown that during early apoptosis HMGB1 is concentrated into the nucleus (Scaffidi et al., 2002), however during late apoptosis HMGB1 can be released from cells (Bell et al., 2006). Recently, evidence has shown that HMGB1 is present in apoptotic cell membrane vesicles (ACMV) and microparticles (MP) from apoptotic cells (Schiller et al., 2013, Spencer et al., 2014). The mechanism of translocation of HMGB1 to these apoptotic MP and subsequent release from apoptotic cells has not been determined. Furthermore, mechanistic control of HMGB1 expression is an area that requires greater exploration, including evaluating the potential impact of PTMs on HMGB1 expression. For instance, there is evidence that protein oxidation can target proteins for proteasomal degradation via ubiquitin-dependent (Yamanaka et al., 2003) or independent mechanisms (Shringarpure et al., 2003).

Ubiquitination is a highly conserved, ATP-dependent post-translational modification resulting in the adduction of ubiquitin onto a target protein. Ubiquitination usually occurs at lysine residues, but in rare examples can also occur at threonine, methionine or serine residues (Wang et al., 2007, Ciechanover, 1998).

Ubiquitin itself can be a target for ubiquitination, and ubiquitination is possible at any of the seven lysine residues or the N terminal methionine of ubiquitin. This property leads to polyubiquitin chain formation and is important for determining the fate of the ubiquitinated target protein (Komander and Rape, 2012). The chain structure and lengths are vitally important for the functional properties of the ubiquitinated target protein (Komander and Rape, 2012).

Classically, ubiquitination is known to be a mechanism for directing the target protein for degradation (Ciechanover, 1998). This function of ubiquitination is usually as a result of Lys48 polyubiquitin chain formation. Lys48 chains are four ubiquitin molecules in length, with the chain taking a closed conformation, mediated through non-covalent interactions

between hydrophobic patches containing an Ile residue (Ile44 or Ile36). An exposed Ile44 patch is recognised by the proteasome (Sloper-Mould et al., 2001, Dikic et al., 2009). Whilst proteasomal degradation of proteins is usually mediated by Lys48 polyubiquitin chains, other polyubiquitin chain, such as Lys11 chains can also target proteins for degradation (Matsumoto et al., 2010).

The ubiquitin-proteasome system is the most common mechanism of regulation of protein expression. This pathway proceeds through ubiquitination of the target protein and targeting to the 26S proteasome through recognition of polyubiquitin chains. The ubiquitin-proteasome system has also been shown to regulate the expression of another DAMP, heat-shock protein 70 (Qian et al., 2006) and as an important system to regulate protein expression during staurosporine (STS)-induced apoptosis (Gama et al., 2006).

However, there are other non-proteolytic functions of ubiquitination including protein trafficking, protein activation, regulation of signalling and lysosomal targeting of membrane proteins (Komander and Rape, 2012). The non-proteolytic functions of ubiquitination are often the consequence of monoubiquitination or Met1- (Kirisako et al., 2006, Tokunaga et al., 2009) and Lys63-linked chain formation (Doil et al., 2009, Huang et al., 2009, Wang et al., 2001, Al-Hakim et al., 2010, Kirkin et al., 2009).

In addition to polyubiquitination, proteins can be monoubiquitinated, leading to a non-proteasomal fate. Examples include targeting p53 for nuclear export (most likely through conformational change exposing a nuclear export sequence) (Li et al., 2003), coordination of DNA repair mediated by monoubiquitinated PCNA (Hoege et al., 2002) and lysosomal targeting of membrane proteins (Raiborg and Stenmark, 2009). An overview of ubiquitin chain linkage types and a summary of the fates of proteins modified with different ubiquitin chain types are shown in Fig.5.1 and Table 5.1.

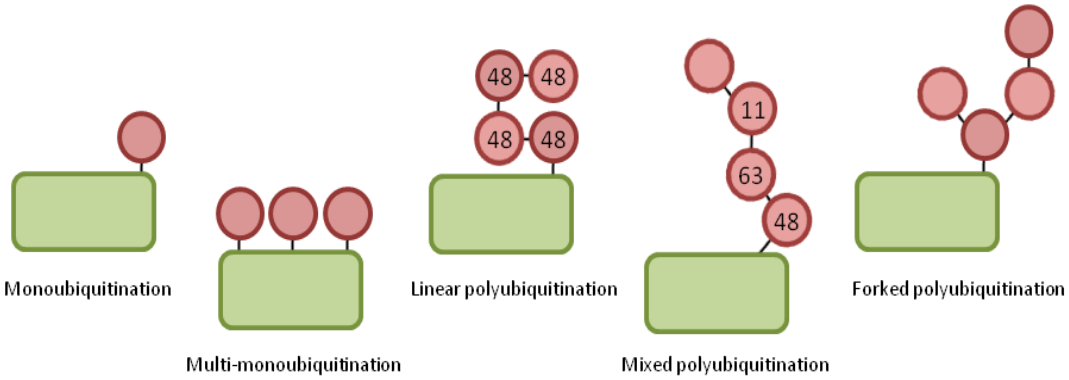

Fig.5.1 – Overview of different ubiquitin chain types. Adapted from (Komander and Rape, 2012).

Ubiquitin linkage	Known fate	Example	References
Lys48 chains (tetraubiquitin)	Proteasomal degradation	IκBα degradation during NF-κB signalling	(Winston et al., 1999, Margottin-Goguet et al., 2003)
Lys63 chains	Protein trafficking	DNA repair, via histone Lys63 chains	(Al-Hakim et al., 2010, Doil et al., 2009, Huang et al., 2009) (Sobhian et al., 2007)
	Protein activation	IKK	(Wang et al., 2001)
	Lysosomal targeting of membrane proteins	FcγR	(Raiborg and Stenmark, 2009, Molfetta et al., 2014)
	Autophagosome targeting	via p62	(Kirkin et al., 2009)
	Proteasomal degradation (rare examples)	Cyclin B1	(Kirkpatrick et al., 2006)
Lys11 chains	Proteasomal degradation	Degradation of cell cycle regulators during mitosis	(Matsumoto et al., 2010)
Lys29 chains	Proteasomal degradation	Ubiquitin fusion proteins in yeast	(Thrower et al., 2000)
Lys6 chains	Unknown	N/A	
Lys27 chains	Unknown	N/A	
Lys33 chains	Unknown	N/A	
Met1 chains (N terminal, linear)	Conformational change	NEMO	(Tokunaga et al., 2009)
Mono-ubiquitination	Protein localisation	Nuclear export of p53	(Li et al., 2003)
	Protein trafficking	DNA repair, mediated by PCNA monoubiquitination	(Hoege et al., 2002)
	Protein cleavage	NF-κB	(Kravtsova-Ivantsiv et al., 2009)
	Transcription regulation	Smad4	(Dupont et al., 2009)
	Lysosomal targeting of membrane proteins	via ESCRT	(Raiborg and Stenmark, 2009)

Table.5.1 Examples of different ubiquitin chains and their defined functions for particular proteins. Table was collated from (Komander and Rape, 2012).

Ubiquitination of proteins can be detected by mass spectrometry, using tryptic digestion of proteins. Tryptic digestion of ubiquitin cleaves the C-terminal glycine-glycine (GlyGly) motif from ubiquitin. This motif (with a mass of 114.1Da) remains attached to the ubiquitinated residue of the target protein (as well as inhibiting cleavage of the ubiquitinated lysine by trypsin), resulting in a branched peptide, and hence can be used to identify a particular residue as a site of ubiquitination (Fig.5.2)(Peng et al., 2003).

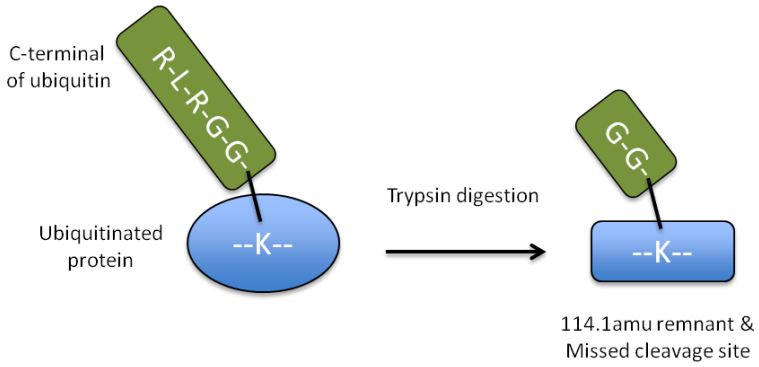

Fig.5.2 – Tryptic digestion leaves a characteristic GlyGly motif on ubiquitinated peptides. Figure adapted from (Denis et al., 2007).

5.1.1 Aims

The aim of this chapter is to identify possible mechanisms governing HMGB1 regulation and release from apoptotic cells, both *in vivo* and *in vitro* that might in turn provide further understanding into the role of HMGB1 signalling during apoptotic cell death. This will also include investigating if HMGB1 can be ubiquitinated (HMGB1-Ub) during normal conditions or during cell death. This aim will be addressed through analysis of APAP-overdose patient samples and a range of cell lines.

5.2 Materials and Methods

5.2.1 Materials

Fetal bovine serum was purchased from Life Technologies (Paisley, UK). Bio-Rad Protein Assay Dye Reagent, Precision Plus Kaleidoscope Standards (molecular weight markers) and non-fat milk was purchased from Bio-Rad Laboratories Ltd (Hemel Hempstead, UK). Amersham Hybond ECL membrane and Amersham Hyperfilm ECL were purchased from GE Healthcare (Little Chalfont, UK). Anti-caspase-3 antibody was purchased from Cell Signaling Technology (MA, USA). Anti-HMGB1 antibody (ab18256) was purchased from Abcam (Cambridge, UK). Anti-ubiquitin antibody was purchased from Dako (Ely, UK). Anti-ubiquitin Lys63 and Lys48 linkage-specific antibodies were purchased from Millipore (MA, USA). Western Lightning Plus-ECL was purchased from Perkin Elmer (Beaconsfield, UK). Annexin V/PI kit was purchased from BD Biosciences (Oxford, UK). CellTiter 96® Aqueous One Solution assay kit and Caspase-Glo 3/7 assay kit were purchased from Promega (Southampton, UK). All other materials were purchased from Sigma-Aldrich (Poole, UK) or Fisher Scientific (Loughborough, UK) unless otherwise indicated.

Sample collection, processing (tryptic digestion) and LC-MS/MS analysis of human APAP overdose patients were performed by Dr Dan Antoine and Dr Roz Jenkins prior to me starting on the work. I was responsible for all the *in vitro* data enclosed in this chapter.

5.2.2 Patient sample collection

Serum samples from patients undergoing APAP hepatotoxicity from Antoine et al (Antoine et al., 2012) were analysed for HMGB1 ubiquitination. The study was prospectively approved by the local human research ethics committee and informed consent was obtained from patients, or next of kin prior to entry into the study. Patients were admitted to the Royal Infirmary of Edinburgh or the University of Kansas Medical Center. APAP hepatotoxicity was defined as the patient having at least two of: ALT>1000U/L,

APAP>4g/day, serum APAP>10mg/L, as per the method described in (Craig et al., 2011). All APAP overdose patients received continuous intravenous N-acetylcysteine (NAC) treatment for 20hr 15min. Blood samples were taken and immediately centrifuged (1000*g*, 15min, 4°C) to isolate serum, which was then stored at -80°C until LC-MS/MS analysis.

5.2.3 LC-MS/MS detection of HMGB1 post-translational modifications (PTMs)

Serum samples from the 10% of APAP overdose patients with the greatest amount of apoptosis (as determined previously by serum cleaved keratin-18 by M30 apoptosense ELISA (Antoine et al., 2012)) or *in vitro* samples (whole cell lysates from MG132-treated mouse embryonic fibroblasts (MEFs) or isolated microparticles (MP)) underwent immunoprecipitation with 5µg anti-HMGB1 rabbit polyclonal antibody (Abcam ab18256). Purified HMGB1 samples were analysed for PTMs by LC-MS/MS as previously described (Antoine et al., 2012, Venereau et al., 2012) with the additional investigation for ubiquitination by looking for the detection of GlyGly adducted residues (Denis et al., 2007, Peng et al., 2003). Reduced cysteine residues within HMGB1 were characterised by thiol-specific alkylation with iodoacetamide (50mM, 30min). Alkylation with iodoacetamide yields a mass-shift of 57amu (atomic mass unit). Sulphonyl (SO_3H) oxidative modification was determined by looking for a mass increase of 48amu on each particular cysteine residue. After the first alkylation step, remaining cysteine residues engaged in a disulphide bond were reduced with 1mM dithiothreitol (DTT) (15min, 4°C). Newly reduced cysteines were then alkylated with *N*-ethylmalemide (NEM) (50mM, 5min, on ice) which yields a mass shift of 125amu.

Samples were run on a hybrid triple quadrupole-linear ion trap mass spectrometer (QTRAP 5500, AB Sciex, Foster City, CA, USA) equipped with a NanoSpray II source by in-line LC using a U3000 HPLC System (Dionex, CA, USA) connected to a 180µm x 20mm nanoAcquity

UPLC C_{18} trap column and a 75µm x 15cm nanoAcquity UPLC BEH130 C_{18} column (Waters, MA, USA) via reducing unions. Spectra were acquired automatically in positive ion mode using information-dependent acquisition (Analyst; Applied Biosystems). Database searching was performed using ProteinPilot 2 (Applied Biosystems) with the latest version of the SwissProt database, with the confidence level set at 80%, and with biological modifications allowed. Individual peptide fragmentation to produce *b* and y ions was used to determine the amino acid sequence and confirm the presence of specific modifications.

5.2.4 Cell culture

THP-1 cells were cultured as described in Chapter 4, Section 4.2.2. Mouse embryonic fibroblasts (MEFs) were cultured in Dulbecco's Modified Eagle Media (DMEM) supplemented with 10% heat-inactivated FBS, 100U/mL penicillin and 100µg/mL streptomycin. All cells were cultured at 37°C, 5% CO_2. MEFs were cultured due to the availability of a stable HMGB1 knockout version of these cells.

5.2.5 Apoptosis induction *in vitro*

THP-1 ($1x10^6$ cells/mL) or MEFs ($4x10^5$ cells/mL) were plated into T25 flasks (5mL), 12-well (1mL) or white-walled 96-well plates (100µL) and allowed to adhere overnight (MEFs). Cells were then dosed with STS or vehicle (DMSO) for 0-24hr and apoptosis was determined by caspase-3 Western blotting, Caspase-Glo 3/7 assay or Annexin V/Propidium iodide (PI) FACS.

5.2.6 Production of THP-1 cytosolic lysates

Following STS dosing, THP-1 cells from T25 flasks were pelleted by centrifugation (300*g*, 5min, 20°C), resuspended in PBS, centrifuged again, and then resuspended in 200µL of buffer A (for cytosolic extraction as described in Chapter 4, Section 4.2.3) followed by centrifugation (1150*g*, 5min, 4°C). Supernatants were removed and stored at -80°C prior to

assessment of protein content by Bradford assay (as described in Chapter 2, Section 2.2.5) and caspase-3 Western blotting.

5.2.7 Western blotting for Caspase-3

20µg of total protein was loaded per sample into 10% acrylamide gels, alongside molecular weight markers. Proteins were separated by running gels for 10min at 90V, followed by 50min at 170V. Proteins were transferred to nitrocellulose membrane for 1hr at 230mA. Membranes were checked for even loading and transfer using Ponceau staining and then blocked in 10% (w/v) non-fat milk for 1hr at RT. All antibodies were made up in 2% non-fat milk/0.1% TBST. Membranes were probed with rabbit anti-caspase-3 antibody (1:2000, 16hr, 4°C) or mouse anti-β actin (1:200000, 1hr, RT), washed (0.1% TBST, 4x5min), and probed with rabbit anti-mouse (1:10000, 1hr, RT) or goat anti-rabbit (1:10000, 1hr, RT). Membranes were washed (0.1% TBST, 4x5min) and probed with ECL reagent. Membranes were imaged using X-ray film.

5.2.8 Annexin V/PI FACS

Following STS treatment, the dosing media in 12-well plates was removed from the cells, MEFs were washed with PBS and removed from the plate by trypsinisation. THP-1 cells, being suspension cells, did not require trypsinisation and were removed in the dosing media. Cells were then pelleted by centrifugation (300*g*, 5min, 20°C), resuspended in PBS, centrifuged again, and resuspended in 0.5mL Annexin V binding buffer. Cells were transferred into FACS tubes and stained with Annexin V-FITC (2µL) and PI (5µL). Samples were incubated in the dark at RT for 15min prior to analysis on a BD FacsCalibur machine. Positive control samples for necrosis (freeze thawed in liquid nitrogen) and apoptosis (1µM STS, 24hr) were stained with only PI or Annexin V respectively. Unstained, healthy cells were used as a negative control. Data was analysed using Cyflogic 1.2.1 software (CyFlo Ltd).

5.2.9 Cytotoxicity assessment

Following STS treatment in 96-well plates, cell viability was determined by CellTiter 96® Aqueous One Solution assay kit as described in Chapter 4, Section 4.2.8.

5.2.10 Caspase-Glo 3/7 assay

Following STS dosing of cells in the 96-well plates, the dosing media was replaced with serum-free media and the Caspase-Glo 3/7 assay was run according to manufacturer's instructions (Promega) using a Varioskan Flash plate reader (Thermo Scientific).

5.2.11 Immunofluorescence (IF)

Immunofluorescence was carried out according to the method in Chapter 4, Section 4.2.7. MEFs ($4x10^5$ cells/well) were plated into the wells, and allowed to adhere overnight. After adherence, cells were dosed with STS (1µM) for 18hr.

5.2.12 Proteasome inhibition

MEFs ($4x10^5$ cells/well) were incubated in 12-well plates overnight to adhere. Cells were then dosed with 10µM MG132 for 1 or 17hr, or 0.1% DMSO as a vehicle control. At the timepoints, media was removed and cells were washed with fresh serum-free media and trypsinised. Cells were pelleted by centrifugation (300*g*, 5min, 4°C) and resuspended in PBS. Cells were re-pelleted, and resuspended in 100µL RIPA buffer supplemented with 2µL/mL protease inhibitor cocktail (PIC). Samples were incubated on ice for 15min and then centrifuged (18,000*g*, 5min 4°C). Supernatants were retained and protein content was determined by Bradford assay (as described in Chapter 2). Western blots for HMGB1 and ubiquitinated proteins were run as described later in this methods section, with 5µg total protein per lane.

5.2.13 Isolation of microparticles (MP)

Microparticles were isolated from MEFs according to the method described in Spencer DM et al (Spencer et al., 2014). Briefly, $120x10^6$ MEFs per treatment condition were cultured in T75 flasks. Cells were dosed, in serum-containing media, with STS (1µM, 24hr) to induce apoptosis or heated to 56°C for 30min to induce necrosis. Control cells were treated with 0.1% DMSO for 24hr. Following the induction of apoptosis or necrosis, the dosing media was removed and centrifuged twice (500*g*, 5min, 4°C) to pellet out any cells. Supernatants were then syringe filtered (1.2µm) to remove any remaining cells. The filtered supernatants were ultracentrifuged (150000*g*, 45min, 10°C) to pellet out MP. The MP pellet was resuspended in 1mL PBS and centrifuged (10000*g*, 30min, RT) to concentrate the MP samples. Pellets were resuspended in 20µL PBS and stored at -80°C. The protein content of MP was determined by Bradford assay (as described in Chapter 2).

5.2.14 Characterisation of MP by flow cytometry

MP were isolated from apoptotic, necrotic and healthy control cells as described previously, and were immediately characterised by flow cytometry on a BD FacsCalibur machine. Submicron sizing beads (Bangs Laboratories, CA) were used to define the size parameters for the determination of MP, as previously published (Spencer et al., 2014). FACS files were analysed using Flowing Software 2.5.1 (University of Turku and Turku Bioimaging, Helsinki, Finland)

5.2.15 Western blotting for MP protein expression

Western blots for HMGB1, total ubiquitin, Lys48- and Lys63-specific ubiquitin chains, histone H2b and β-actin were run on MP samples. Briefly, 5µg of total protein was denatured at 95°C in LDS sample buffer, but not reducing agent for 5min, prior to loading into 10% acrylamide gels. Gels were run, transferred and blocked as described for the caspase-3 Western blot (with the exception that the membrane to be probed for Lys48- and

Lys63- chains was transferred at 30V for 2hr to minimise non-specific binding. All antibodies were made up in 2% non-fat milk/0.1% TBST. Rabbit anti-HMGB1 antibody (1:2000), mouse anti-actin antibody (1:200000), mouse anti-histone H2b (1:2000) or rabbit anti-Lys63 ubiquitin chains (1:500) were applied to blocked membranes for 1hr at RT. Membranes were washed (0.1% TBST, 4x5min) and incubated in secondary antibodies (anti-mouse 1:10000 or anti-rabbit (1:10000 for anti-HMGB1 blot, 1:5000 for anti-Lys63 blot) for 1hr at RT. Membranes were probed with ECL, and imaged on X-ray film. Membranes were then stripped (2% SDS, 0.7% β-mercaptoethanol, 62.5mM Tris (pH6.8), 60°C, 45min), washed (3x10min, 0.1% TBST) and blocked in 10% non-fat milk (1hr, RT). Membranes were reprobed with rabbit anti-ubiquitin (1:1000, overnight, 4°C) or rabbit anti-Lys48 ubiquitin chains (1:500, overnight, 4°C), washed (4x5min), probed with anti-rabbit (1:5000, 1hr, RT), washed again (0.1% TBST, 4x5min), probed with ECL reagent and imaged on X-ray film.

5.2.16 Statistical analysis

Statistical analysis of data was undertaken using GraphPad Prism 5 software. All results are presented as mean±standard error of the mean (SEM). Data were assayed for normality by Shapiro-Wilk test. Normal data were compared by One-Way ANOVA (with either Dunnett's post-hoc test for comparisons between several test groups and a control group, or Bonferroni post-hoc test for comparisons between multiple test groups) or unpaired t-test as indicated. Non-parametric data were compared by Kruskal-Wallis or Mann-Whitney tests as indicated. Results were considered significant when $p<0.05$.

5.3 Results

The collection, preparation (tryptic digestion) and LC-MS/MS analysis of human serum samples from APAP overdose patients was carried out by Dr Dan Antoine and Dr Roz Jenkins.

5.3.1 HMGB1 is ubiquitinated in APAP-overdose patients

In APAP overdose patients exhibiting high levels of apoptosis (high levels of cleaved keratin-18, as determined by Peviva M30 apoptosense ELISA in a previous study (Antoine et al., 2012)), MS/MS analysis revealed the presence of ubiquitination on lysine 30 (K30) and threonine (T136). Ubiquitination was detected by the characteristic ε-glycine-glycine signature on tryptic digested HMGB1 (Peng et al., 2003) (Fig.5.3).

In these serum samples, following tryptic digest, there was detection of a peptide corresponding to amino acid sequence KKHPDASVNFSEFSK with a mass of 1851.0Da, corresponding to a 132.1amu increase on the mass of the amino acids alone. This mass increase was identified on K30-H31, and indicates ubiquitination of K30 (GlyGly) and oxidation of the neighbouring H31 residue (Fig.5.3A).

A second peptide corresponding to amino acid sequence MWNNTAADDKQPYE with a mass of 1796.9Da, corresponding to a 114.1amu increase on the mass of the amino acids alone. This mass increase was identified to be on T136, and corresponds to the GlyGly adduct, indicative of ubiquitination (Fig.5.3B).

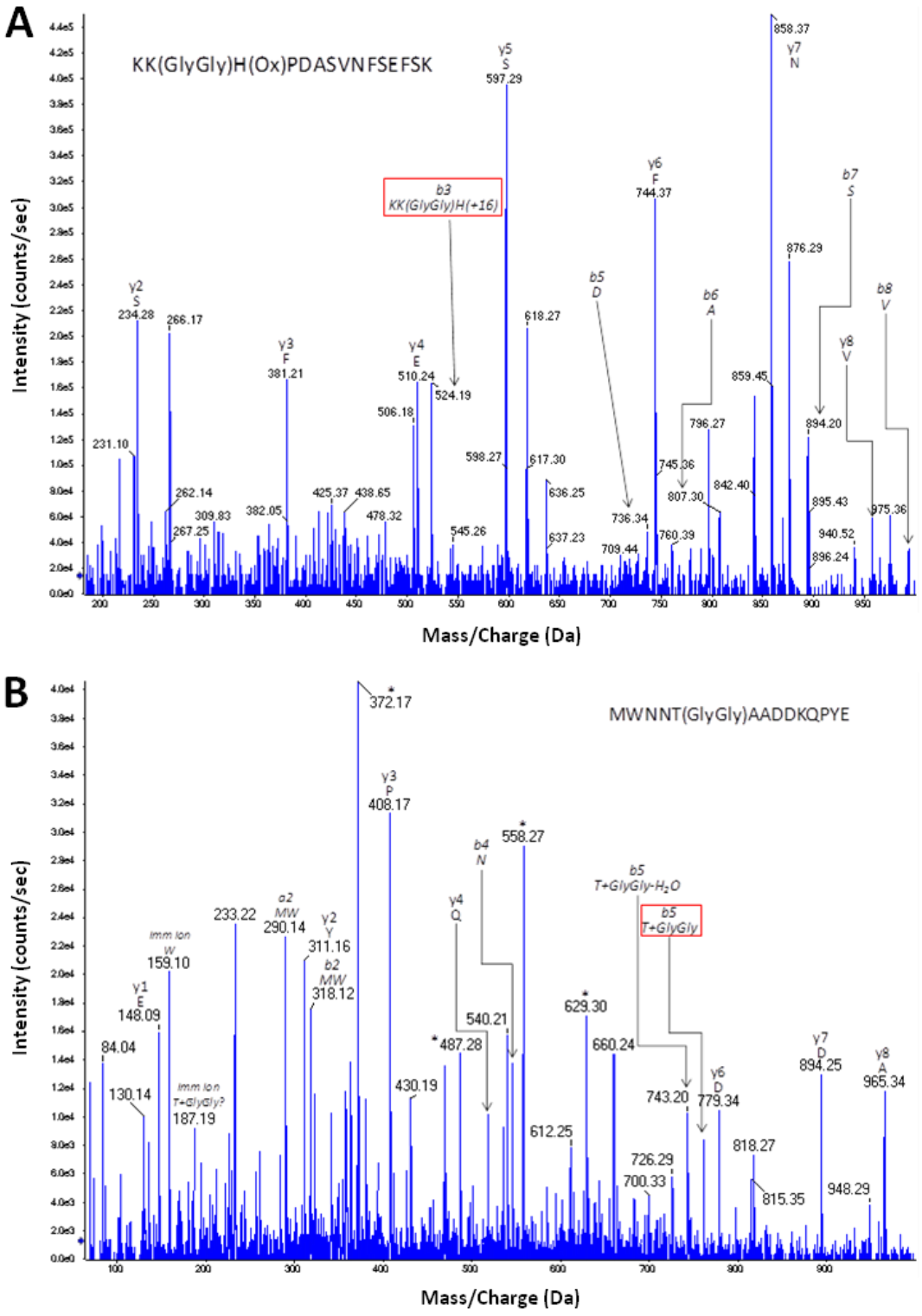

Fig.5.3 – Ubiquitination of HMGB1 in APAP overdose in man. (A) K30 and (B) T136 of HMGB1 are ubiquitinated in the serum of APAP overdose patients that exhibit high levels of cleaved keratin-18. Traces are representative of *n=8* samples, all of which show ubiquitination.

5.3.2 THP-1 cells undergo apoptosis in response to staurosporine (STS) in a dose-dependent manner

Following on from the observation of ubiquitinated HMGB1 in the serum of human APAP overdose patients by Dr Antoine and Dr Jenkins, I investigated the translatability of the findings by inducing apoptosis *in* vitro in THP-1 cells.

Staurosporine (STS) induces apoptosis in THP-1 cells in a dose-dependent manner, as demonstrated by assessment of caspase-3 activation (by Western blot) and Annexin V/PI FACS.

Significant caspase-3 activation is seen at 16hr in response to 1μM and 2μM STS, in comparison with the vehicle control (0.2% DMSO). With 2μM STS, complete cleavage of procaspase-3 to the activated caspase-3 fragments is seen (Fig.5.4) In the Annexin V/PI FACS assay significant apoptosis induction is seen at 16hr with all concentrations of STS investigated (0.25μM+) (Fig.5.5). Apoptosis (Annexin V positive, PI negative) and late apoptosis/dead cells (Annexin V positive, PI positive) are significantly increased in a dose-dependent manner. Apoptosis peaks at 26.8%, seen at 2μM STS, although no significant difference in percentage apoptosis are observed between 0.5 and 2μM. These effects are also associated with a corresponding decrease in viable cells (Annexin V negative, PI negative). Necrosis is largely unaffected by STS.

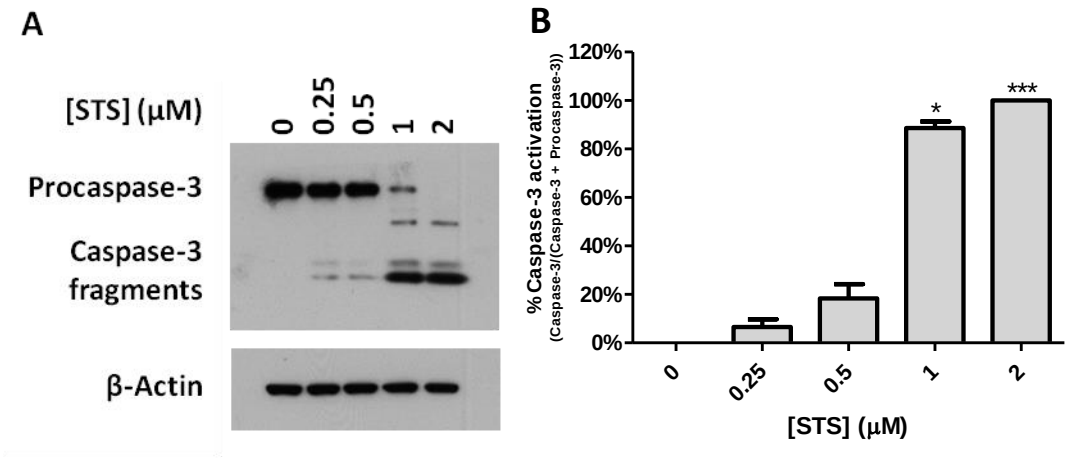

Fig.5.4 – Caspase-3 activation by Western blot in THP-1 cell cytosolic lysates. Following STS treatment (0-2μM) for 16hr, cytosolic lysates were tested for caspase-3 activation by Western blot. Actin was used as a loading control. (A) a representative Western blot of cytosolic caspase-3 activation. (B) caspase-3 as a % of total caspase-3 (procaspase-3 + caspase-3) in cytosolic lysates. Data is represented as mean+SEM of *n=3* experiments, with triplicate samples per condition within each experiment. *=p<0.05, ***=p<0.001 in comparison with control cells as determined by One-Way ANOVA.

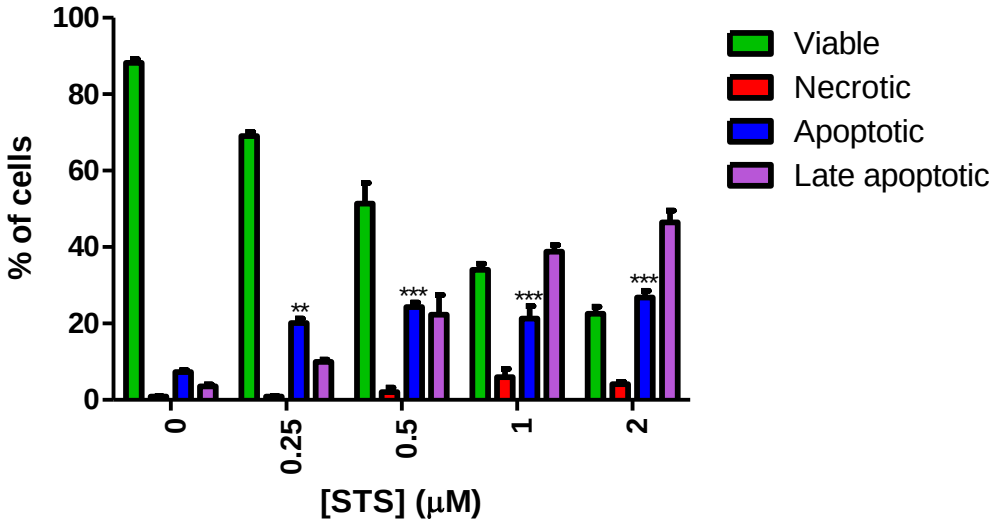

Fig.5.5 – Assessment of apoptosis induction in THP-1 cells by STS as determined by Annexin V/PI FACS. Following STS treatment (0-2μM) for 16hr, cells were stained with Annexin V-FITC or PI, and assessed for induction of cell death. Cell statuses were defined as follows: viable (Annexin V negative, PI negative), necrotic (Annexin V negative, PI positive), apoptotic (Annexin V positive, PI negative) and late apoptotic (Annexin V positive, PI positive). Data is represented as mean+SEM of *n=3* experiments. **=p<0.01, ***=p<0.001 in comparison with control cells as determined by One-Way ANOVA.

5.3.3 THP-1 cells undergo apoptosis in response to staurosporine (STS) in a time- dependent manner

STS also induces apoptosis of THP-1 cells in a time-dependent manner (Fig.5.6). Over a 16hr timecourse with 1μM STS, significant caspase-3 activation compared with control was observed at 4, 8 and 16hr. The percentage caspase-3 activation observed at 16hr was comparable with the activation seen in the dose response experiment at 1μM.

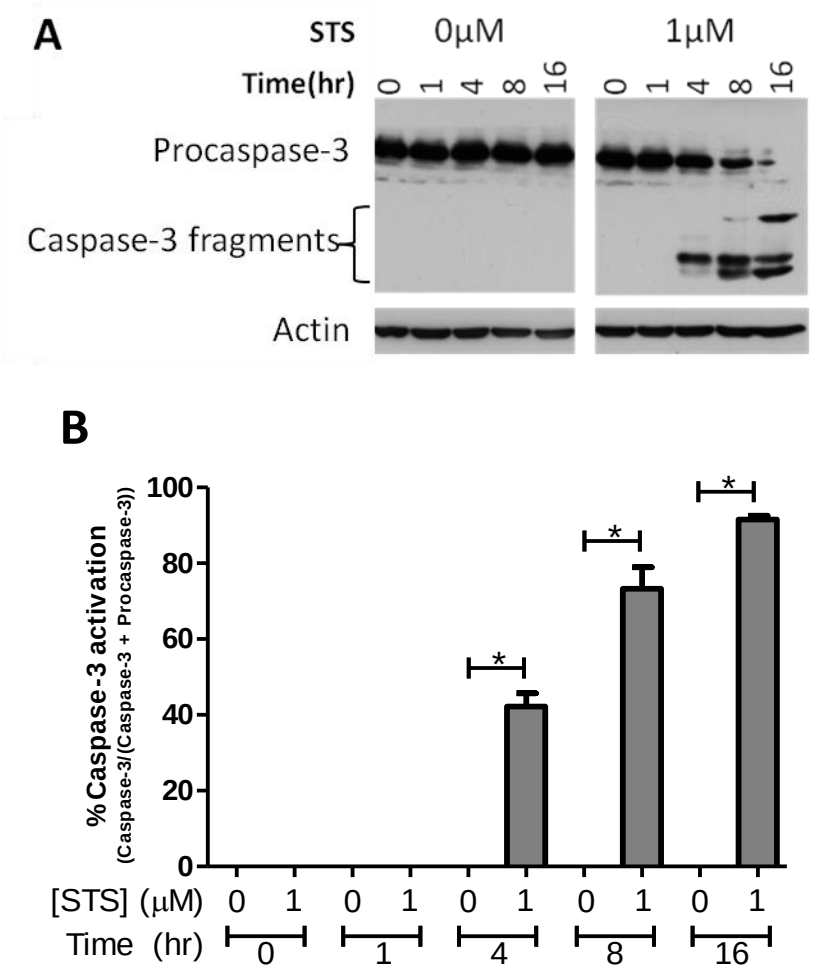

Fig.5.6 – Time-dependent caspase-3 activation by Western blot in THP-1 cell cytosolic lysates. Following STS treatment (1μM) for 0-16hr, cytosolic lysates were tested for caspase-3 activation by Western blot. Actin was used as a loading control. (A) a representative Western blot of cytosolic caspase-3 activation. (B) caspase-3 as a % of total caspase-3 (procaspase-3 + caspase-3) in cytosolic lysates. Data is represented as mean+SEM of *n=3* experiments. *=p<0.05 in comparison with time-matched control as determined by Mann-Whitney test.

5.3.4 THP-1 cell apoptosis is inhibited by Z-VAD-FMK

Pre-treatment for 30min with 50μM Z-VAD-FMK, attenuates STS-induced apoptosis of THP-1 cells, as determined by caspase-3 Western blot and Annexin V/PI FACS. Caspase-3 Western blot data (Fig.5.7) shows that Z-VAD-FMK prevents cleavage of procaspase-3 to the active cleaved caspase-3 fragments. This attenuation of caspase-3 activation is shown at both 0.5 and 1μM STS. Annexin V/PI FACS also shows that pre-treatment of cells with Z-VAD-FMK significantly attenuates apoptosis induction (Fig.5.8). This is shown by a significant decrease in apoptosis at 0.5μM STS with Z-VAD-FMK treatment compared with 0.5μM alone. Additionally, a significant decrease in late apoptosis is seen in cells given the Z-VAD-FMK pre-treatment. Importantly, Z-VAD-FMK pre-treatment also results in a significant prevention of the loss of viable cells at both 0.5 and 1μM STS.

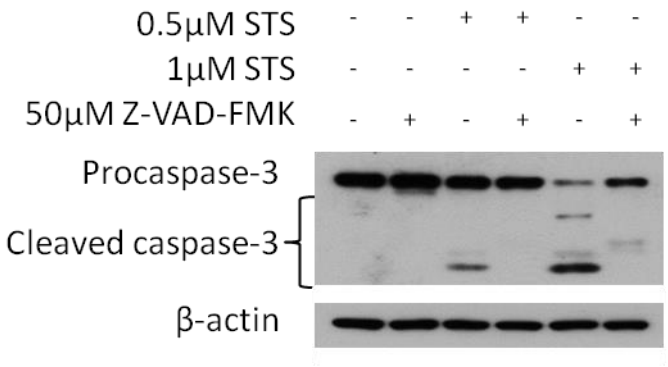

Fig.5.7 – Effect of Z-VAD-FMK on apoptosis induction in THP-1 cells by STS as determined by caspase-3 Western blot. THP-1 cells were pre-treated with Z-VAD-FMK (50μM) for 1hr prior to STS treatment (0.5-1μM) for 16hr. Cytosolic lysates were tested for caspase-3 activation by Western blot. Actin was used as a loading control. A representative Western blot of *n=2* experiments is shown.

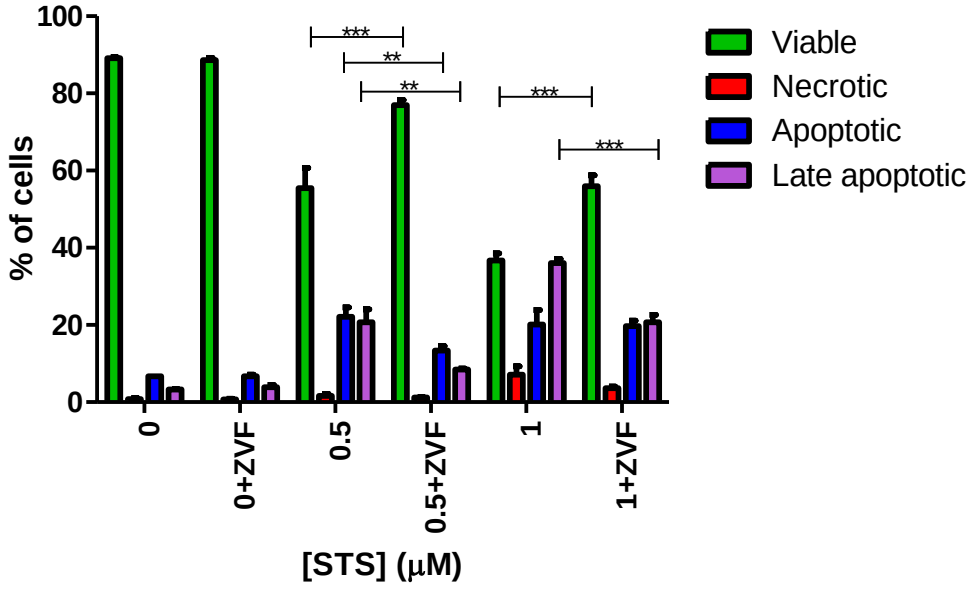

Fig.5.8 – Effect of Z-VAD-FMK on apoptosis induction in THP-1 cells by STS as determined by Annexin V/PI FACS. THP-1 cells were pre-treated with Z-VAD-FMK (50μM) for 1hr prior to STS treatment (0.5-1μM) for 16hr. Cells were stained with Annexin V-FITC or PI, and assessed for induction of cell death. Cell statuses were defined as follows: viable (Annexin V negative, PI negative), necrotic (Annexin V negative, PI positive), apoptotic (Annexin V positive, PI negative) and late apoptotic (Annexin V positive, PI positive). Data is represented as mean+SEM of *n=3* experiments. **=p<0.01, ***=p<0.001 between indicated groups as determined by One-Way ANOVA.

5.3.5 Mouse embryonic fibroblasts (MEFs) undergo dose-dependent apoptosis in response to STS

Following on from the initial findings in THP-1 cells, investigations were carried out in MEFs due to the availability of a stable HMGB1 knockout MEF cell line that could be used for future studies.

MEFs also display a low level of apoptosis in response to STS. Annexin V/PI FACS shows significant induction of apoptosis at 18hr in response to STS at 0.5, 1 and 2µM (Fig.5.9). Late apoptosis and necrosis are not affected by STS dosing. Cell viability of MEFs was determined by MTS assay. In response to 18hr treatment with STS, there was significant loss of cell viability in comparison with vehicle control (0.2% DMSO) (Fig.5.10). The effect of STS on HMGB1 localisation within MEFs was also investigated through immunofluorescence. 1µM STS causes significant morphological changes in the MEFs, with STS-treated cells demonstrating cytoplasmic shrinkage, and adopting a spindly morphology. HMGB1 is also seemingly retained within the nucleus during STS-induced apoptosis (Fig.5.11).

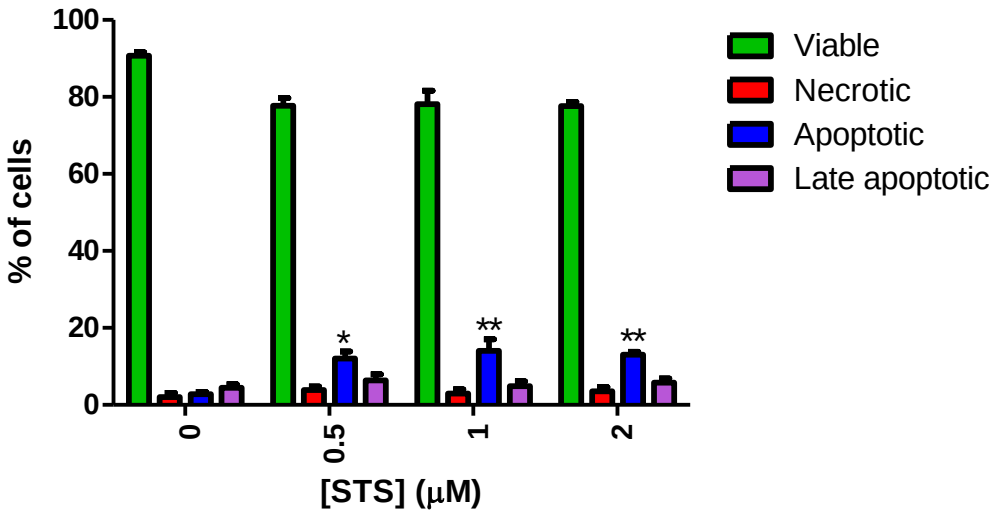

Fig.5.9 – Assessment of apoptosis induction in MEFs by STS as determined by Annexin V/PI FACS. Following STS treatment (0-2μM) for 18hr, cells were stained with Annexin V-FITC or PI, and assessed for induction of cell death. Cell statuses were defined as follows: viable (Annexin V negative, PI negative), necrotic (Annexin V negative, PI positive), apoptotic (Annexin V positive, PI negative) and late apoptotic (Annexin V positive, PI positive). Data is represented as mean+SEM of *n=3* experiments. *=p<0.05, **=p<0.01 in comparison with control cells as determined by One-Way ANOVA.

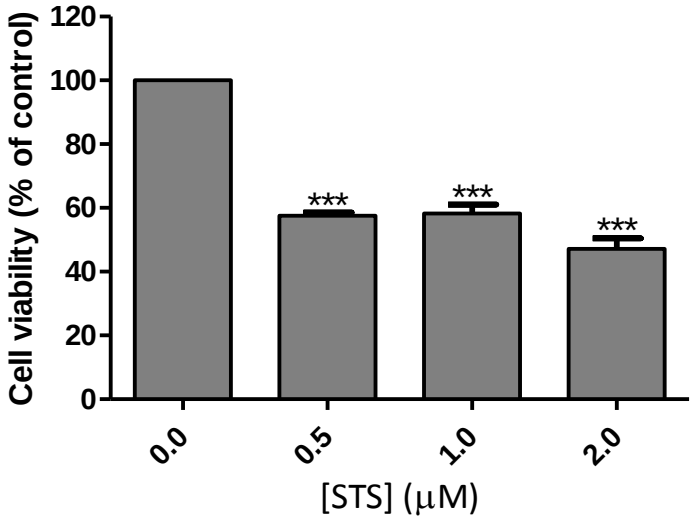

Fig.5.10 – Assessment of MEF cell viability by MTS assay following STS-treatment. Following STS treatment (0-2μM) for 18hr, cell viability was assessed by MTS assay. Data is represented as mean±SEM of *n=3* experiments. ***=p<0.001 in comparison with control cells as determined by Kruskal-Wallis test.

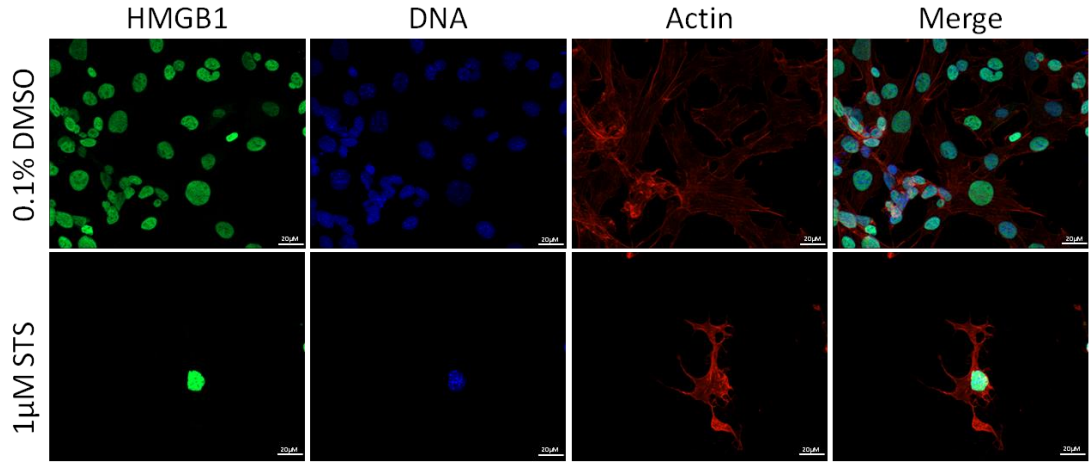

Fig.5.11 – Immunofluorescent microscopy of MEFs stained for HMGB1, following STS (1μM) treatment. HMGB1 was stained using Abcam rabbit polyclonal (ab18256) followed by Alexa Fluor 488 donkey anti-rabbit secondary, DNA was stained using Hoechst, actin was stained using phalloidin. Scale bar is 20μm.p Data is representative of *n=3* experiments.

5.3.6 Mouse embryonic fibroblasts (MEFs) undergo time-dependent apoptosis in response to STS

MEFs also undergo apoptosis in a time-dependent manner in response to STS, as determined by Caspase-Glo 3/7 assay and Annexin V/PI FACS. The Caspase-Glo 3/7 assay was utilised due to a lack of sensitivity of the caspase-3 Western blot using MEF whole cell lysates (Fig.5.12). Annexin V/PI FACS data also shows significant apoptosis induction in MEFs over a 24hr timecourse. There was a significant increase in apoptotic cells at 24hr treatment with 1μM STS (Fig.5.13C). Conversely, there is significant loss of viable cells from 6hr (Fig.5.13A). As seen with the MEF dose response data, there is no effect of STS on the induction of late apoptosis or necrosis (Fig.5.13B,D). Assessment of overall cell viability by MTS assay shows that, over a 24hr timecourse, there is significant loss of cell viability at 18 and 24hr in response to 1μM STS. (Fig.5.14)

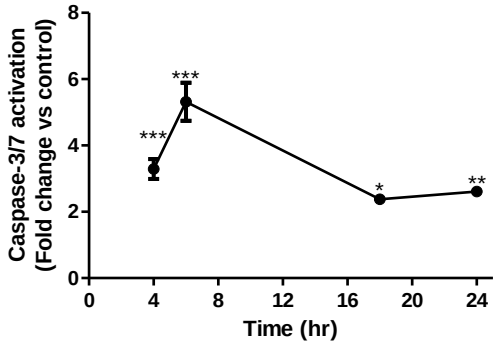

Fig.5.12 – Caspase-3/7 activation in MEFs over a 24hr timecourse following 1μM STS treatment. Data is represented as mean±SEM of *n=3* experiments. *=p<0.05, **=p<0.01, ***=p<0.001 in comparison with time-matched control cells as determined by Kruskal-Wallis test.

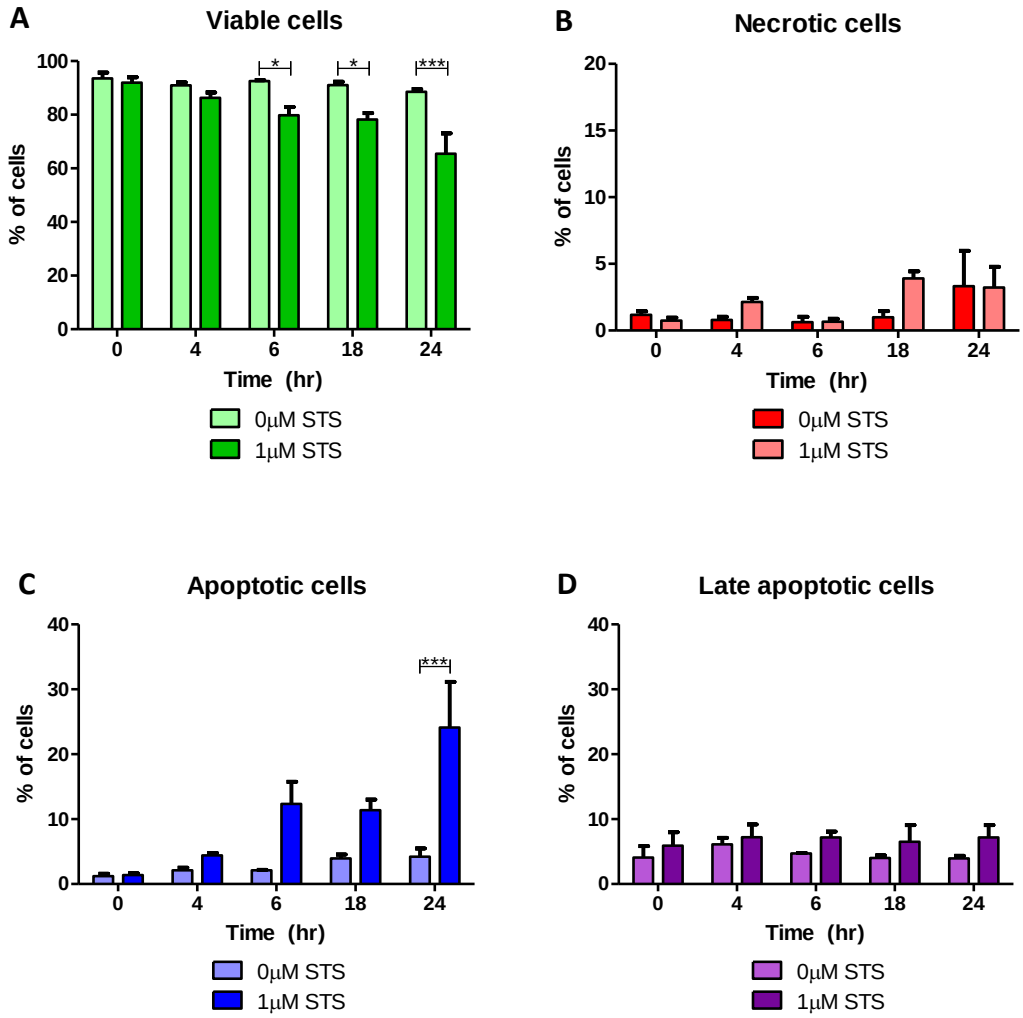

Fig.5.13 – Annexin V/PI FACS assessment of MEFs following 1μM STS treatment, over a 24hr timecourse. Cell statuses were defined as follows: (A) viable (Annexin V negative, PI negative), (B) necrotic (Annexin V negative, PI positive), (C) apoptotic (Annexin V positive, PI negative) and (D) late apoptotic (Annexin V positive, PI positive). *=p<0.05, ***=p<0.001 in comparison with time-matched control cells as determined by One-Way ANOVA.

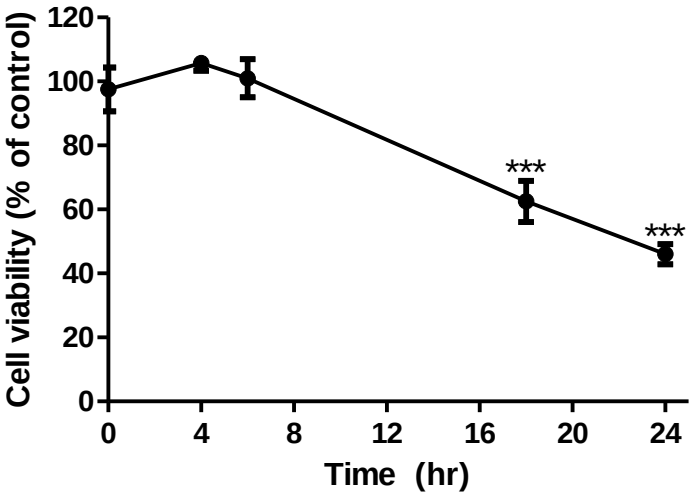

Fig.5.14 – Assessment of MEF cell viability by MTS assay following 1µM STS treatment over a 24hr timecourse. Following STS treatment (1µM) for 0-24hr, cell viability was assessed by MTS assay. Data is represented as mean±SEM of *n=3* experiments. ***=p<0.001 in comparison with control cells as determined by One-Way ANOVA.

5.3.7 The effects of proteasome inhibition on HMGB1 expression

Following on from the successful induction of apoptosis in MEFs, studies were carried out to investigate if HMGB1 is subject to proteasomal degradation. Preliminary data showed that the proteasome inhibitor MG132 (10μM) causes significant accumulation of ubiquitinated proteins in MEFs at 1hr, without an effect on HMGB1 expression. With treatment with MG132 (10μM) for 17hr, the accumulation of ubiquitinated proteins was still seen, however this was associated with a reduction in HMGB1 expression (Fig.5.15).

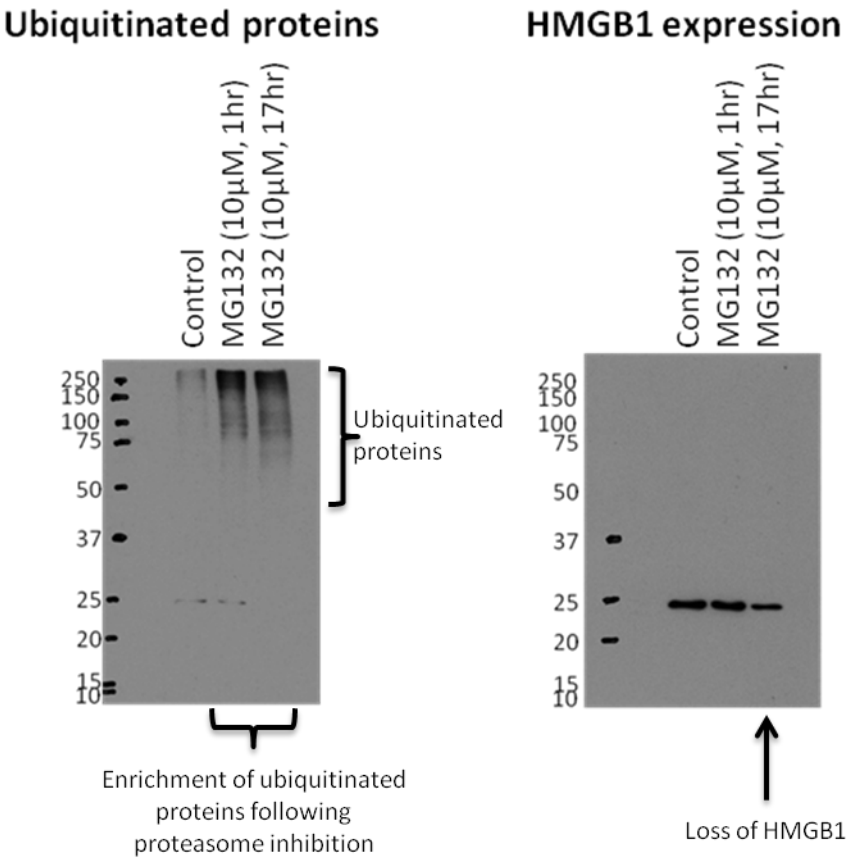

Fig.5.15 – Effects of MG132 on HMGB1 and ubiquitinated protein expression. MEFs were treated with 10μM MG132 for 1hr or 17hr, and whole cell lysates were analysed for ubiquitinated proteins and HMGB1 by Western blot. Data shown is from *n=1* experiment.

5.3.8 Characterisation of microparticles (MP) by flow cytometry

A possible fate of HMGB1-Ub is translocation to apoptotic MP. Recent publications have demonstrated that HMGB1 is expressed in microparticles from apoptotic cells, but without investigation of the mechanism of translocation (Spencer et al., 2014, Schiller et al., 2013). Following isolation of MP from STS-treated MEFs, characterisation of MP, and comparison between control, apoptotic and necrotic MP was undertaken by flow cytometry. Submicron sizing beads (0.2, 0.5, 0.76μm) were used to gate the populations of MP (Fig.5.16).

Following STS-treatment (1μM, 24hr), there was the detection of a new population of submicron particles (Fig.5.17C) that did not appear in PBS alone (Fig.5.17A), or MP isolated from control cells (Fig.5.17B). These apoptotic MP have a greater size and granularity than MP isolated from control cells (Fig.5.17E-F). Additionally, heat treatment of cells (56°C, 30min) results in the formation of a different new population of submicron particles at a similar size (FSC) to those seen in STS-treated cells, however these necrotic MP are more granular than apoptotic MP (as determined by SSC) (Fig.5.17D-F). Overall, characterisation of the MP from control, STS and heat treated MEFs show differences in size and granularity, although there is overlap between the size of apoptotic and necrotic MP. STS treatment results in an increase in the proportion of the apoptotic MP, and heat treatment results in an increase in the proportion of necrotic MP as a percentage of total MP (Fig.5.17G).

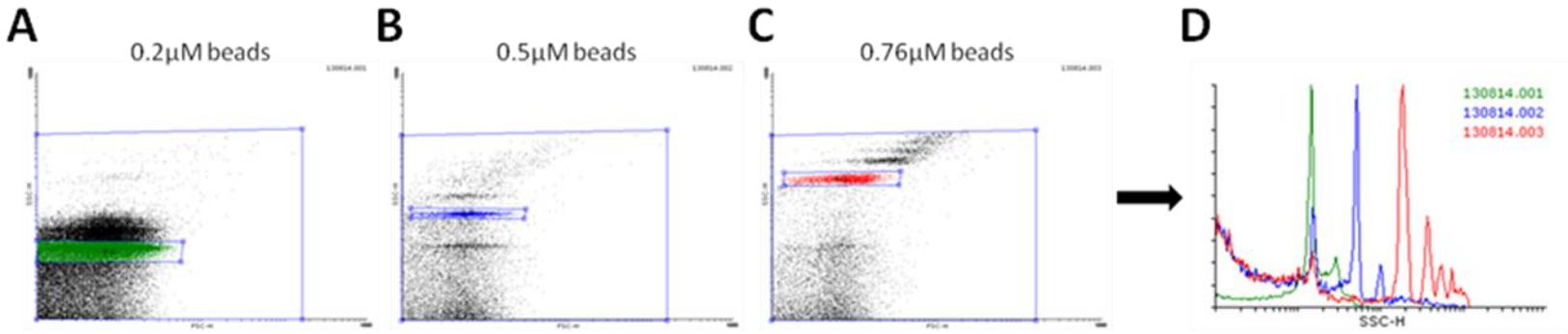

Fig.5.16 – Gating of microparticles using submicron beads. (A) 0.2µm, (B) 0.5µm and (C) 0.76µm beads were used to define microparticles. (D) Combined histogram, showing distinct bead populations. Due to the sensitivity of the machine, gating of MP was done according to granularity (SSC) rather than size directly.

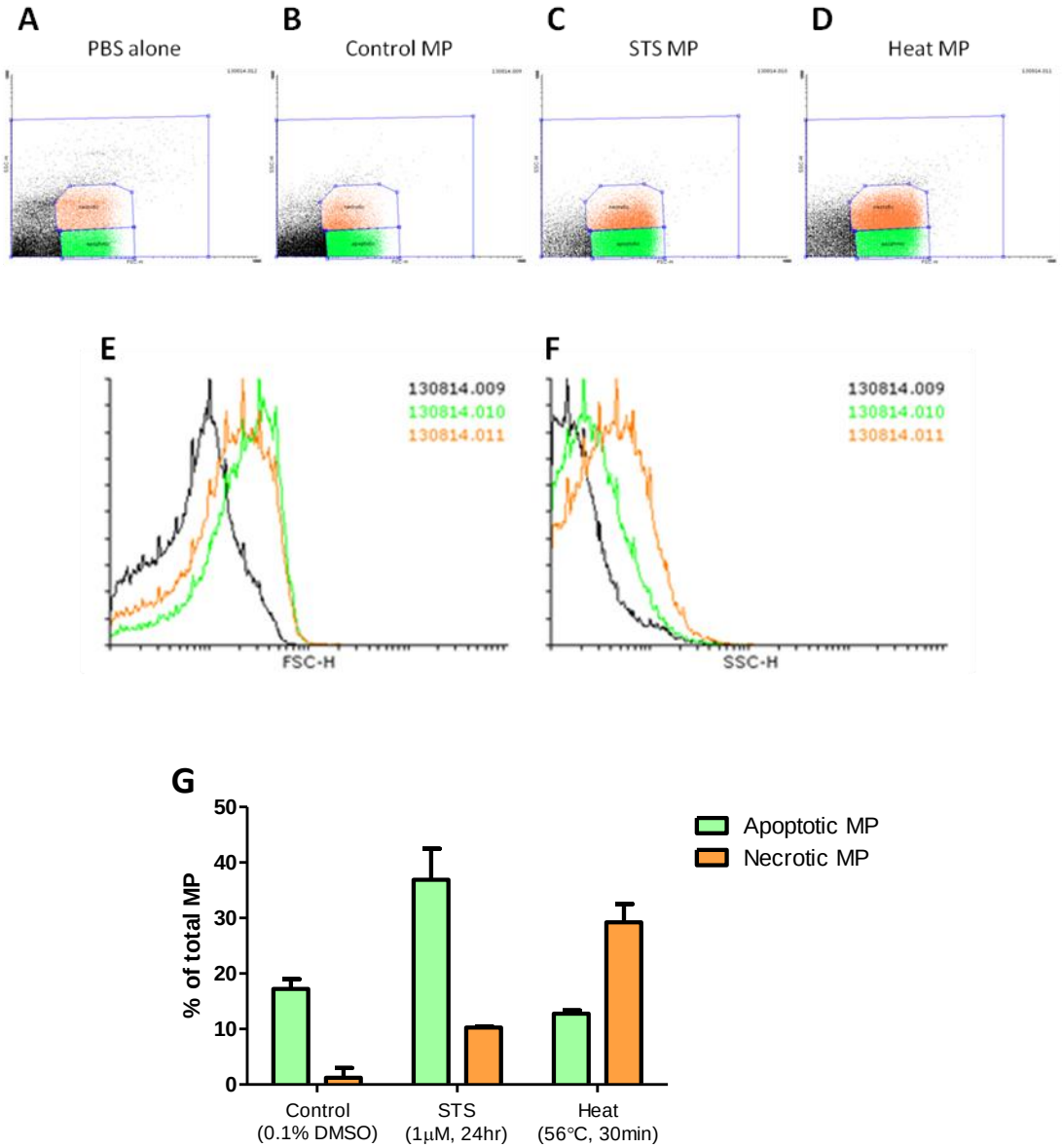

Fig.5.17 – MP from MEFs undergoing different forms of cell death were characterised by flow cytometry. (A) Some submicron particles were detectable in cell-free PBS, and counts were subtracted from MP values from all other treatment groups. Dot plots of (B) MP from control cells, (C) MP from STS-treated cells, (D) MP from heat-treated cells. Histograms showing the (E) FSC and (F) SSC of MP from control cells (black), STS-treated cells (green) and necrotic cells (orange). (G) Analysis of MP populations by treatment condition. Data is represented as mean+SEM of *n=2* experiments.

5.3.9 HMGB1 and ubiquitinated proteins are enriched in apoptotic MP, but not necrotic MP

Characterisation of the protein content of different MP populations was performed by Western blotting (Fig.5.18). HMGB1 was shown to be expressed in both apoptotic and necrotic MP, although there is distinctly greater enrichment of HMGB1 in apoptotic MP compared with necrotic MP (Fig.5.18A). Additionally, ubiquitinated proteins were enriched in apoptotic, but not necrotic MP (Fig.5.18B). The Western blots show polyubiquitin chains at high molecular weights, as well as ubiquitinated protein(s) at approximately 31kDa. Histone H2b was used as a marker of apoptotic MP isolation, as it has been shown previously to be enriched in apoptotic MP in comparison with necrotic MP (Schiller et al., 2013, Schiller et al., 2008). Actin was evenly expressed in all MP populations.

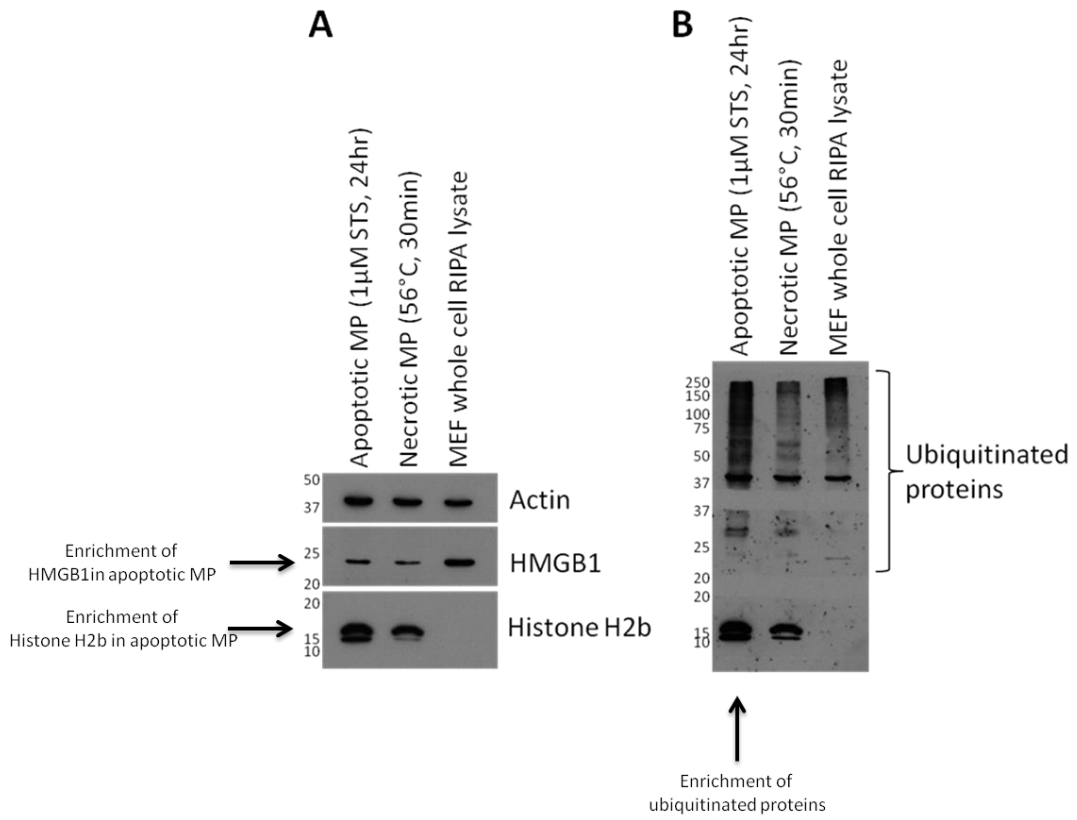

Fig.5.18 – Characterisation of the protein content of MP by Western blot. (A) HMGB1, actin and histone H2b Western blots. (B) Reprobing of membranes for ubiquitin. Incomplete stripping of actin may be responsible for the band seen at 42kDa. Blots are representative of *n=3* individual experiments.

5.3.10 Lys63-linked, but not Lys48-linked Ub chains are enriched in apoptotic MP, but not necrotic MP

The linkage types of ubiquitin chains conjugated to a protein are important for determining the fate of that protein. Lys48-linked chains are commonly associated with directing a protein to proteasomal degradation, whereas Lys63-linked chains are often associated with protein translocation. Hence we sought to identify the type of ubiquitin chains found in the apoptotic MP.

Samples from three individual experiments were pooled and assessed for linkage-specific ubiquitin chains. Enrichment of Lys63- but not Lys48-linked ubiquitin chains was seen in apoptotic MP, compared with necrotic MP (Fig.5.19). In comparison with whole cell lysate from healthy cells, apoptotic MP also show enrichment of Lys63 ubiquitin chains. Healthy cells have greater content of Lys48 ubiquitin chains than MP.

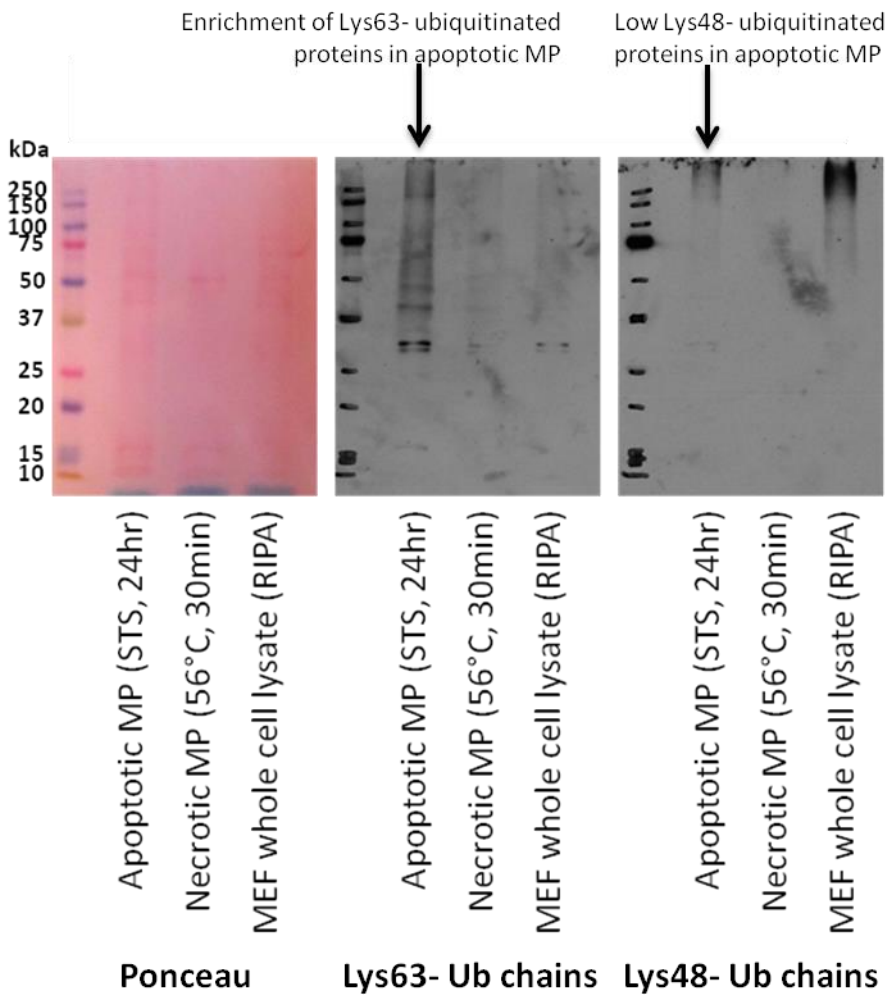

Fig.5.19 – Lys63- and Lys48- linked ubiquitin chains in MP from apoptotic and necrotic cells and whole cell lysates from untreated cells. MP samples from STS or heat-treated MEFs probed for Lys63- or Lys48- linked ubiquitin chains. RIPA lysates of MEFs were probed as a comparison. Blots are representative of pooled samples from *n=3* experiments.

5.3.11 Characterisation of HMGB1 in MG132-treated cells and MP

LC-MS/MS was used to characterise the redox, acetylation and ubiquitination statuses of HMGB1 in MG132-treated MEF cell lysates and MP from MEFs undergoing different mechanisms of cell death. Cysteine thiols in HMGB1 were confirmed by alkylation of the thiol with iodoacetamide (57amu). Cysteines in a disulphide bridge were reduced using DTT and subsequently capped with NEM (125amu). The irreversible sulphonyl oxidation of cysteines was not reduced by DTT treatment. Ubiquitination of HMGB1 was determined by the detection of the signature glycine-glycine (GlyGly) motif (114.1amu) remaining on the ubiquitinated lysine within a peptide following tryptic digest (Peng et al., 2003). Samples were prepared by immunoprecipitation of HMGB1 and tryptic (redox, ubiquitination) or GluC (acetylation) digest. Tryptic digestion of proteins occurs at lysine and arginine residues except if the next residue is a proline.

In whole cell lysates from 1hr MG132-treated MEFs, control MP and necrotic MP, a tryptic peptide corresponding to the amino acid sequence MSSYAFFVQTCR was identified by MS/MS. This peptide corresponds to amino acids 13-24 of HMGB1, but had a molecular weight of 1496.7Da, 57amu greater than the amino acids alone (1439.7). This mass shift of 57amu corresponds to alkylation of C23 by iodoacetamide, and indicates that this cysteine was a thiol (Fig.5.20A). Additionally a second tryptic peptide corresponding to amino acid sequence RPPSAFFLFCSEYRPK was identified by MS/MS. This corresponds with amino acids 97-112 of HMGB1, but had a molecular weight of 2002.2Da, a 57amu shift on the molecular weight of the amino acids alone (1945.2Da). This indicates that C106 is also iodoacetamide alkylated, and hence was also a thiol (Fig.5.20B).

In whole cell lysates from 17hr MG132-treated cells and apoptotic MP, a tryptic peptide corresponding to the amino acid sequence RPPSAFFLFCSEYRPK but with a molecular weight of 1993.2Da was identified as the sulphonyl form of cysteine, indicating caspase-dependent

oxidation of HMGB1 at C106 and suggesting that these cells are undergoing apoptosis (Fig.5.20D). Sulphonyl residues were also detected at C23 in these samples. Additionally, in apoptotic MP, a very low signal was detected at a peptide mass of 1564.7Da in a peptide with the amino acid sequence corresponding to amino acids 13-24. This is a 125amu shift on the mass of the amino acids alone, and corresponds to an NEM adduct on C23, demonstrating that there is also some disulphide HMGB1 seen in apoptotic MP (Fig.5.20C).

GluC digestion of samples was utilised to verify acetylation status of HMGB1. GluC was used, as trypsin would cleave the lysine-rich peptides too small to be amenable for MS/MS analysis. HMGB1 in all samples was shown to be hypoacetylated (data not shown).

In whole cell lysates from both 1hr and 17hr MG132-treated MEFs, as well as control and necrotic MP, there was detection of a peptide corresponding to the sequence HKKKHPDASVNFSE with a mass of 1623.8Da. This peptide corresponds to amino acids 28-41 of HMGB1. This peptide was unmodified and demonstrates no ubiquitination at K30 (Fig.5.21A).

However, in whole cell lysates from apoptotic MP, there was detection of a peptide corresponding to amino acid sequence KKHPDASVNFSEFSK with a mass of 1851.0Da, corresponding to a 132.1Da increase on the mass of the amino acids alone. This mass increase was identified on K30-H31, and indicates ubiquitination of K30 (GlyGly) and oxidation of the neighbouring H31 residue (Fig.5.21B). An overview of the observed HMGB1 isoforms is shown in Table.5.2.

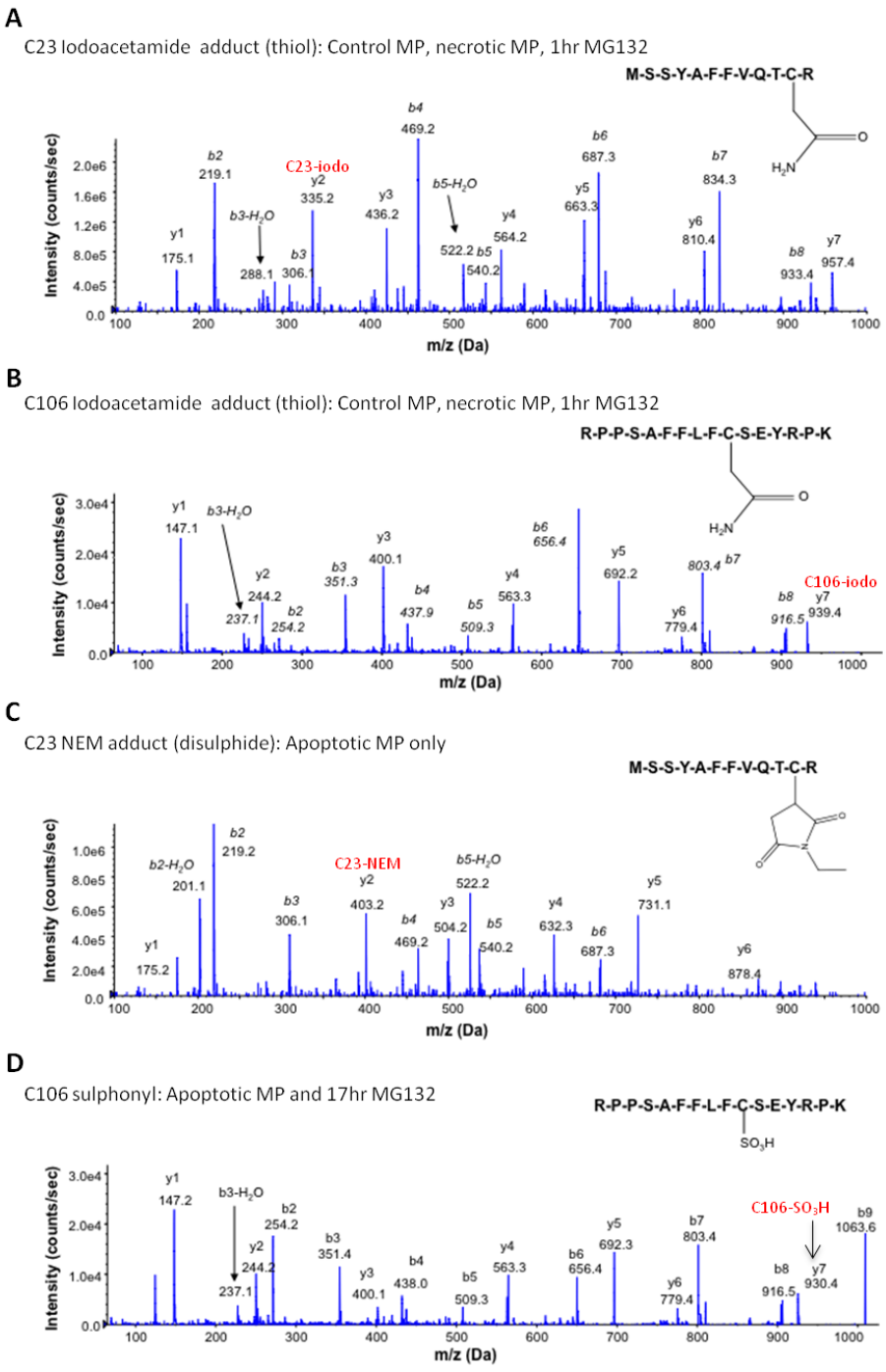

Fig.5.20 – LC-MS/MS characterisation of HMGB1 redox states. Characterisation of C23: MS/MS trace of the peptide containing amino acids 13-24, with an iodoacetamide adduct indicating reduced C23 (A) or with a NEM adduct after DTT reduction of a C23-C45 disulphide bond (C). Characterisation of C106: MS/MS trace of the peptide containing amino acids 97-112 with an iodoacetamide adduct indicating reduced C106 (B) or as a non-reducible sulphonyl C106 (D). In samples with a disulphide bridge, C106 was detected as an iodoacetamide adduct. In samples with a sulphonyl at C106, a sulphonyl was also seen at C23 and C45 (data not shown). Data is representative of traces from either one pooled sample from *n=3* individual experiments (MP samples) or *n=1* experiment (MG132 samples).

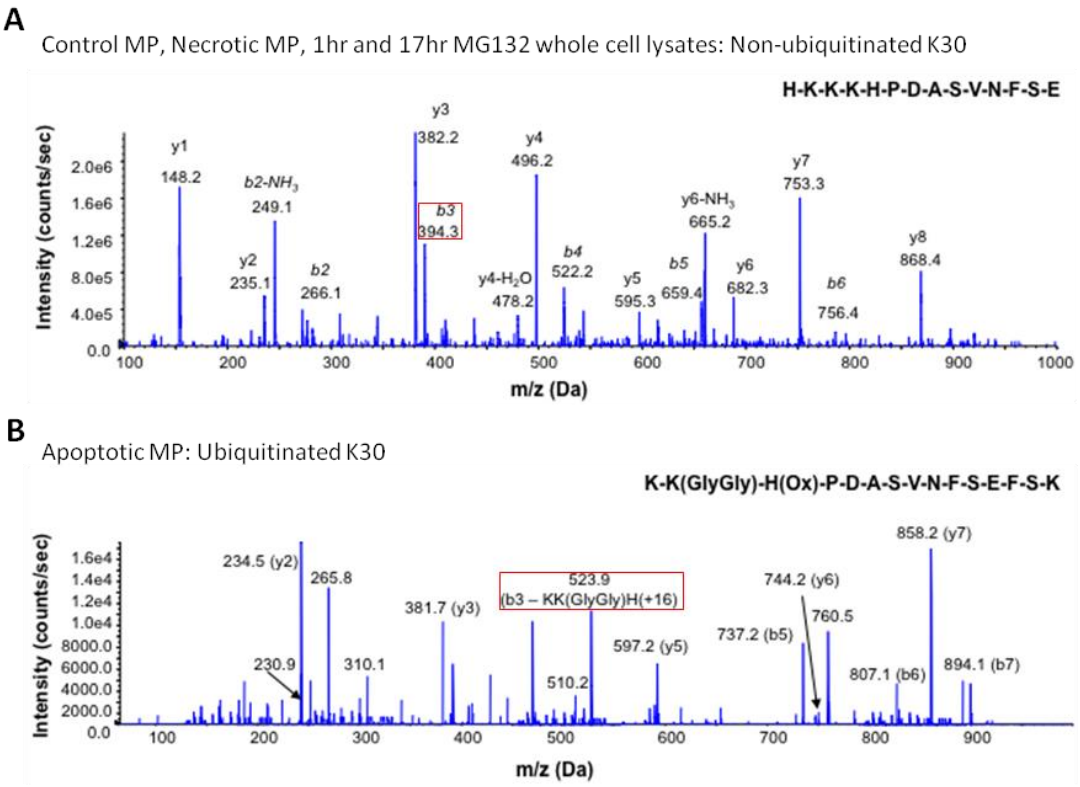

Fig.5.21 – Ubiquitination status of HMGB1 in MP. Characterisation of K30: MS/MS trace of the peptide containing amino acids 29-43, with no modification (A) or a glycine-glycine adduct, indicative of ubiquitination (B) at K30. Data is representative of traces from either one pooled sample from *n=3* individual experiments (MP samples) or *n=1* experiment (MG132 samples).

Table 5.2 – Summary of HMGB1 post-translational status in microparticles (MP) and MG132-treated whole cell lysates as determined by LC-MS/MS.

Treatment	Sample type	Redox			Hyper-Acetylation		Hypo-Acetylation		Ub K30	Non-Ub K30
		Fully reduced HMGB1	Disulphide HMGB1	Sulphonic acid HMGB1	NLS1	NLS2	NLS1	NLS2		
Control (0.1% DMSO, 24hr)	MP									
Necrosis (56°C, 30min)	MP									
Apoptosis (1μM STS, 24hr)	MP		Very low signal							
MG132 (10μM, 1hr)	Whole cell lysate									
MG132 (10μM, 17hr)	Whole cell lysate									

5.4 Discussion

The precise mechanisms regulating the expression and release of HMGB1 during apoptosis are currently unknown. During apoptosis, HMGB1 has been shown to be concentrated within nuclei (Scaffidi et al., 2002) and subject to release later in the apoptotic pathway (Bell et al., 2006). Caspase-dependent oxidation of HMGB1 at cysteines 23, 45 and 106 has been shown to eliminate proinflammatory function (Kazama et al., 2008). Despite this loss of proinflammatory function, HMGB1 may still have an important role as a signalling molecule during apoptosis. Alternatively, HMGB1 may be subject to degradation during apoptosis, to act as a secondary mechanism to prevent undesired HMGB1 release.

Investigations in this chapter demonstrate that HMGB1 is subject to ubiquitination during apoptosis, at K30 and T136, as observed by LC-MS/MS in APAP overdose patients displaying a high incidence of apoptotic cell death (Antoine et al., 2012). Ubiquitination was demonstrated by the characteristic ε-glycine-glycine signature on tryptic digested HMGB1. This ε-glycine-glycine motif is formed when ubiquitin is cleaved at residue 74 by trypsin, leading to the C-terminal glycine residues remaining covalently bound to the target protein peptide (Peng et al., 2003). This novel *in vivo* observation led to work investigating the ubiquitination of HMGB1 *in vitro*.

Investigations *in vitro* using the agent staurosporine (STS) demonstrated the ability of STS to induce apoptosis in a dose- and time-dependent manner in both immune (monocytes: THP-1) and non-immune (fibroblasts: MEFs) cell lines in both murine (MEFs) and human (THP-1) cell lines. STS has previously been utilised as an apoptosis-inducing agent in THP-1 (Zhu et al., 1995, Namgaladze et al., 2008) and MEFs (Liu et al., 2001, Hansen et al., 2006, Urbonaviciute et al., 2008). Additionally, MEFs have been used in studies of the role of

HMGB1 in apoptosis due to the availability of HMGB1(-/-) cells (Scaffidi et al., 2002, Urbonaviciute et al., 2008).

STS is a protein kinase inhibitor, including protein kinase C (PKC), a key protein in many second messenger signalling pathways (Tamaoki et al., 1986) and cyclin dependent kinases (CKD). It is though that inhibition of protein kinases by STS leads to intracellular and mitochondrial stress and activation of the intrinsic pathway of apoptosis. Although the precise mechanisms of STS-induced apoptosis are undefined, intracellular stress caused by STS results in caspase-3-dependent apoptosis (Wang et al., 1996).

Annexin V/PI FACS staining was used to confirm apoptosis induction in response to STS. FITC-coupled Annexin V binds to phosphatidylserine (PS) exposed on the surface of apoptotic cells, whereas PI is a fluorescent dye that intercalates into DNA. PS is expressed on the inner membrane of healthy cells, however during apoptosis, it becomes flipped to the outer membrane, in an event that can be downstream of caspase activation (Suzuki et al., 2010, Marino and Kroemer, 2013). PI is unable to penetrate the cell membrane, so is used as a marker of necrosis, when membrane integrity is lost, allowing PI to access the intracellular DNA. Hence, cells staining Annexin V positive and PI negative were used to indicate apoptosis. During late apoptosis, the cell membrane integrity can also be lost, leading to Annexin V being able to bind to PS on the inner membrane. Hence these cells stain positive for both Annexin V and PI.

The apoptosis-induction data in THP-1 cells was further supported by successful inhibition by the pan-caspase inhibitor Z-VAD-FMK, which attenuated caspase-3 activation and cell-surface PS exposure following STS treatment. The data fits with previous investigations of Z-VAD-FMK in THP-1 cells (Zhu et al., 1995).

In MEFs, apoptosis was further confirmed by Caspase-Glo 3/7 assay. This assay was used as attempts to qualify caspase-3 activation by Western blot were unsuccessful. This may be due to only a small amount of the total caspase-3 requiring activation in order to proceed to apoptosis in MEFs, which is detectable by the Caspase-Glo assay, but not the less sensitive Western blot assay.

MTS assay confirmed a reduction in cell viability of MEFs in response to STS. In comparison with the Annexin V/PI FACS data, the MTS assay apparently shows greater cytotoxicity, this may be a result of STS-mediated mitochondrial stress, preceding PS exposure, however further work would be required to confirm this. Immunofluorescence microscopy showed that during STS-induced apoptosis, HMGB1 is mostly concentrated into the nuclei of cells. This fits with previous observations that demonstrate that HMGB1 is sequestered in the nucleus during apoptosis due to increased binding to chromatin (Scaffidi et al., 2002).

Following confirmation of apoptosis induction, MEFs were taken forward for investigation into the formation of ubiquitinated HMGB1 *in vitro*. Unfortunately attempts to isolate HMGB1-Ub from whole cell lysates from apoptotic cells were unsuccessful, due to a high contaminating background, despite many troubleshooting steps including pre-clearing of beads.

In order to investigate the role of the ubiquitin-proteasome system in the regulation of HMGB1 expression, preliminary studies were undertaken using MEFs treated with the proteasome inhibitor MG132. Proteasome inhibition was confirmed by Western blotting for ubiquitinated proteins, which showed accumulation of ubiquitinated proteins in response to MG132 (10µM) from 1hr through to 17hr, following the known response to proteasome inhibition (Lee and Goldberg, 1998). HMGB1 levels were shown to be unaffected by proteasome inhibition at 1hr, suggesting that under normal conditions HMGB1 is not targeted for proteasomal degradation. However, at 17hr MG132 there was a distinct

decrease in HMGB1 expression. At this timepoint, cells also showed morphological signs of apoptosis, and this also fits with characterisation of MG132-induced apoptosis in the literature (Zhao and Vuori, 2011). The reduction in total HMGB1 expression would suggest that HMGB1 is not targeted for proteasomal degradation during apoptosis, as this would have resulted in an increase in HMGB1 expression. However this data is only preliminary and further work to confirm these findings and apoptosis induction in response to MG132 is required.

Recent evidence has shown that HMGB1 is translocated into microparticles (MP) or membrane vesicles during apoptosis (Schiller et al., 2013, Spencer et al., 2014, Pisetsky, 2014). No mechanism of translocation has been postulated in any of these reports (although HMGB1 does associate with nucleosomes that are released during apoptosis in lupus (Urbonaviciute et al., 2008)). Additionally, non-proteasomal roles of HMGB1 ubiquitination include protein trafficking and relocation. Hence it was investigated if ubiquitination could direct HMGB1 for translocation to apoptotic MP.

Isolation of MP from apoptotic MEFs was confirmed by flow cytometry indicating the appearance of new submicron populations following apoptosis or necrosis induction. There were also different populations seen between the apoptosis and necrosis-inducing conditions, as seen previously (Spencer et al., 2014).

Characterisation of the proteins within apoptotic and necrotic MP by Western blot showed that total ubiquitinated proteins were enriched in apoptotic MP in comparison with necrotic MP. This suggests that ubiquitinated proteins are targeted to apoptotic MP, and may suggest more specific regulation of the contents of apoptotic MP compared with necrotic MP. This would make sense as apoptosis is generally considered to be a more ordered mechanism of cell death compared with the rapid disintegration of the cell during necrosis. Additionally, HMGB1 was enriched in apoptotic MP in comparison with necrotic

MP. Together these data show a correlation between HMGB1 and ubiquitinated proteins in MP from only apoptotic cells. Histone H2b was used as a control for successful isolation of MP, as has been used previously (Schiller et al., 2013, Schiller et al., 2008). However, HMGB1 Western blots for a full range of molecular weights needs to be undertaken to determine if there is a HMGB1 band corresponding to a particular ubiquitin chain band, which would give an estimate of the molecular weight of HMGB1-Ub.

Investigation of specific ubiquitin chains showed that Lys63-linked polyubiquitin chains were enriched in apoptotic MP compared with necrotic MP. Lys63 chain-linked proteins have been shown to have non-proteasomal fates (Komander and Rape, 2012, Al-Hakim et al., 2010, Huang et al., 2009, Doil et al., 2009, Raiborg and Stenmark, 2009), and the enrichment of Lys63 polyubiquitinated proteins in MP suggests this to be another destination for them.

Lys48 chain-linked proteins were present in apoptotic MP, but these were at a lower level than in healthy cell lysates. As it is known that Lys48 polyubiquitin chains usually target proteins for proteasomal degradation (Komander and Rape, 2012), it is not surprising to see less Lys48- chain –linked proteins in apoptotic MP.

LC-MS/MS assessment of whole cell lysates from MEFs treated with MG132 for 1hr or 17hr showed that the longer MG132 treatment induces oxidation of HMGB1 to the sulphonic acid, likely indicative of caspase-dependent oxidation during MG132-induced apoptosis (Zhao and Vuori, 2011, Kazama et al., 2008). Importantly there was no detection of HMGB1-Ub in any of the MG132-treated MEF samples, suggesting that HMGB1-Ub is not present in healthy cells, even with proteasome inhibition (1hr MG132), or cells undergoing apoptosis as a result of proteasome inhibition (17hr MG132). However repetition of this work to further consolidate these findings is required.

LC-MS/MS analysis of HMGB1 in MP showed that control and necrotic MP contained fully reduced HMGB1, whereas apoptotic MP contained mainly sulphonyl HMGB1, but also with a very low signal from disulphide HMGB1. This coincides with observations in the literature of fully reduced HMGB1 in healthy and necrotic cells, but terminally oxidised (by caspases) HMGB1 in apoptosis (Kazama et al., 2008, Venereau et al., 2012, Antoine et al., 2010). Crucially, HMGB1-Ub was detected in apoptotic MP but not necrotic or control cell MP. This shows that ubiquitination of HMGB1 is an apoptosis-dependent process. However apoptotic MP also contained non-ubiquitinated HMGB1, suggesting that ubiquitination is not the sole determining factor for the localisation of HMGB1 into apoptotic MP. Additionally, as the vast majority of HMGB1 in the apoptotic MP was sulphonic but not all was ubiquitinated, this indicates that HMGB1 oxidation likely precedes HMGB1 ubiquitination. It may be that caspase-dependent oxidation of HMGB1 may enable recognition of HMGB1 by ubiquitinating enzymes through a conformational change in HMGB1 A box (Sahu et al., 2008). Future work investigating the timecourse of HMGB1 ubiquitination and caspase activation could be used to confirm the sequence of HMGB1 oxidation and ubiquitination. Furthermore, as the absence of caspase-dependent oxidation results in the absence of HMGB1-Ub, it would be interesting to establish if inhibition of ubiquitination can lead to the modulation of oxidised HMGB1 expression in MP.

MP, as well as apoptotic blebs, are thought to be important as a mechanism of signalling between cells (Spencer et al., 2014, Schiller et al., 2013, Schiller et al., 2008). The mechanisms targeting intracellular contents to MP are poorly understood, and future work should establish if HMGB1-Ub has a functional role in targeting HMGB1 (and possibly associated proteins/DNA) into apoptotic MP. It may be the case that HMGB1 has a more secure interaction with chromatin/DNA in apoptotic cells as has previously been proposed (Scaffidi et al., 2002) and HMGB1-Ub may enable targeting of DNA and associated proteins to MP.

Future work should attempt to isolate a purified HMGB1-Ub population from MP, so that the redox status of this HMGB1 can be confirmed. This may involve the optimisation of an anti-ubiquitin immunoprecipitation method. No acetylation of HMGB1 was seen in any MP (apoptotic, necrotic or control), showing that this PTM is not required for MP localisation, and would not have been expected as this PTM is a feature of immune cells (Bonaldi et al., 2003). Future work should also look to identify if phosphorylation is seen on HMGB1 in MP, to determine if this PTM is responsible for targeting HMGB1 to MP, as it is known to cause translocation (Ge et al., 2014, Youn and Shin, 2006). Whilst the findings demonstrate the identification of HMGB1-Ub in apoptotic MP, investigations to quantify the proportions of non-ubiquitinated vs ubiquitinated HMGB1, as well as redox isoforms, in apoptotic MP should be undertaken, as has been previously been done for HMGB1 acetylation using a synthetic peptide standard (Antoine et al., 2012).

HMGB1 ubiquitination is seen at K30 of HMGB1, a residue which firstly is within NLS1 of HMGB1, and secondly is also subject to acetylation (a PTM that is important for nucleocytosolic translocation of HMGB1 (Bonaldi et al., 2003)). Lysine ubiquitination and acetylation are mutually exclusive, so ubiquitination of HMGB1 at Lys30 will prevent acetylation of this residue, and so may also prevent acetylation-dependent HMGB1 targeting. Through ubiquitination, HMGB1 may be targeted to MP, and allow it to function as an important signalling molecule following release during late apoptosis, as opposed to being retained in the cytosol, or released as a result of acetylation. Hence HMGB1 Lys30 may be an important example of cross-talk between PTMs to regulate protein function during inflammatory conditions. In DILI, the consequences of this cross-talk between the acetylation and ubiquitination of HMGB1 could be to affect the release of HMGB1 from activated immune cells. It has not been shown if acetylation of a particular individual HMGB1 residue is critical for the nucleocytoplasmic translocation and release. However, if HMGB1 ubiquitination leads to a reduction in acetylated HMGB1, and hence HMGB1

release, this could have a protective effect as acetylated HMGB1 is involved in exacerbating the inflammatory response in liver injury and is associated with worse prognosis in AILI (Antoine et al., 2012).

An important point of future investigation arising from the work in this chapter would be to identify the chain sequences of ubiquitination of HMGB1 seen during apoptosis. This could be investigated through immunoprecipitation of HMGB1-Ub from apoptotic cells using ubiquitin chain linkage-specific antibodies. Unfortunately, initial attempts to isolate HMGB1-Ub *in vitro* by immunoprecipitation were unsuccessful for a range of antibody conditions (using anti-HMGB1 and anti-ubiquitin antibodies), total protein contents, bead pre-clearing conditions, and apoptosis intervention conditions.

Another area of interest for future investigation would be the role of HMGB1-Ub as a signalling molecule in apoptosis. This could be explored through inhibition of HMGB1-Ub by a lysine to arginine mutation (K30R) and would also allow further investigation of the function of HMGB1-Ub in the context of an inflammatory response.

The work in this chapter is the first identification of ubiquitinated HMGB1, a PTM seen during apoptosis in man during APAP overdose, and subsequently identified *in vitro* in apoptotic MP. This observation that the HMGB1-Ub is translatable to an *in vitro* model will enable subsequent mechanistic studies that can inform of the situation in man. Additionally, the LC-MS/MS characterisation of HMGB1 post-translational modifications in MP is novel, and defines the PTM status of HMGB1 in this emerging form of cell-to-cell signalling (Distler et al., 2006). This work also demonstrates the fine regulation of HMGB1 localisation and function in apoptotic cell death. In the wider context of liver injury, the identification of HMGB1-Ub during apoptosis could eventually be used to develop strategies to modulate apoptosis and inflammation, as apoptosis is a key form of cell death

during many liver disease such as hepatitis and non-alcoholic fatty liver disease (Guicciardi and Gores, 2005, Wang, 2014).

Chapter Six
Concluding Discussion

CONTENTS

6.1 Introduction

Adverse drug reactions (ADRs) are a burden on both the pharmaceutical and medical sectors, as a result of a high rate of drug attrition during development (Kola and Landis, 2004) and patient morbidity and mortality respectively (Pirmohamed et al., 2004, Wu et al., 2010). ADRs can be classified as “on-target” or “off-target” depending upon the relationship to the pharmacology of the drug. Whilst on-target ADR are related to the pharmacology of the drug, off-target ADRs are not predictable by the pharmacology of the drug, and are therefore often difficult to replicate in pre-clinical models.

Drug-induced liver injury (DILI) is a major subset of ADRs, and responsible for over half of all cases of acute liver failure (Ostapowicz et al., 2002). Current clinically used biomarkers of liver injury have deficiencies in both sensitivity and specificity (Ozer et al., 2008, Antoine et al., 2014a). In addition, currently only around 50% of known hepatotoxins are detectable in animal models (Olson et al., 2000) and 60-70% *in vitro* (Xu et al., 2008) with existing biomarkers. Hence novel, mechanistic and translational biomarkers of liver injury, determined in well-defined liver-injury models, may improve compound testing and clinical intervention strategies (Antoine et al., 2014a).

In order to identify and validate new biomarkers for adverse drug reactions such as DILI, a sequential and strategic approach is required (Fig.6.1). Initial investigation of the clinical ADR can indicate pathways or processes that can be researched for candidate mechanism-based biomarkers. Potential biomarkers can then be characterised through assessment in man, *in vivo* models and *in vitro* systems. Using this approach, the appropriate context for use of the proposed biomarker can be defined, and through further experimental investigation, a greater mechanistic understanding of the processes underlying the ADR can be attained. In-depth knowledge of the mechanisms underlying an ADR and the

mechanistic control of the biomarker can then enable the stratification of patient treatment and development of strategies and therapeutic interventions for the ADR.

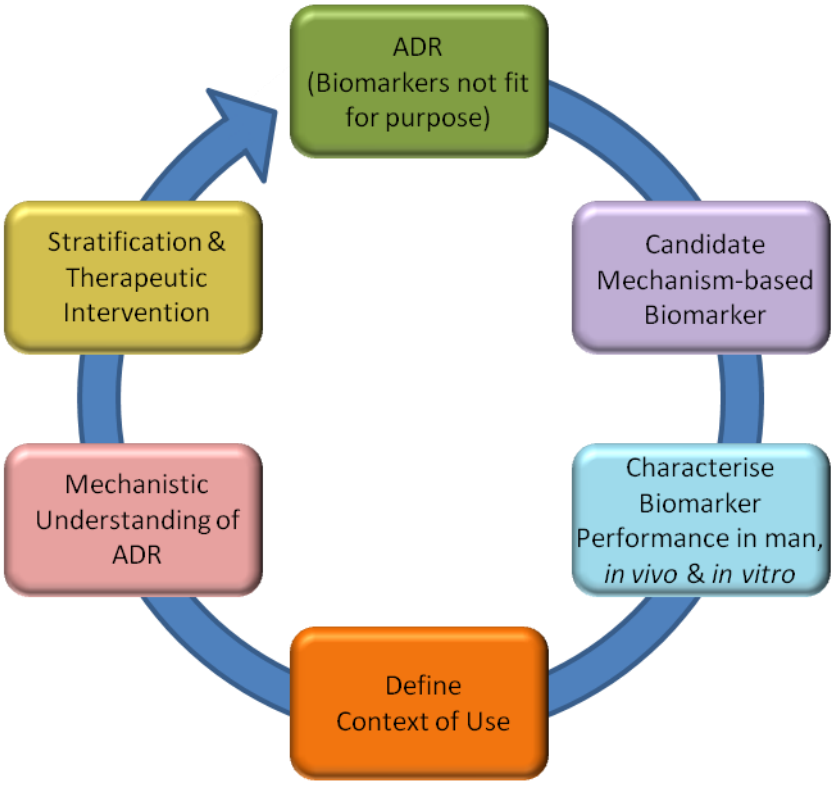

Fig.6.1 – The development of mechanism-based biomarkers for the treatment of ADRs.

A crucial aspect in the process of qualification of a biomarker for an ADR is defining and understanding the translatability of the bioanalyte between man, *in vivo* models and *in vitro* systems (Fig.6.2). Using *in vivo* and *in vitro* systems allows higher throughput investigations, in more controlled conditions, which can then feed back to inform on the clinical situation in man.

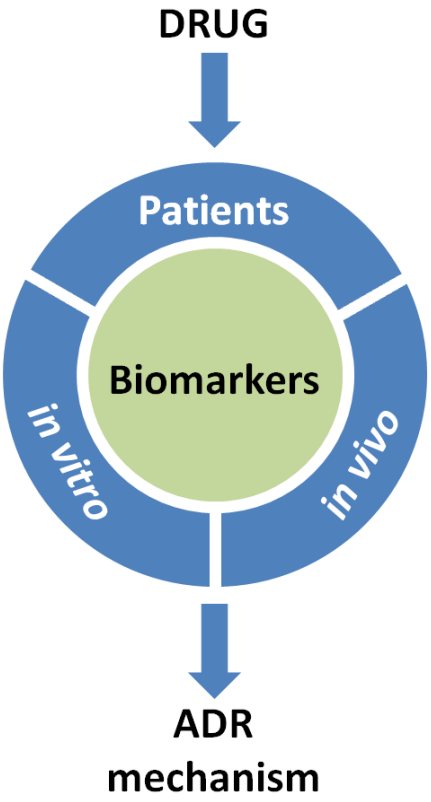

Fig.6.2 – A structured approach to investigating ADRs through *in vivo* and *in vitro* models as well as in man is crucial for understanding the mechanisms of toxicity and development of new biomarkers.

Understanding which aspects of the ADR in man are conserved *in vivo* and *in vitro* allows translational studies to be undertaken that focus on determining the precise molecular mechanisms of toxicity, and hence can guide therapeutic intervention. Establishing the mechanisms of formation and extracellular release of a biomarker are essential for defining the context of potential use of the biomarker.

HMGB1 has shown translational promise as a biomarker of a range of inflammatory conditions, both sterile and non-sterile, and in particular as an acute, sensitive and specific mechanistic biomarker of acetaminophen-induced liver injury (AILI) (Antoine et al., 2012, Antoine et al., 2013a). In AILI in man, serum HMGB1 has been shown to outperform the existing "gold standard" biomarker, serum ALT, for prediction of AILI at first presentation, and prognosis (Antoine et al., 2013a, Antoine et al., 2012). The highly conserved nature of

HMGB1 throughout species allows HMGB1 to be a investigated as a useful translational biomarker of DILI. Additionally, an important advantage of HMGB1 over existing biomarkers of DILI is that HMGB1 is post-translationally modified in a manner specific to the release process. Studies have shown that post-translational modifications (PTMs) of HMGB1 can regulate extracellular function (Yang et al., 2012a, Venereau et al., 2012) and intracellular localisation (Youn and Shin, 2006, Ito et al., 2007, Bonaldi et al., 2003).

Despite the recent exploration into the role of HMGB1 in sterile inflammation, many important research questions were in need of further investigation, such as the precise redox configurations regulating extracellular HMGB1 function and strategies to inhibit HMGB1 extracellular function.

This thesis set out to address the following key areas of HMGB1 functional and mechanistic regulation:

1. Can a chimeric anti-HMGB1 antibody attenuate liver injury in a murine model of acetaminophen overdose?
2. If so, what mechanism(s) of action may be responsible for the attenuation of injury?
3. The extracellular function of HMGB1 is dependent on the redox status of cysteine residues that control proinflammatory capability. How does the specific redox configuration of HMGB1 affect NF-κB activation and cytokine release?
4. HMGB1 has been shown to be subject to many PTMs, and PTMs are known to cross-talk to guide function and localisation of proteins. Oxidation is known to cause conformational changes in proteins, so what effects may HMGB1 oxidation have with regards to other PTMs and the fate of HMGB1 in apoptosis?

The work in this thesis encompassed the template of translational biomarker research. In Chapter 2 and Chapter 3 *in vivo* investigations were used to identify the effect and mechanism of chimeric monoclonal antibody-based intervention of HMGB1 in AILI, using a preclinical model to advance the development of a potentially clinically useful therapeutic for acetaminophen overdose. Work in Chapter 4 investigated the redox modification of HMGB1 function *in* vitro, which fits with *in vivo* observations of toxicity. Chapter 5 explored the mechanistic regulation of HMGB1 PTMs during apoptosis. Following a clinical observation, work was translated into *in vitro* studies, and suggests a novel PTM of HMGB1 that is indicative of a specific mechanism of release, which may be important in understanding the disposition of extracellular HMGB1 during injury.

6.2 Chimeric monoclonal anti-HMGB1 as a potential therapeutic intervention in AILI

A wide range of anti-HMGB1 therapeutics have been used in pre-clinical models of injury and *in vitro* experiments (Musumeci et al., 2014, Lu et al., 2014b, Chen et al., 2013). These have either targeted HMGB1 release, HMGB1 extracellular function, or both and have shown the ability to attenuate inflammation/inflammatory signalling. An important set of these therapeutics are anti-HMGB1 antibodies, which have been used in a wide range of inflammatory conditions. However, the antibodies used in these models have been from non-human species, and hence may lack the translational ability for use in man. The development of a chimeric anti-HMGB1 antibody is the next step towards taking anti-HMGB1 therapeutics to the clinical scenario.

The significance of taking the clinical observation of an ADR to *in vivo* models for the development of possible therapeutics is highlighted in this thesis, through investigations of the chimeric anti-HMGB1 antibody, h2G7. This chimeric anti-HMGB1 antibody builds on

work using a murine anti-HMGB1 antibody (2G7) that has been shown to be effective in a range of disease models (sepsis (Yang et al., 2004), arthritis (Schierbeck et al., 2011), liver I/R (Tsung et al., 2005) and islet transplantation (Gao et al., 2010)) at suppressing inflammation and tissue damage.

h2G7 was produced by cloning the Fab-encoding region of the murine counterpart, 2G7 (IgG2b), onto a human IgG1 backbone. The data shown in Chapters 2 and 3 of this thesis demonstrates the effectiveness of h2G7 at attenuating both the hepatocellular injury and the proinflammatory immune response associated with AILI in a murine model. This data was also the first study of a chimeric HMGB1-targeting antibody as a therapeutic agent in a model of inflammation.

The studies in Chapter 2 showed no differences between h2G7 and the murine counterpart, 2G7, as assessed by markers of hepatocellular damage (ALT and miR-122), immune activation (MCP-1, CXCL1, TNFα and MPO) as well as histological evidence. This proof-of-concept study using a chimeric anti-HMGB1 antibody demonstrated the effectiveness of the antibody, with equivalent activity at 300µg dose as the murine 2G7 antibody. The work using h2G7 builds on the previous work performed using 2G7 to investigate a more clinically relevant antibody treatment, and suggests that h2G7 may have the potential for clinical utility.

Subsequently, investigations into the mechanism of action of h2G7 were undertaken, to identify if h2G7 attenuates AILI through neutralisation of HMGB1, complement-mediated or FcγR-mediated effects. Gaining an understanding of the mechanism of action of h2G7 has informed on potential effects in man. The experiments in Chapter 3 investigated two potential mechanisms (complement-mediated and Fcγ-mediated effects) by utilising modified versions of the h2G7 antibody in the APAP mouse model. Whilst there were limitations with the *in vivo* studies due to mouse and human species differences,

complementary *in vitro* studies using human proteins shows that K322A h2G7 demonstrates attenuated binding to human C1q, and EndoS-treated h2G7 does not bind to human FcγR. This study suggests a neutralisation mechanism of action for h2G7 and also give confidence that the modifications (K322A and EndoS) could be used to remove any immune engagement with h2G7 if taken into man.

There are limitations to the studies, and future experiments using h2G7 should be focussed on determining the cytokine stimulating potential *in vitro* using human cells, such as PBMC, expressing a full contingent of FcγR isoforms. Comprehensive determination of cytokine-stimulating capability has been shown to be a critical step in the safety assessment of monoclonal antibodies, since TGN1412 (Stebbings et al., 2013).

Additionally, a more complete safety profile of h2G7, including studies of route of administration, clearance (especially any differences in half-life between health and disease, and both bound and unbound to HMGB1) and unequivocal definition of the mechanism of action will need to be clearly defined prior to any clinical studies.

Another important consideration for future experiments will be to investigate the affinity of h2G7 for different post-translationally modified HMGB1 isoforms. Currently no redox or acetyl isoform-specific antibodies for HMGB1 have been characterised, and this poses an important challenge for future mechanistic HMGB1 work. There is evidence however of differential activity of different anti-HMGB1 antibodies in preclinical models of sepsis and arthritis (An, 2007), that may be due to recognition of different HMGB1 isoforms. Furthermore, a study has shown that HMGB1 in neutrophils and lymphocytes may have different conformational structures, leading to differential recognition by an anti-HMGB1/HMGB2 antibody that recognises HMGB1 residues 52-56 (Ito et al., 2004). The epitope for 2G7 lies in the region of residues 53-63 of HMGB1, an area within the A box, but 2G7 binding is unaffected by redox-mediated conformational changes in HMGB1

(unpublished observations). Given that the formation of the disulphide bridge between C23 and C45 results in a conformational change in HMGB1, this could perhaps be utilised as a target of HMGB1 isoform-specific antibodies.

The work in these chapters also has wider ranging implications than just the role of HMGB1 in AILI. HMGB1 is important in the pathogenesis of many liver injury conditions, ranging from other acute injury states such as ischemia-reperfusion (I/R) through to chronic liver diseases such as non-alcoholic fatty liver disease, hepatocellular carcinoma and fibrosis (Chen et al., 2013). In liver I/R, anti-HMGB1 antibody treatment has been shown to be effective at reducing injury in mice, suggesting that a chimeric anti-HMGB1 antibody such as h2G7 may be effective at reducing liver I/R injury in man (Tsung et al., 2005).

6.3 Investigating the mechanistic regulation of HMGB1 localisation and function by post-translational modifications (PTMs).

Critical to the validation of a new biomarker is the precise understanding of the mechanisms regulating expression and function, both in intracellular situations and release into biofluids. PTMs alter the expression, localisation and function of proteins, including release, and hence can modulate the disposition of the biomarker in blood.

In Chapters 4 and 5, experiments were undertaken to investigate the functional roles of oxidative PTMs of HMGB1 and their modulation of extracellular function, or how they can influence further PTMs.

Experiments in Chapter 4 investigated, *in vitro*, the effects of modulation of HMGB1 cysteine redox status on cytokine-inducing capability in order to gain a greater understanding of the role of oxidative processes present during inflammation. Conserved cysteines in HMGB1 (C23, C45 and C106) had previously been shown to be subject to redox

modification (Hoppe et al., 2006). As a result it was proposed that HMGB1 extracellular inflammatory function could be regulated by redox of cysteines (Lotze et al., 2007, Rubartelli and Lotze, 2007). Work by Kazama et al demonstrated that during apoptosis, HMGB1 becomes terminally oxidised by caspases, resulting in a loss of inflammatory function (Kazama et al., 2008). However, the precise understanding of the regulation of HMGB1 function by redox was undefined.

The work in Chapter 4 defined the functional importance of HMGB1 redox status on the cytokine-inducing capability of HMGB1 *in vitro*. Cytokine-inducing function is critically dependent upon the presence of a disulphide bridge between cysteines 23 and 45 (C23-C45) and a reduced thiol residue at cysteine 106 (C106). The cytokine-inducing function of HMGB1 is mediated through NF-κB activation as shown by translocation of p65 into the nucleus followed by cytokine release. The requirement for the disulphide bridge, suggests that it alters the conformation of the HMGB1 A box (Sahu et al., 2008), as may oxidation at C106 (which leads to loss of proinflammatory function) (Kazama et al., 2008). Recent work has defined a role for fully reduced HMGB1 as an inducer of chemotaxis (Schiraldi et al., 2012). This demonstrates a highly redox-sensitive regulation of function of extracellular HMGB1 (Fig.6.3). Redox regulation of HMGB1 function enables the local redox environment to govern the proinflammatory function. Intracellular HMGB1 is usually kept in the fully reduced status, due to the reducing environment maintained by reducing systems such as thioredoxin and glutathione. However caspase-dependent oxidation of HMGB1 acts as a safety mechanism to prevent HMGB1-mediated proinflammatory signalling during apoptosis (Kazama et al., 2008). The work in Chapter 4 complements and confirms work in (Yang et al., 2012b) and also fits with *in vivo* observations of AILI (Antoine et al., 2010), conveying the translatability of *in vitro* findings to the *in vivo* scenario.

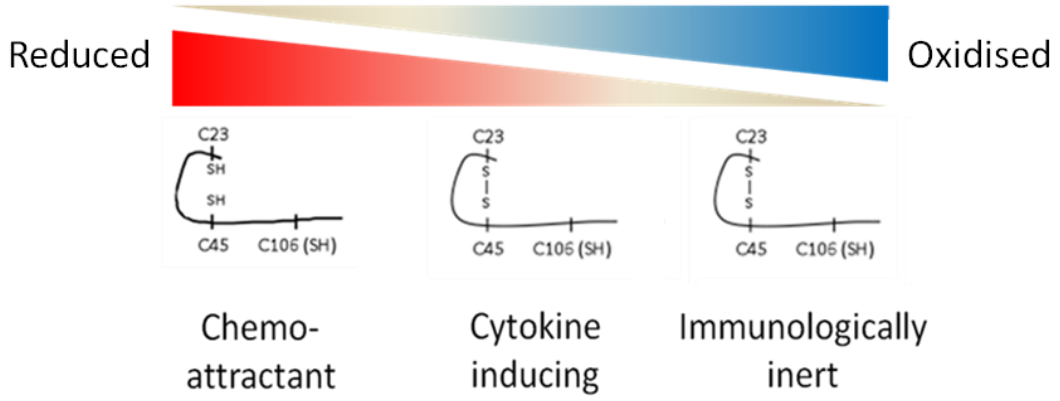

Fig.6.3 – A schematic representation of the effects of HMGB1 redox on proinflammatory function. Figure adapted from (Antoine et al., 2014b, Yang et al., 2012a).

Subsequently, this work was extended to look at mechanisms of PTM cross-talk and regulation of HMGB1 expression during apoptosis. In Chapter 5, apoptosis-specific PTMs were investigated. Oxidation has been shown to be a key regulator of tertiary structure of proteins, and may cause dramatically different functions and fates for the oxidised protein (Spickett and Pitt, 2012, Shringarpure et al., 2003). Additionally, PTMs can cause conformational changes in the molecule that could prevent or enable further PTM formation (cross-talk). Relocation of target proteins can bring them into cellular areas enriched or devoid of the enzymes required for particular PTMs. Protein oxidation has been shown to alter the structure of proteins (Spickett and Pitt, 2012), and as a result may target them for further PTMs such as ubiquitination (Iwai et al., 1998).

LC-MS/MS characterisation of serum HMGB1 in APAP overdose patients who exhibit high levels of apoptosis (as defined by quantification of caspase-cleaved keratin 18) identified ubiquitination of HMGB1, a novel PTM, at residue 30 (K30). It may be the case that oxidation of HMGB1 leads to the ubiquitination, as the ubiquitinating enzymes may recognise a motif in HMGB1 that only becomes accessible following a conformational change induced by the oxidation. This link between the observation of apoptosis and ubiquitinated HMGB1 (HMGB1-Ub) led to the hypothesis that oxidised HMGB1 may be

targeted for ubiquitination. The initial findings in man were subsequently investigated *in vitro* to attempt to define the mechanisms regulating release of ubiquitinated HMGB1 during apoptosis. These studies supported the findings in man, as HMGB1 was only found to be ubiquitinated during apoptosis, but not necrosis or in healthy cells.

Preliminary studies suggested that ubiquitinated HMGB1 is not targeted to the 26S proteasome, as proteasome inhibition using MG132 did not lead to accumulation of HMGB1-Ub during MG132-induced apoptosis. Furthermore, HMGB1-Ub was not detectable in these cell lysates. However analysis of apoptotic microparticles (apoptotic MP) by LC-MS/MS indicated the presence of HMGB1-Ub. These apoptotic MP are released from apoptotic cells, and contain DNA and histones as well as HMGB1 (Schiller et al., 2013, Spencer et al., 2014). This suggests that HMGB1-Ub may be an important cell-cell signalling molecule during apoptotic cell death, another novel function for HMGB1. However, an important caveat is that whilst HMGB1-Ub was only observed in apoptotic MP, not all HMGB1 in apoptotic MP was ubiquitinated, whereas all of the HMGB1 was oxidised (either sulphonyl or disulphide). This suggests that ubiquitination occurs downstream of oxidation.

The identification of ubiquitination of HMGB1 is a novel observation, and is indicative of another layer of PTM-based control of HMGB1 function and localisation. Further work to determine the precise mechanism of ubiquitination (including if HMGB1-Ub is exclusively expressed in apoptotic MP) and the functions of HMGB1-Ub in apoptotic signalling should be investigated. HMGB1-Ub could potentially then be developed as a marker of apoptotic MP in examples of injury where there is significant apoptosis and inform of apoptotic cell death in man.

Another highly interesting area arising from the studies in Chapter 5 is the determination of the hierarchy and cross-talk of PTMs of HMGB1 in different physiological and pathological situations/cell death processes. For example, acetylation of lysine 30 (K30) occurs as a

result of activation of immune cells (Bonaldi et al., 2003), and potentially in parenchymal cells (Evankovich et al., 2010), but this residue is now also a target of ubiquitination. PTMs of a single lysine residue are mutually exclusive and so acetylation could prevent ubiquitination and vice-versa. Additionally, given that three different PTMs (acetylation, methylation and phosphorylation) have independently been shown to direct HMGB1 translocation, it would be interesting to see if they all occur on the same molecule of HMGB1, and if one PTM is dominant. In a very recent study, acetylation of lysines and phosphorylation of serine 35 have been shown to occur together in mice and humans with alcoholic liver disease, alongside the presence of C23-C45 disulphide HMGB1 (Ge et al., 2014).

In addition, apoptosis plays a pivotal role in the progression and resolution of inflammatory liver diseases (Wang, 2014). Any apoptotic cell death in these conditions may also lead to the release of MP containing HMGB1-Ub, and it will be important to identify the functional role of this PTM in different disease conditions.

6.4 Disposition of HMGB1

It is also critically important to understand the disposition of a biomarker as this will influence the potential utility and context of use in man. HMGB1 release is passive from necrotic cells, but is actively released from activated immune cells. Hence HMGB1 is subject to mechanism-specific release, and can inform of the biological situation. Extracellular HMGB1 is detectable in serum and plasma, and is more acutely elevated *in vivo* (Antoine et al., 2010, Antoine et al., 2009) and in man (Antoine et al., 2013a) than ALT during acetaminophen overdose. During AILI, HMGB1 derived from necrotic cells also has a shorter half-life than ALT in mice, although the half-life has not been defined in man (Antoine et al., 2009). However, the half-life of fully reduced and disulphide HMGB1 in human serum has

been determined *in situ* by NMR, with fully reduced HMGB1 exhibiting a half-life of 17±1min before oxidation to the disulphide isoform (Zandarashvili et al., 2013). Furthermore, interactions between HMGB1 and other proteins can modulate the oxidation kinetics and therefore HMGB1 function (Zandarashvili et al., 2013).

The release of HMGB1 from immune cells is dependent upon acetylation at lysine residues within NLS1 and NLS2 that redirect HMGB1 for nucleocytoplasmic translocation and localisation into secretory lysosomes (Bonaldi et al., 2003). HMGB1 is secreted in these secretory lysosomes in an inflammasome-dependent mechanism, dependent on PKR (Lu et al., 2012), and regulated by JAK/STAT signalling (Lu et al., 2014a). Hence the detection of acetylated HMGB1 in serum is indicative of immune cell activation. Conversely, HMGB1 passively released from necrotic cells is fully reduced, and therefore serum detection of this isoform is indicative of necrosis. Importantly, the findings in Chapter 5 indicate a novel HMGB1 PTM, ubiquitination, which is implicated in the release of HMGB1 in apoptosis. Hence, HMGB1-Ub may have future utility as a marker of apoptosis.

The understanding of how HMGB1 is cleared from blood is less well understood, but it is thought that HMGB1 is subject to proteolysis by extracellular proteases. In human serum *in situ*, disulphide HMGB1 exhibits a half-life of 642±49min (Zandarashvili et al., 2013). However, this situation lacks the oxidising ROS that would convert HMGB1 to the sulphonyl form *in vivo* and may alter half-life. Renal clearance of HMGB1 can also be observed in conditions of kidney injury, such as in patients with lupus nephritis (Abdulahad et al., 2012) and murine models of chronic kidney disease (Leelahavanichkul et al., 2011), this would need to be taken into consideration when evaluating HMGB1 levels in patients with kidney injury as a secondary condition.

6.5 Integrating HMGB1 with existing biomarkers for the assessment of DILI

The processes involved in the qualification of new biomarkers for DILI highlights deficiencies in our mechanistic understanding of currently used biomarkers. The current "gold standard" biomarker of DILI, ALT has only been "validated" and "qualified" through extensive use and ease of the assay, and has not formally been qualified against human histology for DILI. Additionally, the quantification of the relationship between ALT release and actual cellular injury has not been defined, nor have the precise mechanisms governing ALT release (Antoine et al., 2013b, Senior, 2012, Antoine et al., 2014a). Furthermore, ALT exists as two functional isoforms, ALT1 and ALT2, with different tissue expression and intracellular localisation profiles, yet current tests do not discriminate between the two (Lindblom et al., 2007, Yang et al., 2002). Finally, no universal normal range has been established for ALT. However, the definition of baseline values for healthy individuals, including assessment of diurnal, gender and age differences is also currently a pressing need with novel biomarkers such as HMGB1. Feedback from the studies of novel biomarkers of DILI, such as HMGB1 could improve our understanding of the currently used, but not strictly defined biomarkers of DILI.

Despite this, ALT still retains clinical utility as a biomarker of liver injury if values are correctly interpreted (Antoine et al., 2013b, Senior, 2012). ALT, in combination with total bilirubin (TBL) (a marker of liver function) offers a high sensitivity and specificity combination for identifying liver injury, which should be used as the benchmark for novel biomarkers of liver injury. Since DILI is a multi-step and multi-cell process, a panel-based biomarker approach that informs of specific mechanisms in a time-dependent manner will be beneficial for earlier and more focussed assessment of injury. Hence novel mechanistic biomarkers of DILI, such as HMGB1, keratin-18 and miR-122 should be utilised alongside

existing biomarkers in order to both complement each other and improve identification of mechanisms of toxicity in DILI.

The investigations in this thesis demonstrate the translational application of HMGB1 between *in vitro, in vivo* models and clinical scenarios, and indicate its potential as a translational and mechanistic biomarker of DILI.

BIBLIOGRAPHY

ABDULAHAD, D. A., WESTRA, J., BIJZET, J., DOLFF, S., VAN DIJK, M. C., LIMBURG, P. C., KALLENBERG, C. G. & BIJL, M. 2012. Urine levels of HMGB1 in Systemic Lupus Erythematosus patients with and without renal manifestations. *Arthritis Res Ther,* 14**,** R184.

ABEYAMA, K., STERN, D. M., ITO, Y., KAWAHARA, K., YOSHIMOTO, Y., TANAKA, M., UCHIMURA, T., IDA, N., YAMAZAKI, Y., YAMADA, S., YAMAMOTO, Y., YAMAMOTO, H., IINO, S., TANIGUCHI, N. & MARUYAMA, I. 2005. The N-terminal domain of thrombomodulin sequesters high-mobility group-B1 protein, a novel antiinflammatory mechanism. *J Clin Invest,* 115**,** 1267-74.

AL-HAKIM, A., ESCRIBANO-DIAZ, C., LANDRY, M. C., O'DONNELL, L., PANIER, S., SZILARD, R. K. & DUROCHER, D. 2010. The ubiquitous role of ubiquitin in the DNA damage response. *DNA Repair (Amst),* 9**,** 1229-40.

ALKALAY, I., YARON, A., HATZUBAI, A., ORIAN, A., CIECHANOVER, A. & BEN-NERIAH, Y. 1995. Stimulation-dependent I kappa B alpha phosphorylation marks the NF-kappa B inhibitor for degradation via the ubiquitin-proteasome pathway. *Proc Natl Acad Sci U S A,* 92**,** 10599-603.

ALLHORN, M., OLIN, A. I., NIMMERJAHN, F. & COLLIN, M. 2008. Human IgG/Fc gamma R interactions are modulated by streptococcal IgG glycan hydrolysis. *PLoS One,* 3**,** e1413.

AMARAL, S. S., OLIVEIRA, A. G., MARQUES, P. E., QUINTAO, J. L., PIRES, D. A., RESENDE, R. R., SOUSA, B. R., MELGACO, J. G., PINTO, M. A., RUSSO, R. C., GOMES, A. K., ANDRADE, L. M., ZANIN, R. F., PEREIRA, R. V., BONORINO, C., SORIANI, F. M., LIMA, C. X., CARA, D. C., TEIXEIRA, M. M., LEITE, M. F. & MENEZES, G. B. 2013. Altered responsiveness to extracellular ATP enhances acetaminophen hepatotoxicity. *Cell Commun Signal,* 11**,** 10.

AN, L. L., L. XU, ET AL. 2007. Targeting different isoforms of HMGB1 leads to different beneficial effects in preclinical models of sepsis and inflammatory arthritis. *J Immunol,* 178(Meeting Abstract Supplement)S197.

ANDRADE, R. J., LUCENA, M. I., FERNANDEZ, M. C., PELAEZ, G., PACHKORIA, K., GARCIA-RUIZ, E., GARCIA-MUNOZ, B., GONZALEZ-GRANDE, R., PIZARRO, A., DURAN, J. A., JIMENEZ, M., RODRIGO, L., ROMERO-GOMEZ, M., NAVARRO, J. M., PLANAS, R., COSTA, J., BORRAS, A., SOLER, A., SALMERON, J., MARTIN-VIVALDI, R. & SPANISH GROUP FOR THE STUDY OF DRUG-INDUCED LIVER, D. 2005. Drug-induced liver injury: an analysis of 461 incidences submitted to the Spanish registry over a 10-year period. *Gastroenterology,* 129**,** 512-21.

ANTOINE, D. J., DEAR, J. W., LEWIS, P. S., PLATT, V., COYLE, J., MASSON, M., THANACOODY, R. H., GRAY, A. J., WEBB, D. J., MOGGS, J. G., BATEMAN, D. N., GOLDRING, C. E. & PARK, B. K. 2013a. Mechanistic biomarkers provide early and sensitive detection of acetaminophen-induced acute liver injury at first presentation to hospital. *Hepatology,* 58**,** 777-87.

ANTOINE, D. J., HARRILL, A. H., WATKINS, P. B. & PARK, B. K. 2014a. Safety biomarkers for drug-induced liver injury - current status and future perspectives. *Toxicology Research,* 3**,** 75-85.

ANTOINE, D. J., HARRIS, H. E., ANDERSSON, U., TRACEY, K. J. & BIANCHI, M. E. 2014b. A systematic nomenclature for the redox states of high mobility group box (HMGB) proteins. *Mol Med,* 20**,** 135-7.

ANTOINE, D. J., JENKINS, R. E., DEAR, J. W., WILLIAMS, D. P., MCGILL, M. R., SHARPE, M. R., CRAIG, D. G., SIMPSON, K. J., JAESCHKE, H. & PARK, B. K. 2012. Molecular forms of HMGB1 and keratin-18 as mechanistic biomarkers for mode of cell death and prognosis during clinical acetaminophen hepatotoxicity. *J Hepatol,* 56**,** 1070-9.

ANTOINE, D. J., LEWIS, P. S., GOLDRING, C. E. & PARK, B. K. 2013b. Are we closer to finding biomarkers for identifying acute drug-induced liver injury? *Biomark Med,* 7**,** 383-6.

ANTOINE, D. J., MERCER, A. E., WILLIAMS, D. P. & PARK, B. K. 2009a. Mechanism-based bioanalysis and biomarkers for hepatic chemical stress. *Xenobiotica,* 39**,** 565-77.

ANTOINE, D. J., WILLIAMS, D. P., KIPAR, A., JENKINS, R. E., REGAN, S. L., SATHISH, J. G., KITTERINGHAM, N. R. & PARK, B. K. 2009b. High-mobility group box-1 protein and keratin-18, circulating serum proteins informative of acetaminophen-induced necrosis and apoptosis in vivo. *Toxicol Sci,* 112**,** 521-31.

ANTOINE, D. J., WILLIAMS, D. P., KIPAR, A., LAVERTY, H. & PARK, B. K. 2010. Diet restriction inhibits apoptosis and HMGB1 oxidation and promotes inflammatory cell recruitment during acetaminophen hepatotoxicity. *Mol Med,* 16**,** 479-90.

ANTONIADES, C. G., QUAGLIA, A., TAAMS, L. S., MITRY, R. R., HUSSAIN, M., ABELES, R., POSSAMAI, L. A., BRUCE, M., MCPHAIL, M., STARLING, C., WAGNER, B., BARNARDO, A., POMPLUN, S., AUZINGER, G., BERNAL, W., HEATON, N., VERGANI, D., THURSZ, M. R. & WENDON, J. 2012. Source and characterization of hepatic macrophages in acetaminophen-induced acute liver failure in humans. *Hepatology,* 56**,** 735-46.

ARMOUR, K. L., CLARK, M. R., HADLEY, A. G. & WILLIAMSON, L. M. 1999. Recombinant human IgG molecules lacking Fcgamma receptor I binding and monocyte triggering activities. *Eur J Immunol,* 29**,** 2613-24.

ARNOLD, J. N., WORMALD, M. R., SIM, R. B., RUDD, P. M. & DWEK, R. A. 2007. The impact of glycosylation on the biological function and structure of human immunoglobulins. *Annu Rev Immunol,* 25**,** 21-50.

BELL, C. W., JIANG, W., REICH, C. F., 3RD & PISETSKY, D. S. 2006. The extracellular release of HMGB1 during apoptotic cell death. *Am J Physiol Cell Physiol,* 291**,** C1318-25.

BELLANCE, N., LESTIENNE, P. & ROSSIGNOL, R. 2009. Mitochondria: from bioenergetics to the metabolic regulation of carcinogenesis. *Front Biosci (Landmark Ed),* 14**,** 4015-34.

BENICHOU, C. 1990. Criteria of drug-induced liver disorders. Report of an international consensus meeting. *J Hepatol,* 11**,** 272-6.

BENKHOUCHA, M., MOLNARFI, N., SANTIAGO-RABER, M. L., WEBER, M. S., MERKLER, D., COLLIN, M. & LALIVE, P. H. 2012. IgG glycan hydrolysis by EndoS inhibits experimental autoimmune encephalomyelitis. *J Neuroinflammation,* 9**,** 209.

BERGSBAKEN, T., FINK, S. L. & COOKSON, B. T. 2009. Pyroptosis: host cell death and inflammation. *Nat Rev Microbiol,* 7**,** 99-109.

BIANCHI, M. E. 2007. DAMPs, PAMPs and alarmins: all we need to know about danger. *J Leukoc Biol,* 81**,** 1-5.

BLAZKA, M. E., ELWELL, M. R., HOLLADAY, S. D., WILSON, R. E. & LUSTER, M. I. 1996. Histopathology of acetaminophen-induced liver changes: role of interleukin 1 alpha and tumor necrosis factor alpha. *Toxicol Pathol,* 24**,** 181-9.

BOCK, K. W., LILIENBLUM, W., FISCHER, G., SCHIRMER, G. & BOCK-HENNING, B. S. 1987. The role of conjugation reactions in detoxication. *Arch Toxicol,* 60**,** 22-9.

BOELSTERLI, U. A. 2003. Diclofenac-induced liver injury: a paradigm of idiosyncratic drug toxicity. *Toxicol Appl Pharmacol,* 192**,** 307-22.

BONALDI, T., TALAMO, F., SCAFFIDI, P., FERRERA, D., PORTO, A., BACHI, A., RUBARTELLI, A., AGRESTI, A. & BIANCHI, M. E. 2003. Monocytic cells hyperacetylate chromatin protein HMGB1 to redirect it towards secretion. *EMBO J,* 22**,** 5551-60.

BONIZZI, G. & KARIN, M. 2004. The two NF-kappaB activation pathways and their role in innate and adaptive immunity. *Trends Immunol,* 25**,** 280-8.

BRADFORD, M. M. 1976. A rapid and sensitive method for the quantitation of microgram quantities of protein utilizing the principle of protein-dye binding. *Anal Biochem,* 72**,** 248-54.

BRENNER, C., GALLUZZI, L., KEPP, O. & KROEMER, G. 2013. Decoding cell death signals in liver inflammation. *J Hepatol,* 59**,** 583-94.

BRUHNS, P., IANNASCOLI, B., ENGLAND, P., MANCARDI, D. A., FERNANDEZ, N., JORIEUX, S. & DAERON, M. 2009. Specificity and affinity of human Fcgamma receptors and their polymorphic variants for human IgG subclasses. *Blood,* 113**,** 3716-25.

CALOGERO, S., GRASSI, F., AGUZZI, A., VOIGTLANDER, T., FERRIER, P., FERRARI, S. & BIANCHI, M. E. 1999. The lack of chromosomal protein Hmg1 does not disrupt cell growth but causes lethal hypoglycaemia in newborn mice. *Nat Genet,* 22**,** 276-80.

CARTER, P. 2001. Improving the efficacy of antibody-based cancer therapies. *Nat Rev Cancer,* 1**,** 118-29.

CHAN, A. C. & CARTER, P. J. 2010. Therapeutic antibodies for autoimmunity and inflammation. *Nat Rev Immunol,* 10**,** 301-16.

CHEN, C. J., SHI, Y., HEARN, A., FITZGERALD, K., GOLENBOCK, D., REED, G., AKIRA, S. & ROCK, K. L. 2006. MyD88-dependent IL-1 receptor signaling is essential for gouty inflammation stimulated by monosodium urate crystals. *J Clin Invest,* 116**,** 2262-71.

CHEN, R., HOU, W., ZHANG, Q., KANG, R., FAN, X. G. & TANG, D. 2013. Emerging role of high-mobility group box 1 (HMGB1) in liver diseases. *Mol Med,* 19**,** 357-66.

CHEN, Z., HAGLER, J., PALOMBELLA, V. J., MELANDRI, F., SCHERER, D., BALLARD, D. & MANIATIS, T. 1995. Signal-induced site-specific phosphorylation targets I kappa B alpha to the ubiquitin-proteasome pathway. *Genes Dev,* 9**,** 1586-97.

CHORNY, A., ANDERSON, P., GONZALEZ-REY, E. & DELGADO, M. 2008. Ghrelin protects against experimental sepsis by inhibiting high-mobility group box 1 release and by killing bacteria. *J Immunol,* 180**,** 8369-77.

CHORNY, A. & DELGADO, M. 2008. Neuropeptides rescue mice from lethal sepsis by down-regulating secretion of the late-acting inflammatory mediator high mobility group box 1. *Am J Pathol,* 172**,** 1297-307.

CIECHANOVER, A. 1998. The ubiquitin-proteasome pathway: on protein death and cell life. *EMBO J,* 17**,** 7151-60.

COLES, B., WILSON, I., WARDMAN, P., HINSON, J. A., NELSON, S. D. & KETTERER, B. 1988. The spontaneous and enzymatic reaction of N-acetyl-p-benzoquinonimine with glutathione: a stopped-flow kinetic study. *Arch Biochem Biophys,* 264**,** 253-60.

COLLIN, M. & OLSEN, A. 2001. EndoS, a novel secreted protein from Streptococcus pyogenes with endoglycosidase activity on human IgG. *EMBO J,* 20**,** 3046-55.

COOPER, C. E., PATEL, R. P., BROOKES, P. S. & DARLEY-USMAR, V. M. 2002. Nanotransducers in cellular redox signaling: modification of thiols by reactive oxygen and nitrogen species. *Trends Biochem Sci,* 27**,** 489-92.

CORDLE, S. R., DONALD, R., READ, M. A. & HAWIGER, J. 1993. Lipopolysaccharide induces phosphorylation of MAD3 and activation of c-Rel and related NF-kappa B proteins in human monocytic THP-1 cells. *J Biol Chem,* 268**,** 11803-10.

CRAIG, D. G., LEE, P., PRYDE, E. A., MASTERTON, G. S., HAYES, P. C. & SIMPSON, K. J. 2011. Circulating apoptotic and necrotic cell death markers in patients with acute liver injury. *Liver Int,* 31**,** 1127-36.

DAMBACH, D. M., WATSON, L. M., GRAY, K. R., DURHAM, S. K. & LASKIN, D. L. 2002. Role of CCR2 in macrophage migration into the liver during acetaminophen-induced hepatotoxicity in the mouse. *Hepatology,* 35**,** 1093-103.

DAVE, S. H., TILSTRA, J. S., MATSUOKA, K., LI, F., DEMARCO, R. A., BEER-STOLZ, D., SEPULVEDA, A. R., FINK, M. P., LOTZE, M. T. & PLEVY, S. E. 2009. Ethyl pyruvate decreases HMGB1 release and ameliorates murine colitis. *J Leukoc Biol,* 86**,** 633-43.

DAVID JOSEPHY, P. 2005. The molecular toxicology of acetaminophen. *Drug Metab Rev,* 37**,** 581-94.

DAVIES, E. C., GREEN, C. F., TAYLOR, S., WILLIAMSON, P. R., MOTTRAM, D. R. & PIRMOHAMED, M. 2009. Adverse drug reactions in hospital in-patients: a prospective analysis of 3695 patient-episodes. *PLoS One,* 4**,** e4439.

DECLERCQ, W., VANDEN BERGHE, T. & VANDENABEELE, P. 2009. RIP kinases at the crossroads of cell death and survival. *Cell,* 138**,** 229-32.

DENIS, N. J., VASILESCU, J., LAMBERT, J. P., SMITH, J. C. & FIGEYS, D. 2007. Tryptic digestion of ubiquitin standards reveals an improved strategy for identifying ubiquitinated proteins by mass spectrometry. *Proteomics,* 7**,** 868-74.

DIGNAM, J. D., LEBOVITZ, R. M. & ROEDER, R. G. 1983. Accurate transcription initiation by RNA polymerase II in a soluble extract from isolated mammalian nuclei. *Nucleic Acids Res,* 11**,** 1475-89.

DIKIC, I., WAKATSUKI, S. & WALTERS, K. J. 2009. Ubiquitin-binding domains - from structures to functions. *Nat Rev Mol Cell Biol,* 10**,** 659-71.

DIMASI, J. A., HANSEN, R. W. & GRABOWSKI, H. G. 2003. The price of innovation: new estimates of drug development costs. *J Health Econ,* 22**,** 151-85.

DISTLER, J. H., HUBER, L. C., GAY, S., DISTLER, O. & PISETSKY, D. S. 2006. Microparticles as mediators of cellular cross-talk in inflammatory disease. *Autoimmunity,* 39**,** 683-90.

DOIL, C., MAILAND, N., BEKKER-JENSEN, S., MENARD, P., LARSEN, D. H., PEPPERKOK, R., ELLENBERG, J., PANIER, S., DUROCHER, D., BARTEK, J., LUKAS, J. & LUKAS, C. 2009. RNF168 binds and amplifies ubiquitin conjugates on damaged chromosomes to allow accumulation of repair proteins. *Cell,* 136**,** 435-46.

DUNCAN, A. R. & WINTER, G. 1988. The binding site for C1q on IgG. *Nature,* 332**,** 738-40.

DUPONT, S., MAMIDI, A., CORDENONSI, M., MONTAGNER, M., ZACCHIGNA, L., ADORNO, M., MARTELLO, G., STINCHFIELD, M. J., SOLIGO, S., MORSUT, L., INUI, M., MORO, S., MODENA, N., ARGENTON, F., NEWFELD, S. J. & PICCOLO, S. 2009. FAM/USP9x, a deubiquitinating enzyme essential for TGFbeta signaling, controls Smad4 monoubiquitination. *Cell,* 136**,** 123-35.

EDWARDS, I. R. & ARONSON, J. K. 2000. Adverse drug reactions: definitions, diagnosis, and management. *Lancet,* 356**,** 1255-9.

ELLIOTT, M. J., MAINI, R. N., FELDMANN, M., KALDEN, J. R., ANTONI, C., SMOLEN, J. S., LEEB, B., BREEDVELD, F. C., MACFARLANE, J. D., BIJL, H. & ET AL. 1994. Randomised double-blind comparison of chimeric monoclonal antibody to tumour necrosis factor alpha (cA2) versus placebo in rheumatoid arthritis. *Lancet,* 344**,** 1105-10.

ENTEZARI, M., JAVDAN, M., ANTOINE, D. J., MORROW, D. M., SITAPARA, R. A., PATEL, V., WANG, M., SHARMA, L., GORASIYA, S., ZUR, M., WU, W., LI, J., YANG, H., ASHBY, C. R., THOMAS, D., WANG, H. & MANTELL, L. L. 2014. Inhibition of extracellular HMGB1 attenuates hyperoxia-induced inflammatory acute lung injury. *Redox Biol,* 2**,** 314-22.

EVANKOVICH, J., CHO, S. W., ZHANG, R., CARDINAL, J., DHUPAR, R., ZHANG, L., KLUNE, J. R., ZLOTNICKI, J., BILLIAR, T. & TSUNG, A. 2010. High mobility group box 1 release from hepatocytes during ischemia and reperfusion injury is mediated by decreased histone deacetylase activity. *J Biol Chem,* 285**,** 39888-97.

EVANS, A. M. 1996. Membrane transport as a determinant of the hepatic elimination of drugs and metabolites. *Clin Exp Pharmacol Physiol,* 23**,** 970-4.

FOELL, D., WITTKOWSKI, H., VOGL, T. & ROTH, J. 2007. S100 proteins expressed in phagocytes: a novel group of damage-associated molecular pattern molecules. *J Leukoc Biol,* 81**,** 28-37.

GAMA, V., YOSHIDA, T., GOMEZ, J. A., BASILE, D. P., MAYO, L. D., HAAS, A. L. & MATSUYAMA, S. 2006. Involvement of the ubiquitin pathway in decreasing Ku70 levels in response to drug-induced apoptosis. *Exp Cell Res,* 312**,** 488-99.

GAO, Q., MA, L. L., GAO, X., YAN, W., WILLIAMS, P. & YIN, D. P. 2010. TLR4 mediates early graft failure after intraportal islet transplantation. *Am J Transplant,* 10**,** 1588-96.

GE, X., ANTOINE, D. J., LU, Y., ARRIAZU, E., LEUNG, T. M., KLEPPER, A. L., BRANCH, A. D., FIEL, M. I. & NIETO, N. 2014. High mobility group box-1 (HMGB1) participates in the pathogenesis of alcoholic liver disease (ALD). *J Biol Chem,* 289**,** 22672-91.

GIBSON, G. S., P. 2001. *Introduction to Drug Metabolism*.

GO, Y. M. & JONES, D. P. 2008. Redox compartmentalization in eukaryotic cells. *Biochim Biophys Acta,* 1780**,** 1273-90.

GOLDIN, R. D., RATNAYAKA, I. D., BREACH, C. S., BROWN, I. N. & WICKRAMASINGHE, S. N. 1996. Role of macrophages in acetaminophen (paracetamol)-induced hepatotoxicity. *J Pathol,* 179**,** 432-5.

GOLDRING, C. E., KITTERINGHAM, N. R., ELSBY, R., RANDLE, L. E., CLEMENT, Y. N., WILLIAMS, D. P., MCMAHON, M., HAYES, J. D., ITOH, K., YAMAMOTO, M. & PARK, B. K. 2004. Activation of hepatic Nrf2 in vivo by acetaminophen in CD-1 mice. *Hepatology,* 39**,** 1267-76.

GRIFFITHS, S. W., KING, J. & COONEY, C. L. 2002. The reactivity and oxidation pathway of cysteine 232 in recombinant human alpha 1-antitrypsin. *J Biol Chem,* 277**,** 25486-92.

GUICCIARDI, M. E. & GORES, G. J. 2005. Apoptosis: a mechanism of acute and chronic liver injury. *Gut,* 54**,** 1024-33.

GUILLIAMS, M., BRUHNS, P., SAEYS, Y., HAMMAD, H. & LAMBRECHT, B. N. 2014. The function of Fcgamma receptors in dendritic cells and macrophages. *Nat Rev Immunol,* 14**,** 94-108.

HANSEN, T. M., SMITH, D. J. & NAGLEY, P. 2006. Smac/DIABLO is not released from mitochondria during apoptotic signalling in cells deficient in cytochrome c. *Cell Death Differ,* 13**,** 1181-90.

HARRIS, H. E., ANDERSSON, U. & PISETSKY, D. S. 2012. HMGB1: a multifunctional alarmin driving autoimmune and inflammatory disease. *Nat Rev Rheumatol,* 8**,** 195-202.

HATAKEYAMA, S. & NAKAYAMA, K. I. 2003. U-box proteins as a new family of ubiquitin ligases. *Biochem Biophys Res Commun,* 302**,** 635-45.

HAWTON, K., WARE, C., MISTRY, H., HEWITT, J., KINGSBURY, S., ROBERTS, D. & WEITZEL, H. 1995. Why patients choose paracetamol for self poisoning and their knowledge of its dangers. *BMJ,* 310**,** 164.

HAYDEN, M. S. & GHOSH, S. 2004. Signaling to NF-kappaB. *Genes Dev,* 18**,** 2195-224.

HENGARTNER, M. O. 2000. The biochemistry of apoptosis. *Nature,* 407**,** 770-6.

HEZAREH, M., HESSELL, A. J., JENSEN, R. C., VAN DE WINKEL, J. G. & PARREN, P. W. 2001. Effector function activities of a panel of mutants of a broadly neutralizing antibody against human immunodeficiency virus type 1. *J Virol,* 75**,** 12161-8.

HOEGE, C., PFANDER, B., MOLDOVAN, G. L., PYROWOLAKIS, G. & JENTSCH, S. 2002. RAD6-dependent DNA repair is linked to modification of PCNA by ubiquitin and SUMO. *Nature,* 419**,** 135-41.

HOLT, M. P., CHENG, L. & JU, C. 2008. Identification and characterization of infiltrating macrophages in acetaminophen-induced liver injury. *J Leukoc Biol,* 84**,** 1410-21.

HOPPE, G., TALCOTT, K. E., BHATTACHARYA, S. K., CRABB, J. W. & SEARS, J. E. 2006. Molecular basis for the redox control of nuclear transport of the structural chromatin protein Hmgb1. *Exp Cell Res,* 312**,** 3526-38.

HORI, O., BRETT, J., SLATTERY, T., CAO, R., ZHANG, J., CHEN, J. X., NAGASHIMA, M., LUNDH, E. R., VIJAY, S., NITECKI, D. & ET AL. 1995. The receptor for advanced glycation end products (RAGE) is a cellular binding site for amphoterin. Mediation of neurite outgrowth and co-expression of rage and amphoterin in the developing nervous system. *J Biol Chem,* 270**,** 25752-61.

HOTCHKISS, R. S., STRASSER, A., MCDUNN, J. E. & SWANSON, P. E. 2009. Cell death. *N Engl J Med,* 361**,** 1570-83.

HREGGVIDSDOTTIR, H. S., LUNDBERG, A. M., AVEBERGER, A. C., KLEVENVALL, L., ANDERSSON, U. & HARRIS, H. E. 2012. High mobility group box protein 1 (HMGB1)-partner molecule complexes enhance cytokine production by signaling through the partner molecule receptor. *Mol Med,* 18**,** 224-30.

HREGGVIDSDOTTIR, H. S., OSTBERG, T., WAHAMAA, H., SCHIERBECK, H., AVEBERGER, A. C., KLEVENVALL, L., PALMBLAD, K., OTTOSSON, L., ANDERSSON, U. & HARRIS, H. E. 2009. The alarmin HMGB1 acts in synergy with endogenous and exogenous danger signals to promote inflammation. *J Leukoc Biol,* 86**,** 655-62.

HUANG, J., HUEN, M. S., KIM, H., LEUNG, C. C., GLOVER, J. N., YU, X. & CHEN, J. 2009. RAD18 transmits DNA damage signalling to elicit homologous recombination repair. *Nat Cell Biol,* 11**,** 592-603.

HUGHES-JONES, N. C. & GARDNER, B. 1979. Reaction between the isolated globular sub-units of the complement component C1q and IgG-complexes. *Mol Immunol,* 16**,** 697-701.

HUGHES, E. N., ENGELSBERG, B. N. & BILLINGS, P. C. 1992. Purification of nuclear proteins that bind to cisplatin-damaged DNA. Identity with high mobility group proteins 1 and 2. *J Biol Chem,* 267**,** 13520-7.

IDUSOGIE, E. E., PRESTA, L. G., GAZZANO-SANTORO, H., TOTPAL, K., WONG, P. Y., ULTSCH, M., MENG, Y. G. & MULKERRIN, M. G. 2000. Mapping of the C1q binding site on rituxan, a chimeric antibody with a human IgG1 Fc. *J Immunol,* 164**,** 4178-84.

ISHIDA, Y., KONDO, T., KIMURA, A., TSUNEYAMA, K., TAKAYASU, T. & MUKAIDA, N. 2006. Opposite roles of neutrophils and macrophages in the pathogenesis of acetaminophen-induced acute liver injury. *Eur J Immunol,* 36**,** 1028-38.

ITO, I., FUKAZAWA, J. & YOSHIDA, M. 2007. Post-translational methylation of high mobility group box 1 (HMGB1) causes its cytoplasmic localization in neutrophils. *J Biol Chem,* 282**,** 16336-44.

ITO, I., MITSUOKA, N., SOBAJIMA, J., UESUGI, H., OZAKI, S., OHYA, K. & YOSHIDA, M. 2004. Conformational difference in HMGB1 proteins of human neutrophils and lymphocytes revealed by epitope mapping of a monoclonal antibody. *J Biochem,* 136**,** 155-62.

IVANOV, S., DRAGOI, A. M., WANG, X., DALLACOSTA, C., LOUTEN, J., MUSCO, G., SITIA, G., YAP, G. S., WAN, Y., BIRON, C. A., BIANCHI, M. E., WANG, H. & CHU, W. M. 2007. A novel role for HMGB1 in TLR9-mediated inflammatory responses to CpG-DNA. *Blood,* 110**,** 1970-81.

IWAI, K., DRAKE, S. K., WEHR, N. B., WEISSMAN, A. M., LAVAUTE, T., MINATO, N., KLAUSNER, R. D., LEVINE, R. L. & ROUAULT, T. A. 1998. Iron-dependent oxidation, ubiquitination, and degradation of iron regulatory protein 2: implications for degradation of oxidized proteins. *Proc Natl Acad Sci U S A,* 95**,** 4924-8.

JACOB, A., SHAH, K. G., WU, R. & WANG, P. 2010. Ghrelin as a novel therapy for radiation combined injury. *Mol Med,* 16**,** 137-43.

JAESCHKE, H. & LIU, J. 2007. Neutrophil depletion protects against murine acetaminophen hepatotoxicity: another perspective. *Hepatology,* 45**,** 1588-9; author reply 1589.

JAMES, L. P., MAYEUX, P. R. & HINSON, J. A. 2003. Acetaminophen-induced hepatotoxicity. *Drug Metab Dispos,* 31**,** 1499-506.

JAMES, L. P., SIMPSON, P. M., FARRAR, H. C., KEARNS, G. L., WASSERMAN, G. S., BLUMER, J. L., REED, M. D., SULLIVAN, J. E. & HINSON, J. A. 2005. Cytokines and toxicity in acetaminophen overdose. *J Clin Pharmacol,* 45**,** 1165-71.

JANG, C. H., CHOI, J. H., BYUN, M. S. & JUE, D. M. 2006. Chloroquine inhibits production of TNF-alpha, IL-1beta and IL-6 from lipopolysaccharide-stimulated human monocytes/macrophages by different modes. *Rheumatology (Oxford),* 45**,** 703-10.

JEFFERIS, R. & LUND, J. 2002. Interaction sites on human IgG-Fc for FcgammaR: current models. *Immunol Lett,* 82**,** 57-65.

JEONG, J. Y. & JUE, D. M. 1997. Chloroquine inhibits processing of tumor necrosis factor in lipopolysaccharide-stimulated RAW 264.7 macrophages. *J Immunol,* 158**,** 4901-7.

JIANG, W. L., TIAN, J. W., FU, F. H., ZHU, H. B. & HOU, J. 2010. Neuroprotective efficacy and therapeutic window of Forsythoside B: in a rat model of cerebral ischemia and reperfusion injury. *Eur J Pharmacol,* 640**,** 75-81.

JOLLOW, D. J., MITCHELL, J. R., POTTER, W. Z., DAVIS, D. C., GILLETTE, J. R. & BRODIE, B. B. 1973. Acetaminophen-induced hepatic necrosis. II. Role of covalent binding in vivo. *J Pharmacol Exp Ther,* 187**,** 195-202.

JU, C., REILLY, T. P., BOURDI, M., RADONOVICH, M. F., BRADY, J. N., GEORGE, J. W. & POHL, L. R. 2002. Protective role of Kupffer cells in acetaminophen-induced hepatic injury in mice. *Chem Res Toxicol,* 15**,** 1504-13.

JUNGHANS, R. P. & ANDERSON, C. L. 1996. The protection receptor for IgG catabolism is the beta2-microglobulin-containing neonatal intestinal transport receptor. *Proc Natl Acad Sci U S A,* 93**,** 5512-6.

KANELLAKIS, P., AGROTIS, A., KYAW, T. S., KOULIS, C., AHRENS, I., MORI, S., TAKAHASHI, H. K., LIU, K., PETER, K., NISHIBORI, M. & BOBIK, A. 2011. High-mobility group box protein 1 neutralization reduces development of diet-induced atherosclerosis in apolipoprotein e-deficient mice. *Arterioscler Thromb Vasc Biol,* 31**,** 313-9.

KAZAMA, H., RICCI, J. E., HERNDON, J. M., HOPPE, G., GREEN, D. R. & FERGUSON, T. A. 2008. Induction of immunological tolerance by apoptotic cells requires caspase-dependent oxidation of high-mobility group box-1 protein. *Immunity,* 29**,** 21-32.

KEIZER, R. J., HUITEMA, A. D., SCHELLENS, J. H. & BEIJNEN, J. H. 2010. Clinical pharmacokinetics of therapeutic monoclonal antibodies. *Clin Pharmacokinet,* 49**,** 493-507.

KEMNA, E., PICKKERS, P., NEMETH, E., VAN DER HOEVEN, H. & SWINKELS, D. 2005. Time-course analysis of hepcidin, serum iron, and plasma cytokine levels in humans injected with LPS. *Blood,* 106**,** 1864-6.

KERR, J. F., WYLLIE, A. H. & CURRIE, A. R. 1972. Apoptosis: a basic biological phenomenon with wide-ranging implications in tissue kinetics. *Br J Cancer,* 26**,** 239-57.

KIM, S. C., SPRUNG, R., CHEN, Y., XU, Y., BALL, H., PEI, J., CHENG, T., KHO, Y., XIAO, H., XIAO, L., GRISHIN, N. V., WHITE, M., YANG, X. J. & ZHAO, Y. 2006. Substrate and functional diversity of lysine acetylation revealed by a proteomics survey. *Mol Cell,* 23**,** 607-18.

KIRISAKO, T., KAMEI, K., MURATA, S., KATO, M., FUKUMOTO, H., KANIE, M., SANO, S., TOKUNAGA, F., TANAKA, K. & IWAI, K. 2006. A ubiquitin ligase complex assembles linear polyubiquitin chains. *EMBO J,* 25**,** 4877-87.

KIRKIN, V., MCEWAN, D. G., NOVAK, I. & DIKIC, I. 2009. A role for ubiquitin in selective autophagy. *Mol Cell,* 34**,** 259-69.

KIRKPATRICK, D. S., HATHAWAY, N. A., HANNA, J., ELSASSER, S., RUSH, J., FINLEY, D., KING, R. W. & GYGI, S. P. 2006. Quantitative analysis of in vitro ubiquitinated cyclin B1 reveals complex chain topology. *Nat Cell Biol,* 8**,** 700-10.

KOEGL, M., HOPPE, T., SCHLENKER, S., ULRICH, H. D., MAYER, T. U. & JENTSCH, S. 1999. A novel ubiquitination factor, E4, is involved in multiubiquitin chain assembly. *Cell,* 96**,** 635-44.

KOKKOLA, R., LI, J., SUNDBERG, E., AVEBERGER, A. C., PALMBLAD, K., YANG, H., TRACEY, K. J., ANDERSSON, U. & HARRIS, H. E. 2003. Successful treatment of collagen-induced arthritis in mice and rats by targeting extracellular high mobility group box chromosomal protein 1 activity. *Arthritis Rheum,* 48**,** 2052-8.

KOLA, I. & LANDIS, J. 2004. Can the pharmaceutical industry reduce attrition rates? *Nat Rev Drug Discov,* 3**,** 711-5.

KOMANDER, D. 2009. The emerging complexity of protein ubiquitination. *Biochem Soc Trans,* 37**,** 937-53.

KOMANDER, D. & RAPE, M. 2012. The ubiquitin code. *Annu Rev Biochem,* 81**,** 203-29.

KOVALOVICH, K., DEANGELIS, R. A., LI, W., FURTH, E. E., CILIBERTO, G. & TAUB, R. 2000. Increased toxin-induced liver injury and fibrosis in interleukin-6-deficient mice. *Hepatology,* 31**,** 149-59.

KRAPP, S., MIMURA, Y., JEFFERIS, R., HUBER, R. & SONDERMANN, P. 2003. Structural analysis of human IgG-Fc glycoforms reveals a correlation between glycosylation and structural integrity. *J Mol Biol,* 325**,** 979-89.

KRAVTSOVA-IVANTSIV, Y., COHEN, S. & CIECHANOVER, A. 2009. Modification by single ubiquitin moieties rather than polyubiquitination is sufficient for proteasomal processing of the p105 NF-kappaB precursor. *Mol Cell,* 33**,** 496-504.

KRETZ-ROMMEL, A. & BOELSTERLI, U. A. 1993. Diclofenac covalent protein binding is dependent on acyl glucuronide formation and is inversely related to P450-mediated acute cell injury in cultured rat hepatocytes. *Toxicol Appl Pharmacol,* 120**,** 155-61.

KROEMER, G., GALLUZZI, L., VANDENABEELE, P., ABRAMS, J., ALNEMRI, E. S., BAEHRECKE, E. H., BLAGOSKLONNY, M. V., EL-DEIRY, W. S., GOLSTEIN, P., GREEN, D. R., HENGARTNER, M., KNIGHT, R. A., KUMAR, S., LIPTON, S. A., MALORNI, W., NUNEZ, G., PETER, M. E., TSCHOPP, J., YUAN, J., PIACENTINI, M., ZHIVOTOVSKY, B., MELINO, G. & NOMENCLATURE COMMITTEE ON CELL, D. 2009. Classification of cell death: recommendations of the Nomenclature Committee on Cell Death 2009. *Cell Death Differ,* 16**,** 3-11.

KUBOTA, T., NIWA, R., SATOH, M., AKINAGA, S., SHITARA, K. & HANAI, N. 2009. Engineered therapeutic antibodies with improved effector functions. *Cancer Sci,* 100**,** 1566-72.

KUMAR, H., KAWAI, T. & AKIRA, S. 2011. Pathogen recognition by the innate immune system. *Int Rev Immunol,* 30**,** 16-34.

LASSER, K. E., ALLEN, P. D., WOOLHANDLER, S. J., HIMMELSTEIN, D. U., WOLFE, S. M. & BOR, D. H. 2002. Timing of new black box warnings and withdrawals for prescription medications. *JAMA,* 287**,** 2215-20.

LAVERTY, H. G., ANTOINE, D. J., BENSON, C., CHAPONDA, M., WILLIAMS, D. & KEVIN PARK, B. 2010. The potential of cytokines as safety biomarkers for drug-induced liver injury. *Eur J Clin Pharmacol,* 66**,** 961-76.

LAWSON, J. A., FARHOOD, A., HOPPER, R. D., BAJT, M. L. & JAESCHKE, H. 2000. The hepatic inflammatory response after acetaminophen overdose: role of neutrophils. *Toxicol Sci,* 54**,** 509-16.

LAZAR, G. A., DANG, W., KARKI, S., VAFA, O., PENG, J. S., HYUN, L., CHAN, C., CHUNG, H. S., EIVAZI, A., YODER, S. C., VIELMETTER, J., CARMICHAEL, D. F., HAYES, R. J. & DAHIYAT, B. I. 2006. Engineered antibody Fc variants with enhanced effector function. *Proc Natl Acad Sci U S A,* 103**,** 4005-10.

LEE, D. H. & GOLDBERG, A. L. 1998. Proteasome inhibitors: valuable new tools for cell biologists. *Trends Cell Biol,* 8**,** 397-403.

LEE, K. J., WOO, E. R., CHOI, C. Y., SHIN, D. W., LEE, D. G., YOU, H. J. & JEONG, H. G. 2004. Protective effect of acteoside on carbon tetrachloride-induced hepatotoxicity. *Life Sci,* 74**,** 1051-64.

LEELAHAVANICHKUL, A., HUANG, Y., HU, X., ZHOU, H., TSUJI, T., CHEN, R., KOPP, J. B., SCHNERMANN, J., YUEN, P. S. & STAR, R. A. 2011. Chronic kidney disease worsens sepsis and sepsis-induced acute kidney injury by releasing High Mobility Group Box Protein-1. *Kidney Int,* 80**,** 1198-211.

LEIST, M., SINGLE, B., CASTOLDI, A. F., KUHNLE, S. & NICOTERA, P. 1997. Intracellular adenosine triphosphate (ATP) concentration: a switch in the decision between apoptosis and necrosis. *J Exp Med,* 185**,** 1481-6.

LI, H., ZHU, H., XU, C. J. & YUAN, J. 1998. Cleavage of BID by caspase 8 mediates the mitochondrial damage in the Fas pathway of apoptosis. *Cell,* 94**,** 491-501.

LI, J., KOKKOLA, R., TABIBZADEH, S., YANG, R., OCHANI, M., QIANG, X., HARRIS, H. E., CZURA, C. J., WANG, H., ULLOA, L., WARREN, H. S., MOLDAWER, L. L., FINK, M. P., ANDERSSON, U., TRACEY, K. J. & YANG, H. 2003a. Structural basis for the proinflammatory cytokine activity of high mobility group box 1. *Mol Med,* 9**,** 37-45.

LI, M., BROOKS, C. L., WU-BAER, F., CHEN, D., BAER, R. & GU, W. 2003b. Mono- versus polyubiquitination: differential control of p53 fate by Mdm2. *Science,* 302**,** 1972-5.

LI, W., ASHOK, M., LI, J., YANG, H., SAMA, A. E. & WANG, H. 2007a. A major ingredient of green tea rescues mice from lethal sepsis partly by inhibiting HMGB1. *PLoS One,* 2**,** e1153.

LI, W., LI, J., ASHOK, M., WU, R., CHEN, D., YANG, L., YANG, H., TRACEY, K. J., WANG, P., SAMA, A. E. & WANG, H. 2007b. A cardiovascular drug rescues mice from lethal sepsis by selectively attenuating a late-acting proinflammatory mediator, high mobility group box 1. *J Immunol,* 178**,** 3856-64.

LI, X., WANG, L. K., WANG, L. W., HAN, X. Q., YANG, F. & GONG, Z. J. 2013. Blockade of high-mobility group box-1 ameliorates acute on chronic liver failure in rats. *Inflamm Res,* 62**,** 703-9.

LINDBLOM, P., RAFTER, I., COPLEY, C., ANDERSSON, U., HEDBERG, J. J., BERG, A. L., SAMUELSSON, A., HELLMOLD, H., COTGREAVE, I. & GLINGHAMMAR, B. 2007. Isoforms of alanine aminotransferases in human tissues and serum--differential tissue expression using novel antibodies. *Arch Biochem Biophys,* 466**,** 66-77.

LIU-BRYAN, R., PRITZKER, K., FIRESTEIN, G. S. & TERKELTAUB, R. 2005. TLR2 signaling in chondrocytes drives calcium pyrophosphate dihydrate and monosodium urate crystal-induced nitric oxide generation. *J Immunol,* 174**,** 5016-23.

LIU, J., LEE, P., GALBIATI, F., KITSIS, R. N. & LISANTI, M. P. 2001. Caveolin-1 expression sensitizes fibroblastic and epithelial cells to apoptotic stimulation. *Am J Physiol Cell Physiol,* 280**,** C823-35.

LIU, K., MORI, S., TAKAHASHI, H. K., TOMONO, Y., WAKE, H., KANKE, T., SATO, Y., HIRAGA, N., ADACHI, N., YOSHINO, T. & NISHIBORI, M. 2007. Anti-high mobility group box 1 monoclonal antibody ameliorates brain infarction induced by transient ischemia in rats. *FASEB J,* 21**,** 3904-16.

LIU, Z. X., GOVINDARAJAN, S. & KAPLOWITZ, N. 2004. Innate immune system plays a critical role in determining the progression and severity of acetaminophen hepatotoxicity. *Gastroenterology,* 127**,** 1760-74.

LIU, Z. X., HAN, D., GUNAWAN, B. & KAPLOWITZ, N. 2006. Neutrophil depletion protects against murine acetaminophen hepatotoxicity. *Hepatology,* 43**,** 1220-30.

LOOD, C., ALLHORN, M., LOOD, R., GULLSTRAND, B., OLIN, A. I., RONNBLOM, L., TRUEDSSON, L., COLLIN, M. & BENGTSSON, A. A. 2012. IgG glycan hydrolysis by endoglycosidase S diminishes the proinflammatory properties of immune complexes from patients with systemic lupus erythematosus: a possible new treatment? *Arthritis Rheum,* 64**,** 2698-706.

LOTZE, M. T., ZEH, H. J., RUBARTELLI, A., SPARVERO, L. J., AMOSCATO, A. A., WASHBURN, N. R., DEVERA, M. E., LIANG, X., TOR, M. & BILLIAR, T. 2007. The grateful dead: damage-associated molecular pattern molecules and reduction/oxidation regulate immunity. *Immunol Rev,* 220**,** 60-81.

LOZANSKI, G., BALLOU, S. P. & KUSHNER, I. 1992. Effect of flurbiprofen on cytokine production by human monocytes and U-937 and THP-1 cell lines. *J Rheumatol,* 19**,** 921-6.

LU, B., ANTOINE, D. J., KWAN, K., LUNDBACK, P., WAHAMAA, H., SCHIERBECK, H., ROBINSON, M., VAN ZOELEN, M. A., YANG, H., LI, J., ERLANDSSON-HARRIS, H., CHAVAN, S. S., WANG, H., ANDERSSON, U. & TRACEY, K. J. 2014a. JAK/STAT1 signaling promotes HMGB1 hyperacetylation and nuclear translocation. *Proc Natl Acad Sci U S A,* 111**,** 3068-73.

LU, B., NAKAMURA, T., INOUYE, K., LI, J., TANG, Y., LUNDBACK, P., VALDES-FERRER, S. I., OLOFSSON, P. S., KALB, T., ROTH, J., ZOU, Y., ERLANDSSON-HARRIS, H., YANG, H., TING, J. P., WANG, H., ANDERSSON, U., ANTOINE, D. J., CHAVAN, S. S., HOTAMISLIGIL, G. S. & TRACEY, K. J. 2012. Novel role of PKR in inflammasome activation and HMGB1 release. *Nature,* 488**,** 670-4.

LU, B., WANG, C., WANG, M., LI, W., CHEN, F., TRACEY, K. J. & WANG, H. 2014b. Molecular mechanism and therapeutic modulation of high mobility group box 1 release and action: an updated review. *Expert Rev Clin Immunol,* 10**,** 713-27.

LUND, J., TAKAHASHI, N., POUND, J. D., GOODALL, M. & JEFFERIS, R. 1996. Multiple interactions of IgG with its core oligosaccharide can modulate recognition by complement and human Fc gamma receptor I and influence the synthesis of its oligosaccharide chains. *J Immunol,* 157**,** 4963-9.

LUO, Q., WANG, Y., FENG, D., XU, Y. & XU, L. 2009. Vasoactive intestinal peptide attenuates concanavalin A-mediated liver injury. *Eur J Pharmacol,* 607**,** 226-33.

LUX, A. & NIMMERJAHN, F. 2013. Of mice and men: the need for humanized mouse models to study human IgG activity in vivo. *J Clin Immunol,* 33 Suppl 1**,** S4-8.

MA, S. & SUBRAMANIAN, R. 2006. Detecting and characterizing reactive metabolites by liquid chromatography/tandem mass spectrometry. *J Mass Spectrom,* 41**,** 1121-39.

MAHER, J. J. 2009. DAMPs ramp up drug toxicity. *J Clin Invest,* 119**,** 246-9.

MALHI, H., GORES, G. J. & LEMASTERS, J. J. 2006. Apoptosis and necrosis in the liver: a tale of two deaths? *Hepatology,* 43**,** S31-44.

MARGOTTIN-GOGUET, F., HSU, J. Y., LOKTEV, A., HSIEH, H. M., REIMANN, J. D. & JACKSON, P. K. 2003. Prophase destruction of Emi1 by the SCF(betaTrCP/Slimb) ubiquitin ligase activates the anaphase promoting complex to allow progression beyond prometaphase. *Dev Cell,* 4**,** 813-26.

MARINO, G. & KROEMER, G. 2013. Mechanisms of apoptotic phosphatidylserine exposure. *Cell Res,* 23**,** 1247-8.

MARQUES, P. E., AMARAL, S. S., PIRES, D. A., NOGUEIRA, L. L., SORIANI, F. M., LIMA, B. H., LOPES, G. A., RUSSO, R. C., AVILA, T. V., MELGACO, J. G., OLIVEIRA, A. G., PINTO, M. A., LIMA, C. X., DE PAULA, A. M., CARA, D. C., LEITE, M. F., TEIXEIRA, M. M. & MENEZES, G. B. 2012. Chemokines and mitochondrial products activate neutrophils to amplify organ injury during mouse acute liver failure. *Hepatology,* 56**,** 1971-82.

MARTIN-MURPHY, B. V., HOLT, M. P. & JU, C. 2010. The role of damage associated molecular pattern molecules in acetaminophen-induced liver injury in mice. *Toxicol Lett,* 192**,** 387-94.

MASSON, M. J., CARPENTER, L. D., GRAF, M. L. & POHL, L. R. 2008. Pathogenic role of natural killer T and natural killer cells in acetaminophen-induced liver injury in mice is dependent on the presence of dimethyl sulfoxide. *Hepatology,* 48**,** 889-97.

MASUBUCHI, Y., BOURDI, M., REILLY, T. P., GRAF, M. L., GEORGE, J. W. & POHL, L. R. 2003. Role of interleukin-6 in hepatic heat shock protein expression and protection against acetaminophen-induced liver disease. *Biochem Biophys Res Commun,* 304**,** 207-12.

MATSUMOTO, M. L., WICKLIFFE, K. E., DONG, K. C., YU, C., BOSANAC, I., BUSTOS, D., PHU, L., KIRKPATRICK, D. S., HYMOWITZ, S. G., RAPE, M., KELLEY, R. F. & DIXIT, V. M. 2010. K11-linked polyubiquitination in cell cycle control revealed by a K11 linkage-specific antibody. *Mol Cell,* 39**,** 477-84.

MATTHEWS, A. M., HINSON, J. A., ROBERTS, D. W. & PUMFORD, N. R. 1997. Comparison of covalent binding of acetaminophen and the regioisomer 3'-hydroxyacetanilide to mouse liver protein. *Toxicol Lett,* 90**,** 77-82.

MEISTER, A. 1983. Transport and metabolism of glutathione and gamma-glutamyl amino acids. *Biochem Soc Trans,* 11**,** 793-4.

MEYER, U. A. 1996. Overview of enzymes of drug metabolism. *J Pharmacokinet Biopharm,* 24**,** 449-59.

MITCHELL, J. R., JOLLOW, D. J., POTTER, W. Z., GILLETTE, J. R. & BRODIE, B. B. 1973. Acetaminophen-induced hepatic necrosis. IV. Protective role of glutathione. *J Pharmacol Exp Ther,* 187**,** 211-7.

MOLFETTA, R., QUATRINI, L., GASPARRINI, F., ZITTI, B., SANTONI, A. & PAOLINI, R. 2014. Regulation of fc receptor endocytic trafficking by ubiquitination. *Front Immunol,* 5**,** 449.

MOLLICA, L., DE MARCHIS, F., SPITALERI, A., DALLACOSTA, C., PENNACCHINI, D., ZAMAI, M., AGRESTI, A., TRISCIUOGLIO, L., MUSCO, G. & BIANCHI, M. E. 2007. Glycyrrhizin binds to high-mobility group box 1 protein and inhibits its cytokine activities. *Chem Biol,* 14**,** 431-41.

MUSUMECI, D., ROVIELLO, G. N. & MONTESARCHIO, D. 2014. An overview on HMGB1 inhibitors as potential therapeutic agents in HMGB1-related pathologies. *Pharmacol Ther,* 141**,** 347-57.

MUZIO, M., STOCKWELL, B. R., STENNICKE, H. R., SALVESEN, G. S. & DIXIT, V. M. 1998. An induced proximity model for caspase-8 activation. *J Biol Chem,* 273**,** 2926-30.

MYERS, T. G., DIETZ, E. C., ANDERSON, N. L., KHAIRALLAH, E. A., COHEN, S. D. & NELSON, S. D. 1995. A comparative study of mouse liver proteins arylated by reactive metabolites of acetaminophen and its nonhepatotoxic regioisomer, 3'-hydroxyacetanilide. *Chem Res Toxicol,* 8**,** 403-13.

NAMGALADZE, D., KOLLAS, A. & BRUNE, B. 2008. Oxidized LDL attenuates apoptosis in monocytic cells by activating ERK signaling. *J Lipid Res,* 49**,** 58-65.

NANDAKUMAR, K. S., COLLIN, M., HAPPONEN, K. E., CROXFORD, A. M., LUNDSTROM, S. L., ZUBAREV, R. A., ROWLEY, M. J., BLOM, A. M. & HOLMDAHL, R. 2013. Dominant suppression of inflammation by glycan-hydrolyzed IgG. *Proc Natl Acad Sci U S A,* 110**,** 10252-7.

NANDAKUMAR, K. S., COLLIN, M., OLSEN, A., NIMMERJAHN, F., BLOM, A. M., RAVETCH, J. V. & HOLMDAHL, R. 2007. Endoglycosidase treatment abrogates IgG arthritogenicity: importance of IgG glycosylation in arthritis. *Eur J Immunol,* 37**,** 2973-82.

NAVARRO, V. J. & SENIOR, J. R. 2006. Drug-related hepatotoxicity. *N Engl J Med,* 354**,** 731-9.

NICOTERA, P., LEIST, M. & FERRANDO-MAY, E. 1998. Intracellular ATP, a switch in the decision between apoptosis and necrosis. *Toxicol Lett,* 102-103**,** 139-42.

OLSON, H., BETTON, G., ROBINSON, D., THOMAS, K., MONRO, A., KOLAJA, G., LILLY, P., SANDERS, J., SIPES, G., BRACKEN, W., DORATO, M., VAN DEUN, K., SMITH, P., BERGER, B. & HELLER, A. 2000. Concordance of the toxicity of pharmaceuticals in humans and in animals. *Regul Toxicol Pharmacol,* 32**,** 56-67.

OSTAPOWICZ, G., FONTANA, R. J., SCHIODT, F. V., LARSON, A., DAVERN, T. J., HAN, S. H., MCCASHLAND, T. M., SHAKIL, A. O., HAY, J. E., HYNAN, L., CRIPPIN, J. S., BLEI, A. T., SAMUEL, G., REISCH, J., LEE, W. M. & GROUP, U. S. A. L. F. S. 2002. Results of a prospective study of acute liver failure at 17 tertiary care centers in the United States. *Ann Intern Med,* 137**,** 947-54.

OVERDIJK, M. B., VERPLOEGEN, S., ORTIZ BUIJSSE, A., VINK, T., LEUSEN, J. H., BLEEKER, W. K. & PARREN, P. W. 2012. Crosstalk between human IgG isotypes and murine effector cells. *J Immunol,* 189**,** 3430-8.

OZER, J., RATNER, M., SHAW, M., BAILEY, W. & SCHOMAKER, S. 2008. The current state of serum biomarkers of hepatotoxicity. *Toxicology,* 245**,** 194-205.

PACHKORIA, K., LUCENA, M. I., MOLOKHIA, M., CUETO, R., CARBALLO, A. S., CARVAJAL, A. & ANDRADE, R. J. 2007. Genetic and molecular factors in drug-induced liver injury: a review. *Curr Drug Saf,* 2**,** 97-112.

PAGET, M. S. & BUTTNER, M. J. 2003. Thiol-based regulatory switches. *Annu Rev Genet,* 37**,** 91-121.

PARK, B. K., LAVERTY, H., SRIVASTAVA, A., ANTOINE, D. J., NAISBITT, D. & WILLIAMS, D. P. 2011. Drug bioactivation and protein adduct formation in the pathogenesis of drug-induced toxicity. *Chem Biol Interact,* 192**,** 30-6.

PARK, B. S., SONG, D. H., KIM, H. M., CHOI, B. S., LEE, H. & LEE, J. O. 2009. The structural basis of lipopolysaccharide recognition by the TLR4-MD-2 complex. *Nature,* 458**,** 1191-5.

PARK, J. S., GAMBONI-ROBERTSON, F., HE, Q., SVETKAUSKAITE, D., KIM, J. Y., STRASSHEIM, D., SOHN, J. W., YAMADA, S., MARUYAMA, I., BANERJEE, A., ISHIZAKA, A. & ABRAHAM, E. 2006. High mobility group box 1 protein interacts with multiple Toll-like receptors. *Am J Physiol Cell Physiol,* 290**,** C917-24.

PARK, J. S., SVETKAUSKAITE, D., HE, Q., KIM, J. Y., STRASSHEIM, D., ISHIZAKA, A. & ABRAHAM, E. 2004. Involvement of toll-like receptors 2 and 4 in cellular activation by high mobility group box 1 protein. *J Biol Chem,* 279**,** 7370-7.

PARK, S. & LIPPARD, S. J. 2011. Redox state-dependent interaction of HMGB1 and cisplatin-modified DNA. *Biochemistry,* 50**,** 2567-74.

PASHEVA, E. A., PASHEV, I. G. & FAVRE, A. 1998. Preferential binding of high mobility group 1 protein to UV-damaged DNA. Role of the COOH-terminal domain. *J Biol Chem,* 273**,** 24730-6.

PENG, J., SCHWARTZ, D., ELIAS, J. E., THOREEN, C. C., CHENG, D., MARSISCHKY, G., ROELOFS, J., FINLEY, D. & GYGI, S. P. 2003. A proteomics approach to understanding protein ubiquitination. *Nat Biotechnol,* 21**,** 921-6.

PIL, P. M. & LIPPARD, S. J. 1992. Specific binding of chromosomal protein HMG1 to DNA damaged by the anticancer drug cisplatin. *Science,* 256**,** 234-7.

PIRES, D. A., MARQUES, P. E., PEREIRA, R. V., DAVID, B. A., GOMIDES, L. F., DIAS, A. C., NUNES-SILVA, A., PINHO, V., CARA, D. C., VIEIRA, L. Q., TEIXEIRA, M. M. & MENEZES, G. B. 2014. Interleukin-4 deficiency protects mice from acetaminophen-induced liver injury and inflammation by prevention of glutathione depletion. *Inflamm Res,* 63**,** 61-9.

PIRMOHAMED, M., JAMES, S., MEAKIN, S., GREEN, C., SCOTT, A. K., WALLEY, T. J., FARRAR, K., PARK, B. K. & BRECKENRIDGE, A. M. 2004. Adverse drug reactions as cause of admission to hospital: prospective analysis of 18 820 patients. *BMJ,* 329**,** 15-9.

PIRMOHAMED, M. & PARK, B. K. 2003. Adverse drug reactions: back to the future. *Br J Clin Pharmacol,* 55**,** 486-92.

PISETSKY, D. S. 2014. The Expression of HMGB1 on microparticles released during cell activation and cell death in vitro and in vivo. *Mol Med,* 20**,** 158-63.

POLANSKA, E., POSPISILOVA, S. & STROS, M. 2014. Binding of histone H1 to DNA is differentially modulated by redox state of HMGB1. *PLoS One,* 9**,** e89070.

PRESCOTT, L. F., ILLINGWORTH, R. N., CRITCHLEY, J. A., STEWART, M. J., ADAM, R. D. & PROUDFOOT, A. T. 1979. Intravenous N-acetylcystine: the treatment of choice for paracetamol poisoning. *Br Med J,* 2**,** 1097-100.

QIAN, S. B., MCDONOUGH, H., BOELLMANN, F., CYR, D. M. & PATTERSON, C. 2006. CHIP-mediated stress recovery by sequential ubiquitination of substrates and Hsp70. *Nature,* 440**,** 551-5.

RAIBORG, C. & STENMARK, H. 2009. The ESCRT machinery in endosomal sorting of ubiquitylated membrane proteins. *Nature,* 458**,** 445-52.

RAUCY, J. L., LASKER, J. M., LIEBER, C. S. & BLACK, M. 1989. Acetaminophen activation by human liver cytochromes P450IIE1 and P450IA2. *Arch Biochem Biophys,* 271**,** 270-83.

ROBERTSON, J. D. & ORRENIUS, S. 2000. Molecular mechanisms of apoptosis induced by cytotoxic chemicals. *Critical Reviews in Toxicology,* 30**,** 609-627.

RODRIGUEZ, J. & LAZEBNIK, Y. 1999. Caspase-9 and APAF-1 form an active holoenzyme. *Genes Dev,* 13**,** 3179-84.

RUBARTELLI, A. & LOTZE, M. T. 2007. Inside, outside, upside down: damage-associated molecular-pattern molecules (DAMPs) and redox. *Trends Immunol,* 28**,** 429-36.

SAHU, D., DEBNATH, P., TAKAYAMA, Y. & IWAHARA, J. 2008. Redox properties of the A-domain of the HMGB1 protein. *FEBS Lett,* 582**,** 3973-8.

SALHANICK, S. D., ORLOW, D., HOLT, D. E., PAVLIDES, S., REENSTRA, W. & BURAS, J. A. 2006. Endothelially derived nitric oxide affects the severity of early acetaminophen-induced hepatic injury in mice. *Acad Emerg Med,* 13**,** 479-85.

SAWA, H., UEDA, T., TAKEYAMA, Y., YASUDA, T., SHINZEKI, M., NAKAJIMA, T. & KURODA, Y. 2006. Blockade of high mobility group box-1 protein attenuates experimental severe acute pancreatitis. *World J Gastroenterol,* 12**,** 7666-70.

SCAFFIDI, P., MISTELI, T. & BIANCHI, M. E. 2002. Release of chromatin protein HMGB1 by necrotic cells triggers inflammation. *Nature,* 418**,** 191-5.

SCHELLER, J., CHALARIS, A., SCHMIDT-ARRAS, D. & ROSE-JOHN, S. 2011. The pro- and anti-inflammatory properties of the cytokine interleukin-6. *Biochim Biophys Acta,* 1813**,** 878-88.

SCHIERBECK, H., LUNDBACK, P., PALMBLAD, K., KLEVENVALL, L., ERLANDSSON-HARRIS, H., ANDERSSON, U. & OTTOSSON, L. 2011. Monoclonal anti-HMGB1 (high mobility group box chromosomal protein 1) antibody protection in two experimental arthritis models. *Mol Med,* 17**,** 1039-44.

SCHIERBECK, H., WAHAMAA, H., ANDERSSON, U. & HARRIS, H. E. 2010. Immunomodulatory drugs regulate HMGB1 release from activated human monocytes. *Mol Med,* 16**,** 343-51.

SCHIERWAGEN, C., BYLUND-FELLENIUS, A. C. & LUNDBERG, C. 1990. Improved method for quantification of tissue PMN accumulation measured by myeloperoxidase activity. *J Pharmacol Methods,* 23**,** 179-86.

SCHILLER, M., BEKEREDJIAN-DING, I., HEYDER, P., BLANK, N., HO, A. D. & LORENZ, H. M. 2008. Autoantigens are translocated into small apoptotic bodies during early stages of apoptosis. *Cell Death Differ,* 15**,** 183-91.

SCHILLER, M., HEYDER, P., ZIEGLER, S., NIESSEN, A., CLASSEN, L., LAUFFER, A. & LORENZ, H. M. 2013. During apoptosis HMGB1 is translocated into apoptotic cell-derived membranous vesicles. *Autoimmunity,* 46**,** 342-6.

SCHIRALDI, M., RAUCCI, A., MUNOZ, L. M., LIVOTI, E., CELONA, B., VENEREAU, E., APUZZO, T., DE MARCHIS, F., PEDOTTI, M., BACHI, A., THELEN, M., VARANI, L., MELLADO, M., PROUDFOOT, A., BIANCHI, M. E. & UGUCCIONI, M. 2012. HMGB1 promotes recruitment of inflammatory cells to damaged tissues by forming a complex with CXCL12 and signaling via CXCR4. *J Exp Med,* 209**,** 551-63.

SENIOR, J. R. 2012. Alanine aminotransferase: a clinical and regulatory tool for detecting liver injury-past, present, and future. *Clin Pharmacol Ther,* 92**,** 332-9.

SGRO, C., CLINARD, F., OUAZIR, K., CHANAY, H., ALLARD, C., GUILLEMINET, C., LENOIR, C., LEMOINE, A. & HILLON, P. 2002. Incidence of drug-induced hepatic injuries: a French population-based study. *Hepatology,* 36**,** 451-5.

SHI, D., POP, M. S., KULIKOV, R., LOVE, I. M., KUNG, A. L. & GROSSMAN, S. R. 2009. CBP and p300 are cytoplasmic E4 polyubiquitin ligases for p53. *Proc Natl Acad Sci U S A,* 106**,** 16275-80.

SHIELDS, R. L., NAMENUK, A. K., HONG, K., MENG, Y. G., RAE, J., BRIGGS, J., XIE, D., LAI, J., STADLEN, A., LI, B., FOX, J. A. & PRESTA, L. G. 2001. High resolution mapping of the binding site on human IgG1 for Fc gamma RI, Fc gamma RII, Fc gamma RIII, and FcRn and design of IgG1 variants with improved binding to the Fc gamma R. *J Biol Chem,* 276**,** 6591-604.

SHIMAZAKI, J., MATSUMOTO, N., OGURA, H., MUROYA, T., KUWAGATA, Y., NAKAGAWA, J., YAMAKAWA, K., HOSOTSUBO, H., IMAMURA, Y. & SHIMAZU, T. 2012. Systemic involvement of high-mobility group box 1 protein and therapeutic effect of anti-high-mobility group box 1 protein antibody in a rat model of crush injury. *Shock,* 37**,** 634-8.

SHRINGARPURE, R., GRUNE, T., MEHLHASE, J. & DAVIES, K. J. 2003. Ubiquitin conjugation is not required for the degradation of oxidized proteins by proteasome. *J Biol Chem,* 278**,** 311-8.

SLOPER-MOULD, K. E., JEMC, J. C., PICKART, C. M. & HICKE, L. 2001. Distinct functional surface regions on ubiquitin. *J Biol Chem,* 276**,** 30483-9.

SOBHIAN, B., SHAO, G., LILLI, D. R., CULHANE, A. C., MOREAU, L. A., XIA, B., LIVINGSTON, D. M. & GREENBERG, R. A. 2007. RAP80 targets BRCA1 to specific ubiquitin structures at DNA damage sites. *Science,* 316**,** 1198-202.

SORKIN, L. S., OTTO, M., BALDWIN, W. M., 3RD, VAIL, E., GILLIES, S. D., HANDGRETINGER, R., BARFIELD, R. C., MING YU, H. & YU, A. L. 2010. Anti-GD(2) with an FC point mutation reduces complement fixation and decreases antibody-induced allodynia. *Pain,* 149**,** 135-42.

SPENCER, D. M., MOBARREZ, F., WALLEN, H. & PISETSKY, D. S. 2014. The expression of HMGB1 on microparticles from Jurkat and HL-60 cells undergoing apoptosis in vitro. *Scand J Immunol,* 80**,** 101-10.

SPICKETT, C. M. & PITT, A. R. 2012. Protein oxidation: role in signalling and detection by mass spectrometry. *Amino Acids,* 42**,** 5-21.

STARKEY LEWIS, P. J., DEAR, J., PLATT, V., SIMPSON, K. J., CRAIG, D. G., ANTOINE, D. J., FRENCH, N. S., DHAUN, N., WEBB, D. J., COSTELLO, E. M., NEOPTOLEMOS, J. P., MOGGS, J., GOLDRING, C. E. & PARK, B. K. 2011. Circulating microRNAs as potential markers of human drug-induced liver injury. *Hepatology,* 54**,** 1767-76.

STEBBINGS, R., EASTWOOD, D., POOLE, S. & THORPE, R. 2013. After TGN1412: recent developments in cytokine release assays. *J Immunotoxicol,* 10**,** 75-82.

SUDA, K., KITAGAWA, Y., OZAWA, S., SAIKAWA, Y., UEDA, M., EBINA, M., YAMADA, S., HASHIMOTO, S., FUKATA, S., ABRAHAM, E., MARUYAMA, I., KITAJIMA, M. & ISHIZAKA, A. 2006. Anti-high-mobility group box chromosomal protein 1 antibodies improve survival of rats with sepsis. *World J Surg,* 30**,** 1755-62.

SUN, P. D. 2003. Structure and function of natural-killer-cell receptors. *Immunol Res,* 27**,** 539-48.

SUTRIAS-GRAU, M., BIANCHI, M. E. & BERNUES, J. 1999. High mobility group protein 1 interacts specifically with the core domain of human TATA box-binding protein and interferes with transcription factor IIB within the pre-initiation complex. *J Biol Chem,* 274**,** 1628-34.

SUZUKI, J., UMEDA, M., SIMS, P. J. & NAGATA, S. 2010. Calcium-dependent phospholipid scrambling by TMEM16F. *Nature,* 468**,** 834-8.

TAKADA, H., MAWET, E., SHIRATORI, Y., HIKIBA, Y., NAKATA, R., YOSHIDA, H., OKANO, K., KAMII, K. & OMATA, M. 1995. Chemotactic factors released from hepatocytes exposed to acetaminophen. *Dig Dis Sci,* 40**,** 1831-6.

TAKANO, K., SHINODA, M., TANABE, M., MIYASHO, T., YAMADA, S., ONO, S., MASUGI, Y., SUDA, K., FUKUNAGA, K., HAYASHIDA, T., HIBI, T., OBARA, H., TAKEUCHI, H., KAWACHI, S., KAWASAKO,

K., OKAMOTO, M., YOKOTA, H., MARUYAMA, I. & KITAGAWA, Y. 2010. Protective effect of high-mobility group box 1 blockade on acute liver failure in rats. *Shock,* 34**,** 573-9.

TAMAOKI, T., NOMOTO, H., TAKAHASHI, I., KATO, Y., MORIMOTO, M. & TOMITA, F. 1986. Staurosporine, a potent inhibitor of phospholipid/Ca++dependent protein kinase. *Biochem Biophys Res Commun,* 135**,** 397-402.

TANG, D., KANG, R., XIAO, W., ZHANG, H., LOTZE, M. T., WANG, H. & XIAO, X. 2009. Quercetin prevents LPS-induced high-mobility group box 1 release and proinflammatory function. *Am J Respir Cell Mol Biol,* 41**,** 651-60.

TANG, Y., LV, B., WANG, H., XIAO, X. & ZUO, X. 2008. PACAP inhibit the release and cytokine activity of HMGB1 and improve the survival during lethal endotoxemia. *Int Immunopharmacol,* 8**,** 1646-51.

THOMAS, J. O. & TRAVERS, A. A. 2001. HMG1 and 2, and related 'architectural' DNA-binding proteins. *Trends Biochem Sci,* 26**,** 167-74.

THORNBERRY, N. A., RANO, T. A., PETERSON, E. P., RASPER, D. M., TIMKEY, T., GARCIA-CALVO, M., HOUTZAGER, V. M., NORDSTROM, P. A., ROY, S., VAILLANCOURT, J. P., CHAPMAN, K. T. & NICHOLSON, D. W. 1997. A combinatorial approach defines specificities of members of the caspase family and granzyme B. Functional relationships established for key mediators of apoptosis. *J Biol Chem,* 272**,** 17907-11.

THROWER, J. S., HOFFMAN, L., RECHSTEINER, M. & PICKART, C. M. 2000. Recognition of the polyubiquitin proteolytic signal. *EMBO J,* 19**,** 94-102.

TIAN, J., AVALOS, A. M., MAO, S. Y., CHEN, B., SENTHIL, K., WU, H., PARROCHE, P., DRABIC, S., GOLENBOCK, D., SIROIS, C., HUA, J., AN, L. L., AUDOLY, L., LA ROSA, G., BIERHAUS, A., NAWORTH, P., MARSHAK-ROTHSTEIN, A., CROW, M. K., FITZGERALD, K. A., LATZ, E., KIENER, P. A. & COYLE, A. J. 2007. Toll-like receptor 9-dependent activation by DNA-containing immune complexes is mediated by HMGB1 and RAGE. *Nat Immunol,* 8**,** 487-96.

TOKUNAGA, F., SAKATA, S., SAEKI, Y., SATOMI, Y., KIRISAKO, T., KAMEI, K., NAKAGAWA, T., KATO, M., MURATA, S., YAMAOKA, S., YAMAMOTO, M., AKIRA, S., TAKAO, T., TANAKA, K. & IWAI, K. 2009. Involvement of linear polyubiquitylation of NEMO in NF-kappaB activation. *Nat Cell Biol,* 11**,** 123-32.

TRAVERS, A. A. 2003. Priming the nucleosome: a role for HMGB proteins? *EMBO Rep,* 4**,** 131-6.

TSUJIMOTO, Y. & SHIMIZU, S. 2005. Another way to die: autophagic programmed cell death. *Cell Death Differ,* 12 Suppl 2**,** 1528-34.

TSUNG, A., SAHAI, R., TANAKA, H., NAKAO, A., FINK, M. P., LOTZE, M. T., YANG, H., LI, J., TRACEY, K. J., GELLER, D. A. & BILLIAR, T. R. 2005. The nuclear factor HMGB1 mediates hepatic injury after murine liver ischemia-reperfusion. *J Exp Med,* 201**,** 1135-43.

U.S. FOOD AND DRUG ADMINISTRATION (FDA). *FAERS Reporting by Patient Outcomes by Year* [Online]. Available: http://www.fda.gov/drugs/guidancecomplianceregulatoryinformation/surveillance/adversedrugeffects/ucm070461.htm [Accessed 22 Sept 2014].

ULLOA, L., OCHANI, M., YANG, H., TANOVIC, M., HALPERIN, D., YANG, R., CZURA, C. J., FINK, M. P. & TRACEY, K. J. 2002. Ethyl pyruvate prevents lethality in mice with established lethal sepsis and systemic inflammation. *Proc Natl Acad Sci U S A,* 99**,** 12351-6.

URBONAVICIUTE, V., FURNROHR, B. G., MEISTER, S., MUNOZ, L., HEYDER, P., DE MARCHIS, F., BIANCHI, M. E., KIRSCHNING, C., WAGNER, H., MANFREDI, A. A., KALDEN, J. R., SCHETT, G., ROVERE-QUERINI, P., HERRMANN, M. & VOLL, R. E. 2008. Induction of inflammatory and immune responses by HMGB1-nucleosome complexes: implications for the pathogenesis of SLE. *J Exp Med,* 205**,** 3007-18.

UZAWA, A., MORI, M., TANIGUCHI, J., MASUDA, S., MUTO, M. & KUWABARA, S. 2013. Anti-high mobility group box 1 monoclonal antibody ameliorates experimental autoimmune encephalomyelitis. *Clin Exp Immunol,* 172**,** 37-43.

VANDEPUTTE, C., GUIZON, I., GENESTIE-DENIS, I., VANNIER, B. & LORENZON, G. 1994. A microtiter plate assay for total glutathione and glutathione disulfide contents in cultured/isolated cells: performance study of a new miniaturized protocol. *Cell Biol Toxicol,* 10**,** 415-21.

VAQUERO, J., BELANGER, M., JAMES, L., HERRERO, R., DESJARDINS, P., COTE, J., BLEI, A. T. & BUTTERWORTH, R. F. 2007. Mild hypothermia attenuates liver injury and improves survival in mice with acetaminophen toxicity. *Gastroenterology,* 132**,** 372-83.

VENEREAU, E., CASALGRANDI, M., SCHIRALDI, M., ANTOINE, D. J., CATTANEO, A., DE MARCHIS, F., LIU, J., ANTONELLI, A., PRETI, A., RAELI, L., SHAMS, S. S., YANG, H., VARANI, L., ANDERSSON, U., TRACEY, K. J., BACHI, A., UGUCCIONI, M. & BIANCHI, M. E. 2012. Mutually exclusive redox forms of HMGB1 promote cell recruitment or proinflammatory cytokine release. *J Exp Med,* 209**,** 1519-28.

VENEREAU, E., SCHIRALDI, M., UGUCCIONI, M. & BIANCHI, M. E. 2013. HMGB1 and leukocyte migration during trauma and sterile inflammation. *Mol Immunol,* 55**,** 76-82.

VIDARSSON, G., STEMERDING, A. M., STAPLETON, N. M., SPLIETHOFF, S. E., JANSSEN, H., REBERS, F. E., DE HAAS, M. & VAN DE WINKEL, J. G. 2006. FcRn: an IgG receptor on phagocytes with a novel role in phagocytosis. *Blood,* 108**,** 3573-9.

WAHAMAA, H., VALLERSKOG, T., QIN, S., LUNDERIUS, C., LAROSA, G., ANDERSSON, U. & HARRIS, H. E. 2007. HMGB1-secreting capacity of multiple cell lineages revealed by a novel HMGB1 ELISPOT assay. *J Leukoc Biol,* 81**,** 129-36.

WANG, C., DENG, L., HONG, M., AKKARAJU, G. R., INOUE, J. & CHEN, Z. J. 2001. TAK1 is a ubiquitin-dependent kinase of MKK and IKK. *Nature,* 412**,** 346-51.

WANG, H., BLOOM, O., ZHANG, M., VISHNUBHAKAT, J. M., OMBRELLINO, M., CHE, J., FRAZIER, A., YANG, H., IVANOVA, S., BOROVIKOVA, L., MANOGUE, K. R., FAIST, E., ABRAHAM, E., ANDERSSON, J., ANDERSSON, U., MOLINA, P. E., ABUMRAD, N. N., SAMA, A. & TRACEY, K. J. 1999. HMG-1 as a late mediator of endotoxin lethality in mice. *Science,* 285**,** 248-51.

WANG, H., LI, W., LI, J., RENDON-MITCHELL, B., OCHANI, M., ASHOK, M., YANG, L., YANG, H., TRACEY, K. J., WANG, P. & SAMA, A. E. 2006. The aqueous extract of a popular herbal nutrient supplement, Angelica sinensis, protects mice against lethal endotoxemia and sepsis. *J Nutr,* 136**,** 360-5.

WANG, H., LIAO, H., OCHANI, M., JUSTINIANI, M., LIN, X., YANG, L., AL-ABED, Y., METZ, C., MILLER, E. J., TRACEY, K. J. & ULLOA, L. 2004. Cholinergic agonists inhibit HMGB1 release and improve survival in experimental sepsis. *Nat Med,* 10**,** 1216-21.

WANG, K. 2014. Molecular mechanisms of hepatic apoptosis. *Cell Death Dis,* 5**,** e996.

WANG, K., ZHANG, S., MARZOLF, B., TROISCH, P., BRIGHTMAN, A., HU, Z., HOOD, L. E. & GALAS, D. J. 2009. Circulating microRNAs, potential biomarkers for drug-induced liver injury. *Proc Natl Acad Sci U S A,* 106**,** 4402-7.

WANG, L., ZHANG, X., LIU, L., CUI, L., YANG, R., LI, M. & DU, W. 2010a. Tanshinone II A down-regulates HMGB1, RAGE, TLR4, NF-kappaB expression, ameliorates BBB permeability and endothelial cell function, and protects rat brains against focal ischemia. *Brain Res,* 1321**,** 143-51.

WANG, L., ZHANG, X., LIU, L., YANG, R., CUI, L. & LI, M. 2010b. Atorvastatin protects rat brains against permanent focal ischemia and downregulates HMGB1, HMGB1 receptors (RAGE and TLR4), NF-kappaB expression. *Neurosci Lett,* 471**,** 152-6.

WANG, X., HERR, R. A., CHUA, W. J., LYBARGER, L., WIERTZ, E. J. & HANSEN, T. H. 2007. Ubiquitination of serine, threonine, or lysine residues on the cytoplasmic tail can induce ERAD of MHC-I by viral E3 ligase mK3. *J Cell Biol,* 177**,** 613-24.

WANG, X., ZELENSKI, N. G., YANG, J., SAKAI, J., BROWN, M. S. & GOLDSTEIN, J. L. 1996. Cleavage of sterol regulatory element binding proteins (SREBPs) by CPP32 during apoptosis. *EMBO J,* 15**,** 1012-20.

WATANABE, T., KUBOTA, S., NAGAYA, M., OZAKI, S., NAGAFUCHI, H., AKASHI, K., TAIRA, Y., TSUKIKAWA, S., OOWADA, S. & NAKANO, S. 2005. The role of HMGB-1 on the development

of necrosis during hepatic ischemia and hepatic ischemia/reperfusion injury in mice. *J Surg Res,* 124**,** 59-66.

WILLIAMS, C. D., BAJT, M. L., SHARPE, M. R., MCGILL, M. R., FARHOOD, A. & JAESCHKE, H. 2014. Neutrophil activation during acetaminophen hepatotoxicity and repair in mice and humans. *Toxicol Appl Pharmacol,* 275**,** 122-33.

WILLIAMS, C. D., FARHOOD, A. & JAESCHKE, H. 2010. Role of caspase-1 and interleukin-1beta in acetaminophen-induced hepatic inflammation and liver injury. *Toxicol Appl Pharmacol,* 247**,** 169-78.

WILLIAMS, D. P., ANTOINE, D. J., BUTLER, P. J., JONES, R., RANDLE, L., PAYNE, A., HOWARD, M., GARDNER, I., BLAGG, J. & PARK, B. K. 2007. The metabolism and toxicity of furosemide in the Wistar rat and CD-1 mouse: a chemical and biochemical definition of the toxicophore. *J Pharmacol Exp Ther,* 322**,** 1208-20.

WINSTON, J. T., STRACK, P., BEER-ROMERO, P., CHU, C. Y., ELLEDGE, S. J. & HARPER, J. W. 1999. The SCFbeta-TRCP-ubiquitin ligase complex associates specifically with phosphorylated destruction motifs in IkappaBalpha and beta-catenin and stimulates IkappaBalpha ubiquitination in vitro. *Genes Dev,* 13**,** 270-83.

WOOF, J. M. & BURTON, D. R. 2004. Human antibody-Fc receptor interactions illuminated by crystal structures. *Nat Rev Immunol,* 4**,** 89-99.

WOOLBRIGHT, B. L., ANTOINE, D. J., JENKINS, R. E., BAJT, M. L., PARK, B. K. & JAESCHKE, H. 2013. Plasma biomarkers of liver injury and inflammation demonstrate a lack of apoptosis during obstructive cholestasis in mice. *Toxicol Appl Pharmacol,* 273**,** 524-31.

WU, T. Y., JEN, M. H., BOTTLE, A., MOLOKHIA, M., AYLIN, P., BELL, D. & MAJEED, A. 2010. Ten-year trends in hospital admissions for adverse drug reactions in England 1999-2009. *J R Soc Med,* 103**,** 239-50.

XU, J. J., HENSTOCK, P. V., DUNN, M. C., SMITH, A. R., CHABOT, J. R. & DE GRAAF, D. 2008. Cellular imaging predictions of clinical drug-induced liver injury. *Toxicol Sci,* 105**,** 97-105.

YAMANAKA, K., ISHIKAWA, H., MEGUMI, Y., TOKUNAGA, F., KANIE, M., ROUAULT, T. A., MORISHIMA, I., MINATO, N., ISHIMORI, K. & IWAI, K. 2003. Identification of the ubiquitin-protein ligase that recognizes oxidized IRP2. *Nat Cell Biol,* 5**,** 336-40.

YANG, D., CHEN, Q., YANG, H., TRACEY, K. J., BUSTIN, M. & OPPENHEIM, J. J. 2007. High mobility group box-1 protein induces the migration and activation of human dendritic cells and acts as an alarmin. *J Leukoc Biol,* 81**,** 59-66.

YANG, H., ANTOINE, D. J., ANDERSSON, U. & TRACEY, K. J. 2013. The many faces of HMGB1: molecular structure-functional activity in inflammation, apoptosis, and chemotaxis. *J Leukoc Biol,* 93**,** 865-73.

YANG, H., HREGGVIDSDOTTIR, H. S., PALMBLAD, K., WANG, H., OCHANI, M., LI, J., LU, B., CHAVAN, S., ROSAS-BALLINA, M., AL-ABED, Y., AKIRA, S., BIERHAUS, A., ERLANDSSON-HARRIS, H., ANDERSSON, U. & TRACEY, K. J. 2010a. A critical cysteine is required for HMGB1 binding to Toll-like receptor 4 and activation of macrophage cytokine release. *Proc Natl Acad Sci U S A,* 107**,** 11942-7.

YANG, H., LUNDBACK, P., OTTOSSON, L., ERLANDSSON-HARRIS, H., VENEREAU, E., BIANCHI, M. E., AL-ABED, Y., ANDERSSON, U., TRACEY, K. J. & ANTOINE, D. J. 2012a. Redox modification of cysteine residues regulates the cytokine activity of high mobility group box-1 (HMGB1). *Mol Med,* 18**,** 250-9.

YANG, H., OCHANI, M., LI, J., QIANG, X., TANOVIC, M., HARRIS, H. E., SUSARLA, S. M., ULLOA, L., WANG, H., DIRAIMO, R., CZURA, C. J., ROTH, J., WARREN, H. S., FINK, M. P., FENTON, M. J., ANDERSSON, U. & TRACEY, K. J. 2004a. Reversing established sepsis with antagonists of endogenous high-mobility group box 1. *Proc Natl Acad Sci U S A,* 101**,** 296-301.

YANG, H., OCHANI, M., LI, J., QIANG, X., TANOVIC, M., HARRIS, H. E., SUSARLA, S. M., ULLOA, L., WANG, H., DIRAIMO, R., CZURA, C. J., WANG, H., ROTH, J., WARREN, H. S., FINK, M. P., FENTON, M. J., ANDERSSON, U. & TRACEY, K. J. 2004b. Reversing established sepsis with

antagonists of endogenous high-mobility group box 1. *Proc Natl Acad Sci U S A,* 101**,** 296-301.

YANG, R., HARADA, T., MOLLEN, K. P., PRINCE, J. M., LEVY, R. M., ENGLERT, J. A., GALLOWITSCH-PUERTA, M., YANG, L., YANG, H., TRACEY, K. J., HARBRECHT, B. G., BILLIAR, T. R. & FINK, M. P. 2006. Anti-HMGB1 neutralizing antibody ameliorates gut barrier dysfunction and improves survival after hemorrhagic shock. *Mol Med,* 12**,** 105-14.

YANG, R., OTTEN, M. A., HELLMARK, T., COLLIN, M., BJORCK, L., ZHAO, M. H., DAHA, M. R. & SEGELMARK, M. 2010b. Successful treatment of experimental glomerulonephritis with IdeS and EndoS, IgG-degrading streptococcal enzymes. *Nephrol Dial Transplant,* 25**,** 2479-86.

YANG, R., ZHANG, S., COTOIA, A., OKSALA, N., ZHU, S. & TENHUNEN, J. 2012b. High mobility group B1 impairs hepatocyte regeneration in acetaminophen hepatotoxicity. *BMC Gastroenterol,* 12**,** 45.

YANG, R., ZOU, X., KOSKINEN, M. L. & TENHUNEN, J. 2012c. Ethyl pyruvate reduces liver injury at early phase but impairs regeneration at late phase in acetaminophen overdose. *Crit Care,* 16**,** R9.

YANG, R. Z., BLAILEANU, G., HANSEN, B. C., SHULDINER, A. R. & GONG, D. W. 2002. cDNA cloning, genomic structure, chromosomal mapping, and functional expression of a novel human alanine aminotransferase. *Genomics,* 79**,** 445-50.

YOUN, J. H. & SHIN, J. S. 2006. Nucleocytoplasmic shuttling of HMGB1 is regulated by phosphorylation that redirects it toward secretion. *J Immunol,* 177**,** 7889-97.

YU, M., WANG, H., DING, A., GOLENBOCK, D. T., LATZ, E., CZURA, C. J., FENTON, M. J., TRACEY, K. J. & YANG, H. 2006. HMGB1 signals through toll-like receptor (TLR) 4 and TLR2. *Shock,* 26**,** 174-9.

ZAMEK-GLISZCZYNSKI, M. J., HOFFMASTER, K. A., NEZASA, K., TALLMAN, M. N. & BROUWER, K. L. 2006. Integration of hepatic drug transporters and phase II metabolizing enzymes: mechanisms of hepatic excretion of sulfate, glucuronide, and glutathione metabolites. *Eur J Pharm Sci,* 27**,** 447-86.

ZANDARASHVILI, L., SAHU, D., LEE, K., LEE, Y. S., SINGH, P., RAJARATHNAM, K. & IWAHARA, J. 2013. Real-time kinetics of high-mobility group box 1 (HMGB1) oxidation in extracellular fluids studied by in situ protein NMR spectroscopy. *J Biol Chem,* 288**,** 11621-7.

ZHANG, J., TAKAHASHI, H. K., LIU, K., WAKE, H., LIU, R., MARUO, T., DATE, I., YOSHINO, T., OHTSUKA, A., MORI, S. & NISHIBORI, M. 2011. Anti-high mobility group box-1 monoclonal antibody protects the blood-brain barrier from ischemia-induced disruption in rats. *Stroke,* 42**,** 1420-8.

ZHANG, Q. & WANG, Y. 2008. High mobility group proteins and their post-translational modifications. *Biochim Biophys Acta,* 1784**,** 1159-66.

ZHAO, M. & VUORI, K. 2011. The docking protein p130Cas regulates cell sensitivity to proteasome inhibition. *BMC Biol,* 9**,** 73.

ZHOU, S., CHAN, E., DUAN, W., HUANG, M. & CHEN, Y. Z. 2005. Drug bioactivation, covalent binding to target proteins and toxicity relevance. *Drug Metab Rev,* 37**,** 41-213.

ZHU, H., FEARNHEAD, H. O. & COHEN, G. M. 1995. An ICE-like protease is a common mediator of apoptosis induced by diverse stimuli in human monocytic THP.1 cells. *FEBS Lett,* 374**,** 303-8.